

ISSN 2313–5891 (Online)

ISSN 2304–974X (Print)

# **Ukrainian Food Journal**

***Volume 12, Issue 1  
2023***

**Kyiv**

**2023**

**Київ**

**Ukrainian Food Journal** is an international scientific journal that publishes articles of the specialists in the fields of food science, engineering and technology, chemistry, economics and management.

**Ukrainian Food Journal** – міжнародне наукове періодичне видання для публікації результатів досліджень фахівців у галузі харчової науки, техніки та технології, хімії, економіки і управління.

**Ukrainian Food Journal** is abstracted and indexed by scientometric databases:

**Ukrainian Food Journal** індексується наукометричними базами:

Index Copernicus (2012)  
EBSCO (2013)  
Google Scholar (2013)  
UlrichsWeb (2013)  
CABI full text (2014)  
Online Library of University of Southern Denmark (2014)  
Directory of Open Access scholarly Resources (ROAD) (2014)  
European Reference Index for the Humanities and the Social Sciences (ERIH PLUS) (2014)  
Directory of Open Access Journals (DOAJ) (2015)  
InfoBase Index (2015)  
Chemical Abstracts Service Source Index (CASSI) (2016)  
FSTA (Food Science and Technology Abstracts) (2018)  
Web of Science (Emerging Sources Citation Index) (2018)  
Scopus (2022)

**Ukrainian Food Journal** включено у перелік наукових фахових видань України з технічних наук, категорія А (Наказ Міністерства освіти і науки України № 358 від 15.03.2019)

**Editorial office address:**

National University  
of Food Technologies  
68 Volodymyrska str.  
Kyiv 01601, **Ukraine**

**Адреса редакції:**

Національний університет  
харчових технологій  
вул. Володимирська, 68  
Київ 01601, **Україна**

e-mail: [ufj\\_nuft@meta.ua](mailto:ufj_nuft@meta.ua)

Scientific Council of the National  
University of Food Technologies  
approved this issue for publication.  
Protocol № 10, 25.05.2023

Рекомендовано вченою радою  
Національного університету  
харчових технологій.  
Протокол № 10 від 25.05.2023

© NUFT, 2023

© НУХТ, 2023

**Ukrainian Food Journal** is an open access journal published by the National University of Food Technologies (Kyiv, Ukraine). The Journal publishes original research articles, short communications, review papers, news and literature reviews dealing with all aspects of food science, technology, engineering, nutrition, food chemistry, economics and management.

Studies must be novel, have a clear connection to food science, and be of general interest to the international scientific community.

**Topic covered by the journal include:**

- Food engineering
- Food chemistry
- Food microbiology
- Food quality and safety
- Food processes
- Automation of food processes
- Food packaging
- Economics
- Food nanotechnologies
- Economics and management

Please note that the Journal does not consider:

1. The articles with medical statements (this topic is not covered by the journal); the subject of research on humans and animals.
2. The articles with statements that do not contain scientific value (solving the typical practical and engineering tasks).

**Periodicity of the Journal**

4 issues per year (March, June, September, December).

**Reviewing a Manuscript for Publication**

The editor in chief reviews the correspondence of the content of a newly submitted article to the Journal Profile, approves the article design, style and illustrative material, can provide suggestions how to improve them, and makes the decision whether to send it for peer-review.

Articles submitted for publication in “Ukrainian Food Journal” are double-blind peer-reviewed by at least two academics appointed by the Editors' Board: one from the Editorial Board and one, not affiliated to the Board and/or the Publisher.

For a **Complete Guide for Authors** please visit our website:

**<http://ufj.nuft.edu.ua>**

## International Editorial Board

### Editor-in-Chief:

**Olena Stabnikova**, PhD, Prof., *National University of Food Technologies, Ukraine*

### Members of Editorial Board:

**Agota Giedrė Raišienė**, PhD, *Lithuanian Institute of Agrarian Economics, Lithuania*

**Báo Thy Vương**, PhD, *Mekong University, Vietnam*

**Cristina Luisa Miranda Silva**, PhD, Assoc. Prof., *Portuguese Catholic University – College of Biotechnology, Portugal*

**Cristina Popovici**, PhD, Assoc. Prof., *Technical University of Moldova*

**Dora Marinova**, PhD, Prof., *Curtin University Sustainability Policy (CUSP) Institute, Curtin University, Australia*

**Egon Schnitzler**, PhD, Prof., *State University of Ponta Grossa, Ponta Grossa, Brazil*

**Eirin Marie Skjøndal Bar**, PhD, Assoc. Prof., *Norwegian University of Science and Technology, Trondheim, Norway*

**Godwin D. Ndossi**, PhD, Prof., *Hubert Kairuki Memorial University, Dar es Salaam, Tanzania*

**Jasmina Lukinac**, PhD, Assoc. Prof., *University of Osijek, Croatia*

**Kirsten Brandt**, PhD, *Newcastle University, United Kingdom*

**Lelieveld Huub**, PhD, *Global Harmonization Initiative Association, The Netherlands*

**Mark Shamtsian**, PhD, Assoc. Prof., *Black Sea Association of Food Science and Technology, Romania*

**María S. Tapia**, PhD, Prof., *Central University of Venezuela, Caracas, Venezuela; COR MEM of the Academy of Physical, Mathematical and Natural Sciences of Venezuela*

**Moisés Burachik**, PhD, *Institute of Agricultural Biotechnology of Rosario (INDEAR), Bioceres Group, Rosario, Argentina*

**Noor Zafira Noor Hasnan**, PhD, *Universiti Putra Malaysia, Selangor, Malaysia*

**Octavio Paredes-López**, PhD, Prof., *The Center for Research and Advanced Studies of the National Polytechnic Institute, Guanajuato, Mexico.*

**Rana Mustafa**, PhD, *Global Institute for Food Security, University of Saskatchewan, Canada*

**Semih Otles**, PhD, Prof., *Ege University, Turkey*

**Sheila Kilonzi**, PhD, *Karatina University, Kenya*

**Sonia Amariei**, PhD, Prof., *University "Ștefan cel Mare" of Suceava, Romania*

**Stanka Damianova**, PhD, Prof., *Ruse University "Angel Kanchev", branch Razgrad, Bulgaria*

**Stefan Stefanov**, PhD, Prof., *University of Food Technologies, Bulgaria*

**Tetiana Pyrog**, PhD, Prof., *National University of Food Technologies, Ukraine*

**Oleksandr Shevchenko**, PhD, Prof., *National University for Food Technologies, Ukraine*

**Viktor Stabnikov**, PhD, Prof., *National University for Food Technologies, Ukraine*

**Umezuruike Linus Opara**, PhD, Prof., *Stellenbosch University, Cape Town, South Africa*

**Yordanka Stefanova**, PhD, Assist. Prof., *University of Plovdiv "Paisii Hilendarski", Bulgaria*

**Yuliya Dzyazko**, PhD, Prof., *Institute of General and Inorganic Chemistry of the National Academy of Sciences of Ukraine*

**Yun-Hwa Peggy Hsieh**, PhD, Prof. Emerita, *Florida State University, USA*

**Yurii Bilan**, PhD, Prof., *Tomas Bata University in Zlin, Czech Republic*

### Managing Editor:

**Oleksii Gubenia**, PhD, Assoc. Prof., *National University of Food Technologies, Ukraine*

## Contents

<b>Food Technology</b> .....	7
<i>Eugenia Covaliov, Tatiana Capcanari, Vladislav Resitca, Aurica Chirsanova</i> Quality evaluation of sponge cake with milk thistle ( <i>Silybum marianum</i> L.) seed powder addition.....	7
<i>Hanna Vovk, Kwankao Karnpakdee, Olga Golubets, Iryna Levchuk, Roland Ludwig, Tamara Nosenko</i> Application of enzymes for press oil production from pumpkin seeds.....	21
<i>Anastasiia Shevchenko, Svitlana Litvynchuk, Vira Drobot, Oleksandr Shevchenko</i> Influence of pumpkin cellulose on conformational transformations in the structure of dough and bread from wheat flour.....	38
<i>Roshanlal Yadav, Sakshi Khurana, Sunil Kumar</i> Comparative study of properties of basmati and non-basmati rice cultivars.	51
<i>Oleh Kuzmin, Victoriia Kiiko, Olena Khareba, Olena Gavrylenko, Mariia Ianchyk, Nataliia Melnyk</i> Ryazhanka with pumpkin puree and flax seeds.....	65
<b>Processes and Equipment</b> .....	80
<i>Taras Pohorilyi</i> Modeling of non-stationary processes heat and mass transfer according to the cellular model of sucrose mass crystallization.....	80
<i>Valentyn Petrenko, Oleksiy Pylypenko, Oleksandr Ryabchuk, Maksym Nalyvaiko</i> Determining the parameters of demarcation of heat exchange modes in the film during vaporization.....	114
<b>Biotechnology, Microbiology</b> .....	130
<i>Viktor Stabnikov, Dmytro Stabnikov, Zubair Ahmed</i> Phosphate recovery and fertilizer production from wastewater using iron-reducing bacteria.....	130

<b>Economics and Management</b> .....	141
<i>Ali Ilhan, Frank Füredi</i> Employment status of Hungarian food delivery workers in the post pandemic era.....	141
<i>Joshua Mabeta, Luboš Smutka</i> Historical and contemporary perspectives of the sugar industry in sub- Saharan Africa.....	157
<b>Abstracts</b> .....	172
<b>Instructions for authors</b> .....	181

## Quality evaluation of sponge cake with milk thistle (*Silybum marianum* L.) seed powder addition

Eugenia Covaliov, Tatiana Capcanari,  
Vladislav Resitca, Aurica Chirsanova

Technical University of Moldova, Chisinau, Republic of Moldova

---

### Abstract

---

#### Keywords:

Sponge cake  
Milk thistle  
Colour  
Texture

---

#### Article history:

Received  
19.09.2022  
Received in  
revised form  
15.02.2023  
Accepted  
31.03.2023

---

#### Corresponding author:

Eugenia Covaliov  
E-mail:  
eugenia.boaghi@  
toap.utm.md

---

#### DOI:

10.24263/2304-  
974X-2023-12-1-  
3

**Introduction.** The characteristics of sponge cakes with partially replaced of wheat flour with milk thistle seed powder are presented in this study.

**Materials and methods.** Milk thistle (*Silybum marianum* L.) seed powder was used to partially replace wheat flour in sponge cake preparation. Baking loss, moisture content, water activity, volume, porosity, texture, crust and crumb colour, sensory analysis, antioxidant activity, and total phenol content were determined in sponge cake with milk thistle seed powder.

**Results and discussion.** Increasing the level of wheat flour substitution with milk thistle powder from 0 to 20% decreases the volume and porosity of cakes. The addition of milk thistle powder influenced the texture and crumb color of the baked sponge cakes. The hardness and chewiness of baked sponge cakes had an upward trend with increasing milk thistle powder amounts, whereas the cohesiveness, resilience and springiness showed a reverse trend. For the crust and crumb colour the  $L^*$  and  $b^*$  values decreased, while the  $a^*$  value increased, showing that darker, redder and less yellow samples were obtained. The milk thistle addition had a positive effect on the total phenols content by increasing it from 63.93 (control sample) to 121.94 mg gallic acid equivalents, (GAE)/100 g (sample with 20% replacement of wheat flour with milk thistle powder). Simultaneously, the highest antioxidant activity (44.70%) was recorded for the sample with 20% milk thistle seed powder. The sensory analysis pointed out that the sponge cake with the replacement of 5 and 10% wheat flour with milk thistle seed powder was the most acceptable.

**Conclusions.** The incorporation of milk thistle seed powder in sponge cake formulations enriched its biological value in terms of total phenol content and antioxidant activity. However, some technological quality parameters decreased. The sensorial evaluation showed that to produce sponge cakes with high quality, replacement of wheat flour with milk thistle seed powder should not exceed 10%.

## Introduction

Pastry products such as cakes or cookies were initially considered as special treats for certain occasions, but nowadays they are consumed much more frequently, even as regular snacks thus contributing to the increase in sugar consumption (Hashem et al., 2018). Sponge cake, either the American version (chiffon cakes, feather or daffodil sponges, angel food cakes, nut sponge cakes) or the European version (génoise, French biscuit, ladyfingers) is the basis of various pastries and confectionery. The basic ingredients are eggs, sugar and wheat flour, their ratio varying from 50:25:25 to 42:42:15%, depending on the preparation method and other used ingredients such as oil, starch, cocoa, and baking powder (Hui, 2007). The majority of macronutrients in the composition of sponge cake are carbohydrates which are provided by flour and sugar and which, if consumed in excess, are stored in the form of adipose tissue, thus contributing to the appearance of obesity, the development of cardiovascular disease and type 2 diabetes (Stanhope, 2016). Two main topics are addressed when improving sponge cake quality: (1) sustainability by capitalizing on white cabbage outer leaves (Prokopov et al., 2015), aquafaba (Mustafa et al., 2018), and ginseng mark (Park et al., 2008); (2) increasing the biological value by incorporating fibers from carrots (Salehi et al., 2016a) or *Euchema* algae powder (Huang and Yang, 2019), high quality proteins from button mushrooms (Salehi, et al., 2016 b), polyphenols from jujube (Najjaa et al., 2020) or olive stone (Jahanbakhshi & Ansari, 2020) powders.

Use of milk thistle (*Silybum marianum* L.) seeds in bakery is in line with main trends in application of novel natural additives for food production (Stabnikova et al., 2021). This novel raw material is still seems to be underestimated in food technology. There are limited data concerning milk thistle seeds chemical composition. According to Apostol et al. (2017) defatted seeds are a good source of protein (20.35%), lipids (11.69%), carbohydrates (38.16%) from which crude fiber (27.24%), and minerals. In the same context, numerous studies have demonstrated the hepatoprotective (Post-White et al., 2007) and anticarcinogenic (Tamayo and Diamond, 2007) effect of the milk thistle seeds. All these properties are due to silymarin, a flavonoid that acts as a protective agent in the human body (Valková et al., 2020).

There are only few studies that present the use of milk thistle seeds in food matrices, this being mostly used for extending the shelf life of the products (Menasra and Fahloul, 2019; Ochrem et al., 2021; Timakova, 2019). Considering this fact, the sponge cake enrichment with milk thistle seeds powder is a valuable and actual topic.

The aim of research was to evaluate the influence of wheat flour replacement with milk thistle seed powder on quality parameters of sponge cakes.

## Materials and methods

### Materials

In the sponge cake production eggs, sugar and wheat flour (premium quality) were used as main ingredients. Defatted by cold pressing milk thistle seed powder (2020 production year) was used to replace the wheat flour in the sponge cake recipe. More than 80% of milk thistle powder consisted of particles with a size of 40–60  $\mu\text{m}$ , however, it was sifted by the same sieve as wheat flour. The powder was added to the sponge cake composition by to substitute 5, 10, 15 and 20% of wheat flour. The physico-chemical indicators of the used raw materials are shown in Table 1.

Table 1

Physico-chemical indicators of the used raw materials

Ingredients	Content, %					Acidity, degrees
	Carbohydrates	Fibers	Proteins	Fat	Moisture	
Wheat flour (premium quality)	73.1	1.3	10.7	0.9	14.0	1.9
Whole eggs	0.7	-	12.7	11.5	74.0	-
Sugar	99.8	-	-	-	-	-
Milk thistle seed powder	10.8	27.0	21.2	7.0	7.0	3.1

### Preparation of sponge cake

The sponge cake was prepared in laboratory conditions using as main raw materials eggs, sugar and wheat flour, and as auxiliary materials salt and milk thistle powder (further as “MT”). The sponge cake formulations are shown in Table 2.

Table 2

Formulations of sponge cake samples

Ingredient, g	Control*	MT5	MT10	MT15	MT20
Wheat flour	100	95	90	85	80
Milk thistle powder	0	5	10	15	20
Egg melange	200	200	200	200	200
Sugar	100	100	100	100	100
Salt	1	1	1	1	1

\*Control, MT5, MT10, MT 15 and MT20: sponge cake prepared with 0%, 10%, 15%, and 20% replacement of wheat flour with milk thistle powder, respectively

The experimental sponge cake samples were prepared as described by Gisslen (2008). Firstly, egg melange, sugar and salt were combined and the bowl was set over a water bath and stirred until the mixture reached 43 °C. The warm mixture was then beaten using a KitchenAid (TILT-Head Stand Mixer) until a light and thick foam was obtained. The wheat flour was mixed with milk thistle seed powder, and then the mix was twice sifted. Then, the flour mix was gently folded into the egg foam until it was all blended in. For each sample 50 g of sponge cake batter was immediately panned (the cake pan with 8 cm in diameter and 4 cm in height) and baked at 180 °C for 20 min.

### Determination of baking loss

Baking loss were determined by weighing the batter before and after baking according to the formula:

$$BL\% = \frac{m_{batter} - m_{sponge}}{m_{batter}} \cdot 100\%$$

where BL is the bakink loss value, %;

$m_{batter}$  is the mass of the batter, g;

$m_{sponge}$  is the mass of the baked sponge cake.

### **Determination of moisture content**

Moisture contents of batters and sponge cakes were determined according to AOAC method 925.10 (AOAC, 2002).

### **Determination of water activity**

Water activity was determined according to (Hussain et al., 2021) using the rotronic water activity meter (INSTRUMART, USA).

### **Determination of porosity**

Porosity was determined as described by Rumeus and Turtoi (2013) using the Juravliov device.

### **Determination of volume of the sponge cake samples**

Volume of the sponge cake samples was determined according to (Lu et al., 2010), by the rapeseed displacement method.

### **Determination of crumb texture**

Crumb texture analysis was carried out after cooling the cakes for 8 h. Small pieces (3x3x3 cm) were cut from the middle of each cake and the crust was removed. The texture profile measurements were taken using a TA.HDplusC texture analyzer (Stable Micro Systems, United Kingdom) with a 36 mm diameter cylindrical probe, 50% compressing and a test speed of 1.0 mm s<sup>-1</sup>.

### **Determination of colour**

Colour evaluation of baked cakes was carried out using a Konica Minolta colorimeter CR-400 (Osaka, Japan). Values of  $L^*$ ,  $a^*$  and  $b^*$  colour coordinates were measured for each cake sample. To assess the impact of milk thistle addition, colour difference  $\Delta E$  and whiteness index ( $WI$ ) were calculated.

$$\Delta E = \sqrt{(L_{sample} - L_0)^2 + (a_{sample} - a_0)^2 + (b_{sample} - b_0)^2}$$
$$WI = 100 - \sqrt{(100 - L)^2 + a^2 + b^2}$$

where  $\Delta E$  is the total colour difference;

$L$  is the lightness of the sponge cake;

$a$  is the redness of the sponge cake;

$b$  is the yellowness of the sponge cake.

### **Determination of total phenol content and antioxidant activity**

The total phenol content was assessed using AOAC Folin Ciocalteu assay (Blainski et al., 2013). The antioxidant activity of researched sponge cake samples was evaluated using the 1,1-diphenyl-2-picryl-hydrazyl (DPPH) free radical (Sharma and Bhat, 2009). In both cases, a DR-5000 spectrophotometer (Hach Lange, Manchester, United Kingdom) was used.

### Sensory evaluation

In order to perform sensory analysis of sponge cakes twenty panelists (median age of 40 years) employed at the Department of Food and Nutrition, Technical University of Moldova were involved. In order to assess the effect of milk thistle on the sensory quality of sponge cake a 5-point hedonic scale ranging from 0 (“dislike extremely”) to 5 (“like extremely”) was used. Quality parameters as appearance, colour, taste, texture and flavour were analyzed using ISO 6658:2017.

### Statistical analysis

All experiments were performed in triplicates. The results are given as mean±standard deviation (SD). The data were statistically analyzed by XLSTAT software (2020 version) with ANOVA.

## Results and discussion

### Effect of milk thistle seed powder addition on sponge cake moisture content, baking loss and water activity

During baking, the sponge cake loses its mass, both moisture and dry matter. Moisture loss accounts for 95-96% of the total baking losses by evaporation from the outer layers of the batter. Dry substance loss consists 4-5% of the total losses and consists from the losses of volatile substances present in the batter (Mondal and Datta, 2008). To determine the impact of the milk thistle seed powder addition on the sponge cake baking losses, batter and cake moisture content was determined. The results are presented in Table 3.

**Table 3**  
Effect of milk thistle seed powder addition on sponge cake baking loss and water activity

Sample	Moisture content, %		Baking loss, %	a <sub>w</sub>
	Batter	Cake		
Control*	48.19±0.03 <sup>a</sup>	38.66±0.11 <sup>c</sup>	9.84±0.06 <sup>a</sup>	0.780±0.008 <sup>b</sup>
MT5	48.16±0.02 <sup>a</sup>	39.01±0.09 <sup>b</sup>	9.42±0.05 <sup>a</sup>	0.781±0.007 <sup>a</sup>
MT10	48.07±0.04 <sup>ab</sup>	39.15±0.12 <sup>b</sup>	9.01±0.02 <sup>b</sup>	0.781±0.011 <sup>a</sup>
MT15	48.04±0.06 <sup>b</sup>	39.86±0.16 <sup>a</sup>	8.88±0.06 <sup>b</sup>	0.780±0.004 <sup>b</sup>
MT20	47.98±0.03 <sup>b</sup>	41.62±0.08 <sup>a</sup>	7.11±0.04 <sup>c</sup>	0.772±0.008 <sup>c</sup>

\* MT5, MT10, MT 15 and MT20: sponge cake prepared with 0%, 10%, 15%, and 20% replacement of wheat flour with milk thistle powder, respectively

**Note:** Results are expressed as mean±standard deviation, insignificant ( $p > 0.05$ ), in each column different letters <sup>a-c</sup> mean significant differences ( $p < 0.001$ ).

At the batter preparation stage, there were no significant differences ( $p < 0.05$ ) in the moisture content, which varied between 47.98 – 48.19%. However, after baking, the moisture variations of the baked samples were higher 38.66– 41.62%. Thus, the addition of milk thistle seed powder in sponge cake formulations contributed to the decrease of baking loss up to 7.11% for the MT20 sample compared to 9.84% for the control sample. This can be explained

by the higher degree of hygroscopicity of the milk thistle seed powder, which is probably due to the high fiber content (27% compared to 1.3% for wheat flour). The same decreasing trends of baking loss were observed when supplementing sponge cake with *Euchema* algae (Huang and Yang, 2019), *Opuntia humifusa* (Kim et al. 2012), coffee silverskin (Ateş et al., 2019).

The water activity of the sponge cake samples did not change significantly ( $P < 0.05$ ), thus it can be mentioned that milk thistle seed powder does not increase the microbiological stability of the sponge cakes. Only in the case of MT20 the  $a_w$  reached the 0.772 value compared to 0.780–0.781 for other samples. A higher water activity (0.900–0.907) of sponge cake was mentioned by Lu et al. (2010) when substituting wheat flour with green tea in amounts of 10, 20 and 30%.

### Effect of milk thistle seed powder addition on sponge cake volume and porosity

Porosity plays an important role for the pastry products (Ghendov-Mosanu et al., 2020). Besides the fact that it contributes to a more attractive commercial appearance, porosity represents a means of facilitating digestibility, as it increases the surface area of saliva and gastric juice action on product components. From the physical point of view, the sponge cake porosity is defined as the ratio of crumb's air pockets volume and the crumb volume (Baeva et al., 2012). In the present research, a direct relationship was established between sponge cake porosity and volume (Pearson correlation coefficient  $r=0.98$ ), and an inversely proportional one between the amount of milk thistle seed powder and these two parameters (Figure 1). Thus, the volume of MT20 sponge cake decreased to 59.56 ml compared to 72.78 ml for the control sponge cake, while porosity decreased from 80.12% (control) to 75.34% (MT20).

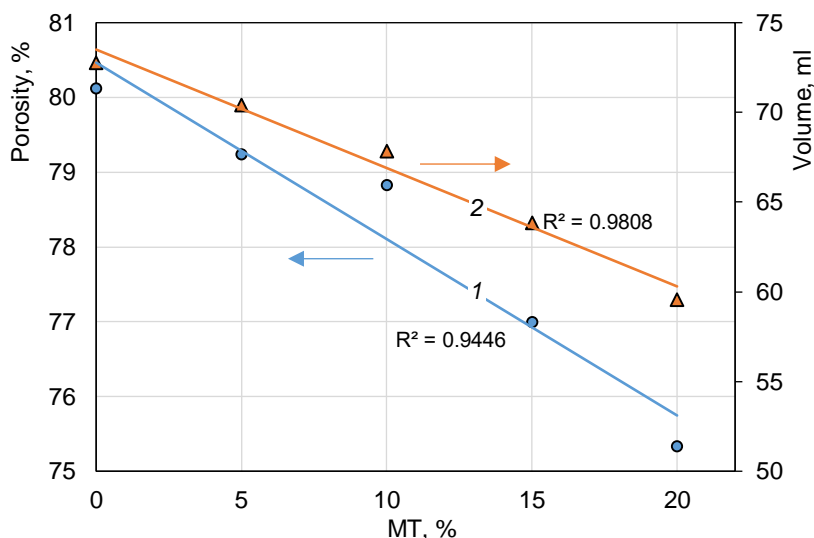


**Figure 1. Relationship between the concentration of milk thistle seed powder and porosity (P) and between the concentration of milk thistle seed powder and volume of the enriched sponge cake (V):**

**1 – Porosity; 2 – Volume**

Regression analysis shows that more than 90% decrease of volume or porosity in the enriched sponge cake is caused by milk thistle seed powder addition. Several studies have shown a decrease in the sponge cake volume when enriching formulations with plant materials (Hosseini Ghaboos et al., 2018; Lu et al., 2010; Maravić et al., 2022).

### **Effect of milk thistle seed powder addition on sponge cake colour**

#### **Crust colour**

The colour of the crust is one of the first quality indicators that are appreciated by the consumer, and which greatly influences its degree of acceptability. The impact of milk thistle seed powder addition on the colour of sponge cake crust and crumb is shown in Table 4. Significant differences between the values of the chromatic parameters of the control sample and those prepared with the addition of milk thistle seed powder were obtained.

The dark brown colour of the crust is mainly due to the Maillard reaction, and the replacement of wheat flour with milk thistle seed powder in sponge cake formulations seems to accelerate this reaction, thus obtaining a darker crust. This may be caused by the high content of amino acids in milk thistle seed powder, the presence of which may intensify the reaction of melanoid formation (Polovnikova et al., 2022). Similarly, numerous studies have shown an increase of total colour difference ( $\Delta E$ ) of sponge cake crust when substituting wheat flour with other plant materials (Jahanbakhshi and Ansari, 2020; Najjaa et al., 2020; Noor Aziah et al., 2011).

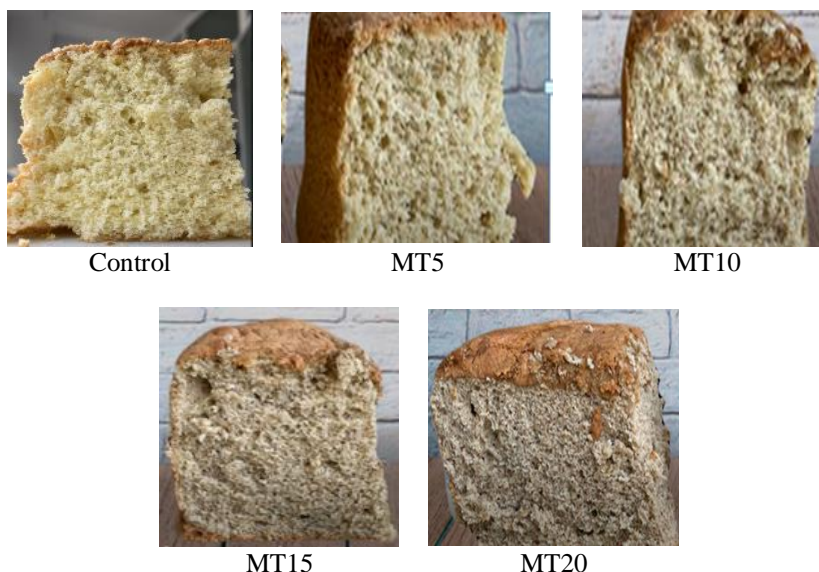


**Figure 2. Cross sections views of sponge cakes enriched with milk thistle seed powder**

Table 4

Effect of milk thistle seed powder addition on sponge cake colour

	Control	MT5*	MT10	MT15	MT20
Crust colour					
<i>L</i>	69.95±1.25 <sup>d</sup>	58.16±1.25 <sup>c</sup>	46.08±1.25 <sup>b</sup>	44.69±1.25 <sup>b</sup>	37.66±1.25 <sup>a</sup>
<i>a</i>	5.82±0.12 <sup>a</sup>	9.68±0.12 <sup>b</sup>	9.87±0.12 <sup>b</sup>	10.38±0.12 <sup>bc</sup>	13.84±0.12 <sup>c</sup>
<i>b</i>	46.99±1.14 <sup>c</sup>	43.42±1.14 <sup>bc</sup>	41.58±1.14 <sup>b</sup>	40.02±1.14 <sup>b</sup>	36.45±1.14 <sup>a</sup>
$\Delta E$	-	12.00±1.09 <sup>a</sup>	24.81±1.09 <sup>b</sup>	26.60±1.09 <sup>b</sup>	34.78±1.09 <sup>c</sup>
Crumb colour					
<i>L</i>	80.33±1.22 <sup>b</sup>	73.95±1.09 <sup>b</sup>	58.88±1.12 <sup>a</sup>	56.45±0.98 <sup>a</sup>	49.69±0.87 <sup>a</sup>
<i>a</i>	-2.90±0.14 <sup>a</sup>	-2.08±0.08 <sup>ab</sup>	0.30±0.01 <sup>ab</sup>	1.51±0.05 <sup>ab</sup>	2.13±0.10 <sup>b</sup>
<i>b</i>	24.75±0.014 <sup>c</sup>	20.27±0.65 <sup>bc</sup>	17.70±0.11 <sup>b</sup>	14.22±0.16 <sup>ab</sup>	10.49±0.20 <sup>a</sup>
$\Delta E$	-	7.84±0.11 <sup>a</sup>	22,80±0,58 <sup>b</sup>	26,47±0,26 <sup>b</sup>	34.17±0.78 <sup>c</sup>
<i>WI</i>	68,25±1,38 <sup>b</sup>	66.93±1.43 <sup>b</sup>	55.23±1.21 <sup>ab</sup>	54.16±1.27 <sup>ab</sup>	48.56±1.10 <sup>a</sup>

\*MT5, MT10, MT 15 and MT20: sponge cake prepared with 0%, 10%, 15%, and 20% replacement of wheat flour with milk thistle powder, respectively

**Note:** Results are expressed as mean±standard deviation, insignificant ( $p > 0.05$ ), in each line different letters <sup>a-d</sup> mean significant differences ( $p < 0.001$ ).

### Crumb colour

Significant differences ( $p < 0.05$ ) were observed among the crumb colour parameters of the sponge cakes variants. The values of luminosity ( $L^*$ ) and yellowness ( $b^*$ ) parameters of the control sponge cake were higher compared with the MT sponge cakes, while the redness ( $a^*$ ) showed a increasing tendency with the MT upward trend. This behaviors of  $L^*$ ,  $a^*$  and  $b^*$  parameters indicate that a darker, redder, and less yellow crumb was obtained because of wheat flour substitution with MT. The decrease of  $L^*$  and  $b^*$  values can be explained by the fact that some compounds of MT are water-soluble, respectively assigning a different colour to the batter mass and the baked product. Similarly, Menasra and Fahloul (2019) mentioned that biscuit became darker with milk thistle powder addition. The ability of milk thistle powder to change the chromatic values of pastry products was also demonstrated by Bortlíková et al. (2019) on its application in functional biscuits formulation. The effect of different ingredients on sponge cake colour was also reported by Lu et al. (2010), who found that green tea powder addition led to an increase in sponge cake lightness and yellowness, and on contrary, to a decrease of  $a^*$  values. It was shown that addition of black garlic powder, Jujube (*Zizyphus lotus* L.), and olive stone powder to sponge cake can lead to a decrease in  $L^*$  and  $b^*$  values but an upward in  $a^*$  values (Jahanbakhshi and Ansari, 2020; J.-S. Lee et al., 2009; Najjaa et al., 2020).

During the research, an inversely proportional relationship was established between the total colour difference  $\Delta E$  and the whiteness index *WI*. With the increase in the MT level in the sponge cake formulation,  $\Delta E$  showed a major upward to 34.17 in the case of the MT20 sample, while *WI* diminished from the value of 68.25 for the control sample to 48.56 for the MT20.

According to Maji & Dingliana, (2018) the just noticeable difference (JND) of colour between two objects ( $\Delta E_{00}^*$ ) equals to 1. Taking into account that the lowest value for  $\Delta E$  was obtained for the MT5 sponge cake ( $\Delta E = 7,84$ ), it can be concluded that all prepared sponge cake variants could be verifiably distinguished according to colour by eyes only.

### Effect of milk thistle seed powder addition on sponge cake texture parameters

Sponge cakes are characterized as having a light, airy texture. In this research the texture of sponge cake samples was analysed in terms of hardness, springiness, resilience, cohesiveness and chewiness (Table 5).

**Table 5**

**Effect of milk thistle seed powder on sponge cake texture parameters**

	Control	MT5	MT10	MT15	MT20
Hardness, g	115.24±4.21 <sup>a</sup>	131.88±5.18 <sup>ab</sup>	134.87±6.01 <sup>b</sup>	158.96±4.34 <sup>c</sup>	177.96±5.26 <sup>c</sup>
Springiness, mm	0.99±0.02 <sup>a</sup>	0.96±0.04 <sup>a</sup>	0.96±0.02 <sup>a</sup>	0.90±0.02 <sup>b</sup>	0.84±0.01 <sup>b</sup>
Chewiness, g·mm	66.57±3.12 <sup>a</sup>	72.27±4.08 <sup>ab</sup>	75.15±4.34 <sup>b</sup>	85.74±6.53 <sup>bc</sup>	96.99±4.22 <sup>c</sup>
Resilience	0.35±0.01 <sup>a</sup>	0.33±0.02 <sup>a</sup>	0.29±0.02 <sup>ab</sup>	0.27±0.01 <sup>b</sup>	0.28±0.01 <sup>ab</sup>
Cohesiveness	0.58±0.02 <sup>b</sup>	0.55±0.01 <sup>a</sup>	0.56±0.01 <sup>b</sup>	0.54±0.03 <sup>a</sup>	0.55±0.01 <sup>a</sup>

Control, MT5, MT10, MT 15 and MT20: prepared with 0, 10, 15 and 20% replacement of wheat flour with milk thistle powder, respectively

**Note:** Results are expressed as mean±standard deviation, insignificant ( $p > 0.05$ ), in each line different letters <sup>a-c</sup> mean significant differences ( $p < 0.001$ ).

Hardness is used to describe the force exerted on the surface of the product when it is deformed under the action of the teeth in the mouth. The softer the product is, the lower hardness it has (Lu et al., 2010). The obtained data show that with the increase in the MT level, the hardness of the sponge also increases from the initial values of 115.24 to 177.96 g. This is probably caused by the fact that the milk thistle fibers absorbed and bounded the water that during baking should have participated in the formation of gluten from the wheat flour. Gluten, in turn, is able to keep CO<sub>2</sub> and air bubbles trapped in the batter structure that during baking increase their volume, thus increasing the porosity and volume of the baked sponge cake (Rodríguez-García et al., 2014). A similar tendency was also noted for the chewiness, which increased with increasing amounts of MT. Springiness and resilience, as they have some similarities, showed a descending trend with the increase of MT concentration. Sponge cake variants had the lowest springiness and resilience of 0.84 mm and 0.28 respectively, when the wheat flour was substituted with MT in a 20% proportion. Likewise, the cohesiveness of the sponge cakes decreased with the increase in the proportion of the MT. Sponge cakes had the lowest cohesiveness values of 0.55 when the proportion of the MT was 20%. However, differences in samples' cohesiveness were not statistically significant ( $p > 0.05$ ). Thus, for the use of the MT sponge cakes as layers for cakes, the revision of the formulation is required, especially regarding the amount of liquid for impregnation in order to obtain a cake with a low hardness and chewiness. Earlier, Lu et al. (2010) have reported the hardness and chewiness to increase, and the springiness and resilience to decrease with the addition of green tea powder (Lu et al., 2010). Contrastingly, Wang et al. (2020) obtained a gradual decline of hardness with the increase of Japonica rice flour proportion in sponge cake formulation, while resilience and springiness increased (Wang et al., 2020).

### Total phenol content and antioxidant activity

The aim of MT addition is actually to enhance the biological value of sponge cake, which is especially conferred by the antioxidants present in MT (Vaknin et al., 2008). According to Yaldiz (2017), milk thistle seeds are rich in tannins and flavonolignans that exhibit a high antioxidant activity (Yaldiz, 2017). In this context, the total polyphenols content and the antioxidant activity of sponge cake variants were determined (Table 6).

**Table 6**  
Total phenol content and antioxidant activity of sponge cakes

Sample	Total Polyphenol Content, mg GAE/100 g	Antioxidant Activity, %
Control	63.93±1.23 <sup>a</sup>	7.86±0.34 <sup>a</sup>
MT5	75.88±1.56 <sup>ab</sup>	14.62±0.27 <sup>ab</sup>
MT10	80.76±2.13 <sup>b</sup>	19.37±0.76 <sup>b</sup>
MT15	90.05±1.97 <sup>b</sup>	23.84±0.47 <sup>c</sup>
MT20	121.24±3.21 <sup>c</sup>	44.70±0.64 <sup>d</sup>

Control, MT5, MT10, MT 15 and MT20: prepared with 0%, 10%, 15%, and 20% replacement of wheat flour with milk thistle powder, respectively

**Note:** Results are expressed as mean±standard deviation, insignificant ( $p > 0.05$ ), in each column different letters <sup>a-d</sup> mean significant differences ( $p < 0.001$ ).

The data show that the MT sponge cake have significantly ( $P > 0.05$ ) higher amount of polyphenols (75.88–121.24 mg GAE/100 g) than the control variant (63.93 mg GAE/100 g). This can be explained by the high content of polyphenols in MT (4.38 mg/g) in comparison with wheat flour (0.33 mg GAE/g). Javeed et al. (2022) reported that milk thistle seed have a polyphenol content of 1.70 mg GAE/g (Javeed et al., 2022). An increase in the antioxidant activity was observed with the increase of MT concentration in sponge cake formulation. The results are in accordance with those mentioned by Nowak et al. (2021) who studied the influence of solvent on the total phenols content and antioxidant activity of different milk thistle parts. In the study was shown that 70% ethanol is the best solvent in order to obtain the highest values for the studied indicators (Nowak et al., 2021). In our study, the same solvent was used.

### Sponge cake sensory scores

The sensory attributes of sponge cake in terms of appearance, crust and crumb colour, crumb texture, taste and flavor were evaluated after 12 hours from preparation. The results of the sensory analysis of sponge cake variants with different MT concentrations are shown in the Table 7.

As noticed, wheat flour substitution by MT in sponge cake formulation did not significantly ( $P < 0.05$ ) influence the crust colour, the lowest liking score being registered for MT20 (4.50). Regarding the crumb colour, the evaluation score manifested a decline as the MT level increased. A similar tendency was noticed for the texture of sponge cake. The taste and flavor of sponge cake counterparts had a significantly lower ( $P > 0.05$ ) acceptability score in the case of MT20. According to the results of the organoleptic analysis, it can be concluded that among the most successful samples were those with a concentration of 5% and 10% MT,

because MT faded the specific smell of egg and the overly sweet taste of sponge cake. In the end, they were appreciated as the most balanced samples. MT15 and MT20 were scored with a lower overall acceptability for the following reasons:

- (1) The samples do not have pleasant crumb colour;
- (2) The samples with 15% and 20% MT have too dominant taste, as well as the aroma of MT is too dominant”;
- (3) In the sample with 20% MT some sandy powder particles are felt.

The control sponge cake reached the highest overall acceptability score (4.94), while the MT20 sponge cake had the lowest value (4.16).

**Table 7**

**Sponge cake sensory evaluation**

	<b>Taste and flavour</b>	<b>Crust colour</b>	<b>Crumb colour</b>	<b>Appearance</b>	<b>Texture</b>	<b>Overall acceptability</b>
Control	4.82±0.04 <sup>b</sup>	5.00 ±0.00 <sup>a</sup>	5.00±0.00 <sup>a</sup>	5.00±0.00 <sup>a</sup>	4.90±0.01 <sup>ab</sup>	4.94±0.04 <sup>ab</sup>
MT5	4.84±0.03 <sup>a</sup>	4.82±0.02 <sup>a</sup>	4.85±0.04 <sup>a</sup>	4.76±0.02 <sup>b</sup>	4.84±0.05 <sup>a</sup>	4.82±0.02 <sup>a</sup>
MT10	4.64±0.04 <sup>b</sup>	4.71±0.03 <sup>a</sup>	4.70±0.05 <sup>a</sup>	4.58±0.05 <sup>b</sup>	4.62±0.03 <sup>b</sup>	4.65±0.05 <sup>b</sup>
MT15	4.43±0.02 <sup>b</sup>	4.62±0.06 <sup>a</sup>	4.42±0.05 <sup>b</sup>	4.50±0.03 <sup>ab</sup>	4.45±0.02 <sup>b</sup>	4.48±0.06 <sup>ab</sup>
MT20	4.13±0.04 <sup>c</sup>	4.50±0.05 <sup>a</sup>	3.82±0.04 <sup>d</sup>	4.26±0.01 <sup>b</sup>	4.10±0.05 <sup>c</sup>	4.16±0.02 <sup>c</sup>

Control, MT5, MT10, MT 15 and MT20: prepared with 0%, 10%, 15%, and 20% replacement of wheat flour with milk thistle powder, respectively

**Note:** Results are expressed as mean±standard deviation, insignificant ( $p > 0.05$ ), in each column different letters <sup>a-d</sup> mean significant differences ( $p < 0.001$ ).

**Conclusions**

1. The replacement of wheat flour with milk thistle powder in sponge cake formulation reduced the baking losses, and enhanced moisture content.
2. The volume and porosity of sponge cakes decreased significantly with the increasing milk thistle powder amounts. The volume decreased from 72.78 ml for the control sponge cake to 59.56 ml when wheat flour was replaced by 20% milk thistle powder. Porosity decreased from 80.12% (control) to 75.34% for the sponge cake with 20 milk thistle powder.
3. The colour of sponge cake crumbs with milk thistle seed powder became darker, less yellow ( $L^*$  and  $b^*$  values decreased) and redder ( $a^*$  values increased). Simultaneously, the whiteness index of sponge cake crumb showed a downward trend with the increase of milk thistle seeds powder addition.
4. The hardness and chewiness of sponge cakes increased with the increasing milk thistle seed powder amount, being in the range of 115.24–177.96 g and 66.57–96.9 g·mm, respectively. A reverse trend was exhibited by springiness, resilience and cohesiveness of sponge cakes.
5. The addition of milk thistle seed powder to the sponge cake formulation led to increase in the polyphenol content and antioxidant activity of cakes.
6. The results of sensory analysis pointed out that a partial replacement of 5 and 10% wheat flour with milk thistle seed powder was the most acceptable.

### Acknowledgments

The research was funded by State Project 20.80009.5107.09 “Improving of food quality and safety through biotechnology and food engineering”, running at Technical University of Moldova.

### References

- AOAC (2002), *Official methods of analysis (3rd ed.)*.
- Apostol L., Iorga C. S., Mo C., Must G. (2017), Nutrient composition of partially deffated milk thistle seeds, *Scientific Bulletin. Series F. Biotechnologies*, 21, pp. 165–169.
- Ateş G., Elmacı Y. (2019), Physical, chemical and sensory characteristics of fiber-enriched cakes prepared with coffee silverskin as wheat flour substitution, *Food Measure*, 13, pp. 755–763, <https://doi.org/10.1007/s11694-018-9988-9>
- Baeva M., Milkova-Tomova I., Angelova S. (2012), Preparation of sponge cakes with flour of topinambur tubers, *Modern Technologies in the Food Industry–2012: Proceedings of the International Conference*, 1, pp. 212–217
- Blainski A., Lopes G., Mello J. (2013), Application and analysis of the folin ciocalteu method for the determination of the total phenolic content from *Limonium Brasiliense L.*, *Molecules*, 18(6), pp. 6852–6865, <https://doi.org/10.3390/molecules18066852>
- Bortlíková V., Kolarič L., Šimko P. (2019), Application of milk thistle (*Silybum marianum*) in functional biscuits formulation, *Acta Chimica Slovaca*, 12(2), pp. 192–199, <https://doi.org/10.2478/acs-2019-0027>
- Ghendov-Mosanu A., Cristea E., Patras A., Sturza R., Padureanu S., Deseatnicova O., Turculeț N., Boestean O., Niculaua M. (2020), Potential application of *Hippophae Rhamnoides* in wheat bread production, *Molecules*, 25(6), pp. 1272, <https://doi.org/10.3390/molecules25061272>
- Gisslen W. (2009), Professional baking, p. 756
- Hashem K. M., He F. J., Alderton S. A., MacGregor G. A. (2018), Cross-sectional survey of the amount of sugar and energy in cakes and biscuits on sale in the UK for the evaluation of the sugar-reduction programme, *BMJ Open*, 8(7), e019075, <https://doi.org/10.1136/bmjopen-2017-019075>
- Hosseini Ghaboos S. H., Seyedain Ardabili S. M., Kashaninejad M. (2018), Physico-chemical, textural and sensory evaluation of sponge cake, *International Food Research Journal*, 25(2), pp. 854–860
- Huang M. & Yang, H. (2019), Eucheuma powder as a partial flour replacement and its effect on the properties of sponge cake, *LWT – Food Science and Technology*, 110, pp. 262–268, <https://doi.org/10.1016/j.lwt.2019.04.087>
- Hui Y. H. (2007), *Handbook of food products manufacturing*, Wiley-Interscience, p. 1221
- Hussain M., Saeed F., Niaz B., Afzaal M., Ikram A., Hussain S., Mohamed A. A., Alamri M. S., Anjum F. M. (2021), Biochemical and nutritional profile of maize bran-enriched flour in relation to its end-use quality, *Food Science & Nutrition*, 9(6), pp. 3336–3345, <https://doi.org/10.1002/fsn3.2323>
- ISO 6658:2017. (2017), Sensory Analysis. Methodology. General Guidance; *International Organization for Standardization*: Geneva, Switzerland, 2017.
- Jahanbakhshi R., Ansari S. (2020), Physicochemical properties of sponge cake fortified by olive stone powder, *Journal of Food Quality*, 2020, pp. 1–11, <https://doi.org/10.1155/2020/1493638>
- Javeed A., Ahmed M., Sajid A. R., Sikandar A., Aslam M., Hassan T., Samiullah Nazir Z., Ji M., Li C. (2022), Comparative assessment of phytoconstituents, antioxidant activity and

- chemical analysis of different parts of milk thistle *Silybum marianum* L., *Molecules*, 27(9), pp. 2641, <https://doi.org/10.3390/molecules27092641>
- Kim J.H., Lee H.J., Lee H.S., Lim E.J., Imm J.Y., Suh H.J. (2012), Physical and sensory characteristics of fibre-enriched sponge cakes made with *Opuntia humifusa*, *LWT – Food Science and Technology*, 47(2), pp. 478-484, <https://doi.org/10.1016/j.lwt.2012.02.011>
- Lee J. S., Kim H. S., Lee Y. J., Jung I. C., Bae J. H., Lee J. S. (2007), Quality characteristics of sponge cakes containing various levels of grifola frondosa powder, *Korean Journal of Food Science and Technology*, 39(4), pp. 400–405.
- Lee J.-S., Seong Y.-B., Jeong B.-Y., Yoon S.-J., Lee I.-S., Jeong Y.-H. (2009), Quality characteristics of sponge cake with black garlic powder added, *Journal of the Korean Society of Food Science and Nutrition*, 38(9), pp. 1222–1228, <https://doi.org/10.3746/jkfn.2009.38.9.1222>
- Lu T.-M., Lee C.-C., Mau J.-L., Lin S.-D. (2010), Quality and antioxidant property of green tea sponge cake, *Food Chemistry*, 119(3), pp. 1090–1095, <https://doi.org/10.1016/j.foodchem.2009.08.015>
- Maji S. & Dingliana J. (2022), Perceptually optimized color selection for visualization, arXiv:2205.14472 [cs.CV], <https://doi.org/10.48550/ARXIV.2205.14472>
- Maravić N., Škrobot D., Dapčević-Hadnadev T., Pajin B., Tomić J., Hadnadev M. (2022), Effect of sourdough and whey protein addition on the technological and nutritive characteristics of sponge cake, *Foods*, 11(14), pp. 1992, <https://doi.org/10.3390/foods11141992>
- Menasra A. & Fahloul D. (2019), Quality characteristics of biscuit prepared from wheat and milk thistle seeds (*Silybum Marianum* (L) Gaertn) flour, *Carpathian Journal of Food Science & Technology*, 11(4), pp. 5-19.
- Mondal A. & Datta A. K. (2008), Bread baking – A review, *Journal of Food Engineering*, 86(4), pp. 465–474, <https://doi.org/10.1016/j.jfoodeng.2007.11.014>
- Mustafa R., He Y., Shim Y. Y., Reaney M. J. T. (2018), Aquafaba, wastewater from chickpea canning, functions as an egg replacer in sponge cake, *International Journal of Food Science & Technology*, 53(10), pp. 2247–2255, <https://doi.org/10.1111/ijfs.13813>
- Najjaa H., Ben Arfa A., Elfalleh W., Zouari N., Neffati M. (2020), Jujube (*Zizyphus lotus* L.): Benefits and its effects on functional and sensory properties of sponge cake, *PLOS ONE*, 15(2), e0227996, <https://doi.org/10.1371/journal.pone.0227996>
- Noor Aziah A. A., Lee Min W., Bhat R. (2011), Nutritional and sensory quality evaluation of sponge cake prepared by incorporation of high dietary fiber containing mango (*Mangifera indica* var. Chokanan) pulp and peel flours, *International Journal of Food Sciences and Nutrition*, 62(6), pp. 559–567, <https://doi.org/10.3109/09637486.2011.562883>
- Nowak A., Florkowska K., Zielonka-Brzezicka J., Duchnik W., Muzykiewicz A., Klimowicz A. (2021), The effects of extraction techniques on the antioxidant potential of extracts of different parts of milk thistle (*Silybum marianum* L.), *Acta Scientiarum Polonorum Technologia Alimentaria*, 20(1), pp. 37–46, <https://doi.org/10.17306/J.AFS.2021.0817>
- Ochrem A., Kułaj D., Pokorska J., Żychlińska-Buczek J., Zapletal P., Draj-Kozak E., Łuszczek-Trojnar E. (2021), Effect of milk thistle addition (*Silybum Marianum* L.) on marinated herring (*Clupea Harengus* L.) meat, *British Food Journal*, 123(7), pp. 2537–2554, <https://doi.org/10.1108/BFJ-09-2020-0829>
- Park Y. R., Han I. J., Kim M. Y., Choi S. H., Shin D. W., Chun S. S. (2008), Quality characteristics of sponge cake prepared with red ginseng marc powder, *Korean Journal of Food and Cookery Science*, 24(2), pp. 236–242
- Polovnikova D., Evlash V., Aksonova O., Gubsky, S. (2022), Muffin enriched with bioactive compounds from milk thistle by-product: baking and physico-chemical properties and sensory characteristics, *Biology and Life Sciences Forum*, 18(1), pp. 49, <https://doi.org/10.3390/Foods2022-12930>

- Post-White J., Ladas E. J., Kelly K. M. (2007), Advances in the use of milk thistle *Silybum Marianum*, *Integrative Cancer Therapies*, 6(2), pp. 104–109, <https://doi.org/10.1177/1534735407301632>
- Prokopov T., Goranova Z., Baeva M., Slavov A., Galanakis, C. M. (2015), Effects of powder from white cabbage outer leaves on sponge cake quality, *International Agrophysics*, 29(4), pp. 493–500, <https://doi.org/10.1515/intag-2015-0055>
- Rodríguez-García J., Sahi S. S., Hernando I. (2014), Optimizing mixing during the sponge cake manufacturing process, *Cereal Foods World*, 59(6), pp. 287–292, <https://doi.org/10.1094/CFW-59-6-0287>
- Rumeus I. & Turtoi M. (2013), Influence of sourdough use on rope spoilage of wheat bread, *Journal of Agroalimentary Processes and Technologies*, 19(1), pp. 94–98
- Salehi et al (2016a), Potential of sponge cake making using infrared-hot air dried carrot, *Journal of Texture Studies*, 47(1), pp. 34–39, <https://doi.org/10.1111/jtxs.12165>
- Salehi et al. (2016b), Improvement of quality attributes of sponge cake using infrared dried button mushroom, *Journal of Food Science and Technology*, 53(3), pp. 1418–1423, <https://doi.org/10.1007/s13197-015-2165-9>
- Sharma O. P. Bhat, T. K. (2009), DPPH antioxidant assay revisited. *Food Chemistry*, 113(4), pp. 1202–1205, <https://doi.org/10.1016/j.foodchem.2008.08.008>
- Stabnikova O., Marinin A., Stabnikov V. (2021), Main trends in application of novel natural additives for food production, *Ukrainian Food Journal*, 10(3), pp. 524–551, <https://doi.org/10.24263/2304-974X-2021-10-3-8>
- Stanhope K. L. (2016), Sugar consumption, metabolic disease and obesity: The state of the controversy, *Critical Reviews in Clinical Laboratory Sciences*, 53(1), pp. 52–67, <https://doi.org/10.3109/10408363.2015.1084990>
- Tamayo C. & Diamond S. (2007), Review of clinical trials evaluating safety and efficacy of milk thistle (*Silybum marianum* [L.] Gaertn.), *Integrative Cancer Therapies*, 6(2), pp. 146–157, <https://doi.org/10.1177/1534735407301942>
- Timakova R. T. (2019), Formation of consumer value of cottage cheese prolonged shelf life when using flour from milk Thistle seeds spotted, *Proceedings of the Voronezh State University of Engineering Technologies*, 81(3), pp. 43–49, <https://doi.org/10.20914/2310-1202-2019-3-43-49>
- Vaknin Y., Hadas R., Schafferman D., Murkhovskiy L., Bashan N. (2008), The potential of milk thistle (*Silybum marianum* L.), an Israeli native, as a source of edible sprouts rich in antioxidants, *International Journal of Food Sciences and Nutrition*, 59(4), pp. 339–346, <https://doi.org/10.1080/09637480701554095>
- Valková V., Ďuranová H., Bilčíková J., Habán M. (2020), Milk thistle (*Silybum Marianum*): a valuable medicinal plant with several therapeutic purposes, *Journal of Microbiology, Biotechnology and Food Sciences*, 9(4), pp. 836–843, <https://doi.org/10.15414/jmbfs.2020.9.4.836-843>
- Wang L., Zhao S., Liu Y., Xiong S. (2020), Quality characteristics and evaluation for sponge cakes made of rice flour, *Journal of Food Processing and Preservation*, 44(7), e14505, <https://doi.org/10.1111/jfpp.14505>
- Yaldiz G. (2017), Effects of potassium sulfate [K<sub>2</sub>SO<sub>4</sub>] on the element contents, polyphenol content, antioxidant and antimicrobial activities of milk thistle [*Silybum Marianum*], *Pharmacognosy Magazine*, 13(49), pp. 102–107, <https://doi.org/10.4103/0973-1296.197641>.

## Application of enzymes for press oil production from pumpkin seeds

Hanna Vovk<sup>1</sup>, Kwankao Karnpakdee<sup>2</sup>, Olga Golubets<sup>3</sup>,  
Iryna Levchuk<sup>3</sup>, Roland Ludwig<sup>2</sup>, Tamara Nosenko<sup>1</sup>

1 – National University of Food Technologies, Kyiv, Ukraine;

2 – University of Natural Resources and Life Sciences (BOKU), Vienna, Austria;

3 – State Enterprise "Ukrmetrteststandard", Kyiv, Ukraine

---

### Abstract

---

#### Keywords:

Enzymatic  
pretreatment  
Press oil  
Pumpkin seeds  
Protease  
Cellulase  
Pectinase

---

#### Article history:

Received 29.10.2022

Received in revised  
form 16.01.2023

Accepted 31.03.2023

---

#### Corresponding author:

Tamara Nosenko  
E-mail:  
tamara\_nosenko@  
ukr.net

---

DOI: 10.24263/2304-  
974X-2023-12-1-4

---

**Introduction.** The aim of this research was to study the effect of pretreatment of pumpkin seed with proteolytic, cellulolytic, and pectolytic enzymes on pressed oil production.

**Materials and methods.** Enzymes, papain, pectinase, cellulase, pepsin, and cellulolytic enzyme mixture Viscozyme L were used in the study. The number of disrupted cells was determined by the amount of easily extractable pumpkin seed oil as result of immediate shaking. To study the cell microstructure, ultramicrotome slices of pumpkin seeds were treated with individual enzymes and enzyme mixtures. The antioxidant activity of the pumpkin seed oil was determined using (DPPH) 2,2-diphenyl-1-picrylhydrazyl radical radical scavenging activity.

**Results and discussion.** The evaluation of cell integrity by immediate hexane extraction (shaking method) showed that all samples treated with different enzymes had a higher oil yield, ranging from 33.2 to 34.1% of seed weight, than the control samples (32.1%). The number of disrupted cells in enzyme treated samples was also higher than the control (64.4%), ranging from 67.6 to 69.5%. The highest amount of damaged cells, 71.0 and 71.1%, was found in the samples treated with mixtures (a) pepsin, Viscozyme L, pectinase and (b) pepsin, cellulase, with the pepsin+ViscozymeL+pectinase mixture was by 7.0% higher than that of the control sample. The enzymatic pretreatment did not significantly affect the free fatty acid content, peroxide value, fatty acid, and phytosterols composition. The antioxidant activity expressed as DPPH radical scavenging capacity of the pressed oil obtained from enzymatically pretreated pumpkin seeds was by 2.7% higher than of control oil.

**Conclusion.** Pretreatment of pumpkin seeds with a mixture of cellulolytic and proteolytic enzymes allowed increasing the yield of oil with high quality characteristics.

## Introduction

Vegetable oils are the source of such essential substances for humans as polyunsaturated fatty acids, fat-soluble vitamins, phytosterols, and others. It is important to include in diet various vegetable oils with different fatty acid compositions and content of valuable micronutrients. Among vegetable oils, pumpkin seed oil is especially valuable due to its biologically active substances, which are useful in the treatment and prevention of many diseases (Dotto et al., 2020; Shaban et al., 2017). In particular, it contains natural antioxidants,  $\omega$ -6 and  $\omega$ -3 acids represented by linoleic and linolenic fatty acids, respectively, as well as squalene, which is a precursor for the synthesis of sterols, steroid hormones, and vitamin D (Dotto et al., 2020; Nosenko et al., 2019a). Carotenoids, tocopherols, and phenolic compounds, as well as oleic acid, are contained in relatively high amounts in pumpkin seed oil (Dotto et al., 2020; Procida et al., 2013; Shaban et al., 2017). Tocopherols of pumpkin seed oil have antihyperglycemic properties (Shaban et al., 2017; Sharma et al., 2013). Phytosterols contained in pumpkin seed oil prevent the development of cardiovascular disease due to the reduction of the level of the low-density lipoprotein cholesterol in the blood. At the same time, phytosterols are able to reduce the risk of some kinds of cancer (Dotto et al., 2020; Shaban et al., 2017).

Nowadays, two methods are used to obtain oil from oil-containing seeds: pressing and solvent extraction. Solvent extraction is considered more efficient allowing the release of almost all oil from oil-containing material. However, in addition to explosive and flammable solvents, numerous studies have found them dangerous to human health, as regular inhalation of its vapors can lead to diseases, such as peripheral neuropathy and sensory loss (Herskowitz et al., 1971; Kutlu et al., 2009). The release of organic solvent vapors into the environment is also negative due to its reaction with air pollutants and ozone formation (Montero-Montoya et al., 2018). Another disadvantage of solvent extraction is that obtained oil has to be refined, which causes the loss of most of its biologically valuable compounds. On the other hand, the pressing, especially cold pressing, is more environmentally friendly, as well as allows to the preservation of valuable natural components in the oil (Yakymenko et al., 2022). However, the pressing never removes the oil from the oil material completely and a significant oil content remains in the pressed cake.

Therefore, the development of pretreatment processes capable of increasing the oil yield during pressing and keeping the oil quality is very important. A promising method is the use of enzymes for disrupting plant cell walls. This potentially increases oil yield, but can also increase the nutritional value and antioxidant activity through the enhanced extraction of oil biologically active substances, such as phytosterols, tocopherols, and phenolic compounds (Kaseke et al., 2021; Latif et al., 2007).

The aim of this work was to study the influence of enzymatic pretreatment of pumpkin seeds on the cell integrity, pressed oil yield as well as its composition.

## Materials and methods

### Materials

Hull-less pumpkin seeds (*Cucurbita pepo*) with an oil content of 49.05% (determined according to ISO, 2009) were supplied by a farm at Doberndorf, Horn, Lower Austria. For pretreatment of pumpkin seeds pepsin, papain, pectinase, cellulase, and Viscozyme L were purchased from Sigma-Aldrich (St. Louis, MO, USA). Pepsin (P7000) produced from

porcine gastric mucosa was purchased from Carl Roth (Karlsruhe, Germany). The declared activity at pH 2.0 and 37 °C is 800–2500 U/mg of solids, where 1 U will produce a change in A 280 of 0.001 per min measured as soluble in trichloroacetic acid products using hemoglobin as substrate. Papain (P3375) was produced from papaya latex crude powder. The declared activity at pH 6.2 (optimum) and 25 °C is 2.1 U/mg of solids, where 1 U will hydrolyze 1 μmol/min of N- $\alpha$ -benzoyl-L-arginine ethyl ester per minute. Cellulase (C2605) is produced by *Aspergillus sp.* The declared activity at pH 4.5 and 50 °C is 1000 CU/g, where 1 CU (cellulase unit) corresponds to the amount of enzyme which produces 1 μmol/min of glucose from carboxymethylcellulose. Pectinase (P2611) is produced from *Aspergillus aculeatus*. The declared activity at pH 3.5 (optimum) and 20 °C is 3800 polygalacturonic units/ml of suspension. The standard activity is determined by measuring the viscosity reduction of a pectic acid solution. Viscozyme L (V2010) is produced by *Aspergillus sp.* (a multi-enzyme mixture containing cellulases,  $\beta$ -glucanase, and hemicellulases like arabinase and xylanase). The declared activity at pH 5.0 and 50 °C is 100 fungal  $\beta$ -glucanase units/g.

### **Enzymatic pretreatment**

To study the enzymatic pretreatment effect on the pumpkin seed cell structure, the seeds were ground using a laboratory mill to a particle size  $\leq 5.0$  mm. Ten g of ground seeds were placed in a 250-ml Erlenmeyer flask, suspended in 10 ml of 100 mM phosphate buffer, pH 5.5, and treated with the enzyme (0.6% w/w). The obtained suspensions were incubated in a water bath for 2.0 h at 48–52 °C with a manual stirring every 20 min. At the end of the incubation, the enzymes were inactivated at 80 °C during 15 min. The control samples were treated under the same conditions as the experimental ones, but without application of enzymes. The initial cell integrity was examined in ground seeds before the treatment.

In some experiments, elevated enzyme amounts (1.8, 3.0 and 6.0% w/w) such as pepsin+Viscozyme L+pectinase, pepsin+cellulase+pectinase, papain+Viscozyme L+pectinase, or papain+cellulase+pectinase in a ratio of 1:1:1 were used under the conditions described above. Each variation of the treatment was performed in triplicate. After incubation and enzyme inactivation, all experimental and control samples were transferred from the flasks into evaporating porcelain cups and dried first in an oven at 100–110 °C for 3.0–3.5 h, and then overnight at room temperature, until moisture content was reached 0–2.0%. The dried material was re-ground in a laboratory mill and used to determine the number of disrupted cells.

### **Evaluation of disrupted cells by the method of immediate oil extraction**

This method is used to determine the amount of easily extractable pumpkin seed oil and can be used to determine the fraction of disrupted plant cells. Therefore, 10 g of the re-ground samples (pretreated or reference samples) was placed in a 250-ml Erlenmeyer flask, mixed with 100 ml of n-hexane, and the contents of the flask were shaken for exactly 3 s. Then the flask was left for exactly 10 s and afterward, the obtained extract was immediately filtered into a weighed Erlenmeyer flask. The filter was washed with several portions of n-hexane and all portions were added to the weighed flask with the obtained extract. The hexane was distilled from the extracts on a rotary evaporator at a rotation speed of 50–54 rpm and at 45 °C. The obtained oil was dried in an oven at 100–105 °C for 1.0 h and then was left overnight under a fume hood for finally solvent removal. Afterward, the flask with dried oil was

weighed. The oil yield determined by the method of immediate extraction ( $a_1$ , %) was calculated using Equation 1:

$$a_1 = \frac{m_1 \cdot 100}{m_2} \quad (1)$$

where  $m_1$  is a mass of the obtained oil (g);  $m_2$  is a mass of the seed sample (g).

The number of disrupted cells ( $x$ , %) was calculated using Equation 2:

$$x = \frac{a_1 \cdot 100}{a_2} \quad (2)$$

where  $a_2$  is the total oil content in pumpkin seeds (%).

From the results of three experimental replicates the mean value and standard deviation were calculated.

### **Pumpkin seed microstructure analysis**

A cross-section of pumpkin seeds was sliced on a microtome. Pumpkin seed slices of 20  $\mu\text{m}$  thickness were treated with pepsin, Viscozyme L, or pectinase as well as the enzyme mixture pepsin+Viscozyme L+pectinase in a microwell plate (same amount of enzymes as in previous experiments was dissolved in 1 ml of a phosphate buffer solution with a pH of 5.5 in each well). All samples were incubated for 2.0 h at 48–52 °C in a microwell plate placed in a petri dish with water in a laboratory oven. Some wells of the plate contained control samples, which were treated under the same conditions, but did not contain enzymes in the buffer solution. After incubation, all enzyme-treated and control samples were transferred to slides and fixed by drying at 65 °C in an oven for 1 h. All fixed samples were stained with Nuclear Fast Red for 5 min, afterward were examined by light microscopy using a microscope Leica DM750 with the camera Leica ICC50 and software Leica Application Suite version 3.0.0. Ten different locations on every sample were imaged and representative images are shown in Figure 3.

### **Pressing of pretreated pumpkin seeds**

For the study of the effect of pumpkin seeds enzymatic pretreatment on the press oil yield, a 200 g of seeds were ground in a laboratory mill to the particle size  $\leq 10.0$  mm. Each seed portion was treated with the 1.8% enzyme mixture pepsin+Viscozim+pectinase in a ratio of 1:1:1 dissolved in 70 ml of a phosphate buffer solution with pH 5.5. The obtained mixture was placed in a glass jar and incubated at 48–52 °C for 2.0 h under constant shaking. The experiment was performed in triplicate. The control samples also were incubated in triplicate under the same conditions as the experimental samples, but without the presence of enzymes in the added buffer solution. After incubation, all samples were transferred from the jars to metal trays and dried in an oven at 100–110 °C for 1.5–2.0 h with thorough manually stirring every 30 min to a moisture content of 3.0–4.3%. Afterward, all dried samples were weighed and pressed on a laboratory screw press at 100–125 °C and a nozzle hole diameter of 6.0 mm. The pressed oil yield in terms of seed weight was calculated using Equation 1. The oil yield in terms of total oil content in the pumpkin seeds was calculated using Equation 2. From the results of three experimental replicates of each control or experimental treatment, a mean value and standard deviation was calculated.

### **Analysis of pumpkin seed residues**

Determination of the oil content in residual pressed cake was performed in the Soxhlet apparatus according to ISO 659:2009. The experiment was performed in triplicate with further calculation of the mean value and standard deviation.

### **Analysis of extracted oil**

#### **Quality parameters**

To evaluate the quality of pressed pumpkin seed oils, free fatty acid (FFA) content and peroxide value (PV) were determined according to the ISO 660:2020, and ISO 3960:2007, respectively. From the results of three replicates of each experiment, the mean value and standard deviation were calculated.

#### **DPPH radical scavenging activity and kinetic analysis**

Determination of the antioxidant activity of the press pumpkin seed oils was carried out by the method of 2,2-diphenyl-1-picrylhydrazyl (DPPH) radical scavenging activity (Broznic et al., 2016). The solution of 2,2-diphenyl-1-picrylhydrazyl at a concentration of 3 mg/100 ml of ethyl acetate, which had an optical density in the range of 0.7–0.9 at a wavelength of 520 nm. To prepare the reaction mixture 15 ml of DPPH solution were added to 100 mg of oil, mixed thoroughly, and the initial absorbance of the reaction mixture was determined at 520 nm ( $A_0$ ). The reaction mixture was kept in the dark place and the absorbance was measured at 520 nm ( $A_t$ ) at a specified time interval (every 5 min) for 25 min. DPPH radicals scavenging effect of the oil solutions ( $AA_{t\%}$ ) at specified time intervals was calculated according to Equation 3:

$$AA_t = \frac{(A_0 - A_t) \cdot 100}{A_0} \quad (3),$$

where  $A_0$  is an absorbance of the freshly prepared DPPH oil solution;

$A_t$  is an absorbance of the DPPH oil solution at time  $t$ .

Antioxidant activity ( $AA_{25\%}$ ) was the total DPPH scavenging for 25 min. The experiment at each time interval was performed in triplicate, and the mean values and standard deviations were calculated.

#### **Fatty acid composition analysis**

Determination of the fatty acid composition of the press pumpkin seed oils was carried out by gas-liquid chromatography of fatty acid methyl esters (Nosenko et al., 2014). For the preparation of fatty acid methyl esters, 100 mg of each oil sample was dissolved in a 2 ml solution (0.5 g/l) of butylated hydroxytoluene in heptane. Then 100  $\mu$ l of sodium in methanol solution (46 mg/ml) was added, solution have been mixed for 2 min and exposed for 15 min. 1 to 2 g of sodium hydrosulfate was added. The samples were filtrated through the anhydrous sodium sulfate, and then 2 ml of butylated hydroxytoluene heptane solution was added. The solution obtained was filtrated one more time through a 0.45  $\mu$ m membrane cellulose filter, and the filter was washed with 1 ml of the same solvent. The two filtrates were combined and the solution was used for analysis. The obtained fatty acid methyl esters were analyzed on Hewlett Packard gas chromatography model HP 6890 with capillary column HP-88 (88%-

cyanopropyl aryl-polysiloxane; 100 m × 0.25 mm; 0.25 μm film thickness (Agilent Technologies)). The temperature of the injector was 280 °C, the detector had a temperature of 290 °C. The temperature steps and heating rates were as follows: holding the temperature at 60 °C for 4 min; heating to 150 °C at 4 °C/min, holding at for 10 min; heating to 180 °C at 3 °C/min, holding for 5 min; heating to 190 °C at 3 °C/min, holding for 2 min, heating to 230 °C at 3 °C/min, holding for 2 min; heating to 260 °C at 4 °C/min, holding for 2 min. The flow rate of carrier gas was 1.2 ml/min, and the sample volume was 1.0 μl. Identification of the fatty acids was performed by comparison of the retention times with a standards mixture of fatty acid methyl esters (37 Component FAME Mix, SUPELCO). Reported data are the mean value and standard deviation of three analytical replicates.

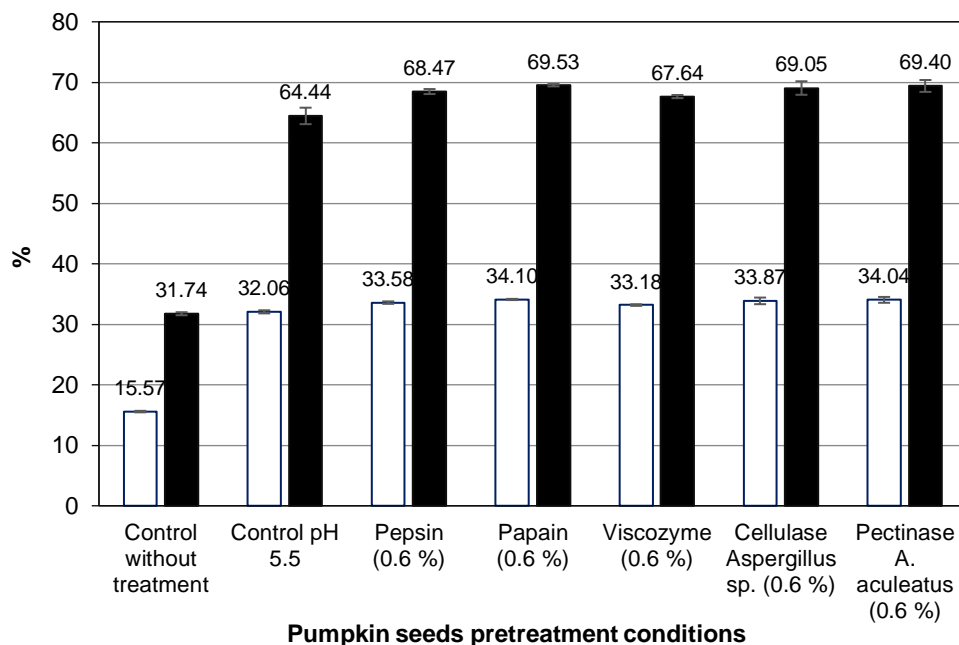
### **Phytosterols composition**

Analysis of phytosterols composition was performed according to ISO 6799:1991. 10 ml of standard betulin solution and 100 ml of alcoholic KOH solution were added to the 100 mg oil sample and boiled in a water bath for 1 h. After cooling, the sample was transferred to a separatory funnel by adding 200 ml of distilled water and 100 ml of diethyl ether, shaken vigorously, and separated the upper ether layer. The washing was repeated 3 times. The combined ether extracts were transferred to another separatory funnel by adding 100 ml of distilled water and shaken gently. After delamination, the aqueous layer was drained, and the washing was repeated 3 times. The upper ether solution was filtered through a pad of sodium sulfate. The solvent was evaporated on a rotary evaporator to give 1 ml of solution. The solution was applied with a micro syringe to the prepared silicon wafer and placed in the developer tank. The plate was removed after distillation and the solvent was allowed to evaporate. Silicon containing the sterol fraction was collected with a micro spatula. The silicon was placed in an Erlenmeyer flask and boiled with 5 ml of diethyl ether in a water bath for 15 min. The solution was cooled and filtered through a paper filter. The silicon from the filter paper was re-extracted and filtered twice more. The residue was dissolved in a minimum amount of solvent for development and analyzed by gas phase chromatography. The measurement was performed on a gas chromatograph CP-3800 (Varian), equipped with a flame ionization detector, electronic gas flow control system, universal injector for the introduction of samples in the split and non-separation modes, and autosampler (CP-8410 Varian). A capillary column MET-Biodiesel with a built-in pre-column (14 m × 0.53 mm; 0.16 μm film thickness) was used under the following conditions: carrier gas flow rate, 5.0 ml/min; flow separation factor 1:10; evaporator temperature, 360 °C; detector temperature, 390 °C; column temperature mode: gradual heating from 160 °C to 340 °C. The sample injection volume was 1 μl. Reported data are the mean value and standard deviation of three analytical replicates.

## **Results and discussion**

### **Effect of the enzyme pretreatment on the cell integrity of pumpkin seeds**

All pumpkin seeds samples, treated with single enzymes, such as pepsin, papain, Viscozyme L, cellulase, and pectinase, gave a higher oil yield with immediate oil extraction, ranging from 33.2 to 34.1%, compared with the oil yield from control samples, 32.1%, which was incubated only with 100 mM phosphate buffer, pH 5.5 (Figure 1). It was found that seed samples treated with different enzymes had also a higher number of disrupted cells, varying from 67.6 to 69.5% (control samples had 64.4%).



□ a<sub>1</sub> - Oil yield in terms of seed weight, % ■ x - The number of destroyed cells, %

**Figure 1. Oil yield (a<sub>1</sub>, %) and number of disrupted cells (x, %) of control samples and samples pretreated with single enzyme, estimated by the method of immediate oil extraction**

It was shown that pretreatment of milled hulled pumpkin seeds with acid protease at pH 5.2 for 2.0 h at 48–52 °C leads to an increase in the number of disrupted cells by 10.4% compared to control samples (Nosenko et al., 2019b). However, the percentage of disrupted cells in control and enzyme-treated samples were 46.7 and 57.1%, respectively, that are lower than it was received in the present study (64.4 and 69.5%). This can be explained by the presence of the husk covering pumpkin seeds in the previous research.

In a study of rapeseed enzymatic pretreatment with cellulase (from *Bacillus subtilis*, 300 units/g, from Enzyme, Ukraine) in the amount of 2.0% (w/w) for 2 h at 40–42 °C a relatively low percentage of disrupted cells in both control and enzyme-treated samples also were found, that was 35 and 50%, respectively (Cherstva et al., 2016). In the present study, the higher percentage of disrupted cells can be associated with significantly higher hydrolysis temperature, while a smaller difference between the number of disrupted cells in the pretreated and control samples may be due to the use of less amount of enzyme by seed weight.

At the same time, the greatest difference in the percentage of disrupted cells was observed between control samples incubated in phosphate buffer at pH 5.5 for 2 h and control samples without this treatment, which indicates that swelling is an important factor to consider in the pretreatment, even without the use of enzymes. A similar result was obtained during the study of the different sunflower seed pretreatment methods effect on the n-hexane oil extraction. Due to the treatment of dehulled seeds with convective heat or steam, the oil yield was by 11% higher than during the extraction of crude seeds for 1.0 h, while the treatment of seeds with Viscozyme L in combination with heat or steam resulted in increased oil yield compared to crude control by 12 and 14%, respectively (Danso-Boateng, 2011).

### Effect of the pretreatment with the enzyme mixtures on the cell integrity

All variations of the pumpkin seed pretreatment with different enzyme mixtures lead to an increase in oil yield during immediate oil extraction and to an increase in the number of disrupted cells in comparison to the control samples (Figure 2). Initially, four different enzyme mixtures were used for seeds treatment for 2.0 h with the amount of mixture for each sample of 1.8% (w/w). The highest amount of disrupted cells 71.0 and 71.1% were detected in samples treated with pepsin+ Viscozyme L+pectinase and pepsin+cellulase+pectinase mixtures, respectively, which was by 6.6% higher than in control samples. A similar result was achieved during the treatment of milled pumpkin seeds with hulls with a mixture of acid protease and cellulase (from *Trichoderma reesei*) in different ratios at pH 5.2, the number of disrupted cells reached 60%, which was by 3% more than in control samples (Nosenko et al., 2019b).

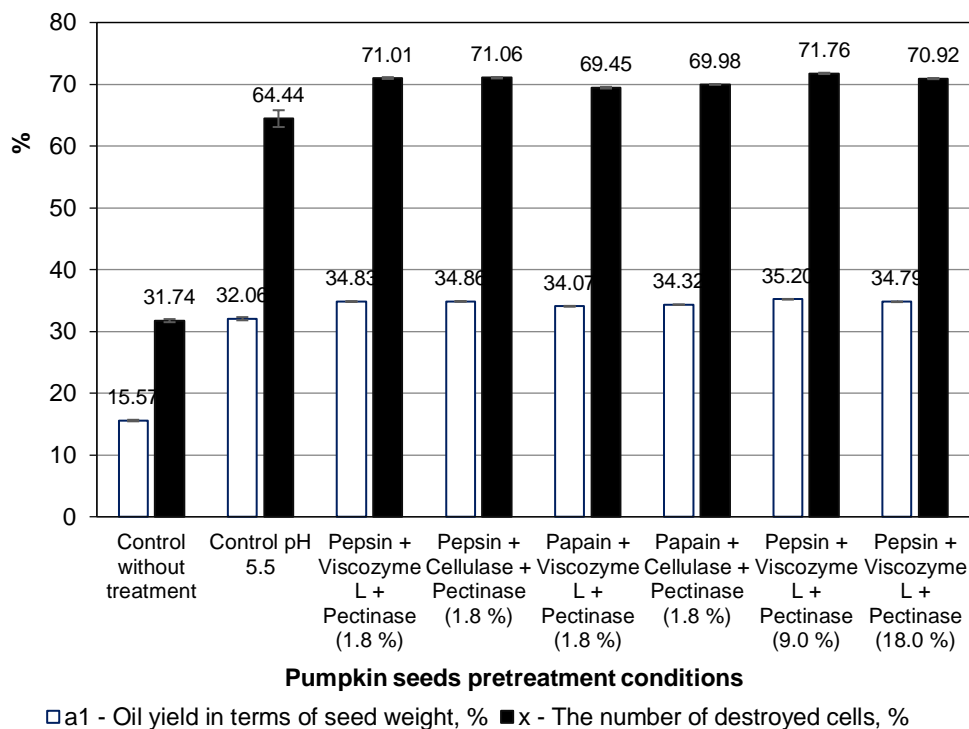


**Figure 2.** Oil yield (a<sub>1</sub>, %) and number of disrupted cells (x, %) of control samples and samples pretreated with enzyme mixtures, estimated by the method of immediate oil extraction

For study of the effect of added enzyme amount, the ground pumpkin seeds were treated with a pepsin+Viscozyme L+pectinase mixture. However, no significant change in the percentage of disrupted cells was observed when the amount of added enzyme mixture was raised 5- or 10-times (9.0 and 18.0% w/w, respectively). An explanation for the ineffectiveness of increased enzyme concentrations is, that the high concentration already saturates available cleavage sites and that an increase beyond a monolayer coverage of the substrate does not lead to a higher activity. Similarly, the soybean- and sunflower seeds were

treated by enzyme mixtures with cellulolytic and pectolytic activities in the amounts from 0.01 to 5.0% by seed weight before oil extraction with n-hexane (Dominguez et al., 1993). It was found that increasing of the enzyme mixture concentration above 1.0% during soybean pre-treatment and more than 2.0% for sunflower seeds did not lead to intensification of oil extraction. In another study of enzymatic pretreatment of rapeseeds with a mixture of protease (from *Bacillus subtilis*, 70 units/g) and cellulase (from *Bacillus subtilis*, 300 units/g) the concentration of enzyme mixture was changed from 0.4 to 1.4% w/w. The optimal enzyme concentration was found to be 0.6%, which allowed achieving a pressed oil yield of 43.1% (Cherstva et al., 2016). Excessive increases in the added enzyme amount and in the enzymatic pretreatment duration are not only economically unprofitable but can also lead to hydrolysis of polysaccharides with the formation of free reducing sugars, which will be quickly caramelized at further drying and prevent the release of oil (Kumar et al., 2017; Latif, 2009).

### **Influence of the enzymatic pretreatment on the pumpkin seed cells microstructure**

To observe the effect of the enzymatic pretreatment on the cell walls and oil bodies within the pumpkin seed cells, microtome slices of pumpkin seeds were enzymatically treated and compared to non-treated samples (Figure 3). Oil bodies are protected by the cell walls and all cells are intact in the control samples of pumpkin seed slices treated with buffer without the addition of enzymes (Figure 3a). Pepsin-treated samples show intact cell walls but also oil bodies which are less stained indicating that the oleosin-containing protein membrane covering the oil body has been partially degraded by the protease (Figure 3b). Pectinase hydrolyzes the pectin gluing cells together, which is visible (Figure 3c). The thickness of the cell walls of pectinase-treated slices was also lower than in the control and pepsin-treated slices, which indicates the presence of cellulases and other cell wall hydrolyzing enzymes. Some ruptured cells have lost their oil bodies, which are visible outside the cells (upper left corner). The effect of Viscozyme L was the largest observed since it is already a mixture of different enzymes and contains cellulases,  $\beta$ -glucanase, and hemicellulases, which have a much bigger effect on the cell wall structures, disrupted a large portion of the cells and released most of the oil bodies from the cells (Figure 3d). A similar result was observed in the treatment of sunflower kernels by Viscozyme L (Danso-Boateng, 2011). The most effective pretreatment of pumpkin seed slices was obtained with a mixture of pepsin+Viscozim+pectinase (Figures 3e and 3f). The cell walls completely disappeared and only residues are observed. Some of the oil bodies are still intact, but also large spots of oil from coagulated oil bodies with some intact oil bodies are visible that indicate a large number of ruptured oleosomes (Figure 3f). In two studies of the pretreatment effect of pomegranate seeds with Pectinex Ultra SPL, Flavorzyme 100 L, and cellulase crude enzymes, as well as the enzymatic treatment of palm fruit fiber with Cellic CTec2, Cellic HTec2, and Pectinex Ultra SPL mixture, significant destruction of cells walls and oleosomes was achieved too (Kaseke et al., 2021; Silvamany and Jamaliah, 2015).

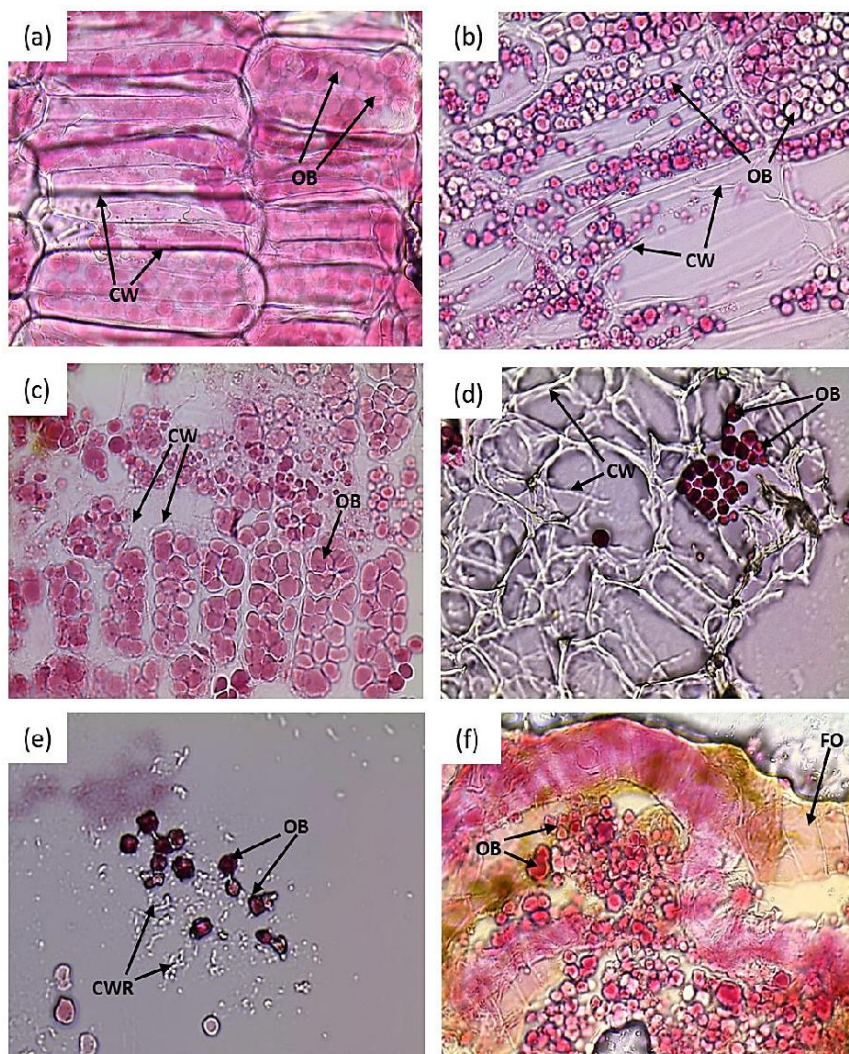


**Figure 3. Pumpkin seed microtome slices stained with Nuclear Fast Red.**

The slices treated without the addition of enzyme (a), pepsin treated slices (b), pectinase treated slices (c), Viscozyme L treated slices (d), the slices treated with pepsin+Viscozyme L+pectinase mixture (e, f).

Magnification = 100 ×, CW – cell walls, OB – oil bodies, CWR – cell wall residues, FO – free oil

During *in vitro* digestion of a walnut oil body dispersion with pepsin, large oil bodies were revealed indicating their coalescence because of surface peptide destruction (Gallier et al., 2013). The effect of pepsin in combination with the cellulolytic, hemicellulolytic, and pectinolytic enzymes becomes clear in the experiment with the enzyme mixture (Fig. 3, e, f), demonstrating that the proteolytic activity is needed for the destruction of membrane protein of oil bodies leading to the coagulation into large oil droplets.

At the same time, it is important to mention that such a complete degradation of the cell wall structure is only possible in the case of microtome slices with a thickness of 20  $\mu\text{m}$ . It is almost impossible to achieve such a degree of destruction with the large particle sizes commonly used for mechanical pressing (0.5 to 5 mm or even intact pumpkin seeds), as enzymes will have a greater effect on smaller particles with a higher specific surface area. Cells inside a large particle are inaccessible to enzymes until the cells around them are degraded.

### Effect of enzymatic pretreatment on press oil yield

The press oil yield from seeds treated with pepsin+Viscozyme L+pectinase mixture was 15.5% (Figure 4), which is by 7.0% higher than in the control samples, while the oil yield calculated to the base of the total oil content in pumpkin seeds is by 14.3% higher compared to control samples (31.6%). A similar result was found in a study of the enzyme-assisted cold pressing of cotton seeds with the highest press oil yield of 12.89% (by seed weight) obtained from samples treated with Kemzyme compared to an oil yield of 8.50% in control samples (Latif et al., 2007). The increase in oil yield by 5.5 and 6.1% compared to the control samples was achieved because of flax- and hemp seed treatment with Viscozyme L, respectively.

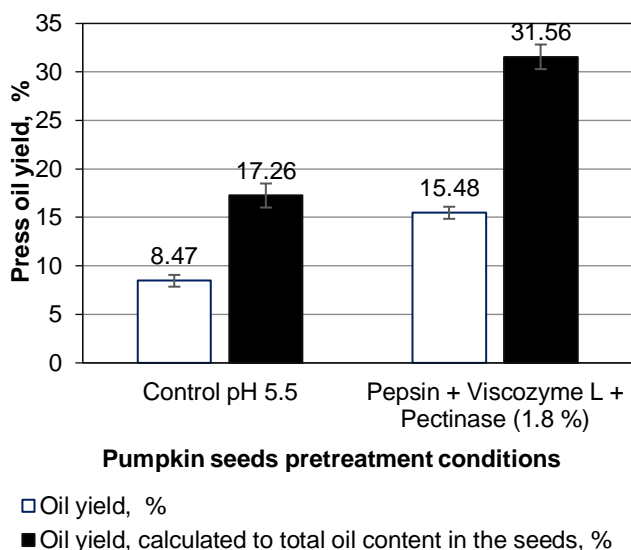


**Figure 4. Press oil yield of control samples and enzymatically pretreated samples**

Low oil yields in both enzyme-treated and control samples may be due to the used parameters of pressing, such as press temperature, nozzle hole diameter, particle size, and moisture content of oil material, which may be not optimally selected for this type of seeds. The residual cake oil content in terms of seed weight decreased from 39.5% in the control samples to 31.8% in samples treated with a pepsin+Viscozyme L+pectinase mixture (Figure 5).

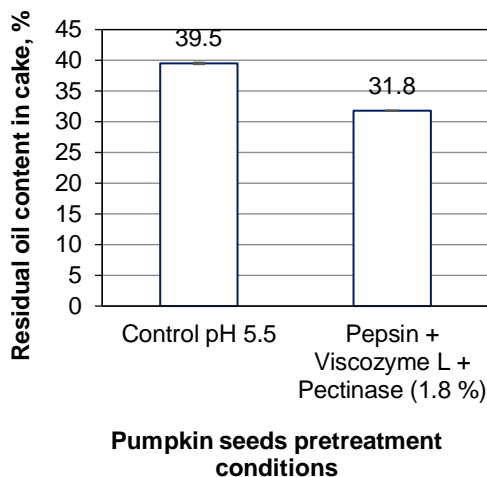


**Figure 5. Residual cake oil content of control samples and enzyme pretreated samples**

### Oil quality and antioxidant activity

Characteristics oil quality and antioxidant activity of pumpkin seed oil are shown in Table 1. The content of free fatty acids in pressed oil from seeds treated with pepsin+Viscozyme L+pectinase mixture was slightly higher compared to the control sample, while its peroxide value is slightly lower than in the control. Similar results were observed after the treatment of cotton seeds with Phytzyme, Kemzyme, and Feedzyme, which led to some increase of free fatty acids in the obtained pressed oil (3.80, 3.90, and 3.60 respectively) compared with the oil obtained from the control (3.22), as well as in flaxseeds treated by Viscozyme L, Kemzyme, and Feedzyme, the peroxide value was slightly lower (1.90, 2.25, and 2.19 meq/kg, respectively) than in the control (2.35 meq/kg) (Anwar et al., 2013;Latif et al., 2007). As a result of hemp seed pre-treatment with Kemzyme, Protex 7L, Viscozyme L, Feedzyme, and Natuzyme, slight variations of free fatty acids (1.73–1.87% as oleic acid) and peroxide value (1.54–1.62 meq/kg) were observed relative to the control (1.75% and 1.57 meq/kg, respectively) (Latif et al., 2009). The decrease of the peroxide value in the oil pressed from enzymatically pretreated seeds may be due to the higher release of tocopherols and increased antioxidant properties compared to the control oil. At the same time, in a study of enzyme-assisted cold-press oil of borage seeds, it was found that the effect of enzymatic pretreatment of seeds on the content of free fatty acids and peroxide values was insignificant (Soto et al., 2007).

**Table 1**  
**Free fatty acids, peroxide value, and DPPH scavenging capacity of control oil and oil from enzyme-treated pumpkin seeds**

Sample	Acid value, mg KOH/g oil	Peroxide value, meq O/kg oil	Antioxidant activity, AA <sub>25</sub> , %
Control	0.94±0.13	1.7±0.04	17.6±0.1
Press oil from enzyme-treated seeds	1.03±0.13	1.6±0.1	20.2±0.1

Enzymatic pretreatment of pumpkin seeds had a positive effect on the oil antioxidant activity, which expressed as a DPPH radical disappearance. The results show that the total DPPH scavenging effect of pressed oil from enzyme-treated seeds was by 2.7% higher than that of control press oil (Table 1). A similar result was obtained during enzymatic treatment of flax seeds, DPPH radical scavenging of press oil from samples treated with Viscozyme L, Feedzyme, and Kemzyme (50.03, 45.30, and 43.01% respectively) was significantly higher compared to DPPH radical disappearance of oil from control seed samples (35.20%) (Anwar et al., 2013). Antioxidant activity of oil from seeds pomegranate cultivar was increased by enzymatic pretreatment from 1.60 to 2.91 mmol Trolox/g of pomegranate seed oil as well as DPPH scavenging effect (Kaseke et al., 2021). DPPH radical disappearance of cold press perilla seed oil was 50.6%, while the perilla seeds oil treated with ultrasound-assisted aqueous enzymatic extraction in combination with cellulase, neutral proteinase, and pectinase had a DPPH scavenging capacity of 70.6% (Li et al., 2017). At the same time, total DPPH radical scavenging of both enzyme-assisted and control pressed pumpkin seed oils was much lower in the current study than reported in other previous studies of this oil's antioxidant properties, where DPPH scavenging activity of pumpkin seed oil obtained by n-hexane extraction was 35.5%, while in unrefined pressed oils from roasted pumpkin seeds, this value ranged from 32.28 to 65.33% (Agustina et al., 2019; Andjelkovic et al., 2010).

The effect of enzymatic pre-treatment of pumpkin seeds on its oil DPPH scavenging capacity over time is shown in Figure 6. DPPH scavenging activity of enzyme-assisted pressed oil is significantly higher at each time point than that of the control pressed oil. The fast, initial phase of the reaction shows a fast disappearance of DPPH radicals within the first 5 min. Afterward, the reaction slows down. In an analogous study of the biphasic DPPH disappearance kinetics in pumpkin seed oil, the first, fast phase occurred between 4.5–6.5 min in oil samples obtained from roasted seed paste, while for cold-pressed oils from unroasted seeds the duration of the first phase was 8.5–10.5 min (Broznic et al., 2016).

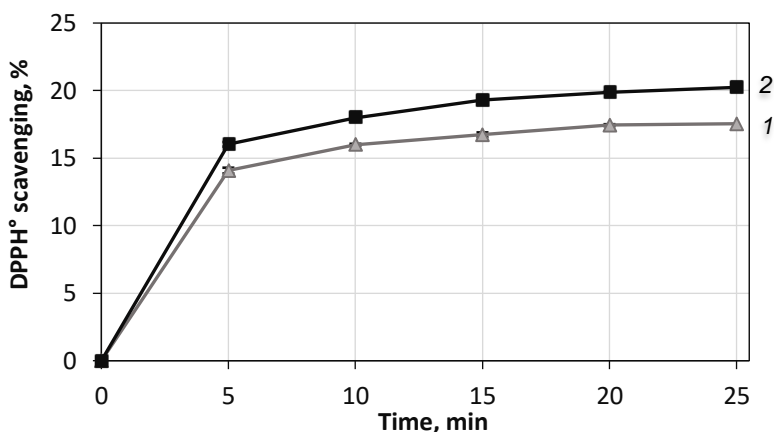


**Figure 6. The kinetics of DPPH scavenging by pumpkin seed oil:**  
**1 – control press pumpkin seed oil, 2 – enzyme pretreated press pumpkin seed oil**

### Fatty acid composition of pumpkin seed oil

The fatty acid composition of control and enzyme-assisted pressed pumpkin seed oils are shown in Table 2. The most abundant fatty acids among unsaturated fatty acids for both control and enzyme-treated samples were linoleic acid (56.2–57.0%) and oleic acid (23.2–24.3%), while the predominant saturated fatty acids were palmitic acid and stearic acid with an amount of 12.1 and 6.0%, respectively. Similarly, the study of the fatty acid composition of 100 different Styrian pumpkin seed oils from different breeding lines showed that the main pumpkin seed oil fatty acids, such as linoleic-, oleic-, palmitic-, and stearic acids, were found in amounts of 43.8–52.4, 28.6–38.1, 11.4–13.3, and 4.8–6.7% respectively (Frühwirth et al., 2007; Procida et al., 2013). The content of these fatty acids varied in the ranges of 44.30–51.58, 33.60–42.59, 9.13–13.35, and 0.27–0.55%, respectively when twelve pumpkin seed oil samples of different origins were analyzed.

**Table 2**  
Fatty acid composition of control oil and oil from enzyme-treated pumpkin seeds

Fatty acid	Content of fatty acid, % of the total content	
	Control press oil	Press oil from enzyme-treated pumpkin seeds
Palmitic acid (C 16:0)	12.07±0.15	12.14±0.15
Palmitoleic acid (cis-9-C 16:1)	0.11±0.05	0.12±0.05
Stearic acid (C 18:0)	5.98±0.10	5.96±0.10
Oleic acid (cis-9-C 18:1)	24.28±0.20	23.23±0.20
Octadecenoic acid (cis-11-C 18:1)	0.51±0.15	0.61±0.15
Linoleic acid (cis, cis-9,12-C 18:2)	56.15±0.20	57.03±0.20
α-Linolenic acid (cis,cis,cis-9,12,15-C 18:3)	0.16±0.20	0.16±0.20
Arachidic acid (C 20:0)	0.38±0.05	0.37±0.05
Behenic acid (C 22:0)	0.11±0.05	0.12±0.05
Saturated fatty acids	18.70	18.75
Monounsaturated fatty acids	24.98	24.03
Polyunsaturated fatty acids	56.32	57.22
Unsaturated fatty acids:Saturated fatty acids	4.35	4.33

Because of enzymatic pretreatment of pumpkin seeds, the content of linoleic acid in the pressed oil increased slightly, while the amount of oleic acid reduced, but also not significantly (Table 2). In spite of the higher polyunsaturated fatty acids amount and lower monounsaturated fatty acids content were observed, however, the unsaturated fatty acids: saturated fatty acids ratio did not change significantly. There also was no significant difference in the amount of palmitic-, palmitoleic-, stearic-, octadecenoic-, α-linolenic-, arachidic-, and behenic acids in the control and enzyme-treated samples. In line with the present study, the research of cotton-, flax-, hemp-, and borage seed cold pressing revealed no significant impact of enzymatic pretreatment on its oil fatty acid profiles (Anwar et al., 2013; Latif et al., 2007; 2009; Soto et al., 2007).

### Phytosterols composition of pumpkin seed oil

The phytosterols composition of pumpkin seed oils is presented in Table 3.

**Table 3**  
Phytosterol composition of of control oil and oil from enzyme-treated pumpkin seeds

Phytosterol	Content of phytosterol, % of the total content	
	Control press oil	Press oil from enzyme-treated pumpkin seeds
Cholesterol	0.77± 0.05	0.82± 0.05
Campesterol	1.74± 0.10	1.78± 0.10
Stigmasterol	1.95±0.15	2.88±0.15
24-Methylcholest-7-enol	0.91±0.05	0.76±0.05
$\alpha$ -Spinasterol+ $\Delta$ 7,22,25-Stigmastatrienol	48.69±0.20	47.46±0.20
$\Delta$ 5-Avenasterol	1.75±0.10	2.56±0.10
$\Delta$ 7,25-Stigmastadienol	22.47±0.20	20.71±0.20
$\Delta$ 7-Stigmastenol	4.81±0.10	4.52±0.10
$\Delta$ 7-Avenasterol	16.90±0.15	18.51±0.15

$\alpha$ -Spinasterol and  $\Delta$ 7,22,25-stigmastatrienol accounted for almost 50% of the total sterol content and were found to be the predominant phytosterols of oils from control and enzyme pretreated pumpkin seed, while  $\Delta$ 7,25-stigmastadienol and  $\Delta$ 7-avenasterol were also present in relatively high amounts 20.7–22.5 and 16.9–18.5%, respectively. Previous studies of the pumpkin seed oil phytosterols composition reported that  $\Delta$ 7-sterols, such as  $\alpha$ -spinasterol,  $\Delta$ 7,22,25-stigmastatrienol,  $\Delta$ 7,25-stigmastadienol,  $\Delta$ 7-avenasterol, and  $\Delta$ 7-stigmastenol, significantly predominate over  $\Delta$ 5-sterols (Dotto et al., 2020; Fruhwirth et al., 2007).

A slight decrease of  $\alpha$ -spinasterol,  $\Delta$ 7,22,25-stigmastatrienol, and  $\Delta$ 7,25-stigmastadienol content was observed in the enzyme-assisted press pumpkin seed oil, while the content of stigmasterol,  $\Delta$ 5-avenasterol, and  $\Delta$ 7-avenasterol slightly increased. Similarly, the stigmasterol content of the oil obtained from enzyme-pretreated pomegranate seed samples was significantly higher (29.8–52.0mg/100 g oil), compared to control pomegranate seed oil samples (20.5–45.8 mg/100 g oil), that might be due to reduced complexation of the phytosterols with the seed polysaccharides and further enhancement of their mass transfer into the oil phase (Kaseke et al., 2021).

### Conclusions

1. Proteolytic enzymes are needed to degrade the oleosin-rich membranes around the oil bodies in seed cells. In the mixtures with cellulolytic, hemicellulolytic and pectinolytic enzymes, proteolytic enzymes help to disrupt pumpkin seed cells synergistically leading to the most prominent increase of oil yield.
2. The yield of press pumpkin seed oil was about 14.3% higher from seeds incubated with a pepsin+Viscozyme L+pectinase mixture at 48–52 °C for 2.0 h at pH 5.5 compared to the seeds pretreated at the same conditions, but without adding enzymes.

3. There was no significant influence of enzyme treatment on the press oil quality and composition, but a slightly higher total DPPH scavenging capacity of oil from enzyme-pretreated seeds was detected. This oil had also higher stigmasterol content.

**Acknowledgment.** The authors gratefully acknowledge the financial support provided by the Ministry of Education and Science of Ukraine (Contract № M/51-2022, 24. 05. 2022). Funding has also been provided by the Austrian Agency for Education and Internationalisation through a Scientific and Technological Cooperation Grant the Ukraine and Austria (WTZ grant Nr. UA 05/2020).

## References

- Agustina N.A., Elisabeth J., Julianti E. (2019), A comparison studies on the chemical characteristics of pumpkin seed oil with extra virgin olive oil and palm olein, *International Conference on Agriculture, Environment, and Food Security 2018 24–25 October 2018, Medan, Indonesia*, 260(1), 012091, <https://doi.org/10.1088/1755-1315/260/1/012091>
- Andjelkovic M., Van Camp J., Trawka A., Verhe R. (2010), Phenolic compounds and some quality parameters of pumpkin seed oil, *European Journal of Lipid Science and Technology*, 112(2), pp. 208–217, <https://doi.org/10.1002/ejlt.200900021>
- Anwar F., Zreen Z., Sultana B., Jamil A. (2013), Enzyme-aided cold pressing of flaxseed (*Linum usitatissimum* L.): Enhancement in yield, quality and phenolics of the oil, *Grasas Aceites*, 64, pp. 463–471, <https://doi.org/10.3989/gya.132212>
- Broznic D., Canadijuresic G., Milin C. (2016), Involvement of  $\alpha$ -,  $\gamma$ - and  $\delta$ -tocopherol isomers from pumpkin (*Cucurbita pepo* L.) seed oil or oil mixtures in the biphasic DPPH disappearance kinetics, *Food Technology and Biotechnology*, 54(2), pp. 200–210, <https://doi.org/10.17113/ftb.54.02.16.4063>
- Cherstva A., Lastovetska A., Nosenko T. (2016), Using of enzymes to extract of rapeseed oil by pressing, *Ukrainian Journal of Food Science*, 4 (1), pp. 85–92.
- Danso-Boateng E. (2011), Effect of enzyme and heat pretreatment on sunflower oil recovery using aqueous and hexane extractions, *International Journal of Chemical, Materials and Biomolecular Sciences*, 4(1), pp. 28–34, <https://doi.org/10.5281/zenodo.1327718>
- Dominguez H., Nunez M.J., Lema J.M. (1993), Oil extractability from enzymatically treated soybean and sunflower: range of operational variables, *Food Chemistry*, 46(3), pp. 277–284, [https://doi.org/10.1016/0308-8146\(93\)90119-Z](https://doi.org/10.1016/0308-8146(93)90119-Z)
- Dotto J. M., Chacha J. S. (2020), The potential of pumpkin seeds as a functional food ingredient: A review, *Scientific African*, 10, e00575, <https://doi.org/10.1016/j.sciaf.2020.e00575>
- Fruhirth G.O., Hermetter A. (2007), Seeds and oil of the Styrian oil pumpkin: Components and biological activities, *European Journal of Lipid Science and Technology*, 109(11), pp. 1128–1140, <https://doi.org/10.1002/ejlt.200700105>
- Gallier S., Tate H., Singh H. (2013), *In vitro* gastric and intestinal digestion of a walnut oil body dispersion, *Journal of Agriculture and Food Chemistry*, 61(2), pp. 410–417, <https://doi.org/10.1021/jf303456a>
- Herskowitz A., Ishii N., Schaumburg H. (1971), n-Hexane neuropathy: A syndrome occurring as a result of industrial exposure, *The New England Journal of Medicine*, 285, pp. 82–85, <https://doi.org/10.1056/NEJM197107082850204>

- Kaseke T., Opara U. L., Fawole O. A. (2021), Effects of enzymatic pretreatment of seeds on the physicochemical properties, bioactive compounds, and antioxidant activity of pomegranate seed oil, *Molecules*, 26(15), 4575, <https://doi.org/10.3390/molecules26154575>
- Kumar S.P.J., Prasad S.R., Banerjee R., Agarwal D.K., Kulkarni K.S., Ramesh K.V. (2017), Green solvents and technologies for oil extraction from oilseeds, *Chemistry Central Journal*, 11(9), pp. 1–9, <https://doi.org/10.1186/s13065-017-0238-8>
- Kutlu G., Gomceli Y. B., Sonmez T., Inan L. E. (2009), Peripheral neuropathy and visual evoked potential changes in workers exposed to n-hexane, *Journal of Clinical Neuroscience*, 16(10), pp. 1296–1299, <https://doi.org/10.1016/j.jocn.2008.12.021>
- Latif S., Anwar F., Ashraf M. (2007), Characterization of enzyme-assisted cold-pressed cottonseed oil, *Journal of Food Lipids*, 14(4), pp. 424–436, <https://doi.org/10.1111/j.1745-4522.2007.00097.x>
- Latif S., Anwar F. (2009), Physicochemical studies of hemp (*Cannabis sativa*) seed oil using enzyme-assisted cold-pressing, *European Journal of Lipid Science and Technology*, 111(10), pp. 1042–1048, <https://doi.org/10.1002/ejlt.200900008>
- Li H., Zhang Z., He D., Xia Y., Liu Q., Li X. (2017), Ultrasound-assisted aqueous enzymatic extraction of oil from perilla seeds and determination of its physicochemical properties, fatty acid composition and antioxidant activity, *Food Science and Technology*, 37(1), pp. 71–77, <https://doi.org/10.1590/1678-457X.29116>
- Montero-Montoya R., Lopez-Vargas R., Arellano-Aguilar O. (2018), Volatile organic compounds in air: Sources, distribution, exposure and associated illnesses in children, *Annals of Global Health*, 84(2), pp. 225–238, <https://doi.org/10.29024/aogh.910>
- Nosenko T., Kot T., Kichshenko V. (2014), Rapeseeds as a source of feed and food proteins, *Polish Journal of Food and Nutrition Science*, 64(2), pp. 109–114, <https://doi.org/10.2478/pjfn-2013-0007>
- Nosenko T., Koroluk T., Usatuk S., Vovk G., Kostinova T. (2019a), Comparative study of walnut and pumpkin seeds oils biological value and oxidative stability, *Food Science and Technology*, 13(1), pp. 60–65, <https://doi.org/10.15673/fst.v13i1.1311>
- Nosenko T., Vovk G., Koroluk T. (2019b), Effect of hydrolytic enzymes pretreatment on the oil extraction from pumpkin seeds, *Ukrainian Food Journal*, 8(1), pp. 80–88, <https://doi.org/10.24263/2304-974X-2019-8-1-9>
- Procida G., Stancher B., Catenia F., Zacchignaa M. (2013), Chemical composition and functional characterisation of commercial pumpkin seed oil, *Journal of the Science and Food Agriculture*, 93(5), pp. 1035–1041, <https://doi.org/10.1002/jsfa.5843>
- Shaban A., Sahu R. P., (2017), Pumpkin seed oil: An alternative medicine, *International Journal of Pharmacogn and Phytochemical Research*, 9(2), pp. 223–227, <https://doi.org/10.25258/phyto.v9i2.8066>
- Sharma A., Sharma A. K., Chand T., Khardiya M., Yadav K. C. (2013), Antidiabetic and antihyperlipidemic activity of *Cucurbita maxima* duchense (pumpkin) seeds on streptozotocin induced diabetic rats, *Journal of PharmacognPhytochemistry*, 1(6), pp. 108–116.
- Silvamany H., Jamaliah M. J. (2015), Enhancement of palm oil extraction using cell wall degrading enzyme formulation, *Malaysian Journal of Analytical Science*, 19(1), pp. 77–87.
- Soto C., Chamy R., Zuniga M. E. (2007), Enzymatic hydrolysis and pressing conditions effect on borage oil extraction by cold pressing, *Food Chemistry*, 102(3), pp. 834–840, <https://doi.org/10.1016/j.foodchem.2006.06.014>
- Yakymenko I., Bubliko N., Salavor O., Nychyk O., Shapovalov Ye. (2022), Energy security of the European Union: challenges of russian energy resources, *Selected Papers of IV International Conference on European Dimensions of Sustainable Development, October 20–21, 2022, Kyiv, NUFT, Kyiv*.

# Influence of pumpkin cellulose addition on conformational transformations in the structure of wheat flour dough and bread

Anastasiia Shevchenko, Svitlana Litvynchuk,  
Vira Drobot, Oleksandr Shevchenko

*National University of Food Technologies, Kyiv, Ukraine*

---

## Abstract

### Keywords:

Pumpkin  
Flour  
Cellulose  
Bread  
Dough  
Spectroscopy

**Introduction.** The aim of the present study was to determine the effect of pumpkin cellulose addition to wheat flour on conformational transformations in the structure of dough and bread.

**Materials and methods.** The granulometric composition, functional and technological properties, and amino acid composition of pumpkin cellulose were compared with those of premium grade wheat flour. The influence of pumpkin cellulose in combination with phospholipids on conformational transformations in the structure of dough and bread was studied by method of infrared spectroscopy in the range of near-infrared regions.

**Results and discussion.** It was found that 96% of the particles of wheat flour of the premium grade passed through a sieve with holes of 132 microns, the remaining 4% – through a sieve with holes of 260 microns. Pumpkin cellulose was much coarser, because all 100% of its particles remained on a sieve (hole size 670 microns). Moisture binding capacity of pumpkin cellulose was 3.6 times higher, and moisture retaining capacity was 2.8 times higher than of wheat flour due to the presence of a significant amount of fibers. The amino acid score of lysine (the limiting amino acid in wheat flour) was 0.44. The amino acid score of methionine (the limiting amino acid in pumpkin cellulose) was 3.16, and the amino acid score of lysine was much higher than in wheat flour 3.49. Partial replacement of wheat flour with pumpkin cellulose (5–15%) increased this indicator for lysine by 6.5–15.2%. It was found that infrared spectra of dough samples after kneading (control sample and sample with the partially flour replacement by pumpkin cellulose) practically overlapped throughout the range of wavelengths. During the fermentation process conformational changes of functional groups occurred intensively as well as changes in structural and mechanical properties. The dough ball of the control sample thinned faster. Shape-retaining ability improved with increasing replacement percentage of wheat flour with pumpkin cellulose.

**Conclusions.** The partial replacement of wheat flour with pumpkin cellulose enhanced the biological value of bread and changed the structural and mechanical properties improving shape-retaining ability of dough but decreasing dimensional stability of bread.

---

### Article history:

Received  
29.09.2022  
Received in revised  
form 12.02.2023  
Accepted  
31.03.2023

---

### Corresponding author:

Anastasiia  
Shevchenko  
E-mail:  
nastyusha8@ukr.net

---

### DOI:

10.24263/2304-  
974X-2023-12-1-5

---

## Introduction

The modern food industry is characterized by the production of food with useful properties having health benefits (Ivanov et al., 2021). Simultaneously, taking into account ecological and economic requirements, it is promising to convert the waste of food processing into valuable products using them as additives to increase the nutritional value of food (Dora et al., 2020; Jin et al., 2018; Shevchenko et al., 2023; Stabnikova et al., 2021). Thus, it was relevant to include in the recipes of bread pumpkin processing products with a high content of dietary fibers, which are generated during production of puree, juice, candied fruit and pumpkin oil (Jacobo-Valenzuela et al., 2011; Shevchenko et al., 2023).

Study of the influence of pumpkin residue powder (5 – 20%) and pumpkin pomace (10 – 50%) on the quality of wheat bread showed that an initial increase in the addition of pumpkin residue (5%) indicated an increase in bread volume, which began to decrease in case of higher amounts (10 – 20%) (Ozola et al., 2015). Sensory evaluation (appearance, surface, crust, porosity, texture, crumb, taste and aroma) of wheat bread with pumpkin by-products showed high consumer acceptance, except for the sample with 50% pomace addition. The total content of carotene in bread increased due to the addition of pumpkin by-products (Ahmed et al., 2011). For the production of wheat bread, it was recommended to add from 5% to 10% of pumpkin powder and up to 30% of pumpkin pomace to the dough.

The addition of pumpkin flour to the recipe of wheat bread affected its antioxidant activity and total phenolic content. Bread was made by partially replacing wheat flour with pumpkin flour in amounts from 5% to 20%. Bread enriched with 20% pumpkin flour had the highest antioxidant activity measured by ABTS scavenging activity – 81.74% compared to the control sample – 76.59%. The highest phenolic content – 5.39 mg/g (calculated as gallic acid equivalent) was observed in bread enriched with 20% pumpkin flour, compared to 1.38 mg/g in the control sample. That is, the antioxidant activity of bread increased significantly (Wahyono et al., 2020).

It was found that the introduction of pumpkin puree in the amount from 5 to 25% in the recipe of wheat bread practically did not affect the amount of washed gluten from the dough. However, the compression strain of raw gluten was 68.5–94.7 units, which was worse than for samples without it. In bread with pumpkin puree the content of pectin was 0.03 mg/100g, while pectin was absent in the control sample. The content of vitamins and minerals increased, thereby increasing the nutritional value of bread (Bayramov et al., 2022).

As pumpkin products are rich in beta-carotene, a fat-soluble provitamin A carotenoid, it is recommended to add these raw materials to the food products in combination with lipids (Li et al., 2016). A significant content of them is in lecithin that makes it a valuable additive for enriching bread.

Raw materials introduced in bread influence its structure, so the aim of the present study was to determine the effect of pumpkin cellulose addition on conformational transformations of the structure of dough and bread made from wheat flour.

## Materials and methods

### Materials

Dough samples and bread were prepared from main components – premium wheat flour, salt and pressed baker's yeast. Sunflower lecithin was added in the amounts of 3% by weight of flour (Partridge et al., 2019). 5, 7, 10, 15% pumpkin cellulose was added to replace wheat flour. A sample without pumpkin cellulose was the control sample. All components were mixed and analyzed immediately after kneading and after 3.5 hours of the fermentation. Bread was obtained using a monophasic way of dough preparation.

## Methods

### Size of the flour particles

Sieve analysis was used for determining size of the particles of flour and cellulose. Sieves with different hole sizes were used: No 33/36 (35) (220  $\mu\text{m}$ ), No 27 (260  $\mu\text{m}$ ), No 067 (670), No 49/52 PA (43) (132  $\mu\text{m}$ ), No 41/43 (38) (160  $\mu\text{m}$ ). Sieves were sequentially placed one under the other from the sieve with the largest holes on top to the sieve with the smallest holes at the bottom. The raw material was loaded onto a sieve with the largest hole size and sieved using a vibratory drive device. The percentage ratio of the residue on the sieves and the passage through the sieves was determined (Patwa et al., 2014).

### Moisture binding and retaining capacity

For determining moisture binding capacity, 0.5 g of raw material was placed in pre-weighed centrifuge tubes, 50 ml of distilled water was added, and tubes were centrifuged at 3500 rpm for 10 minutes. The excess water was drained, the raw materials in the test tubes were dried and weighed.

Moisture binding capacity (MBC) was calculated by the formula:

$$\text{MBC} = \frac{m_1}{m_2} \cdot 100,$$

where  $m_1$  is weight of precipitate, g;  $m_2$  is weight of the original flour, g.

For determining the moisture retaining capacity the same method was used. The study differed in that after adding water, the mixture was placed in a water bath for heating for 30 minutes.

Moisture retaining capacity (MRC) was calculated by the formula:

$$\text{MRC} = \frac{m_1 - m_2}{m} \cdot 100,$$

where  $m_1$  is weight of tube with flour and water retained, g;  $m_2$  is weight of tube with flour, g;  $m$  is weight of flour, g.

### Fat binding and fat retaining capacities

The procedure for determination of fat binding and retaining capacities was the same as in the determination of moisture binding and retaining capacities, but instead of water, 15 ml of refined sunflower oil was added.

Fat binding capacity (FBC, %) was determined as the difference between the fat content in the flour suspension ( $F_1$ ) and the amount of fat released after centrifugation ( $F_2$ ):

$$\text{FBC} = F_1 - F_2,$$

Fat retention capacity (FRC, %) was determined as the difference between the fat content in the flour suspension ( $F_1$ ) and the amount of fat released during heat treatment ( $F_{\text{rel}}$ ) (Suriano et al., 2017):

$$\text{FRC} = F_1 - F_{\text{rel}}$$

### Stability of emulsion

For determining the stability of emulsion, oil and water were mixed in a water bath and cooling. 4 calibrated centrifuge tubes (50 ml) were filled with the obtained emulsion and centrifuged at a frequency of 500 rpm for 5 minutes. Then the volume of the emulsified layer was determined.

The stability of the emulsion was calculated by the formula (Silva et al., 2016):

$$SE = \frac{V_1}{V_2} \cdot 100,$$

where SE is stability of the emulsion, %;  $V_1$  is a volume of emulsified oil, ml;  $V_2$  is a total emulsion volume, ml.

### **Emulsifying ability**

7 g of sample was suspended in 100 ml of water in a homogenizer at a frequency of 66.6 rpm for 60 s. Then 100 ml of sunflower oil was added and the mixture was emulsified in a homogenizer at a frequency of 1500 rpm for 5 minutes. After that, the emulsion was put into 4 calibrated centrifuge tubes with (50 ml) and centrifuged at 500 rpm for 10 minutes. Then the volume of emulsified oil in the layer was determined.

Emulsifying ability was calculated by the formula (Silva et al., 2016):

$$EA = \frac{V_1}{V} \cdot 100,$$

where EA is emulsifying ability, %;  $V_1$  is a volume of emulsified oil, ml;  $V$  is a total emulsion volume, ml.

### **Essential amino acid composition**

Amino acid composition in pumpkin cellulose, wheat flour and bread was determined by ion exchange chromatography (Litvynchuk et al., 2022). The process consisted of two stages: hydrolysis of proteins and their quantitative estimation. For this purpose, automatic analyzer of amino acids T-339 (Mikrotechna, Czech Republic) was used. The elution of amino acids was conducted using Li-citrate buffers with pH  $2.75 \pm 0.01$ ;  $2.95 \pm 0.01$ ;  $3.2 \pm 0.02$ ;  $3.8 \pm 0.02$ ;  $5.0 \pm 0.2$  in turn. For Amino detecting amino acids photometer Unicam SP 800 (Great Britain) was used at a wavelength of 560 nm. The process of rectification with a ninhydrin solution was applied. The results of detection were registered by the peaks of light absorption of ninhydrin-positive substances in an eluent. The ratio of concentrations of this substance in solution is direct with these peaks. For obtaining a comparison sample the prototype was diluted in Li-citrate buffer and inflicted on an ion exchange column. The content of every amino acid expressed per 100 g protein.

### **Amino acid score**

Amino acid score was calculated as the ratio of a gram of the limiting amino acid in the food to the same amount of the corresponding amino acid in the standard protein:

$$EAA_{\text{score}} = \frac{EAA_{\text{lim}}}{EAA_{\text{FAO}}},$$

where  $EAA_{\text{score}}$  is amino acid score;  $EAA_{\text{lim}}$  is amount of the limiting amino acid in the sample, g;  $EAA_{\text{FAO}}$  is amount of the corresponding amino acid in the reference standard, the hen's egg protein, g (Caire-Juvera et al., 2013). The Food and Agriculture Organization (FAO) and World Health Organization (WHO) accepted the essential amino acid composition of the hen's egg protein as a reference standard (Lunven et al., 1973).

### Shape-retaining capacity

Shape-retaining capacity was determined by dynamics of changes of spread of the dough ball during fermentation. Dough balls with the weigh of 100 g were placed on transparent glass surface at temperature of 30°C for 180 min. Diameter of dough ball was measured every 30 minutes (Arpül et al., 2015).

### Near-infrared reflection spectroscopy

Spectra of dough and bread was determined by method of infrared spectroscopy in near infrared range from 1330 to 2370 nm. Infrapid spectrometer (Labor-Mim, Hungary) was used to obtain the reflection spectra from smooth surface of shredded samples. The process consisted of two stages: on the first stage, the spectrometer recorded the reflectance spectrum from referential sample, on the second stage a reflection spectrum from the researched sample. The intensity of reflection was measured in dough after kneading and fermentation and in bread (Shevchenko and Litvynchuk, 2022b). The reflection intensity was calculated as transformation of relative reflection coefficient to spectral index (Yip et al., 2012).

### Statistical analysis

The data represents the mean of a minimum three replicates  $\pm$  standard deviation (S.D.). Graphical presentation of experimental data was performed using program Microsoft Excel 2010.

### Results and discussions

Microbiological, biochemical processes in the dough, its structural and mechanical properties, structural changes are significantly influenced by the chemical composition and size of the components of the recipe. It was found that 96% of the particles of wheat flour of the premium grade passed through a sieve with holes of 132 microns, the remaining 4% – through a sieve with holes of 260 microns. Pumpkin cellulose is much coarser, because all 100% of its particles remained on a sieve with hole size 670 microns.

In the process of dough preparation, biochemical, colloidal processes and structure formation of the dough system take place. As a result the structural and mechanical properties of dough and bread are formed. A significant role in these processes belong to the ability of biopolymers of raw materials to absorb and retain moisture and fat, which is introduced with recipe components (Table 1).

**Table 1**  
**Functional and technological properties of premium wheat flour and pumpkin cellulose**

Indicator, %	Wheat flour	Pumpkin cellulose
Moisture binding capacity	90.7 $\pm$ 2.13	330 $\pm$ 2.93
Moisture retaining capacity	148 $\pm$ 2.89	415 $\pm$ 3.02
Fat binding capacity	146 $\pm$ 2.89	216 $\pm$ 2.90
Fat retaining capacity	164 $\pm$ 2.89	280 $\pm$ 2.91
Emulsifying ability	36 $\pm$ 0.50	27 $\pm$ 0.52
Stability of emulsion	31 $\pm$ 0.51	6.8 $\pm$ 0.24

Functional and technological properties of raw materials, particularly the ability to bind and retain moisture and fat, form an emulsion were important (Berton et al., 2002). Due to these characteristics of the raw materials viscoelastic dough was formed, which provided structure and technological properties of dough to obtain high quality bread. Raw materials with less particle exchange usually have a higher index moisture binding capacity and moisture retaining capacity (Changgao et al., 2022). However, both indicators resulted significantly higher in pumpkin cellulose than in wheat flour because of the higher content of fiber present in pumpkin cellulose (Jurgita et al., 2014). Moisture binding capacity of pumpkin cellulose was 3.6 times higher, and moisture retaining capacity 2.8 times higher than of premium wheat flour. The increase of moisture binding capacity of pumpkin cellulose was explained by release of side polar groups of protein, areas of fibers, which had hydrophilic properties and soluble molecules (Qiao et al., 2019).

Meanwhile, values of fat binding and fat retaining capacities were higher for pumpkin cellulose than for wheat flour 1.5 and 1.7 times, respectively. It was explained by the higher content of hydrophobic polysaccharides in pumpkin cellulose. The different distribution of hydrophobic and hydrophilic particles in the composition of pumpkin cellulose compared to wheat flour caused higher values of fat binding and fat retaining capacities (Wang et al., 2017)

In the recipe of bakery products, fat components of plant or animal origin were used, which were difficult to be distributed evenly during the dough kneading process. The ability to form stable emulsions was characterized by emulsifying ability and stability of emulsion. The decrease of these properties for pumpkin cellulose was because it contained lignin, which promoted the formation of interpolymeric bonds between polysaccharides resulting in binding of protein molecules (Aminzadeh et al., 2017).

Pumpkin cellulose contained a large amount of dietary fiber and protein (Shevchenko et al., 2023). The content of essential amino acids (EAA) in pumpkin cellulose was significantly higher than in premium wheat flour (Table 2).

**Table 2**  
**Content of essential amino acids (EAA) in pumpkin cellulose and premium wheat flour**

EAA	Content, g/100 g of raw material	
	Wheat flour	Pumpkin cellulose
Valine	0.42±0.01	1.64±0.01
Isoleucine	0.36±0.01	1.36±0.01
Leucine	0.71±0.02	2.57±0.02
Lysine	0.23±0.01	1.35±0.01
Methionine	0.40±0.01	0.78±0.01
Threonine	0.28±0.01	1.12±0.01
Tryptophan	0.13±0.01	0.72±0.01
Phenylalanine	0.52±0.01	1.86±0.01

The protein of wheat flour was not complete; therefore, to increase the biological value of bread, it was advisable to add pumpkin cellulose. The protein profile of bread with it will increase. The amino acid score, that is the percentage content of each amino acid in relation to its content in the protein taken as a standard, of the limiting amino acid in wheat flour, lysine, was 0.44. The amino acid score of every standard amino acid was 1. For methionine – the limiting amino acid in pumpkin cellulose it was 3.16, and the amino acid score of lysine was much higher than in wheat flour, 3.49. It was found that the amino acid score of the

limiting EAA in pumpkin cellulose was higher than 1. It indicated that the protein of it was complete. Therefore, pumpkin cellulose will increase content of essential amino acids in bread when it is added to the recipe compared to the control sample that was bread without pumpkin cellulose (Table 3).

**Table 3**  
Content of essential amino acids (EAA) in bread with partial replacement of wheat flour with pumpkin cellulose

EAA	Content, g/100 g of bread				
	Control	Pumpkin cellulose to replace wheat flour, %			
		5	7	10	15
Leucine	0.71±0.01	1.14±0.02	1.28±0.02	1.48±0.02	1.76±0.02
Isoleucine	0.39±0.01	0.40±0.01	0.41±0.01	0.41±0.01	0.42±0.01
Methionine	0.31±0.01	0.42±0.01	0.46±0.01	0.52±0.01	0.59±0.01
Lysine	0.23±0.01	0.25±0.01	0.26±0.01	0.26±0.01	0.27±0.01
Phenylalanine	0.68±0.01	0.64±0.01	0.62±0.01	0.61±0.01	0.58±0.01
Threonine	0.28±0.01	0.47±0.01	0.54±0.01	0.62±0.01	0.75±0.01
Valine	0.43±0.01	0.70±0.01	0.80±0.01	0.93±0.01	1.11±0.01
Tryptophan	0.09±0.01	0.23±0.01	0.27±0.01	0.34±0.01	0.43±0.01

The amino acid score for all essential amino acids in bread showed that the limiting amino acid was lysine with score 0.46. Partial replacement of wheat flour with pumpkin cellulose (5–15%) increased lysine score by 6.5–15.2% (Table 4).

**Table 4**  
Amino acid score of essential amino acids (EAA) in bread with partial replacement of wheat flour with pumpkin cellulose

EAA	Amino acid score				
	Control	Pumpkin cellulose to replace wheat flour, %			
		5	7	10	15
Leucine	1.11	1.76	1.98	2.28	2.70
Isoleucine	1.06	1.09	1.09	1.11	1.12
Methionine	0.97	1.31	1.43	1.59	1.82
Lysine	0.46	0.49	0.50	0.52	0.53
Phenylalanine	1.23	1.15	1.12	1.09	1.04
Threonine	0.77	1.28	1.45	1.68	2.01
Valine	0.93	1.53	1.73	1.99	2.37
Tryptophan	0.98	2.45	2.95	3.62	4.56

Nutrients of recipe components of dough and bread contained various functional groups, the change and redistribution of which was largely influenced by the protein composition of the recipe components and their properties. Chemical composition of wheat flour and pumpkin cellulose differed. It was assumed that pumpkin cellulose addition will affect the change in the structural units – OH, NH and SH groups in dough and bread. These units were analyzed in the near infrared region using the reflection spectrum (Baslar et al.,

2011). The results of research of dough and bread samples with the minimum researched replacement (5%) of wheat flour with pumpkin cellulose (Figure 1a) showed that spectra of control dough sample and samples with replacement after kneading and after fermentation, as well as bread samples had a similar character. However, the intensity of reflection was different.

It was found that samples of dough after kneading (control sample and sample with the replacement part of wheat flour by pumpkin cellulose) practically overlapped throughout the range of wavelengths except for the extremum at the wavelength 1930 nm where relative reflection coefficient was 0.47 and 0.49. Overlapping was explained by the fact that the biopolymers of the recipe components did not have time to interact. The difference on the wavelength 1930 nm was explained by the higher moisture binding capacity of pumpkin cellulose (Table 1) which required adding more water to the dough.

Since the proteins of the recipe components were involved in the formation of the gluten frame, they underwent changes during the formation and fermentation of the dough. The lowest extremum at a wavelength of 2100 nm characterized protein substances of the dough (Kröncke and Benning, 2022). The relative reflection coefficient of the control sample and the sample with replacement after kneading was 0.37.

During the fermentation process, conformational changes of functional groups occurred intensively, so spectra of the fermented dough were situated below. The intensity of reflection of the control dough sample was lower than of the sample with pumpkin cellulose. The relative reflectance of the control sample and sample with replacement at a wavelength of 2100 nm was 0.25 and 0.29. It meant that proteins of pumpkin cellulose did not participate in the formation of gluten. This was explained by the fact that its proteins had a globular structure, and pumpkin cellulose contained a large amount of dietary fibers. They were embedded in the gluten framework and delayed its development (Alfaris et al., 2022). That is why the structure of the protein matrix of dough with this component was less stable and more weakened.

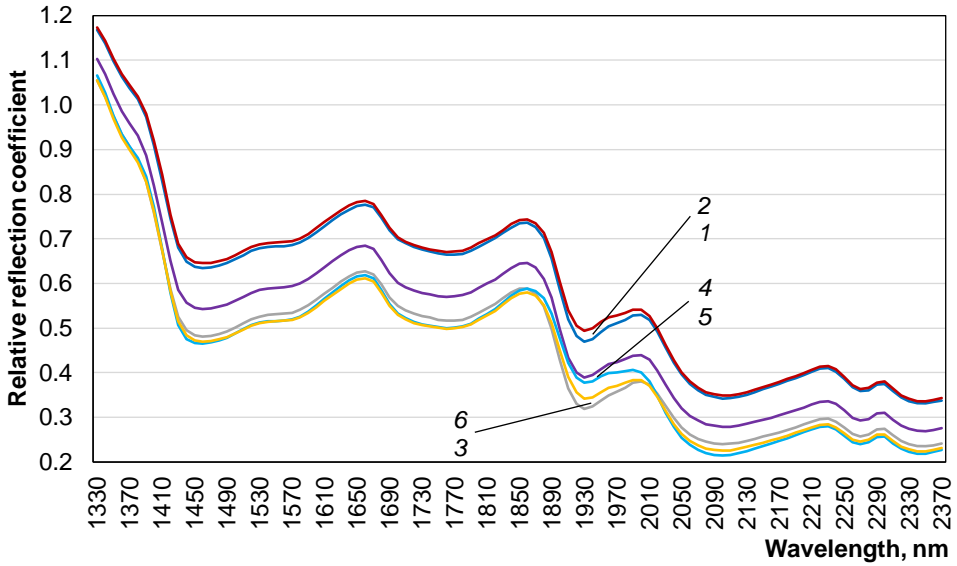
The infrared spectra of bread in terms of intensity practically coincided with the control sample of the dough after fermentation. High temperatures led to the destruction of macromolecules of protein, splitting peptide bonds (Zhou et al., 2021).

The spectra of dough and bread with 15% pumpkin cellulose had a similar character as when replacing 5% (Figure 1b).

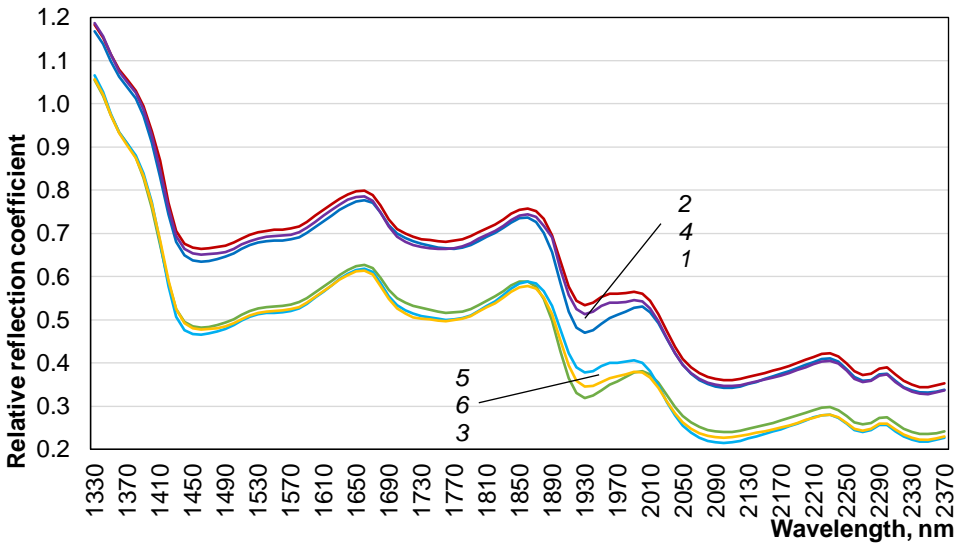
The spectra of the dough after mixing, as in the case of 5% pumpkin cellulose, had the highest relative reflectance in the entire range of wavelengths. However, due to the introduction of a large amount of dietary fiber, the development of the gluten framework of the dough was delayed, pumpkin cellulose significantly binded water and the fermentation process slowed down. It is very visible at the wavelength of 2100 nm because the relative reflectance of the sample of dough with 5% pumpkin cellulose after fermentation was 0.36, which is significantly higher than the control sample and the sample with 5% replacement.

The spectrum of the dough of the control sample after fermentation was close to the spectra of bread. The difference was observed at the wavelength of 1930 nm, which is because of the different moisture content in the samples. Technologically it confirms that the addition of 15% pumpkin cellulose will contribute more to less dilution of the dough ball during fermentation (Figure 2).

It was found that during the period of fermentation, the dough ball of the control sample thinned faster. This is explained by the fact that the content of fiber and pentosans in pumpkin cellulose increased viscosity of the dough system in samples with this recipe component (Apostol et al., 2020). Shape-retaining ability improved with increasing replacement percentage.



*a*



*b*

**Figure 1. Reflection spectra of dough and bread:**  
*a* – with 5% pumpkin cellulose; *b* – with 15% pumpkin cellulose

- 1 - Control sample of the dough after kneading
- 2 - Sample of dough with 5% pumpkin cellulose after kneading
- 3 - Control sample of the dough after 3.5 hours of fermentation
- 4 - Sample of dough with 5% pumpkin cellulose after 3.5 hours of fermentation
- 5 - Control sample of bread
- 6 - Sample of bread with 5% of pumpkin cellulose

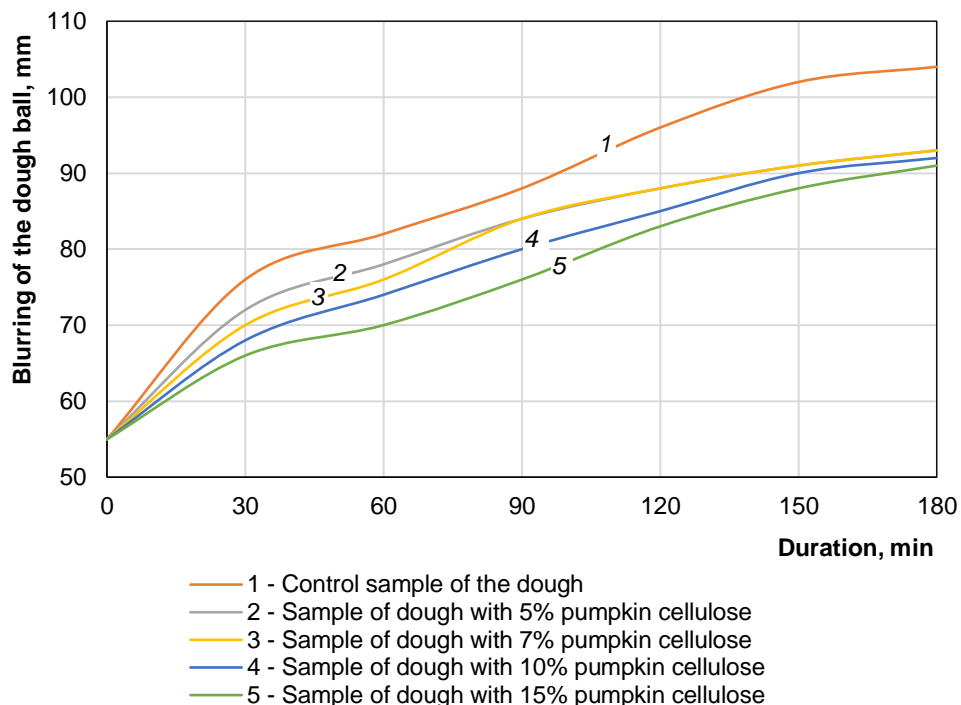


**Figure 3. Dynamics of changes in the shape-retaining ability of the dough during fermentation**

Thus, pumpkin cellulose improved the biological value of bread due to the higher content of dietary fiber, protein and complete amino acid profile. It also affected the structural and mechanical properties of dough and bread improving shape-retaining ability of dough but decreasing dimensional stability of bread.

## Conclusions

1. The pumpkin cellulose had larger particle sizes than wheat flour because all 100% of its particles remained on a sieve with hole size 670 microns. At the same time 96% of the particles of wheat flour of the premium grade passed through a sieve with holes of 132 microns.
2. Pumpkin cellulose binds water 3.6 times better and retains water 2.8 times better than wheat flour.
3. The limiting amino in wheat flour is lysine with amino acid score 0.44. Addition of pumpkin cellulose in bread (5–15%) increased the amino acid score for lysine by 6.5–15.2%.
4. During the fermentation process in dough with pumpkin cellulose conformational changes of functional groups occurred more intensively than in samples without it.
5. Addition of pumpkin cellulose affected the structural and mechanical properties of dough and bread, improving shape-retaining ability of dough but decreasing dimensional stability of bread.

## References

- Ahmed J., Al-Foudari M., Al-Salman F., Almusallam A. S. (2014), Effect of particle size and temperature on rheological, thermal, and structural properties of pumpkin flour dispersion, *Journal of Food Engineering*, 124, pp. 43–53, <https://doi.org/10.1016/j.jfoodeng.2013.09.030>
- Alfaris N. A., Gupta A. K., Khan D., Khan M., Wabaidur S. M., Altamimi J. Z., Alothman Z. A., Aldayel T. S. (2022), Impacts of wheat bran on the structure of the gluten network as studied through the production of dough and factors affecting gluten network, *Food Science and Technology (Campinas)*, 42(3), <https://doi.org/10.1590/fst.37021>
- Aminzadeh S., Zhang L., Henriksson G. (2017), A possible explanation for the structural inhomogeneity of lignin in LCC networks, *Wood Science and Technology*, 51(2), pp. 1365–1376, <https://doi.org/10.1007/s00226-017-0941-6>
- Apostol L., Mosoiu C., Iorga S. C., Sanmartin A. M. (2020), Effect of the addition of pumpkin powder on the physicochemical qualities and rheological properties of wheat flour, *Romanian Biotechnological Letters*, 25(3), pp. 1594-1600, <https://doi.org/10.25083/rbl/25.3/1594.1600>
- Arpul O., Sylchuk T., Kulinich V., Usatiuk O. (2015), The use of plant materials in culinary products out of yeasted dough, *Food and Environment Safety*, 14(1), pp. 1–6.
- Baslar M., Ertugay M.F. (2011), Determination of protein and gluten quality-related parameters of wheat flour using near-infrared reflectance spectroscopy (NIRS), *Turkish Journal of Agriculture and Forestry*, 35(2), pp. 139–144, <https://doi.org/10.3906/tar-0912-507>
- Bayramov E., Aliyev S., Gasimova A., Gurbanova S., Kazimova I. (2022), Increasing the biological value of bread through the application of pumpkin puree, *Eastern-European Journal of Enterprise Technologies*, 2(11(116)), pp. 58–68, <https://doi.org/10.15587/1729-4061.2022.254090>
- Berton B., Scher J., Villieras F., Hardy J. (2002), Measurement of hydration capacity of wheat flour: Influence of composition and physical characteristics, *Powder Technology*, 128(2), 326-331, [https://doi.org/10.1016/S0032-5910\(02\)00168-7](https://doi.org/10.1016/S0032-5910(02)00168-7)
- Caire-Juvera G., Vázquez-Ortiz F.A., Grijalva-Haro M.I. (2013), Amino acid composition, score and in vitro protein digestibility of foods commonly consumed in Northwest Mexico, *Nutricion Hospitalaria*, 28(2), pp. 365-371, <https://doi.org/10.3305/nh.2013.28.2.6219>
- Choi Y.S., Kim H.W., Hwang K.E., Song D.H., Park J.H., Lee S.Y., Choi M.S., Choi J.H., Kim C.J. (2012), Effects of pumpkin (*Cucurbita maxima* Duch.) fiber on physicochemical properties and sensory characteristics of chicken frankfurters, *Food Science of Animal Resources*, 32, pp. 174–183, <https://doi.org/10.5851/kosfa.2012.32.2.174>
- Changgao S., Olkhovikov O., Xiaojin G., Marynin A., Sichen Z., Shevchenko A., Botong S., Yue Z. (2022), Research and comparative analysis of the qualitative parameters of food powders produced from grain raw materials using an improved jet mill, *Technology Audit and Production Reserves*, 6(3(68)), pp. 36–43, <https://doi.org/10.15587/2706-5448.2022.271557>
- Dora M., Wesana J., Gellynck X., Seth N., Dey B., Steur H. (2020), Importance of sustainable operations in food loss: evidence from the Belgian food processing industry, *Annals of Operations Research, Springer*, 290(1), pp. 47-72, <https://doi.org/10.1007/s10479-019-03134-0>

- Ivanov V., Shevchenko O., Marynin A., Stabnikov V., Gubenia O., Stabnikova O., Shevchenko A., Gavva O., Saliuk A. (2021), Trends and expected benefits of the breaking edge food technologies in 2021-2030, *Ukrainian Food Journal*, 10(1), pp. 7–36, <https://doi.org/10.24263/2304-974X-2021-10-1-3>
- Jacobo-Valenzuela N., Maróstica-Junior M.R., Zazueta-Morales J. de J., Gallegos-Infante J.A. (2011). Physicochemical, technological properties and health-benefits of *Cucurbita moschata* Duchense vs. Cehualca, *Food Research International*, 44(9), 2587–2593, <https://doi.org/10.1016/j.foodres.2011.04.039>
- Jin, Q., Yang, L., Poe, N., Huang, H. (2018), Integrated processing of plant-derived waste to produce value-added products based on the biorefinery concept, *Trends in Food Science & Technology*, 74, pp. 119-131, <https://doi.org/10.1016/j.tifs.2018.02.014>
- Jurgita K., Jariene E., Danilcenko H., Černiauskiene J., Wawrzyniak A., Hamulka J., Juknevičienė E. (2014), Chemical composition of pumpkin (*Cucurbita maxima* D.) flesh flours used for food, *Journal of Food Agriculture and Environment*, 12(3), pp. 61-64, <https://doi.org/10.1234/4.2014.5357>
- Kröncke N., Benning R. (2022), Determination of moisture and protein content in living mealworm larvae (*Tenebrio molitor* L.) using near-infrared reflectance spectroscopy (NIRS), *Insects*, 13, p. 560, <https://doi.org/10.3390/insects13060560>
- Li W., Zhai S., Jin H., Wen W., Liu J., Xia X., He Z. (2016), Genetic variation of carotenoids in Chinese bread wheat cultivars and the effect of the 1BL.1RS translocation, *Frontiers of Agricultural Science and Engineering*, 3(2), pp. 124-130, <https://doi.org/10.15302/J-FASE-2016094>
- Litvynchuk S., Galenko O., Cavicchi A., Ceccanti C., Mignani C., Guidi L., Shevchenko A. (2022), Conformational changes in the structure of dough and bread enriched with pumpkin seed flour, *Plants*, 11, 2762, <https://doi.org/10.3390/plants11202762>
- Lunven P., Marcq C., Carnovale E., Fratoni A. (1973), Amino acid composition of hen's egg, *British Journal of Nutrition*, 30(2), 189-194, <https://doi.org/10.1079/BJN19730024>
- Ozola L., Straumite E., Galoburda R. (2015), Quality parameters of wheat bread enriched with pumpkin (*Cucurbita moschata*) by-products, *Acta Universitatis Cibiniensis. Series E: Food Technology*, 19(2), pp. 3-14, <https://doi.org/10.1515/auaft-2015-0010>
- Partridge D., Lloyd K. A., Rhodes J. M., Walker A. W., Johnstone A. M., Campbell B.J. (2019), Food additives: Assessing the impact of exposure to permitted emulsifiers on bowel and metabolic health – introducing the FADiets study, *Nutrition Bulletin*, 44(4), pp. 329–349, <https://doi.org/10.1111/nbu.12408>
- Patwa A., Malcolm B., Wilson J., Ambrose K. (2014), Particle size analysis of two distinct classes of wheat flour by sieving, *Transactions of the ASABE (American Society of Agricultural and Biological Engineers)*, 57(1), pp. 151–159, <https://doi.org/10.13031/trans.57.10388>
- Qiao B., Jiménez-Ángeles F., Nguyen T. D., Olvera de la Cruz M. (2019), Water follows polar and nonpolar protein surface domains, *Proceedings of the National Academy of Sciences*, 116(39), pp. 19274–19281, <https://doi.org/10.1073/pnas.1910225116>
- Shevchenko A., Litvynchuk S. (2022), Influence of rice flour on conformational changes in the dough during production of wheat bread, *Ukrainian Journal of Food Science*, 10(1), pp. 5–15, <https://doi.org/10.24263/2310-1008-2022-10-1-3>
- Shevchenko A., Fursik O., Drobot V., Shevchenko O. (2023), The use of wastes from the flour mills and vegetable processing for the enrichment of food products. In O. Stabnikova, O. Shevchenko, V. Stabnikov, O. Paredes-López (Eds.), *Bioconversion of waste to value-added products*, (pp. 2-24), CRC Press, Boca Raton, <https://doi.org/10.1201/9781003329671-1>

- Silva B.V., Barreira J.C.M, Oliveira M.B.P. (2016), Natural phytochemicals and probiotics as bioactive ingredients for functional foods: Extraction, biochemistry and protected-delivery technologies, *Trends in Food Science & Technology*, 50(5), pp. 144–158, <https://doi.org/10.1016/j.tifs.2015.12.007>
- Stabnikova O., Marinin A., Stabnikov V. (2021), Main trends in application of novel natural additives for food production, *Ukrainian Food Journal*, 10(3), pp. 524–551, <https://doi.org/10.24263/2304-974X-2021-10-3-8>
- Suriano F., Bindels L. B., Verspreet J., Courtin C. M., Verbeke K., Cani P.D., Neyrinck A.M., Delzenne N.M. (2017), Fat binding capacity and modulation of the gut microbiota both determine the effect of wheat bran fractions on adiposity, *Scientific Reports*, 7, 5621, <https://doi.org/10.1038/s41598-017-05698-y>
- Wang L., Ye F., Li S., Wei F., Chen J., Zhao G. (2017), Wheat flour enriched with oat β-glucan: A study of hydration, rheological and fermentation properties of dough, *Journal of Cereal Science*, 75, pp. 143–150, <https://doi.org/10.1016/j.jcs.2017.03.004>
- Wahyono A., Dewi A.C., Oktavia S., Jamilah S., Kang W.W. (2020), Antioxidant activity and total phenolic contents of bread enriched with pumpkin flour, *IOP Conference Series: Earth and Environmental Science*, 411, 012049, <https://doi.org/10.1088/1755-1315/411/1/012049>
- Yip W.L., Gausemel I., Sande S.A., Dyrstad K. (2012), Strategies for multivariate modeling of moisture content in freeze-dried mannitol-containing products by near-infrared spectroscopy, *Journal of Pharmaceutical and Biomedical Analysis*, 70, pp. 202–211, <https://doi.org/10.1016/j.jpba.2012.06.043>
- Zhou Y., Dhital S., Zhao C., Ye F., Chen J., Zhao G. (2021), Dietary fiber-gluten protein interaction in wheat flour dough: Analysis, consequences and proposed mechanisms, *Food Hydrocolloids*, 111, 106203, <https://doi.org/10.1016/j.foodhyd.2020.106203>

## Comparative study of properties of basmati and non-basmati rice cultivars

Roshanlal Yadav<sup>1</sup>, Sakshi Khurana<sup>2</sup>, Sunil Kumar<sup>3</sup>

1 – Lakshmibai College, University of Delhi, India

2 – Bhaskaracharya College of Applied Sciences, University of Delhi, India

3 – Maharaja Ganga Singh University, India

---

### Abstract

#### Keywords:

Basmati rice  
Amylose  
Milling  
Cooking  
Textural

**Introduction.** The aim of this study was to analyze the physicochemical, cooking, textural and milling properties of different basmati and non-basmati rice cultivars.

**Materials and methods.** The de-husking and milling of the paddy were performed using a laboratory mill, and the head rice recovery was determined using Adair's methods. The milled rice was analyzed for moisture, ash, protein, and amylose content. The textural attributes of cooked grains were analyzed using Texture Profile Analysis.

**Results and discussion.** The study presented the milling and chemical properties of different rice cultivars, which affect the quality and market value of rice. The recovery of milled rice was found to vary among cultivars, with Pusa Basmati (PB)-6 exhibiting the highest recovery and PB-1121 having the highest husk percentage. Head rice recovery was highest in P-44 and lowest in PB-6, while the moisture content of the milled rice grain ranged from 10.75 to 11.84%. PB-1121 had the highest ash content, while P-2819 had the lowest ash and protein content. Basmati varieties had significantly lower starch content and higher amylose content than the non-basmati cultivar. In terms of physical properties, the bulk density measurements showed that PB-6 had the lowest bulk density, while P-44 had the highest bulk density. When it came to true density, P-2819 stood out with the highest value. Additionally, the study found that basmati varieties tended to have longer grains compared to non-basmati varieties. Furthermore, when examining the length-to-breadth ratio, PB-1121 stood out with the highest ratio, suggesting a relatively slender and elongated grain shape. The cooking properties of the rice cultivars investigated in the study revealed interesting variations. P-2819 demonstrated the shortest cooking time, whereas PB-1121 showed the longest cooking time. The elongation ratio was found to be higher in basmati varieties compared to non-basmati varieties. When considering water uptake, PB-1121 exhibited the highest ratio, implying that it absorbed more water during cooking. Additionally, the solid loss was highest in P-2819 and lowest in PB-1121. In reference to textural properties, P-2819 exhibited the highest hardness, whereas PB-1121 had the lowest. The adhesiveness of the non-basmati variety was higher than that of the basmati variety, indicating a stickier texture. PB-1121 had the lowest gumminess, indicating a lesser tendency for the grains to become gummy. The correlation study revealed significant relationships between rice properties. Cooking time correlated positively with true density, length to breadth ratio, hardness, gumminess, and chewiness. Elongation ratio correlated positively with amylose content, porosity, length, length to breadth ratio, and 1000 kernel weight. Water uptake ratio showed multiple positive correlations.

**Conclusion.** By leveraging these insights, stakeholders can enhance the quality, market value, and overall satisfaction of rice products.

---

#### Article history:

Received  
28.11.2022  
Received in  
revised form  
16.01.2023  
Accepted  
31.03.2023

---

#### Corresponding author:

Roshanlal  
Yadav  
E-mail:  
roshanfst@  
gmail.com

---

#### DOI:

10.24263/2304-  
974X-2023-12-  
1-6

## Introduction

Rice (*Oryza sativa*) is a crucial cereal crop that serves as a staple food for more than half of the world's population, providing 20% of its dietary energy supply (Panigrahi et al., 2018). With approximately 95% of its production in Asia, rice comes in countless varieties, with India being a significant contributor. Basmati rice, which constitutes only 1% of India's total rice production, is a registered geographical indicator product of India known for its characteristic aroma, exceptional cooking and textural properties, and unique flavor due to the hydrolysis of starch (Prom-U-Thai and Rerkasem, 2020). Basmati rice is considered one of the most acceptable classes of rice globally, especially for its soft and fluffy texture, and is an outstanding example of long-grain flavor rice varieties (Sliwinska-Bartel et al., 2021). Non-basmati rice, on the other hand, is rice that does not have the characteristics of basmati rice, which can have diverse shapes and sizes such as long-slender, short-thick, beads, or even round, with properties entirely different from basmati rice (Bhattacharjee et al., 2002). Researchers have studied various rice varieties, including their physical properties, milling characteristics, physicochemical properties, and cooking characteristics to establish the differences between the various cultivars grown worldwide (Shobhan et al., 2016; Yadav et al., 2014). Moreover, physicochemical and cooking properties of rice cultivars from Pakistan and found significant differences in amylose content, water uptake, and cooking time (Murtaza et al., 2022). With the increasing demand for rice globally, there is a tremendous amount of scope to carry out further research on different rice cultivars to improve their yield, quality, and nutritional content to meet the growing needs of the population.

Consumer acceptance of rice is influenced by the milling degree, i.e. the percentage of bran removed from the brown rice grain. Milling produces white rice with a higher market value than brown rice. Besides influencing the colour, the milling degree also improves the cooking behaviour of rice. Brown rice has poor water absorption capacity and cooks slower than white rice (Nzonzo and Mogambi, 2016). In general, 'head rice' comprises kernels that are 75-80 percent of the whole kernel. The quality of milled rice is measured on the yield of 'head rice'. The market value of 'broken' is reduced to about half that of head rice and the milling process is one of the factors responsible for brain damage and loss besides losses caused due to harvesting, drying or handling (Nzonzo and Mogambi, 2016). One of the exceptional characteristics of basmati rice cultivars is kernel elongation during cooking, which has a complex inheritance pattern. Other important basmati features- aroma and slenderness are effortlessly inherited and simple to transfer. Consumers prefer rice that is elongated in length when cooked. The phenomenon of elongation is influenced by numerous genetic or physicochemical factors, including genotypes, ageing temperature, ageing time, water uptake, amylose content and gelatinization temperature (Faruq and Prodhan, 2013).

The physicochemical properties like grain weight and size, including the length, breadth and length: breadth ratio, damaged rice, moisture, ash, protein, starch and amylose content, have a significant impact on the marketing value of rice. Grain size and shape are the properties that vary with the variety of grain under consideration. Determination of the physical properties of the grain, including dimensional analysis, bulk density and thousand grains weight, is essential for the design and development of storage bins that help prevent spoilage by molds and insect infestation (Pandiselvam et al., 2015). Thus, the physicochemical, organoleptic and cooking properties are very significant for the consumers to evaluate the superiority and preference of rice (Verma and Srivastav, 2020). Moreover, the physicochemical properties and amylose content collectively determine rice's thermal/cooking quality (Sujatha et al., 2004). Water uptake is conventionally defined as the grams of water absorbed per gram of rice in a given time when rice is cooked directly in boiling

water. It is affected by grain surface area per unit weight. Therefore, more petite and more slender grains would cook in a shorter period than bigger and rounder grains. Soaking before cooking not only cuts down cooking time but also enhances kernel elongation. Bhattacharya (2011) reported that water uptake, which is influenced by grain surface area per unit weight, affects the cooking time and kernel elongation of rice. The author also noted that soaking before cooking enhances kernel elongation and reduces cooking time. Concerning this, the present study evaluated the essential properties of certain developed Indian rice cultivars.

## **Materials and methods**

### **Materials**

The Indian Agricultural Research Institute, Pusa, Delhi, provided four paddy cultivars, including two non-basmati (P-44 & P-2819) and two basmati (PB-1121 & PB-6), for this study.

### **De-husking and milling of paddy**

The paddy seeds of various selected cultivars were hulled using a laboratory model of Paddy de husker and the milling was performed with a rice miller (McGill type, Osawa Industries Pvt. Ltd, India). After de-husking, the percentage of husk and recovery of rice grain were measured and after milling, the head rice recovery was determined using Adair's methods (Adair, 1952).

### **Chemical properties of milled rice**

Moisture, ash and protein content of different cultivars of milled rice grain were determined using the standard analysis methods (AOAC, 2000). Amylose content was determined by using the method of Juliano (1971) with some minor modifications. 0.1 g of rice flour was taken in a test tube and 1 mL ethanol (95%) and 9 mL of 1N sodium hydroxide were added. The samples were heated in a boiling water bath, cooled for about one h, and the final volume was made up to 100 mL with distilled water. 5 mL of this sample solution was taken in a test tube and 1 mL of 1 N acetic acid followed by 2 mL of iodine solution were added into it and the absorbance of the solution was measured at 620 nm.

### **Physical properties of rice kernel**

The dimensional parameters such as grain length (L) and breadth (B) of milled rice were measured with vernier calipers. The measurement was performed by using 10 grains in each sample; thus, averages of 10 grains were recorded. The ratio of length and breadth (L/B) ratio, was also determined for milled rice (Kaur et al., 2011). The Gravimetric properties viz., 1000 kernels weight of each sample was determined by counting randomly selected 1000 kernels. The bulk density was determined using the mass/volume relationship. It was determined by tenderly pouring the grains into a 100 mL graduated cylinder and it was weighed. The actual density was determined using the kerosene displacement method by immersing a weighted quantity of rice grains in the known volume of kerosene. Porosity (%) was estimated with the help of values obtained from bulk and true density and by using the following equation:

$$\text{Porosity (\%)} = 1 - (\text{Bulk density} / \text{True Density}) \times 100$$

### **Cooking properties of milled rice**

The cooking properties of milled rice were observed using the method of Yadav et al. (2014). The milled head rice (2 g) of each cultivar was cooked with 20 mL distilled water, taken in a test tube of 50 mL and cooked in a boiling water bath. The cooking time was determined by analyzing a few grains at different time intervals during cooking till no white core was left. The elongation ratio of rice grain was measured by dividing the length of cooked grain by the length of the uncooked grain. To determine water uptake, the weight of cooked rice and uncooked rice was measured carefully, and water absorption was determined based on water gained after cooking. Solid loss in gruel was measured by completely drying left-out cooking water in a hot air oven at 105 °C.

### **Texture profile analysis (TPA)**

The textural attributes of cooked grains were observed using T.A. X.T. Plus, Stable Microsystems, UK. TPA in terms of hardness, adhesiveness, springiness, cohesiveness, gumminess, chewiness and resilience were measured according to the method given by Li et al. (2016) with some minor modifications. Three cooked rice kernels were positioned centrally under a probe (35mm) on the base plate, and the test was carried out by selecting the force vs distance compression program; other settings were as follows: Strain, 90%; Pre-Test Speed, 0.5 mm/s; Test Speed, 0.5 mm/s; Post-Test Speed, 2.00 mm/s; Trigger Force (auto), 0.05 N.

### **Statistical analysis**

The experiments were conducted in triplicate, and the mean values along with standard deviations were calculated using SPSS 25. The significant difference was analyzed using Tukey pairwise comparisons ( $P < 0.05$ ). Pearson correlation was calculated using SPSS 25 to determine the relationship between various physical, chemical, cooking, and textural properties of different rice grain varieties.

## **Results and discussion**

### **Milling and chemical properties of various rice cultivars**

The market value of rice generally depends on its milling performance because of the total recovery; the proportion of head and broken rice categorizes its quality. The milling properties of rice cultivars are presented in Table 1; after milling, various properties like husk percentage, milled rice and head rice percentage were observed. Maximum husk percentage was measured in PB-1121 and P-2819; minimum was estimated in PB-6, followed by PB-44. Reciprocally, the recovery of milled rice was observed maximum in PB-6. In terms of head rice recovery most excellent recovery (71.77%) was calculated for P-44 and significantly least (63.23%) recovery was observed for PB-6. Sandhu et al. (2018) also reported that milling recovery varied from 49.43% to 77.08% for some Indian rice varieties. Similarly, Falade and Christopher (2015) observed that milling recovery varied from 45.74% to 68.24% for six Nigerian rice cultivars. They also reported that a recovery equal to or less than 50% is undesirable. Moreover, similar milling properties of different rice varieties were reported in earlier studies (Kaur et al., 2011; Rather et al., 2016; Verma and Srivastav, 2020). A studies conducted by Li et al. (2021) and Ertop et al. (2020) examined the impact of milling

degree on the physical and chemical properties of rice flour, and found that the milling process significantly affects the flour quality. Similarly, a study by Yuliana et al. (2020) investigated the milling characteristics and physicochemical properties of Indonesian rice varieties, and found that the milling efficiency has a significant impact on the head rice yield and total milling recovery. The study revealed that the more efficient milling process resulted in a higher total milling recovery, indicating that a larger quantity of milled rice was obtained from the same amount of raw paddy. Moreover, research by Sandhu et al. (2018) and Falade and Christopher (2015) provides evidence of the significant variation in milling recovery among different rice cultivars. In their studies, milling recovery was found to range from 45.74 to 77.08% for six Nigerian rice cultivars and from 49.43 to 77.08% for some Indian rice varieties. A recovery equal to or less than 50% was deemed undesirable by Falade and Christopher, further highlighting the importance of milling performance in determining rice quality and market value.

The chemical properties such as moisture, ash, protein, starch and amylose of the milled rice grain are presented in Table 1. The moisture content was estimated in the range of 10.75 to 11.84%. Previous studies have conducted moisture content analysis on various rice cultivars, revealing a range of values across different investigations. For instance, Elbashir (2005) reported moisture contents ranging from 8.6 to 10.9% in their study. Similarly, Kaur et al. (2011) found moisture contents between 10.05 and 12.61% in another research, while He et al. (2021) observed moisture contents ranging from 11.15 to 13.40% in their study. The ash content was measured maximum in PB-1121 and significantly lower was observed for P-2819. No trend of difference in ash contents was observed between basmati and non-basmati varieties, as reported by Kaur et al. (2011). However, their tested varieties ranged between 0.24 to 0.62% ash content, while Verma and Srivastav (2020) ranged between 0.48 to 0.85% in different varieties of rice. The protein content was observed in the range of 5.87 to 7.27%, and it was observed highest for cultivar PB-6 and lowest for P-2819. Several studies have investigated the protein content of various rice cultivars, providing valuable insights into the range of protein levels observed. For instance, Elbashir (2005) reported protein content ranging from 6.2% to 8% in different rice cultivars. In another study by Verma and Srivastav (2020), protein content in aromatic rice varieties was found to be within the range of 7.23 to 9.51%. Similarly, Sandhu et al. (2018) observed protein content ranging from 7.92 to 8.02% in short and long grain Indica rice cultivars. Starch content was observed to be higher for non-basmati cultivars, i.e. P-2819 and P-44 and lower for basmati cultivars, i.e. PB-6 and PB-1121.

The amylose content usually has considerable effects on the cooking characteristics and eating quality of rice apart from being a significant decider of the textural properties (hardness and adhesiveness) of cooked rice (Suwannaporn et al., 2007). The amylose content was significantly lower for variety P-44 and highest for variety PB-1121. The amylose content is an ancillary characteristic of rice and should range from 20–25% for basmati varieties. Ahuja et al. (1995) reported amylose content in different basmati rice varieties cultivated in India, ranging from 19.10 to 27.14%. This amylose content was in accordance with non-aromatic IRRI (International Rice Research Institute) varieties. The amylose content in non-aromatic rice varieties can range from around 20% to over 30%, depending on the specific variety and growing conditions (Butardo et al., 2019). Research has also shown that rice flour with a higher amylose content tends to ferment more slowly than rice flour with a lower amylose content. This is because amylose is less soluble in water than amylopectin, and therefore more resistant to enzymatic breakdown during fermentation (Medvid et al., 2017).

**Table 1**

**Milling and chemical compositions of different rice cultivars**

<b>Properties, %</b>	<b>PB-6</b>	<b>PB-1121</b>	<b>P-2819</b>	<b>P-44</b>
Husk	12.00±0.30 <sup>c</sup>	17.03±0.15 <sup>a</sup>	17.00±0.20 <sup>a</sup>	12.73±0.25 <sup>b</sup>
Milled Rice	88.00±0.30 <sup>a</sup>	82.97±0.15 <sup>c</sup>	83.00±0.20 <sup>c</sup>	87.27±0.25 <sup>b</sup>
Head Rice	63.23±1.08 <sup>c</sup>	68.23±1.08 <sup>b</sup>	68.17±0.76 <sup>b</sup>	71.77±0.32 <sup>a</sup>
Moisture Content	11.64±0.17 <sup>b</sup>	10.75±0.36 <sup>c</sup>	11.44±0.20 <sup>b</sup>	11.84±0.07 <sup>b</sup>
Ash	0.39±0.01 <sup>b</sup>	0.43±0.02 <sup>a</sup>	0.32±0.01 <sup>c</sup>	0.42±0.02 <sup>ab</sup>
Protein	7.27±0.06 <sup>a</sup>	7.06±0.05 <sup>a</sup>	5.87±0.18 <sup>c</sup>	6.62±0.22 <sup>b</sup>
Total Starch	69.58±0.14 <sup>b</sup>	69.29±0.14 <sup>b</sup>	70.59±0.13 <sup>a</sup>	70.29±0.16 <sup>a</sup>
Amylose Content	20.28±0.16 <sup>b</sup>	21.54±0.19 <sup>a</sup>	17.07±0.08 <sup>c</sup>	16.12±0.18 <sup>d</sup>

All data are reported as mean±SD (n=3)

Different alphabets in superscripts indicate significant differences (p<0.05) among various rice cultivar

**Physical properties of different varieties of milled rice**

Grading of rice grain based on physical characteristics such as length, breadth, density, and porosity is crucial for consumer acceptance of a particular variety. In Table 2, the physical properties of four different varieties of milled rice are presented. The bulk density (BD) was found to be the lowest for variety PB-6 and the highest for P-44, indicating that longer grains have a lower bulk density, and PB-6 would require more storage space while P-44 would require the least. The true density was observed to be significantly higher in P-2819, which is consistent with findings reported by Kaur et al. (2011) for different rice cultivars grown in India. The relationship between bulk density and true density is presented in the form of porosity, and it was observed that basmati varieties have a higher value than non-basmati varieties, which agrees with previous studies (Singh et al., 2005). The lengths of all the varieties ranged from 7.10 to 7.80 mm, with lower values observed for non-basmati varieties and higher values for basmati varieties. Similar results were observed in different previous studies of basmati and non-basmati cultivars (Kaur et al., 2011). Moreover, the width was measured in the range from 1.53 to 1.77 mm, with the maximum estimated for P-2819 and the minimum for PB-1121.

**Table 2**

**Physical properties of different variety of milled rice grains**

<b>Properties</b>	<b>PB-6</b>	<b>PB-1121</b>	<b>P-2819</b>	<b>P-44</b>
Bulk Density (g/ml)	0.68±0.01 <sup>b</sup>	0.69±0.01 <sup>ab</sup>	0.70±0.01 <sup>ab</sup>	0.72±0.01 <sup>a</sup>
True Density (g/ml)	1.27±0.01 <sup>a</sup>	1.29±0.01 <sup>a</sup>	1.24±0.01 <sup>c</sup>	1.26±0.01 <sup>ab</sup>
Porosity (%)	46.60±1.00 <sup>a</sup>	46.50±1.19 <sup>a</sup>	43.39±1.04 <sup>b</sup>	43.27±0.65 <sup>b</sup>
Length (mm)	7.47±0.06 <sup>b</sup>	7.80±0.10 <sup>a</sup>	7.10±0.10 <sup>bc</sup>	7.20±0.17 <sup>b</sup>
Width (mm)	1.70±0.10 <sup>ab</sup>	1.53±0.06 <sup>b</sup>	1.77±0.06 <sup>a</sup>	1.63±0.06 <sup>ab</sup>
L/B Ratio	4.40±0.26 <sup>b</sup>	5.09±0.13 <sup>a</sup>	4.02±0.09 <sup>b</sup>	4.42±0.23 <sup>b</sup>
1000 Kernel Weight (g)	19.27±0.15 <sup>b</sup>	20.43±0.40 <sup>a</sup>	18.27±0.25 <sup>c</sup>	18.50±0.20 <sup>c</sup>

All data are reported as mean±SD (n=3)

Different alphabets in superscripts indicate significant differences (p<0.05) among various rice cultivar

A length to breadth (L/B) ratio is used to classify the shape of rice grains; the higher value of the L/B ratio indicates slender shapes, whereas intermediate, medium, round or bold shapes of grains are indicated by a lower L/B ratio (Verma and Srivastav, 2020).

In this study, the L/B ratio was significantly higher in PB-1121. As per the provisions of the Seed Act, 1966, length, breadth and L/B ratio are primary quality characteristics of Basmati rice, for which it has also laid down standards. According to it, the minimum average precooked milled rice length should be 6.61 mm, the average precooked milled rice breadth  $\leq 2.00$  mm and the minimum length/breadth ratio of precooked milled rice should be 3.50. Ahuja et al. (1995) reported length varying between 6.74 mm to 7.10 mm, breadth 1.65 mm to 1.78 mm and L/B ratio 3.84 to 4.08, while for Kaur et al. (2011), these values were 6.77 mm to 8.23 mm, 1.54 mm to 1.75 mm and 3.86 to 5.01, respectively for different basmati rice varieties. Furthermore, Kaur et al. (2011) also reported significantly higher length, lower breadth and higher L/B ratio of basmati varieties compared to non-basmati rice cultivars. The physical property was also estimated as 1000 kernel weight, which varied from 18.27 to 20.43 g. Other researchers observed 1000 kernel weight ranging from 14.53 to 18.89g for rice grown in different countries such as America, Pakistan, Egypt, Thailand and Sudanese (Elbashir, 2005).

### Cooking properties of different varieties of milled rice grains

The present study evaluated the cooking properties of various milled rice grains and reported the results in Table 3. The cooking time varied significantly among the different rice varieties, with the lowest cooking time (22.83 min) observed for P-2819 and the highest cooking time observed for PB-1121. The elongation ratio was also found to vary significantly, with basmati varieties exhibiting significantly higher values than non-basmati ones. The Seed Act 1966 states that the minimum elongation ratio of basmati rice should be 1.70.

Table 3

Cooking properties of different variety of milled rice grains

Properties	PB-6	PB-1121	P-2819	P-44
Cooking Time (min)	25.33±0.58 <sup>a</sup>	27.00±1.00 <sup>a</sup>	22.83±0.29 <sup>b</sup>	26.50±0.50 <sup>a</sup>
Elongation Ratio	2.05±0.05 <sup>a</sup>	1.80±0.10 <sup>b</sup>	1.57±0.06 <sup>c</sup>	1.47±0.06 <sup>c</sup>
Water Uptake (g/g)	2.57±0.03 <sup>a</sup>	2.69±0.09 <sup>a</sup>	2.23±0.06 <sup>b</sup>	2.33±0.04 <sup>b</sup>
Solid Loss (g/g)	3.65±0.10 <sup>c</sup>	3.21±0.09 <sup>d</sup>	4.44±0.12 <sup>a</sup>	3.93±0.05 <sup>b</sup>

All data are reported as mean±SD (n=3)

Different alphabets in superscripts indicate significant differences ( $p < 0.05$ ) among various rice cultivar

The water uptake ratio was observed to be maximum for PB-1121 and minimum for P-2829. Basmati rice varieties are known to have lower bulk density and an amorphous structure, which allows for more water absorption in the grain (Lisle et al., 2000). Furthermore, a negative correlation between water uptake and bulk density was also observed in the present study. After cooking, the solid loss was significantly higher for the P-2819 cultivar and significantly lower for the PB-1121 cultivar. Solid loss was found to have a positive correlation with total starch content, with non-basmati varieties exhibiting significantly higher starch content than basmati ones. Non-basmati rice kernels are known to crack during soaking, allowing the cell contents to leach into the cooking water, resulting in

higher solid loss (Hirannaiah et al., 2001). The results of the present study are consistent with those of previous researchers who have reported higher elongation ratio, higher water uptake, and lower solid loss for basmati rice varieties (Yadav et al., 2014).

### Textural properties of cooked rice grain

Texture profile analysis (TPA) is a widely used method for evaluating the textural properties of rice the results of presented study is embedded in Table 4. Hardness was significantly higher for P-2819, and the lowest was estimated for PB-1121. Adhesiveness is the negative area for the first compression cycle representing the work needed to overcome the attractive forces between the probe and food and it was calculated higher for non-basmati variety when compared to basmati variety. The hardness of rice rich in amylose rice was mainly attributed to leached amylose, which forms several layers of thick coating on the cooked rice (Yu et al., 2009). Previous investigations have also proven that rice with low amylose content would have a soft texture, while waxy rice would exhibit a hard, adhesive, and sticky texture (Moongngarm et al., 2012; Tao et al., 2020). The researchers also observed increasing hardness with an increase in amylose content. Li (2017) showed that rice with comparable amylose contents could exhibit different textural attributes. Besides, they may have the same texture even with utterly different amylose contents, possibly due to complexities in characterizing the structure of amylose. Springiness was measured in the range from 0.02 to 0.03.

**Table 4**  
Texture profile analysis (TPA) of different variety of cooked rice grains

Rice Cultivar	PB-6	PB-1121	P-2819	P-44
Hardness(g)	1900.32±107.06 <sup>b</sup>	1562.11±243.27 <sup>c</sup>	2471.07±194.65 <sup>a</sup>	1775.70±67.29 <sup>bc</sup>
Adhesiveness (g.sec)	-336.01±19.69 <sup>b</sup>	-329.62±111.48 <sup>b</sup>	-559.00±129.00 <sup>a</sup>	-640.67±155.90 <sup>a</sup>
Springiness	0.03±0.00 <sup>a</sup>	0.02±0.00 <sup>a</sup>	0.03±0.01 <sup>a</sup>	0.02±0.01 <sup>a</sup>
Cohesiveness	0.55±0.04 <sup>a</sup>	0.53±0.05 <sup>a</sup>	0.48±0.08 <sup>a</sup>	0.52±0.10 <sup>a</sup>
Gumminess	1070.46±33.67 <sup>ab</sup>	835.16±178.05 <sup>c</sup>	1230.27±49.11 <sup>a</sup>	915.67±157.47 <sup>bc</sup>
Chewiness	27.55±0.91 <sup>ab</sup>	18.59±5.67 <sup>b</sup>	33.37±4.61 <sup>a</sup>	21.25±4.19 <sup>b</sup>
Resilience	1.18±0.19 <sup>a</sup>	1.31±0.43 <sup>a</sup>	1.03±0.25 <sup>a</sup>	1.06±0.45 <sup>a</sup>

All data are reported as mean±SD (n=3)

Different alphabets in superscripts indicate significant differences (p<0.05) among various rice cultivar

Cohesiveness is the ratio of the positive force area during the second cycle of compression to that of the first cycle, which was estimated from 0.48 to 0.55. Gumminess is the product of hardness and cohesiveness; it was observed significantly lower for variety PB-1121, whereas significantly higher was measured for P-2819. The chewiness is the product of gumminess and springiness, and similar to gumminess, the maximum was calculated for P-2819 and the minimum was reported for PB-1121. No significant difference was observed for resilience among different cultivars of a cooked rice grain, and it was observed in the range from 1.03 to 1.31. Similar results of textural properties of cooked rice grains were observed by Sethupathy et al. (2021), who found that the hardness, adhesiveness, and gumminess of rice grains varied significantly among different cultivars.

### Correlation study

The correlation investigation was established among different physical, chemical, cooking and textural properties (Table 5 A-B). Cooking time showed a highly significant and positive correlation with true density and L/B ratio, whereas there was a negative correlation with solid loss, hardness, gumminess and chewiness. Elongation ratio showed a highly significant positive correlation with amylose content ( $r = 0.802$ ) and porosity ( $r = 0.741$ ), whereas there was a negative correlation with total starch and bulk density. Water uptake ratio showed a significant ( $P \leq 0.01$ ) positive correlation with amylose content, true density, porosity, length, L/B ratio and 1000 KW. Solid loss indicated a significantly higher correlation with total starch, hardness and chewiness. Total starch showed a significant ( $P \leq 0.05$ ) positive correlation with bulk density, width and hardness. Moreover, amylose content showed a higher significant positive correlation with true density, porosity, length, 1000KW and adhesiveness. Interestingly, no positive correlation was observed between bulk density and other parameters. True density showed a significant ( $P \leq 0.01$ ) positive correlation with porosity, length, L/B ratio and 1000KW.

**Table 5-A**  
Correlation between some physical, chemical, cooking and textural parameters of rice

	<b>Cooking Time</b>	<b>Elongation Ratio</b>	<b>Water Uptake Ratio</b>	<b>Solid Loss</b>	<b>Total Starch</b>	<b>Amylose Content</b>	<b>Bulk Density</b>
Elongation Ratio	0.126						
Water Uptake Ratio	0.591*	0.701*					
Solid Loss	-0.0792**	-0.529	-0.930**				
Total Starch	-0.0592*	-0.711**	-0.965**	0.924**			
Amylose Content	0.385	0.802**	0.912**	-0.812**	-0.915**		
Bulk Density	0.021	-0.722**	-0.555	0.4	0.597*	-0.709**	
True Density	0.867**	0.481	0.847**	-0.938**	-0.871**	0.752**	-0.404
Porosity	0.41	0.741**	0.802**	-0.737**	-0.843**	0.860**	-0.894**
Length	0.650*	0.54	0.909**	-0.919**	-0.866**	0.875**	-0.569
Width	-0.707*	-0.068	-0.615*	0.688*	0.608*	-0.424	-0.084
LB Ratio	0.743**	0.274	0.816**	-0.864**	-0.787**	0.673*	-0.188
1000 KW	0.609*	0.518	0.889**	-0.928**	-0.888**	0.880**	-0.527
Hardness	-0.890**	-0.217	-0.667*	0.876**	0.677*	-0.474	0.15
Adhesiveness	0.26	0.683*	0.688*	-0.584*	-0.732**	0.814**	-0.491
Springiness	-0.443	0.305	-0.193	0.378	0.096	-0.11	-0.417
Cohesiveness	0.178	0.329	0.325	-0.381	-0.392	0.269	-0.297
Gumminess	-0.888**	0.017	-0.475	0.689*	0.478	-0.319	-0.105
Chewiness	-0.887**	0.021	-0.474	0.730**	0.433	-0.301	-0.131
Resilience	0.244	0.194	0.285	-0.369	-0.271	0.322	-0.441

\*\* Correlation is significant at the 0.01 level (2-tailed)

\* Correlation is significant at the 0.05 level (2-tailed)

Porosity showed higher significant and positive correlation with length ( $r = 0.813$ ) and 1000KW ( $r = 0.777$ ). The length of uncooked grains was highly correlated with the L/B ratio and 1000KW. A strong positive correlation was established between the L/B ratio and 1000KW. The hardness of cooked rice grain demonstrated a higher significant and positive correlation with gumminess ( $r = 0.816$ ) and chewiness ( $r = 0.896$ ). From this correlation study, it was measured that the increase in the cohesiveness of cooked rice grain is due to an increase in the springiness, whereas gumminess was observed directly related to the chewiness of cooked rice grain. The given correlation investigation among different physical, chemical, cooking, and textural properties is supported by several previous studies. For example, a study conducted by Bhardwaj et al. (2019) reported a significant positive correlation between elongation ratio and amylose content in rice. Similarly, a study by Wang et al. (2010) also reported a positive correlation between amylose content and water uptake ratio in rice. Moreover, the positive correlation between true density and cooking time is also supported by a study by Pokhrel et al. (2020). The negative correlation between solid loss, hardness, gumminess, chewiness, and cooking time is also reported in a study by Zhu et al. (2020). Furthermore, the positive correlation between total starch and hardness is supported by a study by Li and Gilbert (2018). The positive correlation between amylose content and true density, porosity, length, 1000KW, and adhesiveness is also supported by studies by Verma and Srivastav (2020).

**Table 5-B**  
Correlation between some physical, chemical, cooking and textural parameters of rice  
(Cont.)

	<b>True Density</b>	<b>Porosity</b>	<b>Length</b>	<b>Width</b>	<b>LB Ratio</b>	<b>1000 KW</b>
Porosity	0.771**					
Length	0.857**	0.813**				
Width	-0.600*	-0.236	-0.599*			
LB Ratio	0.768**	0.506	0.843**	-0.934**		
1000 KW	0.845**	0.777**	0.934**	-0.618*	0.831**	
Hardness	-0.865**	-0.526	-0.713**	0.602*	-0.708**	-0.760**
Adhesiveness	0.591*	0.632*	0.569	-0.29	0.45	0.626*
Springiness	-0.289	0.156	-0.377	0.402	-0.451	-0.363
Cohesiveness	0.24	0.323	0.33	-0.213	0.272	0.328
Gumminess	-0.783**	-0.309	-0.527	0.604*	-0.632*	-0.592*
Chewiness	-0.750**	-0.272	-0.602*	0.535	-0.620*	-0.616*
Resilience	0.316	0.455	0.539	-0.086	0.28	0.426
	<b>Hardness</b>	<b>Adhesiveness</b>	<b>Springiness</b>	<b>Cohesiveness</b>	<b>Gumminess</b>	<b>Chewiness</b>
Adhesiveness	-0.258					
Springiness	0.443	-0.025				
Cohesiveness	-0.399	-0.08	-0.067			
Gumminess	0.816**	-0.348	0.46	0.162		
Chewiness	0.896**	-0.187	0.687*	-0.091	0.901**	
Resilience	-0.403	-0.138	-0.285	0.726**	0.037	-0.271

\*\* Correlation is significant at the 0.01 level (2-tailed)

\* Correlation is significant at the 0.05 level (2-tailed)

## Conclusions

1. Milling performance, as indicated by the recovery of milled rice and head rice recovery, varied among the cultivars. PB-6 exhibited the highest milled rice recovery, indicating better milling efficiency, while PB-1121 had the lowest recovery. P-44 had the highest head rice recovery, suggesting a higher percentage of intact rice grains, whereas PB-6 had the lowest head rice recovery.
2. The chemical composition of milled rice also differed among the cultivars. Moisture content ranged from 10.75 to 11.84%, indicating similar moisture levels across the varieties. PB-1121 had the highest ash content, which may affect the nutritional composition and sensory attributes of rice. Protein content varied from 5.87 to 7.27%, with PB-6 exhibiting the highest protein content. Starch content was higher in non-basmati cultivars compared to basmati cultivars, indicating potential differences in cooking and texture. PB-1121 had the highest amylose content, which may contribute to its characteristic texture and cooking properties.
3. Physical characteristics, including length, breadth, density, and porosity, are important factors influencing consumer acceptance. Basmati varieties generally displayed higher length, lower breadth, and higher length-to-breadth (L/B) ratio compared to non-basmati varieties, contributing to their desirable appearance. PB-1121 had the highest L/B ratio among the cultivars. Bulk density was lowest for PB-6 and highest for P-44, while true density was highest in P-2819, indicating differences in grain compactness.
4. Cooking properties varied among the rice varieties, with P-2819 exhibiting the lowest cooking time and PB-1121 showing the highest cooking time. Basmati varieties displayed higher elongation ratio and water uptake ratio compared to non-basmati varieties, indicating their ability to absorb more water and elongate during cooking. P-2819 had higher solid loss, which might affect its overall texture, while PB-1121 had lower solid loss, indicating a firmer texture after cooking.
5. Textural properties, such as hardness, adhesiveness, and gumminess, also differed among the cultivars. P-2819 exhibited the highest hardness and gumminess, potentially resulting in a chewier texture, while PB-1121 had the lowest hardness, suggesting a softer texture. Adhesiveness was higher in non-basmati varieties compared to basmati varieties, indicating variations in stickiness.
6. The correlation analysis provided insights into the relationships between different properties of rice grains. Cooking time positively correlated with true density and L/B ratio, suggesting that denser and elongated grains require longer cooking. Conversely, cooking time showed negative correlations with solid loss, hardness, gumminess, and chewiness, indicating that softer and less sticky grains tend to cook faster. Elongation ratio showed positive correlations with amylose content and porosity, indicating that higher amylose content and increased porosity contribute to greater elongation during cooking. Water uptake ratio displayed positive correlations with amylose content, true density, porosity, length, L/B ratio, and 1000 kernel weight, suggesting that these factors influence the water absorption capacity of rice grains.

**Acknowledgments.** The authors would like to thank Bhaskaracharya College of Applied Sciences (University of Delhi), Delhi, India for providing laboratory facility to conduct this research.

## References

- Adair C. R. (1952), The McGill miller method for determining the milling quality of small samples of rice, *Rice Journal*, 55, pp. 21–23, Available at: <https://eurekamag.com/research/013/857/013857121.php>
- Ahuja S. C., Panwar D. V. S., Ahuja U., Gupta K. R. (1995), Basmati Rice: The Scented Pearl. *Directorate of Publications, CCS Haryana Agricultural University*, Hisar, Available at: <https://www.cabdirect.org/cabdirect/abstract/19960704648>
- AOAC International. (2000), *Official Methods of Analysis of AOAC International (17th ed.)*, Gaithersburg, USA: AOAC International Inc, Available at: <https://law.resource.org/pub/us/cfr/ibr/002/aoac.methods.1.1990.pdf>
- Bhattacharjee P., Singhal R. S., Kulkarni P. R. (2002), Basmati rice: A review, *International Journal of Food Science and Technology*, 37(1), pp. 1–12, <https://doi.org/10.1046/j.1365-2621.2002.00541.x>.
- Bhattacharya K. R. (2011), *Rice Quality: A Guide to Rice Properties and Analysis*, Elsevier. Available at: <https://www.elsevier.com/books/rice-quality/bhattacharya/978-1-84569-485-2>
- Zhu L., Bi S., Wu G., Zhang H., Wang L., Qian H., Jiang H. (2020). Comparative analysis of the texture and physicochemical properties of cooked rice based on adjustable rice cooker, *LWT Food Science & Technology*, 130, 109650, <https://doi.org/https://doi.org/10.1016/j.lwt.2020.109650>.
- Verma D. K., Srivastav P. P. (2020). Exploring the physicochemical and cooking properties of some Indian aromatic and non-aromatic rice (*Oryza sativa* L.) cultivars, *ORYZA-An International Journal on Rice*, 57(2), pp. 146–161, <https://doi.org/10.35709/ory.2020.57.2.9>.
- Elbashir L. T. M. (2005), Physicochemical properties and cooking quality of long and short rice (*Oryza sativa*) grains. *Master's thesis, University of Khartoum*, Available at: <https://www.osti.gov/etdweb/servlets/purl/20655574>
- Ertop M. H., Bektaş M., Atasoy, R. (2020), Effect of cereals milling on the contents of phytic acid and digestibility of minerals and protein, *Ukrainian Food Journal*, 9(1), pp. 136–147, <https://doi.org/10.24263/2304-974X-2020-9-1-12>.
- Falade K. O., Christopher A. S. (2015), Physical, functional, pasting and thermal properties of flours and starches of six Nigerian rice cultivars, *Food Hydrocolloids*, 44, pp. 478–490, <https://doi.org/10.1016/j.foodhyd.2014.10.005>
- Faruq G., Prodhan M. Z. H. (2013). Kernel elongation in rice, *Journal of the Science of Food and Agriculture*, 93(3), pp. 449–456, <https://doi.org/10.1002/jsfa.5983>
- Pokhrel A., Dhakal A., Sharma S., Poudel A. (2020). Evaluation of physicochemical and cooking characteristics of rice (*Oryza sativa* L.) landraces of lamjung and Tanahun Districts, Nepal, *International Journal of Food Science*, 2020, pp. 1589150, <https://doi.org/10.1155/2020/1589150>
- He Y., Chen F., Shi Y., Guan Z., Zhang N., Campanella O. H. (2021), Physico-chemical properties and structure of rice cultivars grown in Heilongjiang province of China, *Food Science & Human Wellness*, 10(1), pp. 45–53, <https://doi.org/10.1016/j.fshw.2020.05.010>
- Hirannaiah B. V., Bhashyam M. K., Ali S. Z. (2001), An improved cooking quality test for basmati rice, *Journal of Food Science and Technology*, 38(2), pp. 116–119, Available at: <http://ir.cftri.res.in/id/eprint/2996>
- Juliano B. O. (1971), A simplified assay for milled rice amylose, *Cereal Science Today*, 16, pp. 334–340, Available at: <https://cir.nii.ac.jp/crid/1390282681385870336>

- Kang M. Y., Rico C. W., Lee S. C. (2011). Comparative analysis of the physicochemical properties of rice endosperm from cultivars with diverse amylose content. *Journal of Crop Science and Biotechnology*, 14(3), pp. 219–225, <https://doi.org/10.1007/s12892-010-0020-0>
- Kaur S., Panesar P. S., Bera, M. B. (2011), Studies on evaluation of grain quality attributes of some basmati and non-basmati rice cultivars, *Journal of Food Quality*, 34(6), pp. 435–441, <https://doi.org/10.1111/j.1745-4557.2011.00417.x>
- Panigrahi A. K., Bharathi M., Kumaravadeivel N. (2018), Morphological Characterization of Advanced Backcross Population for Yield and Yield Attributing Character in Rice (*Oryza sativa* L.), *International Journal of Current Microbiology & Applied Sciences*, 7(2), pp. 2812–2819, <https://doi.org/10.20546/ijcmas.2018.702.342>
- Li H. (2017). Understanding the texture of cooked rice from the molecular, instrumental and sensory levels. *Doctoral Dissertation, The University of Queensland*, Available at: <https://core.ac.uk/download/pdf/86629549.pdf>
- Li H., Prakesh S., Nicholson T. H. (2016), The importance of amylose and amylopectin fine structure for textural properties of cooked rice grains, *Food Chemistry*, pp. 196, 702–711, <https://doi.org/10.1016/j.foodchem.2015.09.112>
- Lisle K. J., Martin M., Fitzgerald M. A. (2000), Chalky and translucent rice grains differ in starch composition, structure and cooking properties, *Cereal Chemistry*, 77, pp. 627–632, <https://doi.org/10.1094/CCHEM.2000.77.5.627>
- Medvid I., Shydlovska O., Dotsenko V. (2017), Influence of fermentative modification of rice flour starch on bread quality for patients with celiac disease, *Ukrainian Food Journal*, 6(4), pp. 632–647, <https://doi.org/10.24263/2304974X-2017-6-4-5>
- Bhardwaj R., Salgotra R. K. Sharma M. (2019), Studies on correlation of amylose content and grain dimensions in Basmati rice (*Oryza sativa* L.), *Electronic Journal of Plant Breeding*, 10(2), pp. 364-369, Available at: <https://ejplantbreeding.org/index.php/EJPB/article/view/3098>
- Moongnarm A., Bronlund J. E., Grigg N., Sriwai N. (2012), Chewing behavior and bolus properties as affected by different rice types, *International Journal of Medical and Biological Sciences*, 6, pp. 51–56, Available at: <https://mro.massey.ac.nz/handle/10179/12162>
- Murtaza G., Huma N., Sharif M.K., Zia M.A. (2022). Probing a best suited brown rice cultivar for the development of extrudates with special reference to Physico-chemical, microstructure and sensory evaluation, *Food Science and Technology*, 42, pp. e103521, <https://doi.org/10.1590/fst.103521>
- Nzozzo D., Mogambi H. (2016), An analysis of communication and information communication technologies adoption in irrigated rice production in Kenya, *International Journal of Education Research*, 4(12), pp. 295–316, Available at: <http://ijern.com/journal/2016/December-2016/23.pdf>
- Pandiselvam R., Thirupathi V., Mohan S. (2015), Engineering properties of rice. *Agricultural Engineering International: CIGR Journal*, 17(3), pp. 69–78, Available at: [https://www.academia.edu/82298435/Engineering\\_Properties\\_of\\_Rice](https://www.academia.edu/82298435/Engineering_Properties_of_Rice)
- Prom-U-Thai C., Rerkasem B. (2020), Rice quality improvement. A review, *Agronomy for Sustainable Development*, 40(4), 28, <https://doi.org/10.1007/s13593-020-00633-4>
- Rather T. A., Malik M. A., Dar, A. H. (2016), Physical, milling, cooking, and pasting characteristics of different rice varieties grown in the valley of Kashmir India, *Cogent Food & Agriculture*, 2(1), pp. 1178694, <https://doi.org/10.1080/23311932.2016.1178694>

- Li H., Gilbert R. G. (2018), Starch molecular structure: The basis for an improved understanding of cooked rice texture, *Carbohydrate Polymers*, 195, pp. 9–17, <https://doi.org/10.1016/j.carbpol.2018.04.065>
- Sandhu R. S., Singh N., Kaler R. S. S., Kaur A., Shevkani K. (2018), Effect of degree of milling on physicochemical, structural, pasting and cooking properties of short and long grain *Indica* rice cultivars, *Food Chemistry*, 260, pp. 231–238, <https://doi.org/10.1016/j.foodchem.2018.03.092>
- Sethupathy P., Sivakamasundari S. K., Moses J. A., Anandharamkrishnan, C. (2021), Effect of varietal differences on the oral processing behavior and bolus properties of cooked rice, *International Journal of Food Engineering*, 17(3), pp. 177–188, <https://doi.org/10.1515/ijfe-2020-0097>
- Shobhan N. V., Veerapaga, N., Rao, S. (2016), Physical properties and milling characteristics of rice (*Oryza sativa* L.), *International Journal of Agricultural Sciences*, 8(59), pp. 3301–3305, Available at: <http://www.bioinfopublication.org/jouarchive.php?opt=&jouid=BPJ0000217>
- Singh N., Kaur L., Sodhi N. S., Sekhon K. S. (2005), Physicochemical, cooking and textural properties of milled rice from different Indian rice cultivars, *Food Chemistry*, 89, pp. 253–259, <https://doi.org/10.1016/j.foodchem.2004.02.032>
- Sliwiska-Bartel M., Burns D. T., Elliott C. (2021), Rice fraud a global problem: A review of analytical tools to detect species, country of origin and adulterations, *Trends in Food Science & Technology*, 116, pp. 36–46, <https://doi.org/10.1016/j.tifs.2021.06.042>
- Butardo, V. M., Sreenivasulu, N., Juliano, B. O. (2019), Improving rice grain quality: State-of-the-art and future prospects. *Rice Grain Quality: Methods and Protocols*, 1892, pp. 19–55, <https://doi.org/10.1007/978-1-4939-8914-0-2>
- Sujatha S. J., Ahmad R., Bhat P. R. (2004), Physicochemical properties and cooking qualities, qualities of two varieties of raw and parboiled rice cultivated in the coastal region of Dakshina Kannada, India, *Food Chemistry*, 86(2), pp. 211–216, <https://doi.org/10.1016/j.foodchem.2003.08.018>
- Suwannaporn P., Pitiphunpong S., Champangern S. (2007), Classification of rice amylose content by discriminant analysis of physicochemical properties, *Starch-Starke*, 59, pp. 171–177, <https://doi.org/10.1002/star.200600565>
- Tao K., Yu W., Prakash S., Gilbert R. G. (2020), Investigating cooked rice textural properties by instrumental measurements, *Food Science & Human Wellness*, 9, pp. 130–135, <https://doi.org/10.1016/j.fshw.2020.02.001>
- Verma D. K., Srivastav P. P. (2020), Exploring the physicochemical and cooking properties of some Indian aromatic and non-aromatic rice (*Oryza sativa* L.) cultivars, *Oryza-An International Journal on Rice*, 57(2), pp. 146–161, <https://doi.org/10.35709/ory.2020.57.2.9>
- Wang L., Xie B., Shi J., Xue S., Deng Q., Wei Y., Tian, B. (2010), Physicochemical properties and structure of starches from Chinese rice cultivars, *Food Hydrocolloids*, 24(2–3), pp. 208–216, <https://doi.org/10.1016/j.foodhyd.2009.09.007>
- Yadav R. B., Khatkar B. S., Yadav B. S. (2014), Morphological, physicochemical and cooking properties of some Indian rice (*Oryza sativa* L.) cultivars. *Journal of Agricultural Technology*, 3(2), pp. 203–210, Available at: [http://www.ijat-aatsea.com/pdf/Nov\\_V3\\_no2\\_07/5-IJAT2007\\_14-P%20203-210.pdf](http://www.ijat-aatsea.com/pdf/Nov_V3_no2_07/5-IJAT2007_14-P%20203-210.pdf)
- Yu S., Ma Y., Sun D. W. (2009), Impact of amylose content on starch retrogradation and texture of cooked milled rice during storage, *Journal of Cereal Science*, 50, pp. 139–144, <https://doi.org/10.1016/j.jcs.2009.04>

## Ryazhanka with pumpkin puree and flax seeds

Oleh Kuzmin<sup>1</sup>, Victoriia Kiiko<sup>1,2</sup>, Olena Khareba<sup>3</sup>,  
Olena Gavrylenko<sup>2</sup>, Mariia Ianchyk<sup>1</sup>, Nataliia Melnyk<sup>1</sup>

1 – National University of Food Technologies, Kyiv, Ukraine

2 – Ukrainian State Scientific and Research Institute "Resurs", Kyiv, Ukraine

3 – National Academy of Agrarian Sciences of Ukraine, Kyiv, Ukraine

---

### Abstract

---

#### Keywords:

Ryazhanka  
Pumpkin  
Flax seeds  
Nutritional value  
Sensory

---

#### Article history:

Received 2.09.2022

Received in revised  
form 14.03.2023

Accepted 31.03.2023

---

#### Corresponding author:

Oleh Kuzmin  
E-mail:  
kuzmin\_ovl@ukr.net

---

DOI: 10.24263/2304-  
974X-2023-12-1-7

---

**Introduction.** The aim of this research was to study the influence of pumpkin puree and flax seeds addition on nutritional value, physicochemical and sensory properties of Ryazhanka.

**Materials and methods.** Ryazhanka samples were prepared with the addition of pumpkin puree and flax seeds. The titrated acidity was determined by the Turner method, and the active acidity was measured using pH-meter. The fat content was determined using Gerber's acid method, and sensory evaluations were conducted by an expert panel.

**Results and discussion.** Pumpkin puree and flax seeds were used in Ryazhanka preparation. It was shown that the addition of 4–8% flax seeds to Ryazhanka with 10% pumpkin puree reduced the titrated acidity to 64–70 °T and increased the active acidity to pH 4.6–4.7. Similarly, the addition of 4–8% flax seeds with 15% pumpkin puree reduced the titrated acidity to 61–68 °T and increased the active acidity to 4.6–4.7. When 20% pumpkin puree and 4–8% flax seeds were added simultaneously, the titrated acidity decreased to 60–65 °T, and the active acidity increased to 4.6–4.8. The optimal conditions for achieving physico-chemical stability in Ryazhanka were observed for samples added with 10% pumpkin puree and 4% flax seeds.

The addition of pumpkin puree (10%) and flax seeds (4%) to Ryazhanka resulted in increased content of water-soluble vitamins, such as 0.570 mg (184% increase) of vitamin C, 0.062 mg (295% increase) of vitamin B<sub>1</sub>, 0.003 mg (2% increase) of vitamin B<sub>2</sub>, and an increase in fat-soluble vitamins including vitamin E and β-carotene. Furthermore, the addition of flax seeds increased the content of polyunsaturated fatty acids, particularly the increase of omega-3 fatty acids from 0 to 0.80 g and omega-6 fatty acids from 0 to 0.20 g.

Comparing the control sample, the addition of pumpkin puree and flax seeds to Ryazhanka affected its shelf life at temperatures ranging from 0 to 6 °C, extending it to no more than 7 days.

**Conclusions.** The proposed recipe of Ryazhanka with pumpkin puree and flax seeds improves its nutrient composition, stabilizes its physicochemical parameters, enhances sensory properties, and expands the range of options to cater to the preferences of fermented milk drink consumers.

## Introduction

Ryazhanka is a popular and traditional fermented milk drink in Ukraine. It is produced by fermenting curdled milk with pure cultures of the thermophilic lactic acid bacteria *Streptococcus salivarius* subsp. *thermophiles* (Aidarbekova and Aider, 2022). Improving the quality and expanding the range of fermented milk drinks (Buldo et al., 2021) requires the enhancement of preventive properties (Oh et al., 2014). This involves utilizing non-traditional raw materials (Tavares and Malcata, 2019), which is significant for Ryazhanka technology (Moreno-Montoro et al., 2018; Zhang et al., 2022). Application of natural plant additives including pumpkin and flax seeds in food products allows to enhance their nutritional value and supply the consumers with different valuable substances essential for health (Ivanov et al., 2021; Stabnikova et al., 2021).

Pumpkin is an innovative functional product that is used in various food products such as jelly, jam, marmalade, chutney, sauce, puree, juice, candies, bars, flakes, chips, cookies, cakes, halva, pickles, pies, and bread (Ahmad and Khan, 2019; Chikpah et al., 2022; Dhiman et al., 2009; Hussain et al., 2022; Montesano et al., 2018). It serves as a valuable raw material for the production of food products with therapeutic and preventive benefits. Pumpkin's rational composition of nutrients, nutraceuticals, and functional ingredients makes it an excellent choice to be added to Ryazhanka to improve its nutritional properties.

Since pumpkin crops are seasonal and prone to microbial spoilage and postharvest quality changes due to their high moisture content, they need to be dried or frozen to increase their shelf life and improve nutrient bioavailability (Akpinar et al., 2003; Korese et al., 2021; Monteiro et al., 2018; Ropelewska et al., 2022). Drying helps reduce moisture content and water activity to levels that significantly inhibit microbial, enzymatic, and chemical spoilage (Chikpah et al., 2022; Monteiro et al., 2018; Seremet (Ceclu) et al., 2016). Additionally, drying reduces the volume and weight of the product, resulting in reduced costs for packaging, transportation, and storage of agricultural food products, while also expanding its food supply applications. Therefore, innovative forms of processing pumpkin raw materials include powders, extracts, isolates, purees, biologically active substances, and functional food products. Pumpkin flour can be used as a supplement to cereal crop flour for producing bakery products, pasta, soups, instant noodles, mixtures for child feeding, natural dyes in pasta products, and flour mixtures (Ahmad and Khan, 2019; Dhiman et al., 2009; Hussain et al., 2022; Montesano et al., 2018). Moreover, dried pumpkin can be rehydrated and used to make stews and soups (Doymaz, 2007).

Flaxseed is rich in nutrients and offers various health benefits. It is known for being a rich source of omega-3 fatty acids, which can help reduce body fat levels and improve cardiovascular health (Marpalle et al., 2014). Flaxseed contains lipids (40%), protein (21%), dietary fiber (28%), ash (4%), and other soluble components such as sugars, phenolic acids, and lignans (approximately 6%) (Fitzpatrick, 2011). Therefore, incorporating flax seeds into the diet can be a beneficial addition for individuals seeking to improve their health. Moreover, flax seeds can serve as an innovative raw material in Ryazhanka technology.

The aim of this work is to enhance the nutrient composition of Ryazhanka by incorporating pumpkin puree and flax seeds, while further stabilizing the physicochemical parameters and improving the sensory properties of Ryazhanka.

## Materials and methods

### Materials

The main raw materials used for the production of Ryazhanka included high-grade and «Extra» grade whole cow's milk, cow cream, pure cultures of lactic acid bacteria

(*Streptococcus thermophilus*, *Lactococcus lactis*), pasteurized pumpkin puree (*Cucurbita moschata* Duchesne ex Poiret), and flax seeds (*Linum usitatissimum* L).

Ryazhanka samples were prepared according to the following compositions: control sample (sample 1) prepared using the classic recipe; samples 2–10, which were variations of Ryazhanka compositions with 10–20% pumpkin puree and 4–8% flax seeds.

### **Physicochemical and sensory analysis methods**

The following methods were used to evaluate the physicochemical and sensory properties of Ryazhanka with pumpkin puree and flax seeds:

Taste, smell, color, appearance, and consistency analysis (ISO 6658:1985 Sensory analysis. Methodology. General guidance; ISO 6564:1985 Sensory analysis. Methodology. Flavour profile methods).

Determination of fat content by the gravimetric method (ISO 1211:1999 Milk. Determination of fat content. Gravimetric method).

Titrateable acidity analysis (ISO/TS 11869:2012 Determination of titrateable acidity).

Measurement of active acidity and pH using continuous pH measurement (ISO 26323:2009 Milk products. Determination of the acidification activity of dairy cultures by continuous pH measurement (CpH)).

The sensory evaluation was conducted using a scoring method, where highly qualified and experienced experts evaluated the sensory attributes of the Ryazhanka samples (Khareba et al., 2021; Kuzmin et al., 2021).

### **Calculation and analytical method**

To determine the nutritional value and nutrient composition of Ryazhanka with pumpkin puree and flax seeds, a calculation-analytical method was employed. This method involves converting the data to 100 grams of plant raw material and combining the nutritional composition data with the database information (NatureClaim 2015-2023). The energy value of the samples was calculated using energy conversion coefficients and presented as kcal/100g by summing the percentage composition of fats, proteins, and total carbohydrate content multiplied by coefficients of 9, 4, and 4 respectively.

## **Results and discussions**

### **Physicochemical parameters of Ryazhanka with pumpkin puree and flax seeds**

The standard range for titrateable acidity in Ryazhanka is 70–110 °T, while the active acidity should be within the range of pH 4.6–4.0. The control Ryazhanka prepared using the classical technology had a titrateable acidity of 73 °T (Figure 1) and an active acidity of 4.56 pH (Figure 2).

The addition of 10–20% pumpkin puree to the Ryazhanka recipe resulted in a decrease in titrateable acidity from 73 °T to 70–65 °T due to the presence of organic acids, primarily malic acid, in the pumpkin puree. The addition of 10% pumpkin puree increased the active acidity from pH 4.56 to pH 4.60. Addition of 15–20% pumpkin puree stabilized the active acidity at pH 4.62. However, it should be noted that the optimal range lies within the 10% pumpkin puree content. Increasing the pumpkin puree content to 15–20% led to a decrease in titrateable acidity to 68–65 °T, which is below the standard value of 70 °T. Additionally, the increase in pumpkin puree content to 15–20% resulted in an increase in active acidity to pH 4.62, which exceeds the standard value of pH 4.6.

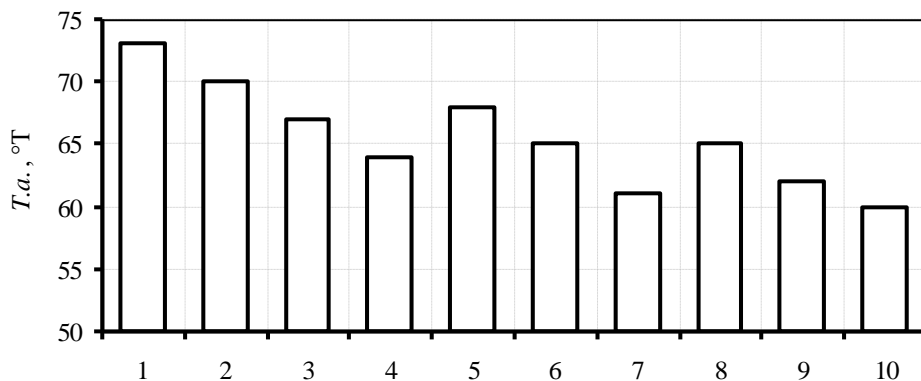


**Figure 1. Dependence of the titratable acidity (*T.a.*) of Ryazhanka on the content of pumpkin puree and flax seeds:**

1 – control sample; 2 – 10% pumpkin puree and 4% flax seeds; 3 – 10% pumpkin puree and 6% flax seeds; 4 – 10% pumpkin puree and 8% flax seeds; 5 – 15% pumpkin puree and 4% flax seeds; 6 – 15% pumpkin puree and 6% flax seeds; 7 – 15% pumpkin puree and 8% flax seeds; 8 – 20% pumpkin puree and 4% flax seeds; 9 – 20% pumpkin puree and 6% flax seeds; 10 – 20% pumpkin puree and 8% flax seeds

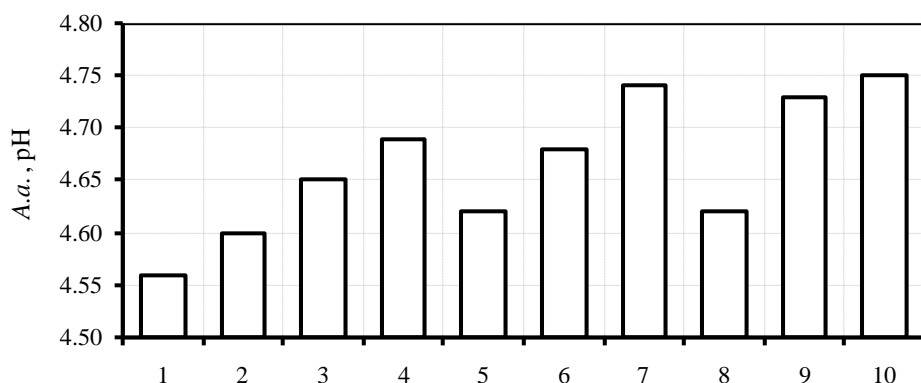


**Figure 2. Dependence of active acidity (*A.a.*) of Ryazhanka on the content of pumpkin puree and flax seeds:**

1 – control sample; 2 – 10% pumpkin puree and 4% flax seeds; 3 – 10% pumpkin puree and 6% flax seeds; 4 – 10% pumpkin puree and 8% flax seeds; 5 – 15% pumpkin puree and 4% flax seeds; 6 – 15% pumpkin puree and 6% flax seeds; 7 – 15% pumpkin puree and 8% flax seeds; 8 – 20% pumpkin puree and 4% flax seeds; 9 – 20% pumpkin puree and 6% flax seeds; 10 – 20% pumpkin puree and 8% flax seeds

Addition of flax seeds to Ryazhanka, which contains polyunsaturated fatty acids (omega-3 acids), has an impact on the reduction of titrated acidity and an increase in active acidity of the product, depending on the flax seed content. When adding 4–8% flax seeds to Ryazhanka along with 10% pumpkin puree, the titrated acidity of the product is reduced to 70–64 °T, while the active acidity increases to pH 4.60-4.69. Adding 4–8% flax seeds along with 15% pumpkin puree reduces the titrated acidity of Ryazhanka to 68–61 °T and increases the active

acidity to pH 4.62–4.74. Similarly, adding 4–8% flax seeds with 20% pumpkin puree reduces the titrated acidity of Ryazhanka to 65–60 °T and increases the active acidity to pH 4.62–4.75. However, the limiting range for the Ryazhanka recipe is the content of 4% flax seeds. Increasing the content of flax seeds to 6–8% leads to the following effects:

(a) a reduction in the titrated acidity of Ryazhanka to 67–64 °T when adding 10% pumpkin puree, to 65–61 °T when adding 15% pumpkin puree, and to 62–60 °T when adding 20% pumpkin puree, which is lower than the standard value of 70 °T;

(b) an increase in the active acidity to pH 4.65–4.69 when adding 10% pumpkin puree, to pH 4.68–4.74 when adding 15% pumpkin puree, and to pH 4.73–4.75 when adding 20% pumpkin puree, which exceeds the normalized value of pH 4.60.

Based on preliminary observations, it can be concluded that titrated and active acidity of Ryazhanka are inversely correlated, following a one-to-one relationship. An increase in titrated acidity by 1 °T leads to a decrease in the active acidity of Ryazhanka by 0.0151 (Figure 3).

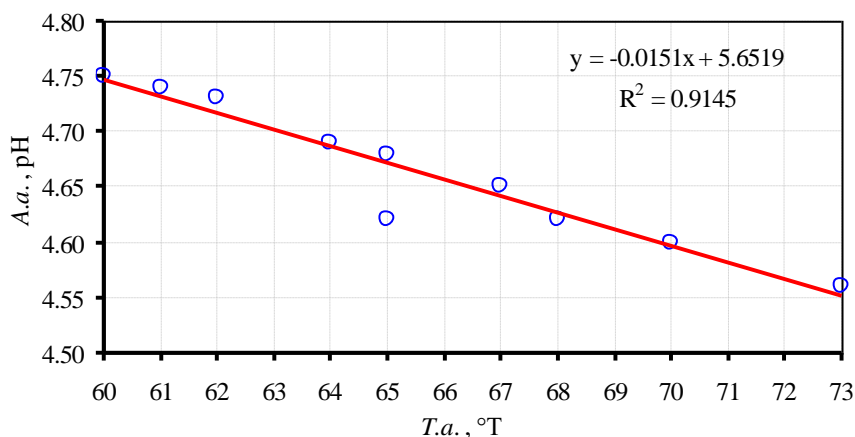


**Figure 3. Dependence of active acidity (A.a.) on titratable acidity (T.a.)**

The addition of pumpkin puree and flax seeds has an impact on the titrated and active acidity of Ryazhanka, as these ingredients contain organic acids that can alter the acid-base balance of the final product. The optimal values of titrated and active acidity for Ryazhanka are achieved with the simultaneous addition of 10% pumpkin puree and 4% flax seeds, which sets a limit on increasing the content of these ingredients. Furthermore, the addition of pumpkin puree and flax seeds can have a positive effect on the nutritional value and sensory characteristics of Ryazhanka, including its appearance, consistency, taste, aroma, and color.

### **Sensory evaluation of Ryazhanka with pumpkin puree and flax seeds**

The sensory evaluation of Ryazhanka with 10% pumpkin puree and 4% flax seeds is shown in Figure 4a. Figure 4b represents the sample with 15% pumpkin puree and 6% flax seeds, while Figure 4c illustrates Ryazhanka with 20% pumpkin puree and 8% flax seeds.

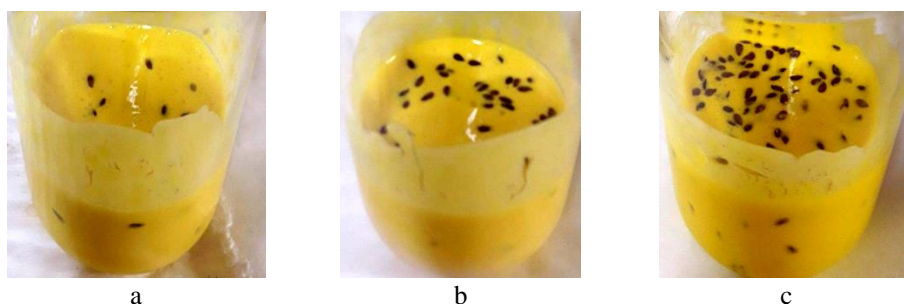


**Figure 4. Ryazhanka with different amounts of pumpkin puree and flax seeds:**  
 a – 10% pumpkin puree and 4% flax seeds;  
 b – 15% pumpkin puree and 6% flax seeds;  
 c – 20% pumpkin puree and 8% flax seeds

Based on the results of the point assessment, profilograms were constructed (Figure 5-6).

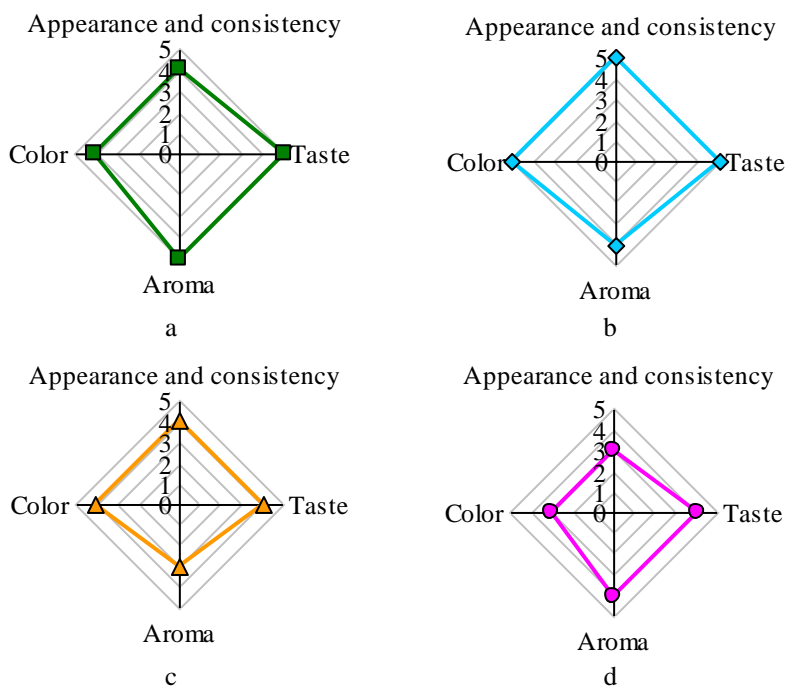


**Figure 5. Profilograms of sensory indicators of the quality of Ryazhanka depending on the content of pumpkin puree and flax seeds:**  
 a – control sample; b – 10% pumpkin puree and 4% flax seeds; c – 10% pumpkin puree and 6% flax seeds; d – 10% pumpkin puree and 8% flax seeds

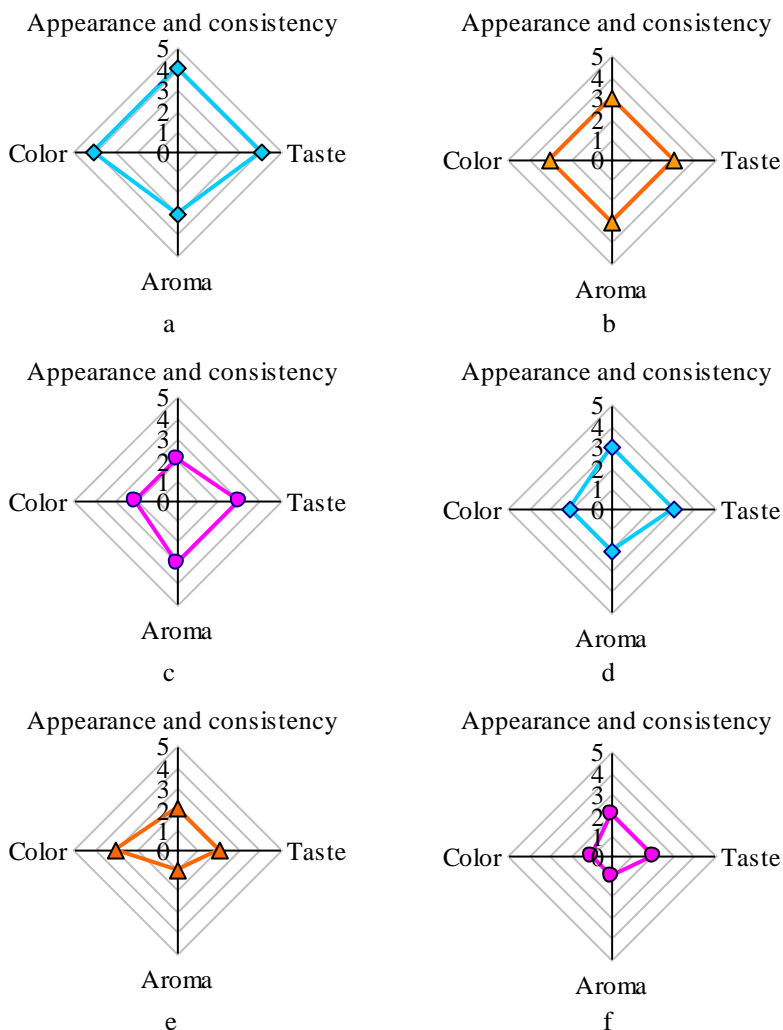


**Figure 6. Profilograms of sensory indicators of the quality of Ryazhanka depending on the content of pumpkin puree and flax seeds:**

a – 15% pumpkin puree and 4% flax seeds; b – 15% pumpkin puree and 6% flax seeds; c – 15% pumpkin puree and 8% flax seeds; d – 20% pumpkin puree and 4% flax seeds; e – 20% pumpkin puree and 6% flax seeds; f – 20% pumpkin puree and 8% flax seeds

Profile analysis revealed that Ryazhanka with the addition of 10% pumpkin puree and 4% flax seeds exhibited the highest sensory indicators (Figure 5b), with an average score of 4.75 points.

Evaluation of the sensory properties of the samples showed that the addition of up to 10% pumpkin puree and 4% flax seeds to Ryazhanka resulted in improved sensory parameters. The addition of pumpkin puree contributed to a soft, sweet, and pleasant aroma in Ryazhanka, while flax seeds added crunch, texture, and a natural flavor. These findings

are consistent with a study by Mousavi et al. (2019), which demonstrated the positive effects of flax seeds on the sensory properties of yogurt, particularly its texture and taste. Flax seeds imparted a richer flavor and aroma to the yogurt and improved its texture by forming a gel structure. However, it should be noted that flax seeds contain polysaccharides that can increase viscosity and affect the texture of fermented dairy products (Fitzpatrick, 2011). Therefore, to achieve the desired consistency of Ryazhanka with flax seeds, strict adherence to the prescribed their amount in the recipe and close control over the production process are necessary.

Increasing the content of pumpkin puree over 10% and flax seeds over 4% negatively impacts the quality of Ryazhanka. The average sensory index decreased from 3.75 to 1.50 points with a deterioration in appearance, texture, taste, aroma and color. A higher amount of pumpkin puree leads to an overly pronounced pumpkin flavor in the final product, resulting in excessively expressive color in Ryazhanka. Similar results were observed when adding sea buckthorn to Ryazhanka in amounts of 2.5, 5.0 and 7.5% (Ge et al., 2022). The authors found that samples with higher sea buckthorn content exhibited a more red-yellow color.

An increased level of flax seed can introduce a bitter aftertaste that may be undesirable to some consumers, thus caution is advised when incorporating this ingredient. This finding was supported by Mousavi et al. (2019), who reported a decreasing trend in sensory scores, including taste, mouthfeel, appearance, and overall acceptance, in samples containing high amounts of flaxseed. Higher amount of flax seeds alter the texture of Ryazhanka, making it thicker and reducing its sweetness. The oil content in flax seeds can also impart a slightly oily texture to Ryazhanka. The addition of flax seeds generally enhances the nutritional value of Ryazhanka due to their beneficial elements, such as omega-3 fatty acids.

### Recipe development

Based on the conducted research, a recipe was developed incorporating the most successful combination of components for Ryazhanka with pumpkin puree (10%) and flax seeds (4%), as shown in Table 1.

**Table 1**  
**Ryazhanka with pumpkin puree and flax seeds**

Raw material	Component amount (kg)	Percentage (%)
Pasteurized milk	859.98	85.998
Leaven	0.02	0.002
Pumpkin puree	100	10
Flax seeds	40	4
Total	1000	100

The production of Ryazhanka using this proposed recipe will result in a product enriched with biologically valuable substances, improved sensory properties, and an expanded range of this fermented milk beverage.

### Justification of raw material processing technology

In addition to pumpkin, other plant materials such as garlic, black pepper, and basil leaves can be added to the Ryazhanka recipe. These ingredients have been shown to have

immune-strengthening properties (Ahmad et al., 2022). The use of spicy-aromatic plant raw materials in the restaurant industry has been proven to enhance the biological value and antioxidant capacity of dishes, thereby improving their sensory properties (Khareba et al., 2021; Kuzmin et al., 2021; Shevchenko et al., 2022).

Flax seeds are particularly valuable as a raw material. Various flax seed products, including whole flax seeds, ground meal, and extracted oil or mucilage, can be used in food preparation (Kajla et al., 2015). These products have been suggested as nutritional additives in a variety of dietary items, such as baked cereal products, ready-to-eat cereals, fiber bars, salad toppings, meat extenders, bread, muffins, and spaghetti (Singh et al., 2011; 2012).

### Nutritional and energy value

Calculated nutritional and energy value of Ryazhanka with pumpkin puree and flax seeds is shown in Table 2.

**Table 2**  
Calculated nutritional and energy value of Ryazhanka with pumpkin puree and flax seeds per 100 g of the finished product

Indicator	Control sample – Ryazhanka*	Ryazhanka with 10% pumpkin puree and 4% flax seeds**	+/-
Nutritional value			
Proteins, g	2.7	3.1	0.4
Fats, g	2.5	2.9	0.4
Carbohydrates, g	4.0	4.2	0.2
Energy (calorie) value			
Calorie content, kcal	49.30	55.30	6.00
Energy value, kJ	206.41	231.53	25.12
Vitamins			
C, mg	0.310	0.880	0.570
B <sub>1</sub> , mg	0.021	0.083	0.062
B <sub>2</sub> , mg	0.127	0.130	0.003
E, mg	0.000	0.010	0.010
β-carotene, mg	0.000	0.051	0.051
Minerals			
K, mg	141.00	172.30	31.300
Ca, mg	123.00	117.80	-5.200
Mg, mg	15.00	32.20	17.200
Na, mg	47.00	42.90	-4.100
Fatty acids			
Omega-3, g	0.00	0.80	0.800
Omega-6, g	0.00	0.20	0.200

\*The nutritional composition of Ryazhanka, according to the manufacturer's quality certificate, indicates a fat content of 2.5% per 100 g.

\*\*Recalculation for 86 grams of Ryazhanka with the addition of 10 grams of pumpkin puree and 4 grams of flax seeds, based on the combined nutritional data from the database (NatureClaim 2015-2023).

A comparison of the nutritional value, energy content, vitamin and mineral content, and fatty acid composition was conducted for 100 g of the control sample product – Ryazhanka and Ryazhanka with the addition of 10 g of pumpkin puree (10%) and 4 g of flax seeds (4%).

The addition of 10% pumpkin puree and 4% flax seeds to Ryazhanka compared to the control resulted in an increase in protein by 0.4 g (15%), fats by 0.4 g (16%), and carbohydrates by 0.2 g (5%). This led to a 6.00 kcal (12%) increase in calorie content and a 25.12 kJ (12%) increase in energy value. The presence of proteins in pumpkin puree and essential amino acids (Ezzat et al., 2022) confirms these findings. Additionally, *Cucurbita moschata* Duchesne ex Poiret contains 5.0-7.0% total sugars.

The addition of pumpkin puree and flax seeds to Ryazhanka increased the content of water-soluble vitamins: C by 0.570 mg (184%), B<sub>1</sub> by 0.062 mg (295%), and B<sub>2</sub> by 0.003 mg (2%). It also increased the content of fat-soluble vitamins: E by 0.010 mg and β-carotene by 0.051 mg. *Cucurbita moschata* Duchesne ex Poiret contains vitamin C, 4.8–7.6 mg/100 g, as well as vitamins B<sub>1</sub>, B<sub>2</sub>, E, and carotenoids. The addition of pumpkin puree and flax seeds to Ryazhanka increased the content of minerals: K by 31.3 mg (22%) and Mg by 17.2 mg (115%) due to the presence of minerals in pumpkin. However, replacing Ryazhanka with pumpkin puree and flax seeds led to a decrease in the content of such minerals as Ca by 5.2 mg (-4%) and Na by 4.1 mg (-9%).

Pumpkin fruits are rich in phenolic substances, including phenolcarboxylic acids and flavonols (Chikpah et al., 2022; Hussain et al., 2022), essential oils (Hussain et al., 2022), dietary fibers (Ahmad and Khan, 2019; Ezzat et al., 2022; Montesano et al., 2018), polysaccharides and pectin (Ezzat et al., 2022), peptides (Hussain et al., 2022), and phytosterols (Ezzat et al., 2022).

Flax seed (*Linum usitatissimum* L.) has a unique nutrient profile due to its oil content, ranging from 29% to 45% of the seed (Fitzpatrick, 2011; Marpalle et al., 2014). It is high in polyunsaturated fatty acids (73% of total fatty acids), moderate in monounsaturated fatty acids (18%), and low in saturated fatty acids (9%). Linoleic acid constitutes approximately 16% of total fatty acids (Morris, 2001), and flax seed oil's main nutritional advantage is its high level of α-linolenic acid (50-60%), an essential omega-3 fatty acid (Fitzpatrick, 2011; Morris, 2001). Adding flax seeds to Ryazhanka increased the content of omega-3 fatty acids from 0 to 0.80 g and omega-6 fatty acids from 0 to 0.20 g (Table 2). Flax seed mucilage, which constitutes about 20% of the flax seed, contains gum-like polysaccharides (Fitzpatrick, 2011). Flax seed also contains approximately 1-2% total phenolic compounds (Fitzpatrick, 2011).

The addition of pumpkin puree to the Ryazhanka enriches it with biologically active compounds that exhibit a wide range of biological activities: antioxidant, immunomodulatory, anti-inflammatory, antibacterial, antiviral, cardioprotective, hepatoprotective, cytoprotective, antidiabetic, anticancer, anti-aging, and prebiotic effects (Chikpah et al., 2022; Ezzat et al., 2022; Hussain et al., 2022; Yang et al., 2007). These properties make it useful to improve human health in current post COVID 19 period (Hussain et al., 2022).

Flax seed can be used in Ryazhanka technology as an additional ingredient to improve the nutritional value and texture of the product. Flax seed is a rich source of dietary fiber, omega-3 and omega-6 fatty acids, lignans, and other beneficial substances that can enhance the health benefits of Ryazhanka.

### **Sensory evaluation of Ryazhanka**

The sensory indicators of Ryazhanka with an optimal content of pumpkin puree (10%) and flax seeds (4%) are presented in Table 3.

**Table 3**  
**Sensory evaluation of Ryazhanka with pumpkin puree (10%) and flax seeds (4%)**

<b>Indicator</b>	<b>Research results of Ryazhanka according to a new recipe</b>
Appearance and consistency	Homogenous, with a broken clot, pumpkin puree and flax seeds evenly distributed throughout the mass
Taste	Sour milk, with a pronounced taste of pumpkin puree
Aroma	Clean, sour milk with a pronounced smell of pumpkin
Color	Uniform throughout the mass: light yellow

The impact of 4% flaxseed on the sensory characteristics of Ryazhanka is limited. The presence of mucilage in flax seeds increases the viscosity of Ryazhanka, resulting in reduced fluidity and increased resistance to destruction. Using more than 4% flaxseed can lead to the formation of a thick consistency that may be unpleasant for consumers. Hence, the optimal amount of flax seeds in Ryazhanka should be restricted to 4%. Similarly, the content of pumpkin puree should be limited to 10% as it affects the pleasant taste, aroma, and creaminess of Ryazhanka. Exceeding the 10% threshold may alter the consistency of the product.

### **Research of physicochemical parameters**

There is a need to study the influence of pumpkin puree and flax seeds on the quality and properties of Ryazhanka, including the duration of storage. The study of physico-chemical indicators was carried out based on the indicators of the mass fraction of fat and titrated acidity in two parallel tests. The final result was taken as the arithmetic mean of two parallel tests.

The results of changes in the titrated acidity of the control sample (Ryazhanka) and Ryazhanka with the addition of 10% pumpkin puree and 4% flax seeds during storage are shown in Figure 7.

The results from Figure 7 show that on the first day of the study, Ryazhanka with 10% pumpkin puree and 4% flax seeds had a titrated acidity of 72 °T. Over the storage period, the titrated acidity increased to 86 °T on the 4th day, 100 °T on the 6th day, and 107 °T on the 7th day. These findings are in line with data reported by Dan et al. (2019), Huang et al. (2020), and Zhang et al. (2022).

Based on the research results, it can be concluded that the addition of 10% pumpkin puree and 4% flax seeds influences the titrated acidity of Ryazhanka compared to the control sample. However, the experimental sample did not reach the upper limit of normalized titrated acidity (110 °T) during the 7-day storage period. Therefore, the shelf life of Ryazhanka with 10% pumpkin puree and 4% flax seeds, stored at temperatures between 0 and 6 °C, is determined to be no more than 7 days.

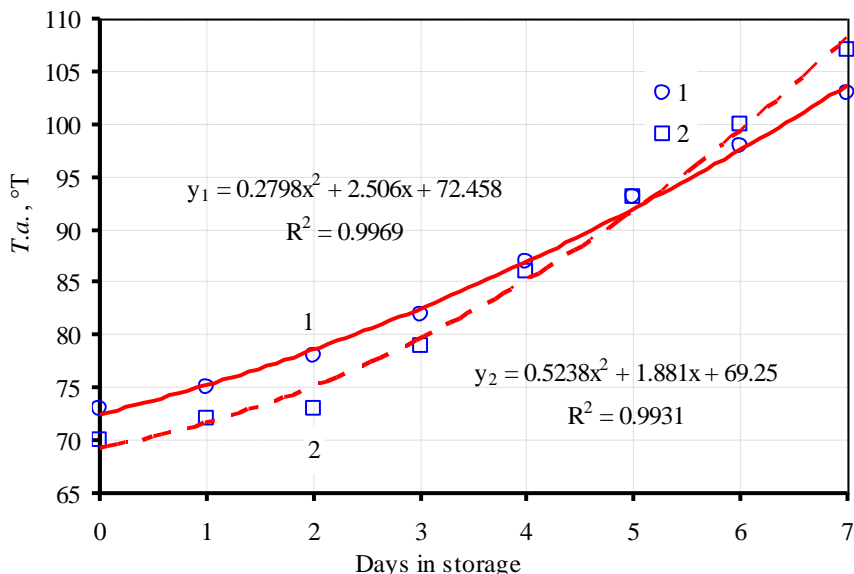


**Figure 7. Changes in the titrated acidity of Ryazhanka with pumpkin puree and flax seeds during storage:**

*1 – a control sample made according to the traditional recipe; 2 – sample according to the developed recipe with pumpkin puree (10%) and flax seeds (4%)*

Similar findings were observed in a study on fermented baked milk with sea buckthorn, where the authors noted a slight impact of sea buckthorn on the initial acidity of the samples. Over the subsequent 21 hours, the trends in titrated acidity of sea buckthorn fermented baked milk were comparable (Ge et al., 2022). These results align with the indicators highlighted in another study by Samilyk and Helikh (2020), which examined the addition of strawberry powder, candied beetroot, and strawberry jam to a yogurt recipe. The authors found no negative effects on the fermentation process and no significant increase in titrated acidity.

## Conclusions

1. The effect of pumpkin puree and flax seeds addition on the active and titrated acidity of Ryazhanka was studied. The results showed that adding 4-8% flax seeds and 10% pumpkin puree reduced the titrated acidity to 64-70 °T and increased the active acidity to pH 4.60-4.69. Similarly, adding 4-8% flax seeds and 15% pumpkin puree reduced the titrated acidity to 61-68 °T and increased the active acidity to pH 4.62-4.74. Furthermore, adding 4-8% flax seeds and 20% pumpkin puree decreased the titrated acidity to 60-65 °T and increased the active acidity to pH 4.62-4.75.
2. The optimal conditions for modifying the content of pumpkin puree and flax seeds in Ryazhanka to stabilize the physicochemical parameters were determined to be 10% pumpkin puree and 4% flax seeds.
3. It was determined that an increase in titrated acidity by 1 °T leads to a decrease in the active acidity of Ryazhanka by 0.0151 pH – an inverse correlation.

4. Based on the results of a study of the sensory indicators of Ryazhanka with pumpkin puree and flax seeds in comparison with Ryazhanka made according to traditional technology, it was established that the addition of 10% pumpkin puree and 4% flax seeds provides pleasant sensory properties, in particular with a uniform light yellow color, the taste and smell of pure sour milk with a pronounced taste of pumpkin.
5. When calculating the nutritional and energy value of the new type of Ryazhanka, an increase in the amount of proteins, fats, and carbohydrates was established by 15%, 16%, and 5%, respectively. The energy value of Ryazhanka with pumpkin puree and flax seeds increased by 12% compared to Ryazhanka made according to the traditional recipe.
6. Adding pumpkin puree and flax seeds to Ryazhanka affected the titrated acidity, and based on the research findings, the shelf life of Ryazhanka at temperatures between 0 °C and 6 °C was determined to be no more than 7 days.
7. The recipe of Ryazhanka with pumpkin puree and flax seeds was developed taking into account the quality indicators that meet the requirements of consumers and the needs of the production chain. This research enables the expansion of fermented milk product varieties and increases the production and consumption of Ryazhanka with enhanced health benefits.

**Acknowledgments.** The scientific and technical development was carried out by an inter-university team and is directly related to scientific, scientific-practical and innovative activities within the framework of the Memorandum of Cooperation No. 43/22 between the Institute of Vegetable and Melon Growing of the National Academy of Agrarian Sciences of Ukraine and the National University of Food Technologies dated 09/01/2022 (09/01/2022-08/31/2027). The implementation of the Memorandum on joint actions is aimed at deepening cooperation between scientific institutions, which does not contradict the current legislation of Ukraine.

## References

- Ahmad G., Khan A.A. (2019), Pumpkin: horticultural importance and its roles in various forms: a review, *International Journal of Horticulture & Agriculture*, 4, pp. 1–6, <https://doi.org/10.15226/2572-3154/4/1/00124>
- Ahmad M.H., Afzal M.F., Imran M., Khan M.K., Ahmad N. (2022), Nutrition: A strategy for curtailing the impact of COVID-19 through immunity booster foods, In: El Hiba O., Radhakrishnan J., Balzano T., Isbaine F. (eds.), *Handbook of Research on Pathophysiology and Strategies for the Management of COVID-19*, pp. 253–269, IGI Global, <https://doi.org/10.4018/978-1-7998-8225-1.ch016>
- Aidarbekova S., Aider M. (2022), Production of Ryazhanka, a traditional Ukrainian fermented baked milk, by using electro-activated whey as supplementing ingredient and source of lactulose, *Food Bioscience*, 46, 101526, <https://doi.org/10.1016/j.fbio.2021.101526>
- Akpınar E.K., Midilli A., Bicer Y. (2003), Experimental investigation of drying behaviour and conditions of pumpkin slices via a cyclone-type dryer, *Science of Food and Agriculture*, 83, pp. 1480–1486, <https://doi.org/10.1002/jsfa.1565>
- Buldo P., Sokolowsky M., Hoegholm T. (2021), The role of starter cultures on oral processing properties of different fermented milk products, *Food Hydrocolloids*, 114, 106571, <https://doi.org/10.1016/j.foodhyd.2020.106571>
- Chikpah S.K., Korese J.K., Sturm B., Hensel O. (2022), Colour change kinetics of pumpkin (*Cucurbita moschata*) slices during convective air drying and bioactive compounds of the dried products, *Journal of Agriculture and Food Research*, 10, 100409, <https://doi.org/10.1016/j.jafr.2022.100409>
- Dan T., Chen H., Li T., Tian J., Ren W., Zhang H., Sun T. (2019), Influence of *Lactobacillus*

- plantarum* p-8 on fermented milk flavor and storage stability, *Frontiers in Microbiology*, 9, 3133, <https://doi.org/10.3389/fmicb.2018.03133>
- Dhiman A., Sharma K., Attri S. (2009), Functional constituents and processing of pumpkin: A review, *Journal of Food Science and Technology*, 46, pp. 411–417.
- Doymaz İ. (2007), The kinetics of forced convective air-drying of pumpkin slices, *Journal of Food Engineering*, 79(1), pp. 243–248, <https://doi.org/10.1016/j.foodeng.2006.01.049>.
- Ezzat S.M., Adel R., Abdel-Sattar E. (2022), Pumpkin bio-wastes as source of functional ingredients. In: Ramadan M.F., Farag M.A. (eds.), *Mediterranean Fruits Bio-wastes*, pp. 667–696, Springer, Cham, [https://doi.org/10.1007/978-3-030-84436-3\\_29](https://doi.org/10.1007/978-3-030-84436-3_29)
- Fitzpatrick K.C. (2011), Health benefits of flaxseed, In: *Omega-3 Oils*, pp. 213–264, <https://doi.org/10.1016/B978-1-893997-82-0.50013-X>
- Ge X., Tang N., Huang Y., Chen X., Dong M., Rui X., Zhang Q., Li W. (2022), Fermentative and physicochemical properties of fermented milk supplemented with sea buckthorn (*Hippophae eleagnaceae* L.), *LWT*, 153, 112484, <https://doi.org/10.1016/j.lwt.2021.112484>
- Huang Z., Huang L., Xing G., Xu X., Tu C., Dong M. (2020), Effect of co-fermentation with lactic acid bacteria and *K. marxianus* on physicochemical and sensory properties of goat milk, *Foods*, 9(3), 299, <https://doi.org/10.3390/foods9030299>
- Hussain A., Kausar T., Sehar S., Sarwar A., Ashraf A.H., Jamil M.A., Noreen S., Rafique A., Iftikhar K., Aslam J., Qudoos M.Y., Majeed M.A., Zerlasht M. (2022), Utilization of pumpkin, pumpkin powders, extracts, isolates, purified bioactives and pumpkin based functional food products: A key strategy to improve health in current post COVID 19 period: An updated review, *Applied Food Research*, 2(2), 100241, <https://doi.org/10.1016/j.afres.2022.100241>
- Ivanov V., Shevchenko O., Marynyn A., Stabnikov V., Gubenia O., Stabnikova O., Shevchenko A., Gavva O., Saliuk A. (2021), Trends and expected benefits of the breaking edge food technologies in 2021–2030, *Ukrainian Food Journal*, 10(1), pp. 7–36, <https://doi.org/10.24263/2304-974X-2021-10-1-3>
- Kajla P., Sharma A., Sood D.R. (2015), Flaxseed – a potential functional food source, *Journal of Food Science and Technology*, 52, pp. 1857–1871, <https://doi.org/10.1007/s13197-014-1293-y>
- Khareba O., Kuzmin O., Khareba O., Marynchenko V., Karputina M., Koretska I. (2021), Antioxidant characteristics of non-traditional spicy-aromatic vegetable raw materials for restaurant technology, *Ukrainian Food Journal*, 10(2), pp. 301–320, <https://doi.org/10.24263/2304-974X-2021-10-2-8>
- Korese J.K., Achaglinkame M.A., Chikpah S.K. (2021), Effect of hot air temperature on drying kinetics of palmyra (*Borassus aethiopum* Mart.) seed-sprout fleshy scale slices and quality attributes of its flour, *Journal of Agriculture and Food Research*, 6, 100249, <https://doi.org/10.1016/j.jafr.2021.100249>
- Kuzmin O., Stukalska N., Mykhonik L., Koval O., Polyovyk V., Berezova G. (2021), Antioxidant characteristics of tea-herbal compositions, *Ukrainian Food Journal*, 10(4), pp. 807–827, <https://doi.org/10.24263/2304-974X-2021-10-4-14>
- Marpalle P., Sonawane S.K., Arya S.S. (2014), Effect of flaxseed flour addition on physicochemical and sensory properties of functional bread, *LWT – Food Science and Technology*, 58(2), pp. 614–619, <https://doi.org/10.1016/j.lwt.2014.04.003>
- Montesano D., Blasi F., Simonetti M.S., Santini A., Cossignani L. (2018), Chemical and nutritional characterization of seed oil from *Cucurbita maxima* L. (var. Berrettina) pumpkin, *Foods*, 7(3), 30, <https://doi.org/10.3390/foods7030030>
- Monteiro R.L., Link J.V., Tribuzi G., Carciofi B.A.M., Laurindo J.B. (2018), Effect of multi-flash drying and microwave vacuum drying on the microstructure and texture of pumpkin slices, *LWT*, 96, pp. 612–619, DOI: 10.1016/j.lwt.2018.06.023
- Moreno-Montoro M., Navarro-Alarcon M., Bergillos-Meca T., Gimenez-Martinez R., Sanchez-Hernandez S., Olalla-Herrera M. (2018), Physicochemical, nutritional, and organoleptic characterization of a skimmed goat milk fermented with the probiotic strain *Lactobacillus plantarum* C4, *Nutrients*, 10 (5), 633, <https://doi.org/10.3390/nu10050633>
- Morris D.H. (2001), Essential nutrients and other functional compounds in flaxseed, *Nutrition Today*, 36, pp. 159–162, <https://doi.org/10.1097/00017285-200105000-00012>
- Mousavi M., Heshmati A., Garmakhany A.D., Vahidinia A., Taheri M. (2019), Texture and

- sensory characterization of functional yogurt supplemented with flaxseed during cold storage, *Food Science & Nutrition*, 7, pp. 907–917, <https://doi.org/10.1002/fsn3.805>
- NatureClaim 2015-2023 [Internet]. Information on food nutrition facts; [cited 2023 March 8]. Available from: <https://natureclaim.com/nutrition>
- Oh N.S., Kwon H.S., Lee H.A., Joung J.Y., Lee J.Y., Lee K.B., Shin Y.K., Baick S.C., Park M.R., Kim Y., Lee K.W., Kim S.H. (2014), Preventive effect of fermented Maillard reaction products from milk proteins in cardiovascular health, *Journal of Dairy Science*, 97(6), pp. 3300–3313, <https://doi.org/10.3168/jds.2013-7728>
- Ropelewska E., Popińska W., Sabanci K., Aslan M.F. (2022), Flesh of pumpkin from ecological farming as part of fruit suitable for non-destructive cultivar classification using computer vision, *European Food Research and Technology*, 248, pp. 893–898, <https://doi.org/10.1007/s00217-021-03935-3>
- Samilyk M., Helikh A., Ryzhkova T., Bolgova N., Nazarenko Y. (2020), Influence of the structure of some types of fillers introduced to the yogurt recipe on changes in its rheological indicators, *Eastern-European Journal of Enterprise Technologies*, 2(11), 104, pp. 46–51, <https://doi.org/10.15587/1729-4061.2020.199527>
- Seremet Ceclu L., Botez E., Nistor O.V., Andronoiu D.G., Mocanu G.D. (2016), Effect of different drying methods on moisture ratio and rehydration of pumpkin slices, *Food Chemistry*, 195, pp. 104–109, DOI: 10.1016/j.foodchem.2015.03.125
- Shevchenko O., Kuzmin O., Melnyk O., Khareba V., Frolova N., Polyovyk V. (2022). Antioxidant properties of water-alcohol infusions of tea-herbal compositions based on yerba mate, *Ukrainian Food Journal*, 11(3), pp. 403–415, <https://doi.org/10.24263/2304-974X-2022-11-3-6>
- Singh K.K., Mridula D., Rehal J., Barnwal P. (2011), Flaxseed: a potential source of food, feed and fiber, *Critical Reviews in Food Science and Nutrition*, 51(3), pp. 210–222, <https://doi.org/10.1080/10408390903537241>
- Singh K.K., Jhamb S.A., Kumar R. (2012), Effect of pretreatments on performance of screw pressing for flaxseed, *Journal of Food Process Engineering*, 35(4), pp. 543–556, <https://doi.org/10.1111/j.1745-4530.2010.00606.x>
- Stabnikova O., Marinin A., Stabnikov V. (2021), Main trends in application of novel natural additives for food production, *Ukrainian Food Journal*, 10(3), pp. 524–551, <https://doi.org/10.24263/2304-974X-2021-10-3-8>
- Tavares T., Malcata F.X. (2019), Chapter 10 – Alternative Dairy Products Made With Raw Milk, Editor(s): Nero L.A., De Carvalho A.F., *Raw Milk*, Academic Press, pp. 223–234, <https://doi.org/10.1016/B978-0-12-810530-6.00010-9>
- Yang X., Zhao Y., You L. (2007), Chemical composition and antioxidant activity of an acidic polysaccharide extracted from *Cucurbita moschata* Duchesne ex Poirlet, *Journal of Agricultural and Food Chemistry*, 55, pp. 4684–4690, <https://doi.org/10.1021/jf070241r>
- Zhang Z., Guo S., Wu T., Yang Y., Yu X., Yao S. (2022), Inoculum size of co-fermentative culture affects the sensory quality and volatile metabolome of fermented milk over storage, *Journal of Dairy Science*, 105(7), pp. 5654–5668, <https://doi.org/10.3168/jds.2021-21733>
- Zhang X., Yang J., Zhang C., Chi H., Zhang C., Zhang J., Li T., Liu L., Li A. (2022), Effects of *Lactobacillus fermentum* HY01 on the quality characteristics and storage stability of yak yogurt, *Journal of Dairy Science*, 105(3), pp. 2025–2037, <https://doi.org/10.3168/jds.2021-20861>

# Modeling of non-stationary processes heat and mass transfer according to the cellular model of sucrose mass crystallization

Taras Pohorilyi

National University of Food Technologies, Kyiv, Ukraine

---

## Abstract

### Keywords:

Temperature  
Concentration  
Solution  
Crystal  
Massecuite

**Introduction.** The purpose of this work is to determine the influence of variable thermophysical characteristics on non-stationary diffusion mass flows of sucrose during sugar mass crystallization.

**Materials and methods.** In order to obtain quantitative values of nonstationary diffusion mass flows for intercrystalline sucrose solutions surrounding sugar crystals was calculated by numerical methods simultaneously for two systems of heat and mass transfer: 1) the system of 7 nonstationary thermal conductivity problems; 2) the system consisting of three nonstationary diffusion mass transfer problems.

**Results and discussion.** For a number of the relative sugar massecuite boiling time values 0.15-1.0 based on two systems (10 subsystems) simultaneous numerical solution of nonstationary parabolic type differential equations in partial derivatives (the first system consisted of 7 subsystems – for non-stationary thermal conductivity problems in each of the 7 areas; the second system includes three subsystems – for non-stationary diffusion mass transfer problems for 4 areas) found respectively: non-stationary temperature distributions in each of the 7 regions (4 regions with intercrystalline solutions, 2 sugar crystals and massecuite); nonstationary sucrose diffusion mass flows in each of the 4 intercrystalline sucrose solutions regions of the whole considered two cells and massecuite system. When the value of the relative sugar massecuite boiling time 0.15 when the whole cells system moving along the heating tube, the substance is first transferred from the intercrystalline sucrose solution of the smaller crystal to the intercrystalline sucrose solution of the larger crystal during 2.41–2.7 s (depending on constant or variable thermophysical characteristics). Starting from this moment of time  $\tau_{k,2}$  to 3.95 s (at sugar massecuite boiling time values 0.15) when the system of cells leaves the heating tube, the situation changes to the opposite. So, in this case, only one extremum of the diffusive mass flow was clearly defined (the minimum on the graph is reached at the moment of time 1.29–1.45 s, which determines the maximum sucrose mass transfer from a smaller crystal to a larger crystal). No clear maximum has been established in this case. At the relative time 1.0 of sugar massecuite boiling two clearly defined extremes (minimum and maximum) were obtained for both constant and variable thermophysical characteristics.

**Conclusions.** Features of variable thermophysical characteristics influence on the non-stationary sucrose diffusion mass flows in the cellular model are shown.

---

### Article history:

Received  
1.10.2022  
Received in  
revised form  
25.02.2023  
Accepted  
31.03.2023

---

### Corresponding author:

Taras Pohorilyi  
E-mail:  
pogorilytm@  
ukr.net

---

### DOI:

10.24263/2304-  
974X-2023-12-1-  
8

## Introduction

The complexity of the sucrose mass crystallization during the sugar syrup production is due to the simultaneous and mutually influencing non-stationary heat and mass exchange processes.

In this paper, by means of a numerical experiment based on the developed mathematical model [Pogoriliyy, 2015 b; Pogoriliyy, 2015 c; Pogoriliyy, 2016 a], the peculiarities and influence of non-stationary diffusive sucrose mass flows with variable thermophysical characteristics under the cellular model of mass crystallization.

Crystallisation of sucrose is the most energy-intensive step in the industrial production of sugar (Alewijn et al., 2013; Hartel et al., 1991; Shamim et al., 2016).

The process of sugar crystallization is difficult enough to describe. This is due to the need to simultaneously take into account all non-stationary technological and all non-stationary thermophysical parameters that affect the sugar crystallization process (Duroudier, 2016; Rózsa et al., 2016; Kulinchenko et al., 2012).

The problem of crystallization of a single sugar crystal, sucrose mass crystallization, as well as related processes that directly affect these complex processes at the modern level were dealt with by a number of authors: (Bruno et al., 2019; Georgieva et al., 2003; Nagy et al., 2013; Osmanbegovic et al., 2022; Romero-Bustamante et al., 2022; Rózsa et al., 2016; Sánchez-Sánchez et al., 2017; Suarez et al., 2011; Tkachenko et al., 2020; Vetter et al., 2022).

Note that considering the proposed solutions to the sucrose mass crystallization problem in industrial conditions (Bruno et al., 2019; Georgieva et al., 2003; Rózsa et al., 2016; Sánchez-Sánchez et al., 2017; Tkachenko et al., 2020), it can conclude that there is no single generally accepted approach to this issue today. Therefore, the problem arises in creating the most universal mathematical model of the sucrose mass crystallization process in industrial conditions.

One of the main tasks that the author set before himself is that the mathematical model would describe as fully as possible the heat and mass exchange process, which occurs between the constituent parts of the multiphase system, which is a sugar masseccuite.

Based on the literature review, it can also be concluded that taking into account all factors affecting the sucrose crystallization process is a rather difficult task when creating a mathematical model (Rózsa et al., 2016). Note that taking into account simultaneously all technological, thermophysical and hydrodynamic factors that affect the sucrose mass crystallization process is practically an extremely difficult or even impossible task. In view of this, when developing a mathematical model they were forced to accept a number of simplifications. Thus, the mathematical model of the mass crystallization process being developed should be classified as an idealized model.

This paper proposes one of the next steps in the mathematical model development of the sucrose mass crystallization process.

In the continuation of the works (Pogoriliy, 2015 a, b, c; 2016 a) sugar masseccuite is considered from the point of view of a cellular model.

Assume that in each cell a «sugar crystal» is surrounded by a certain corresponding «intercrystalline sucrose solution amount» (Pohorilyi, 2016 a) during the entire time of boiling the sugar masseccuite.

The purpose of this work is to determine the influence of variable thermophysical characteristics on non-stationary diffusion mass flows of sucrose during sugar mass crystallization.

## Materials and methods

In this work, as well as in works (Pogoriliyy, 2015 b, c; Pogorilyy, 2016 a), it consider a system consisting of two cells that are in contact with each other, as well as the massecuite region. Each of the considered cells includes a «sugar crystal» and an «intercrystalline sucrose solution surrounding the corresponding crystal». The considered cells are of different sizes. Therefore, one crystal and the intercrystalline solution surrounding it will have a larger size, respectively, the other will have a smaller size.

In general, we believe that hydrodynamic interactions between cells can occur only between the outer boundaries of the intercrystalline sucrose solutions regions of such cells. That is, in other words, in each cell, the region of the intercrystalline sucrose solution is as if «glued» only to its sugar crystal, which is inside the region of the intercrystalline sucrose solution during the entire time of boiling the sugar massecuite.

Areas of intercrystalline sucrose solutions of different cells can generally move relative to each other. However, in this case, we assume that in the considered system «two cells—the massecuite region» from the moment of entering the heating tube until the moment of its exit, the system components do not change the order of their location relative to each other and do not change their size. With this assumption, we fix the volume both for the crystal and for the intercrystalline sucrose solution, as well as for the area of the massecuite during the entire time  $\tau$  of their stay in the heating tube.

Such an assumption was forced to be accepted, since it is not possible to take into account the dynamic changes of both crystal sizes and sizes of intercrystalline sucrose solutions surrounding the corresponding crystals, at this stage of creating a mathematical model.

We consider the non-stationary heat exchange process, which occurs both internally between the components in each cell of the entire system (that is, between the crystals and the corresponding intercrystalline sucrose solutions in each cell), and between them. At the same time, we also consider the non-stationary heat exchange between all the components of the two cells of this system and the massecuite region.

At the same time, simultaneously with the non-stationary heat exchange processes mentioned above, we consider non-stationary mass transfer processes that occur both internally between the components of each of the entire system considered cells (that is, between the crystals and the corresponding intercrystalline sucrose solutions in each cell), and between the cells themselves (we consider by determination of diffusion mass transfer processes between intercrystalline sucrose solutions of the first and second cells).

Since the simulation of non-stationary processes as heat transfer and mass transfer simultaneously for the entire system «two cells—the massecuite region» («larger sugar crystal–intercrystalline sucrose solution of a larger crystal»–«smaller sugar crystal–intercrystalline sucrose solution of a smaller crystal»–massecuite”) is quite a difficult task, so it should be carried out in several stages.

At the first stage, for the simplest geometric model case of the massecuite representation, the mathematical model described only the non-stationary temperature distribution for the system, which included only one cell («sugar crystal–intercrystalline sucrose solution») and the massecuite region (Pogorilyy, 2015 a).

Further, the non-stationary temperature distribution in the system «sugar crystal–intercrystalline sucrose solution– massecuite» was considered, taking into account the different location of the cell «sugar crystal–intercrystalline sucrose solution» in relation to the heating tube surface. Next, the case was considered for a more complex geometric model of the massecuite representation, when the mathematical model described a non-stationary

temperature distribution for a more complex system, which already included two cells of different sizes («larger crystal–intercrystalline solution of sucrose of a larger crystal»–«smaller crystal–intercrystalline sucrose solution of a smaller crystal») and the massecuite area (Pogoriliy, 2015 b).

At the second stage, the case was considered when the mathematical model simultaneously described the non-stationary temperature distribution for each component of the entire two cells system and the massecuite region (“«larger sugar crystal–intercrystalline sucrose solution of a larger crystal»–«smaller sugar crystal–intercrystalline sucrose solution of a smaller crystal»–massecuite”), and non-stationary sucrose concentrations distribution in all intercrystalline solutions regions of this system (Pogorilyy, 2015 c).

Next, we considered the case when the mathematical model simultaneously described the non-stationary temperature distribution for the each entire system component of two cells and the massecuite area (“«larger sugar crystal–intercrystalline sucrose solution of a larger crystal»–«smaller sugar crystal–intercrystalline sucrose solution of a smaller crystal»–massecuite”), and non-stationary sucrose diffusive mass fluxes in all intercrystalline solutions regions of this system (Pogorilyy, 2016 a).

We note that in the last work, several mathematical model variants were considered, when either all steels or simultaneously all variable thermophysical characteristics that took part in the calculations were taken into account.

However, for a more complete understanding of the sucrose mass crystallization process, it is worth establishing how certain factors individually affect this process.

For this purpose, it is necessary to conduct more thorough studies on solving the question of whether taking into account dynamically changing thermophysical characteristics separately for the sugar crystal, separately for the intercrystalline sucrose solution, and separately for the massecuite region affects the sucrose mass crystallization process. Provided that, if such impacts occur, establish the nature and determine the weight of such impacts.

So, in this work, we consider the system of two cells and the massecuite region (“«larger sugar crystal–intercrystalline sucrose solution of the larger crystal»–«smaller sugar crystal–intercrystalline sucrose solution of the smaller crystal»– massecuite”) inside the heating tube of the vacuum apparatus heating chamber (Figure 1).

From the 3D model of the system “«larger sugar crystal–intercrystalline sucrose solution of a larger crystal»–«smaller sugar crystal–intercrystalline sucrose solution of a smaller crystal»–massecuite” in the inside of the heating tube of the vacuum apparatus heating chamber, by projection, we will move to the 2D model, where all components of the system under consideration (Figure 2).

Finally, in the 2D model (Figure 2), by selecting the regions according to the minimum size of the overall size  $b_{cr,2}$  (Figure 1) of the smaller crystal #2, which will participate in the heat and mass transfer processes, we moved to a one-dimensional formulation of such problems.

Therefore, the main task: to find the values of diffusion mass flows at the corresponding boundaries «sugar crystal–intercrystalline sucrose solution» in each cell of the considered system and between intercrystalline sucrose solutions of neighboring cells (Figure 2).

Also, at the same time, we will consider the diffusive mass transfer between intercrystalline sucrose solutions of different cells of the entire system, which consists of two cells of different sizes and massecuite “«larger sugar crystal–intercrystalline sucrose solution of a larger crystal»–«smaller sugar crystal–intercrystalline sucrose solution of a smaller crystal»–massecuite”).

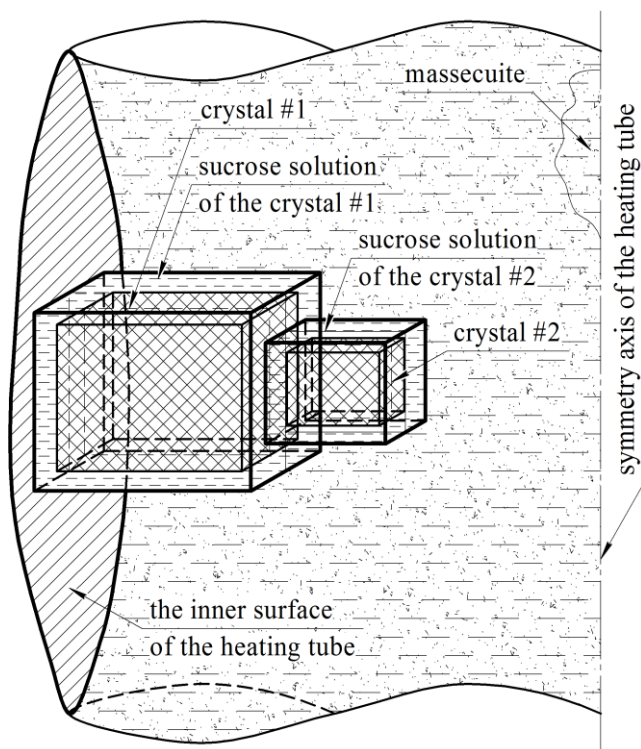


**Figure 1. Three-dimensional geometric model of two cells and the massecuite area (“«larger sugar crystal #1–intercrystalline sucrose solution of larger crystal #1»–«smaller sugar crystal #2–intercrystalline sucrose solution of smaller crystal #2»–massecuite”) inside the heating tube of the vacuum apparatus heating chamber**

The solution of such a complex problem is based on the simultaneous solution of a system of the non-stationary parabolic type differential equations in partial derivatives, which will describe non-stationary heat transfer problems (for seven regions: (#1), (#2), (#3), (#4), (#5), (#6) and (#7)) for the entire system «larger cell–smaller cell–massecuite» and the system of three unsteady diffusion mass transfer problems (for four regions: separately for region (#1)), separately for area (#6), and simultaneously for two areas (#3) and (#4) for all components of the larger and smaller cells in the form of intercrystalline sucrose solutions.

Non-stationary problems of heat transfer and mass transfer for the system “«larger sugar crystal–intercrystalline sucrose solution of a larger crystal»–«smaller sugar crystal–intercrystalline sucrose solution of a smaller crystal»–massecuite” were considered for the case of this entire system contact with the inner heating (boiling) tubes surface of the vacuum apparatus heating chamber (Figure 1).

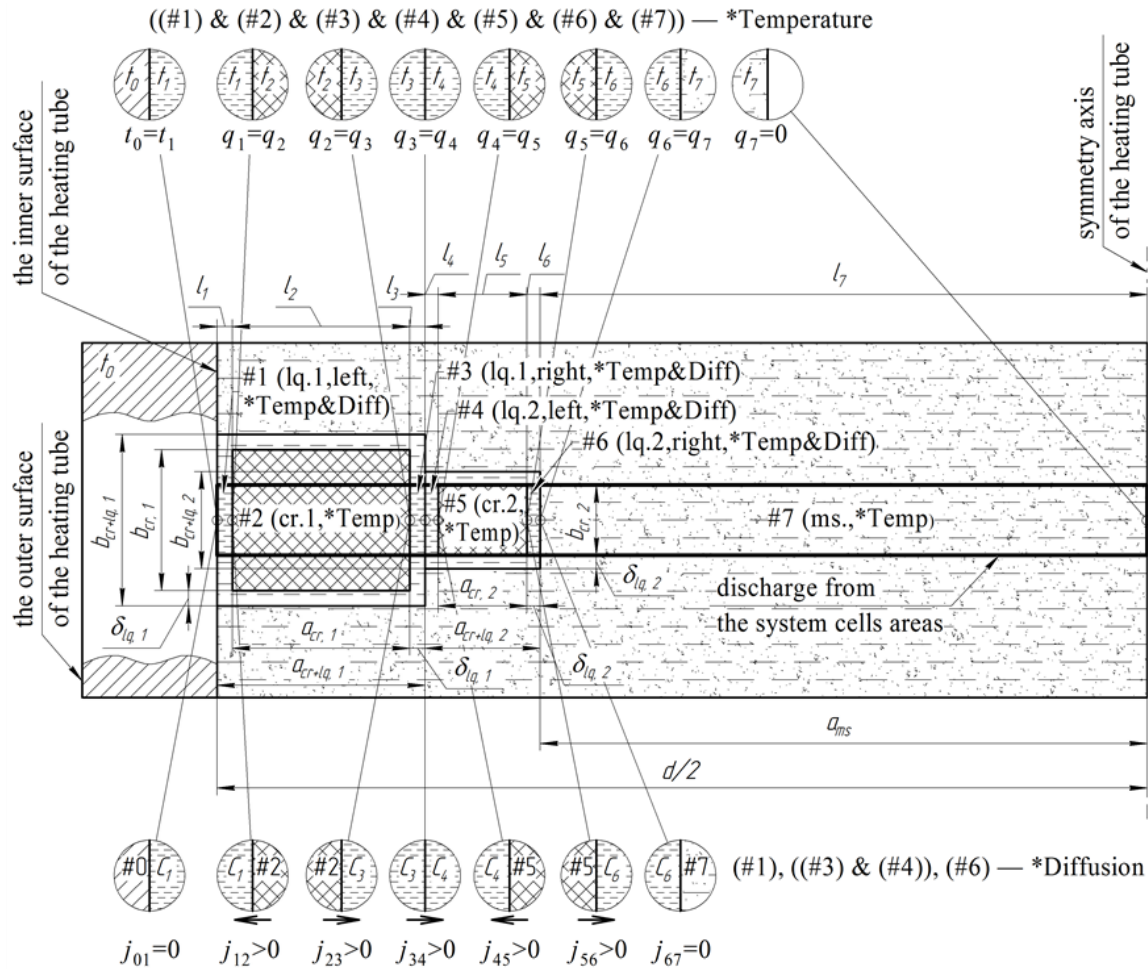


**Figure 2.** Selection from the 2D projection of the system “larger sugar crystal–intercrystalline sucrose solution of a larger crystal»–«smaller sugar crystal–intercrystalline sucrose solution of a smaller crystal»–massecuite” regions that simultaneously receive training in non-stationary heat exchange processes (simultaneously between regions (#1), (#2), (#3), (#4), (#5), (#6) and (#7)) and diffusive mass exchanges (separately for region (#1), separately for region (#6), and simultaneously for two regions (#3) and (#4)) for the calculation of non-stationary diffusive mass fluxes of sucrose.

Designation on Figure 2:

\*) For areas:

\*Temp—only the non-stationary problem of thermal conductivity was considered;

\*Temp&Diff— the non-stationary thermal conductivity problem and the non-stationary diffusive mass transfer problem were considered at the same time

\*) in the footnotes above for heat flows  $q_i$ , (where  $i = 1..7$ ) boundary conditions are indicated on each separate internal boundary;

\*) in the footnotes below for diffusion sucrose mass flows  $j_{mm}$ , (where the coefficients  $(mm)=\{21; 23; 34; 54; 56\}$ ) on each separate boundary, an arrow indicates the positive direction of the sucrose mass flow accepted in the calculations (the reverse direction is negative )

It is worth noting that in this case two different concepts regarding the term "time" are considered:

a)  $\tau/\tau_c$  – the relative time of boiling sugar massecuite; as a rule, the complete cooking time of the sugar massecuite reaches the order of several hours; the relative time  $\tau/\tau_c$  varies within 0–1; where 0 corresponds to the beginning of boiling sugar massecuite; and 1 corresponds to the completion of boiling sugar massecuite; almost all technological, thermophysical indicators depend on this parameter;

b)  $\tau_c$  is the residence time of the system «larger sugar crystal–intercrystalline sucrose solution of a larger crystal»–«smaller sugar crystal–intercrystalline sucrose solution of a smaller crystal»–massecuite” in the middle of the heating tube of the heating chamber; in this case, the order of magnitude is from a few seconds to a dozen seconds, and in turn, also depends on the relative time of boiling the sugar massecuite  $\tau/\tau_c$ .

The initial moment of time  $\tau_{k,0} = 0$  of the contact of the «larger cell–smaller cell–massecuite» system with the heat carrier was taken to be the time when the entire «two cells–massecuite » system enters the lower part of the vertically located heating tube.

The final contact moment of time  $\tau_{c,end}$  of the «larger cell–smaller cell–massecuite» system with the heat carrier was taken to be the moment when the entire «two cells–massecuite» system simultaneously leaves the upper part of the vertically located heating tube of the vacuum apparatus.

The issue of determining the residence time value  $\tau_{c,end}$  of the «two cells– massecuite» system inside the heating tube of the vacuum apparatus heating chamber depending on the relative boiling time  $\tau/\tau_c$  of the sugar massecuite in industrial conditions was considered in (Pohorilyi, 2016 a).

Let us immediately note that the technological and thermophysical characteristics for each of the «two cells–massecuite» system components: for crystals, for intercrystalline solutions of sucrose and for massecuite, as well as the diffusion mass transfer coefficient only for the intercrystalline sucrose solutions regions of two cells, will depend on the relative time of boiling sugar massecuite  $\tau/\tau_c$ .

However, we note that due to the fact that the boiling sugar massecuite time can reach several hours, and the residence time of the «two cells–massecuite» system inside the heating tube of the heating chamber is on the order of several seconds, we consider the problem of heat and mass transfer to be quasi-stationary with respect to the variable relative boiling time  $\tau/\tau_c$  of sugar massecuite; and, at the same time, we consider the contact of the «two cells–massecuite» system with the inner wall of the heating tube of the vacuum apparatus heating chamber to be non-stationary with respect to the time variable. It is precisely in this sense that in this paper a study of non-stationarity in relation to heat and mass transfer processes is carried out.

As for the relative boiling time  $\tau/\tau_c$ , ten different values were recorded in this study from the moment of sugar crystal formation, which corresponds to  $\tau/\tau_c = 0.15$ , and until the end of the sugar massecuite boiling, which corresponds to  $\tau/\tau_c = 1.0$ , namely:  $\tau/\tau_c = 0.15; 0.2; 0.3; 0.4; 0.5; 0.6; 0.7; 0.8; 0.9; 1.0$ . For each of the above fixed relative time values of sugar massecuite boiling  $\tau/\tau_c$ , all technological parameters were found and recorded:

- a) dry substances content in the intercrystalline sucrose solution;
- b) purity of intercrystalline sucrose solution;
- c) mass content of sucrose in intercrystalline sucrose solution;
- d) mass content of crystals in massecuite.

On the basis of these fixed values, as well as depending on the temperature  $t$ , the necessary thermophysical parameters were found for intercrystalline solutions of sucrose in both cells and for massecuite.

Note that in this work, the impact of taking into account variable thermophysical characteristics coefficients on the sucrose mass crystallization process is investigated through the determination of diffusion mass flows in each of the considered cells, as well as diffusion mass exchange between the cells themselves. This is done in order to determine the influence weight of these considerations on each individual component of the «two cells–massecuite» system, and in the future to be able to apply the most optimal approach when creating further mathematical models of the sucrose mass crystallization process.

Let's explain what exactly the «fixed» coefficients and «variable» coefficients contribute to the research understanding.

«constant» coefficients means that at the beginning of the calculation of non-stationary heat and mass transfer processes, all necessary coefficients are calculated when:

a) to the corresponding value of the relative boiling time  $\tau/\tau_c = 0.15; 0.2; 0.3; 0.4; 0.5; 0.6; 0.7; 0.8; 0.9; 1.0$  (that is, all coefficients depend on the relative boiling time  $\tau/\tau_c$ );

b) but each time all the necessary coefficients are calculated precisely at the initial temperature  $t_0$  of the entire system «two cells–massecuite», which enters the lower part of the entry into the heating tube of the heating chamber.

We denote the calculation option with «constant» thermophysical coefficients by (I).

«variable» coefficients means that, just as for «constant» at the beginning of the non-stationary processes calculation of heat and mass transfer, all the necessary coefficients are calculated at the corresponding value of the relative boiling time  $\tau/\tau_c = 0.15; 0.2; 0.3; 0.4; 0.5; 0.6; 0.7; 0.8; 0.9; 1.0$  (that is, all coefficients depend on the relative boiling time  $\tau/\tau_c$ ).

At the first time step, as well as for the «constant» coefficients, those coefficients that depend on temperature are calculated at the initial temperature  $t_0$  of the entire «two cells–massecuite» system, which enters the lower part of the entry into the heating tube of the heating chamber.

But at each subsequent step (starting from the second step) in time  $\tau_c$  for the calculation of non-stationary heat and mass transfer problems, all the necessary coefficients are calculated already at the current temperature  $t$  of each component of the «two cells–massecuite» system, where the current value of the temperature  $t$  is taken from the previous step made calculations.

Note that in this work, research was conducted when «variable» thermophysical coefficients were taken into account:

- separately only for crystals (we denote this calculation version of variable thermophysical coefficients through (II a));
- separately only for intercrystalline solutions of sucrose (we denote this variant of calculating variable thermophysical coefficients through (II b));

- separately only for massecuite (we denote this version of the calculation of variable thermophysical coefficients through (II c)).

All «variable» thermophysical coefficients for the entire «two cells–massecuite» system were also taken into account at the same time (we denote this variant of the calculation of all variable thermophysical coefficients by (III)).

As mentioned earlier, the non-stationary distribution of temperatures in all seven regions (Figure 2) was determined based on the solution of one non-stationary thermal conductivity problem simultaneously for:

- #1 – the left area of the intercrystalline sucrose solution of the larger crystal 1 of the first cell;
- #2 – regions of the larger crystal 1 of the first cell;
- #3 – the right area of the intercrystalline sucrose solution of the larger crystal 1 of the first cell;
- #4 – the left area of the intercrystalline sucrose solution of smaller crystal 2 of the second cell;
- #5 – areas of the smaller crystal 2 of the second cell;
- #6 – the right area of the intercrystalline sucrose solution of smaller crystal 2 of the second cell;
- #7 – massecuite areas.

Together with the non-stationary temperature distribution, the sought non-stationary concentrations distribution in all four regions (Figure 2) of intercrystalline solutions was determined based on the simultaneous solution of three different non-stationary diffusion mass transfer problems:

- separately for area #1 (the left intercrystalline sucrose solution area of larger crystal 1 of the first cell);
- at the same time for regions #3 and #4 (intercrystalline solutions belonging to crystals of different sizes), which are in contact with each other according to the ideal law of diffusion mass transfer;
- separately for area #6 (the right area of the intercrystalline sucrose solution of smaller crystal 2 of the second cell).

Next, on the basis of the obtained solutions of three non-stationary diffusion mass transfer problems the values of  $j(\tau)$ , ( $\text{kg}/(\text{m}^2\cdot\text{s})$ ), non-stationary diffusive mass flows for intercrystalline sucrose solution regions as a function of time  $\tau$ , (s). Since we have four different intercrystalline sucrose solution regions (#1, #3, #4, #6, Figure 2), in order to distinguish the diffusion mass flows for each boundary of each separate region, we denote them by  $j_{mn}(\tau)$ , ( $(mn)=\{01; 12; 23; 34; 45; 56; 67\}$ ), (Figure 2), where:

- $j_{01}(\tau)$ ,– diffusive mass exchange between the left border of region #1 (that is, the left intercrystalline sucrose solution region of the first cell, Figure 2) and the heating wall of the vacuum apparatus heating chamber; since such a mass exchange for the system «two cells–massecuite» and an impermeable heating wall in this direction is absent due to physical considerations, the mass exchange directly of area #1 with the heating wall is also absent, therefore  $j_{01}(\tau) = 0$ , ( $\text{kg}/(\text{m}^2 \text{ s})$ );
- $j_{12}(\tau)$ ,– diffusive mass exchange between the right border of region #1 (ie, the left intercrystalline sucrose solution region of the first larger cell, Figure 2) and the larger sugar crystal (region #2, Figure 2) of the first cell of the «two cells–massecuite»; if diffusive mass transfer occurs from the side of region #2 of the larger crystal to the side of region #1 of the intercrystalline sucrose solution, then we accept this direction

- as positive,  $j_{12}(\tau) > 0$ , (Figure 2); if the diffusive mass transfer occurs from the side of region #1 of the intercrystalline sucrose solution in the direction of region #2 of the larger crystal of the first cell, then we take this direction of movement of sucrose as negative,  $j_{12}(\tau) < 0$ ;
- $j_{23}(\tau)$ ,– diffusive mass exchange between the left border of region #3 (ie, the right intercrystalline sucrose solution region of the first larger cell, Figure 2) and the larger sugar crystal (region #2, Figure 2) of the first cell of the «two cells–massecuite» system; if diffusive mass transfer occurs from the side of region #2 of the larger crystal to the side of region #3 of the intercrystalline sucrose solution, then we accept this direction as positive,  $j_{23}(\tau) > 0$ , (Figure 2); if the diffusive mass transfer occurs from the side of region #3 of the intercrystalline sucrose solution in the direction of region #2 of the larger crystal of the first cell, then this direction of sucrose movement is taken as negative,  $j_{23}(\tau) < 0$ ;
  - $j_{34}(\tau)$ ,– diffusive mass exchange between the right border of region #3 (ie, the right region of the intercrystalline sucrose solution of the first larger cell, Figure 2), and the left border of region #4 (ie, the left region of the intercrystalline sucrose solution of the second smaller cell, Figure 2); in fact, this is the sought-after mass exchange between neighboring cells of the «two cells–massecuite» system in the recrystallization theory; if diffusive mass transfer occurs from the side of region #3 of the intercrystalline sucrose solution of the larger first cell to the side of region #4 of the intercrystalline sucrose solution of the smaller second cell, then we accept this direction as positive,  $j_{34}(\tau) > 0$ , (Figure 2); if the diffusion mass transfer occurs from the side of region #4 of the intercrystalline sucrose solution of the smaller crystal of the second cell in the direction of region #3 of the intercrystalline sucrose solution of the larger crystal of the first cell, then this direction of sucrose movement is taken as negative,  $j_{34}(\tau) < 0$ ;
  - $j_{45}(\tau)$ ,– diffusive mass exchange between the right border of region #4 (ie, the left region of the intercrystalline sucrose solution of the second smaller cell, Figure 2) and the smaller sugar crystal (region #5, Figure 2) of the second smaller cell of the «two cells–massecuite»; if diffusive mass transfer occurs from the side of the smaller crystal #5 to the side of region #4 of the intercrystalline sucrose solution, then we accept this direction as positive,  $j_{45}(\tau) > 0$ , (Figure 2); if the diffusive mass transfer occurs from the side of region #4 of the intercrystalline sucrose solution in the direction of region #5 of the smaller crystal of the second cell, then this direction of sucrose movement is taken as negative,  $j_{45}(\tau) < 0$ ;
  - $j_{56}(\tau)$ ,– diffusive mass exchange between the left border of region #6 (ie, the right region of the intercrystalline sucrose solution of the second smaller cell, Figure 2) and the smaller sugar crystal (region #5, Figure 2) of the second cell of the «two cells–massecuite»; if diffusive mass transfer occurs from the side of region #5 of the smaller sugar crystal to the side of region #6 of the intercrystalline sucrose solution, then we accept this direction as positive,  $j_{56}(\tau) > 0$ , (Figure 2); if the diffusive mass transfer occurs from the side of region #6 of the intercrystalline sucrose solution in the direction of region #5 of the smaller crystal of the second cell, then this direction of sucrose movement is taken as negative,  $j_{56}(\tau) < 0$ ;

- $j_{67}(\tau)$ , – diffusive mass exchange between the right border of region #6 (ie, the right region of the intercrystalline sucrose solution of the second smaller cell, Figure 2), and region #7 of the massecuite of the «two cells–massecuite» system; note that although for physical reasons such a diffusion mass exchange generally occurs, it is not possible to investigate such a diffusion mass exchange directly at this stage. Therefore, we accept the value of the diffusion mass flow between the region #6 of the intercrystalline sucrose solution and the region #7 of the massecuite  $j_{67}(\tau)=0$ .

Thus, on the basis of one system of equations of the non-stationary heat transfer problem and three systems of equations of the non-stationary diffusion mass transfer problems we determine the desired non-stationary diffusion mass flows  $j_{mn}(\tau)$ , ( $mn=\{01; 12; 23; 34; 45; 56; 67\}$ ).

Solve a complex system of non-stationary differential equations for the non-stationary heat transfer problem and three systems of equations of non-stationary diffusion mass transfer problems as well as finding non-stationary diffusive mass flows is a rather difficult task even under the condition of using constant thermophysical characteristics. Using analytical methods, it is difficult to solve such a system of equations even for a system that consists of three regions (in our case, there are seven of them). Therefore, the non-stationary system of problems was solved using numerical methods: the control volume method (Eymard et al., 2000; LeVeque, 2002). Diffusion mass flows were searched: for constant thermophysical characteristics (case I, accepted earlier), for alternately variable thermophysical characteristics (cases II a, II b, and II c), and for the case when the thermophysical characteristics were all variable at the same time (case III).

Note that when calculating the sucrose diffusion mass flows  $j_{mn}(\tau)$ , ( $m=0-6, n=m+1$ ), used the first and second order of their approximation. This paper presents the results of only the second order of approximation.

When calculations were carried out, the initial temperature of the components of the «two cells–massecuite» system was assumed to be the same for all areas (#1)–(#7), (Figure 2) at the same time and equal to  $t_{i,0} = 75 \text{ }^\circ\text{C}$ , ( $i = \overline{1,7}$ ).

The temperature of the inner wall  $t_0$  of the heating tube was assumed to be constant over the entire height of this tube, i.e., during the entire time of contact with the «two cells–massecuite» system and equal to  $t_0 = 100 \text{ }^\circ\text{C}$ .

When performing calculations the initial concentration for all intercrystalline sucrose solutions components of the «two cells–massecuite» system, that is, for all areas (#1), (#3)–(#4), (#6), (Figure 2), was simultaneously assumed to be the same and equal to  $C_{i,0} = C_{i,0}(t_{i,0}) = 77,594\%$  (Pohorilyi, 2016 a). In this work, the initial concentration was calculated at the supersaturation factor  $SS = 1$ .

Based on the research conducted (Pohorilyi, 2016 a), the contact time  $\tau_c$  of the «two cells–massecuite» system with the wall of the heating tube of the vacuum apparatus heating chamber depended non-linearly on the relative time of boiling sugar massecuite  $\tau/\tau_c$ . The following values were found:

- for the relative boiling time  $\tau/\tau_c = 0,15$ , the contact time is equal to  $\tau_{k,\text{end}} = 3,95 \text{ s}$ ;
- at  $\tau/\tau_c = 1,0$ , the contact time is equal to  $\tau_{k,\text{end}} = 67,93 \text{ s}$ .

When using numerical methods, time discretization was  $\Delta\tau_k = 0.01 \text{ s}$ .

In this work, the following crystal size values were adopted:  $a_{cr,1} = 5,0 \cdot 10^{-4} \text{ m}$ ,  $a_{cr,2} = 2,5 \cdot 10^{-4} \text{ m}$ , (Figure 2), (Kulinchenko et al., 2012; Crestani et al., 2021; Zhong et al., 2022). On the basis of the conducted research (Pohorilyi, 2016 a), all other required dimensions of the thickness of the intercrystalline sucrose solution layer were obtained:

$\delta_{\text{li},1} = 4,29 \cdot 10^{-5}$  m,  $\delta_{\text{li},2} = 3,73 \cdot 10^{-5}$  m, and the size of the massecuite region:  $a_{\text{ms}} = 4,83896 \cdot 10^{-2}$  m, (Figure 2). The size of the layer thickness was calculated based on the massecuite volume in the vacuum apparatus at the moment of introducing the seed into it according to the data given in (Kulinchenko et al., 2012).

The discretization by coordinate, i.e., the partition grid, for each of the regions (#1)–(#7), (Figure 2) was adopted as follows:

- regions of intercrystalline sucrose solutions (#1), (#3), (#4), (#6), (Figure 2), the grid is uniform, the number of calculated points of division is  $n_1 = n_3 = n_4 = n_6 = 10$ ;
- regions of sugar crystals (#2), (#5), (Figure 2), the grid is uniform, the number of calculation points of division is  $n_2 = n_5 = 20$ ;
- the massecuite area (#7), (Figure 2), the grid is uneven, the number of calculation points of division  $n_7 = 100$ .

## Results and discussion

On the basis of calculations carried out at the same time for:

- systems of equations of non-stationary thermal conductivity and
- three systems of non-stationary diffusive mass transfer equations for which during the entire contact time  $\tau_c$  of the «two cells–massecuite» system with the inner surface of the heating tube of the vacuum apparatus heating chamber, the calculations were carried out according to five different variants of the calculation (in all five cases, the technological indicators were fixed at a certain relative time value of the boiling sugar massecuite  $\tau/\tau_c$ , ( $\tau/\tau_c = 0.15–1.0$ ) according to which the calculation was made):
- I) all thermophysical characteristics (coefficients) are fixed at the initial temperature  $t_{i,0} = 75$  °C, ( $i = \overline{1,7}$ ), and at a certain value of the relative time of boiling sugar massecuite  $\tau/\tau_c$ , ( $\tau/\tau_c = 0.15–1.0$ ) according to which the calculation was carried out;
- II a) at the initial temperature  $t_{i,0} = 75$ °C, ( $i = \overline{1,7}$ ), and at a certain value of the relative time of boiling sugar massecuite  $\tau/\tau_c$ , ( $\tau/\tau_c = 0.15–1.0$ ) only thermophysical coefficients were recorded: all for the crystal, diffusion coefficient for the intercrystalline solution of sucrose and all for the massecuite; thermophysical coefficients (thermal conductivity coefficient, heat capacity coefficient and density) for the intercrystalline sucrose solution during the entire calculation time  $\tau_c$  were dependent on the current temperature  $t_i(\tau)$ , ( $i = \overline{1,7}$ ), at a certain value of the relative time of boiling sugar massecuite  $\tau/\tau_c$ , ( $\tau/\tau_c = 0.15–1.0$ ) according to which the calculation was carried out;
- II b) at the initial temperature  $t_{i,0} = 75$ °C, ( $i = \overline{1,7}$ ), and at a certain value of the relative time of boiling sugar massecuite  $\tau/\tau_c$ , ( $\tau/\tau_c = 0.15–1.0$ ), only thermophysical coefficients were recorded: all for intercrystalline sucrose solution and all for massecuite; thermophysical coefficients (thermal conductivity coefficient, heat capacity coefficient and density) for the crystal during the entire calculation time  $\tau_c$  were assumed to be dependent on the current temperature  $t_i(\tau_c)$ , ( $i = \overline{1,7}$ );

- II c) at the initial temperature  $t_{i,0} = 75 \text{ }^\circ\text{C}$ , ( $i = \overline{1,7}$ ), and at a certain value of the relative time of boiling sugar massecuite  $\tau/\tau_c$ , ( $\tau/\tau_c = 0.15\text{--}1.0$ ), only thermophysical coefficients are fixed: all for the crystal and all for the intercrystalline solution; thermophysical coefficients (thermal conductivity coefficient, heat capacity coefficient and density) for massecuite depend on the current temperature  $t_i(\tau_c)$ , ( $i = \overline{1,7}$ ), but are fixed at a certain value of the relative time of boiling sugar massecuite  $\tau/\tau_c$ , ( $\tau/\tau_c = 0.15\text{--}1.0$ );
- III) all thermophysical coefficients: for the crystal, for the intercrystalline solution, and for the massecuite depend on the current temperature  $t_i(\tau_c)$ , ( $i = \overline{1,7}$ ), but are fixed at a certain value of the relative time of boiling sugar massecuite  $\tau/\tau_c$ , ( $\tau/\tau_c = 0.15\text{--}1.0$ ).

Due to the limited scope of the article, this paper shows the dependences of the diffusion mass flows  $j_{mn}(\tau)$ , ( $m=1\text{--}5$ ,  $n=m+1$ ), at the boundaries of intercrystalline sucrose solutions of the «two cells–massecuite» system (Figure 2) depending on the contact time  $\tau$  for only two cases of the relative time of boiling sugar massecuite  $\tau/\tau_c$ : at the moment of formation of the structured crystals mass ( $\tau/\tau_c = 0.15$ ) and at the final moment of the sugar massecuite boiling time ( $\tau/\tau_c = 1.0$ ).

Distribution of unsteady diffusion mass flows of sucrose  $j_{mn}(\tau)$ , ( $m=1\text{--}5$ ,  $n=m+1$ ), at the boundaries of intercrystalline sucrose solutions regions (#1), (#3), (#4) and (#6), (Figure 2) depending on the contact time  $\tau$  of the «two cells–massecuite» system with the inner heating tube surface of the vacuum apparatus heating chamber at the relative time of boiling sugar massecuite  $\tau/\tau_c = 0.15$  is presented in the following graphs below:

- the unsteady diffusion mass flow of sucrose  $j_{12}(\tau)$  on the right border of the area (#1), where the movement of matter from the area (#2) of the larger crystal of the first cell to the area (#1) of the intercrystalline sucrose solution is taken as the positive direction (Figure 3);
- unsteady diffusion mass flow of sucrose  $j_{23}(\tau)$  on the left border of the area (#3), where the movement of matter from the area (#2) of the larger crystal of the first cell to the area (#3) of the intercrystalline sucrose solution is taken as the positive direction (Figure 4);
- unsteady diffusion sucrose mass flow  $j_{34}(\tau)$  between the right border of the region (#3) and the left border of the region (#4), where the movement of matter from the region (#3) of the intercrystalline sucrose solution of the larger crystal of the first cell to the region (#4) intercrystalline sucrose solution of the smaller crystal of the second cell (Figure 5);
- unsteady diffusion mass flow of sucrose  $j_{45}(\tau)$  on the right border of the region (#4), where the movement of matter from the region (#5) of the smaller crystal of the second cell to the region (#4) of the intercrystalline sucrose solution is taken as the positive direction (Figure 6);
- unsteady diffusion mass flow of sucrose  $j_{56}(\tau)$  on the left border of the area (#6), where the movement of matter from the area (#5) of the smaller crystal of the second cell to the area (#6) of the intercrystalline sucrose solution is taken as the positive direction (Figure 7).

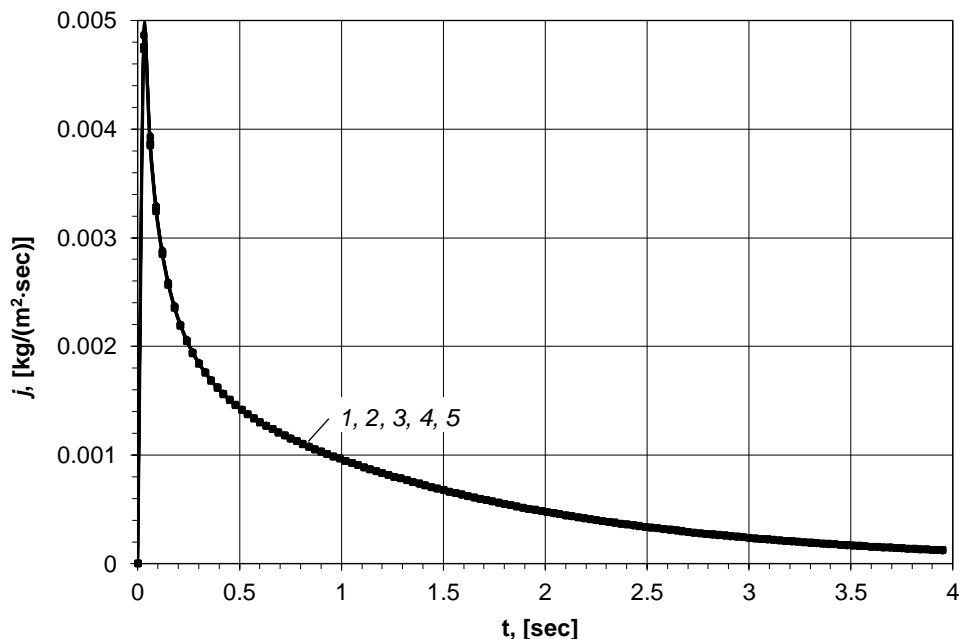


**Figure 3. Dependence of the sucrose diffusion mass flow  $j_{12}(\tau)$  on the contact time  $\tau$  of the «two cells–massecuite» system with the inner surface of the heating tube of the vacuum apparatus heating chamber on the border (Figure 2) of area (#1), (intercrystalline sucrose solution of the first larger cell) and area (#2), (larger sugar crystal of the first cell) with the relative time of boiling sugar massecuite  $\tau/\tau_c = 0.15$ ; [value  $j_{12}(\tau) > 0$  if sucrose is transferred from region (#2) (larger sugar crystal of the first cell) to region (#1) (intercrystalline sucrose solution of the first larger cell), (Figure 2, bottom footnote)].**

**\* Designations:**

1 – all thermophysical characteristics (coefficients): for the crystal, for the intercrystalline sucrose solution and for the massecuite there are constant values (option I);

2 – thermophysical characteristics (coefficients):

all for the crystal, diffusion coefficient for the intercrystalline sucrose solution and all for the massecuite are constant values;

thermal conductivity coefficient, heat capacity coefficient and density for the intercrystalline sucrose solution, are variable values (option II, a);

3 – thermophysical characteristics (coefficients):

all for intercrystalline sucrose solution and all for massecuite are constant values;

thermal conductivity coefficient, heat capacity coefficient and density for the crystal are variable quantities (option II, b);

4 – thermophysical characteristics (coefficients):

all for the crystal, all for the intercrystalline solution are constant values;

thermal conductivity coefficient, heat capacity coefficient and density for massecuite, are variable quantities (option II, c);

5 – all thermophysical characteristics (coefficients):

for the crystal, for the intercrystalline solution, and for the massecuite are variable values (option III).

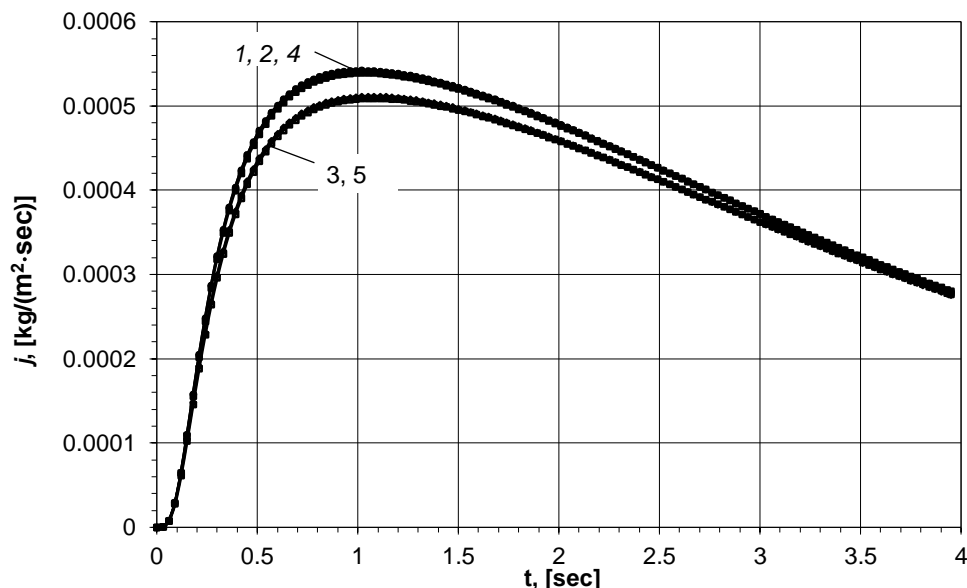


**Figure 4. Dependence of the sucrose diffusion mass flow  $j_{23}(\tau)$  on the contact time  $\tau$  of the «two cells–massecuite» system with the inner surface of the heating tube of the vacuum apparatus heating chamber on the border (Figure 2) of region (#2), (larger sugar crystal of the first cell) and region (#3), (intercrystalline sucrose solution of the first larger cell) with the relative time of boiling sugar massecuite  $\tau/\tau_c = 0.15$ ;**

**[value  $j_{23}(\tau) > 0$  if sucrose is transferred from region (#2) (larger sugar crystal of the first cell) to region (#3) (intercrystalline sucrose solution of the first larger cell), (Figure 2, bottom footnote)].**

**\* Designations:**

1 – all thermophysical characteristics (coefficients): for the crystal, for the intercrystalline sucrose solution and for the massecuite there are constant values (option I);

2 – thermophysical characteristics (coefficients):

all for the crystal, diffusion coefficient for the intercrystalline sucrose solution and all for the massecuite are constant values;

thermal conductivity coefficient, heat capacity coefficient and density for the intercrystalline sucrose solution, are variable values (option II, a);

3 – thermophysical characteristics (coefficients):

all for intercrystalline sucrose solution and all for massecuite are constant values;

thermal conductivity coefficient, heat capacity coefficient and density for the crystal are variable quantities (option II, b);

4 – thermophysical characteristics (coefficients):

all for the crystal, all for the intercrystalline solution are constant values;

thermal conductivity coefficient, heat capacity coefficient and density for massecuite, are variable quantities (option II, c);

5 – all thermophysical characteristics (coefficients):

for the crystal, for the intercrystalline solution, and for the massecuite are variable values (option III).

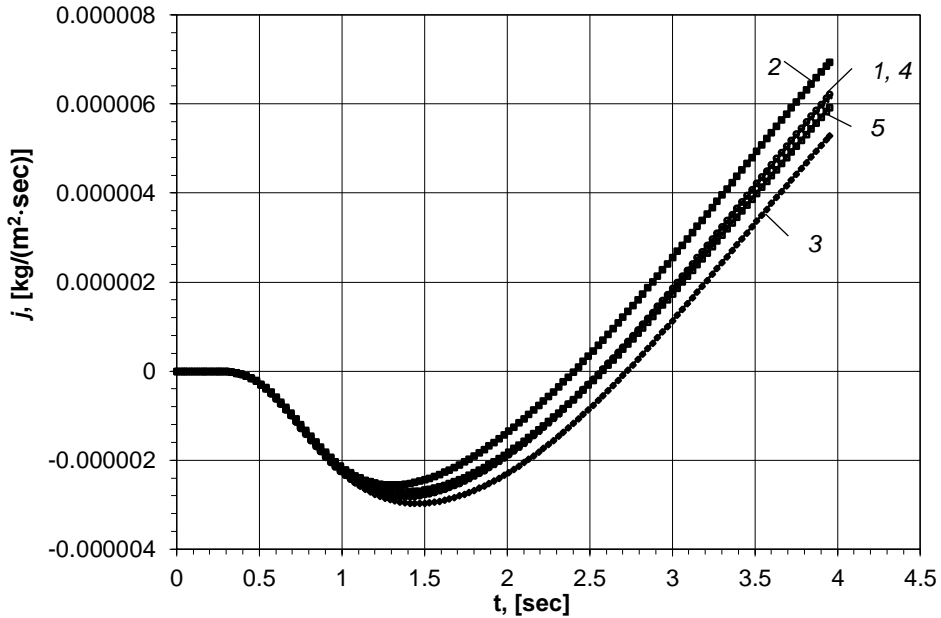


**Figure 5. Dependence of the sucrose diffusion mass flow  $j_{34}(\tau)$  on the contact time  $\tau$  of the «two cells–massecuite» system with the inner surface of the heating tube of the vacuum apparatus heating chamber on the border (Figure 2) of region (#3), (intercrystalline sucrose solution of the first larger cell) and region (#4), (intercrystalline sucrose solution of the second smaller cell) with the relative time of boiling sugar massecuite  $\tau/\tau_c = 0.15$ ;**

**[value  $j_{34}(\tau) > 0$  if sucrose is transferred from region (#3) (intercrystalline sucrose solution of the first larger cell) to region (#4) (intercrystalline sucrose solution of the second smaller cell), (Figure 2, footnote)].**

**\* Designations:**

- 1 – all thermophysical characteristics (coefficients): for the crystal, for the intercrystalline sucrose solution and for the massecuite there are constant values (option I);
- 2 – thermophysical characteristics (coefficients): all for the crystal, diffusion coefficient for the intercrystalline sucrose solution and all for the massecuite are constant values; thermal conductivity coefficient, heat capacity coefficient and density for the intercrystalline sucrose solution, are variable values (option II, a);
- 3 – thermophysical characteristics (coefficients): all for intercrystalline sucrose solution and all for massecuite are constant values; thermal conductivity coefficient, heat capacity coefficient and density for the crystal are variable quantities (option II, b);
- 4 – thermophysical characteristics (coefficients): all for the crystal, all for the intercrystalline solution are constant values; thermal conductivity coefficient, heat capacity coefficient and density for massecuite, are variable quantities (option II, c);
- 5 – all thermophysical characteristics (coefficients): for the crystal, for the intercrystalline solution, and for the massecuite are variable values (option III).

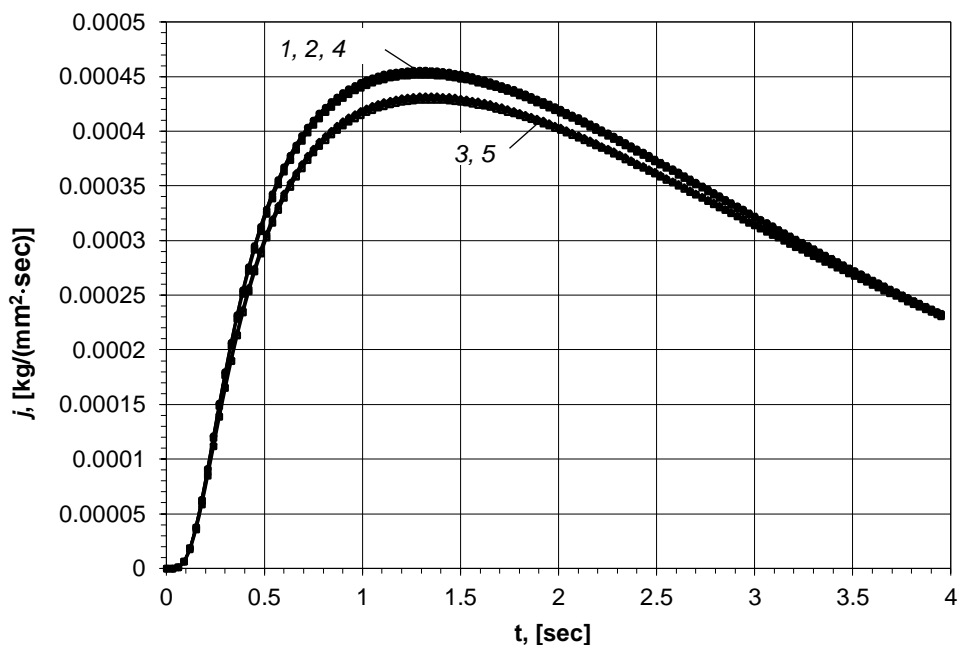


**Figure 6. Dependence of the sucrose diffusion mass flow  $j_{45}(\tau)$  on the contact time  $\tau$  of the «two cells–massecuite» system with the inner surface of the heating tube of the vacuum apparatus heating chamber on the border (Figure 2) of area (#4), (intercrystalline sucrose solution of the second smaller cell) and area (#5), (smaller sugar crystal of the second cell) with the relative time of boiling sugar massecuite  $\tau/\tau_c = 0.15$ ;**

[value  $j_{45}(\tau) > 0$  if sucrose is transferred from region (#5) (smaller sugar crystal of the second cell) to region (#4) (intercrystalline sucrose solution of the second smaller cell), (Figure 2, bottom footnote)].

**\* Designations:**

1 – all thermophysical characteristics (coefficients): for the crystal, for the intercrystalline sucrose solution and for the massecuite there are constant values (option I);

2 – thermophysical characteristics (coefficients):

all for the crystal, diffusion coefficient for the intercrystalline sucrose solution and all for the massecuite are constant values;

thermal conductivity coefficient, heat capacity coefficient and density for the intercrystalline sucrose solution, are variable values (option II, a);

3 – thermophysical characteristics (coefficients):

all for intercrystalline sucrose solution and all for massecuite are constant values;

thermal conductivity coefficient, heat capacity coefficient and density for the crystal are variable quantities (option II, b);

4 – thermophysical characteristics (coefficients):

all for the crystal, all for the intercrystalline solution are constant values;

thermal conductivity coefficient, heat capacity coefficient and density for massecuite, are variable quantities (option II, c);

5 – all thermophysical characteristics (coefficients):

for the crystal, for the intercrystalline solution, and for the massecuite are variable values (option III).

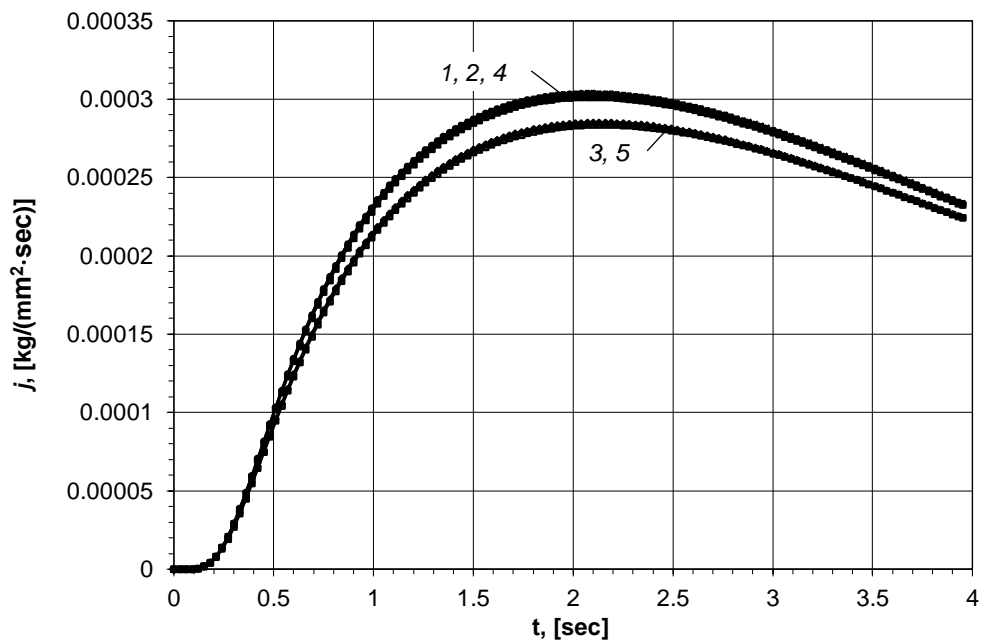


**Figure 7. Dependence of the sucrose diffusion mass flow  $j_{s6}(\tau)$  on the contact time  $\tau$  of the «two cells–massecuite» system with the inner surface of the heating tube of the the vacuum apparatus heating chamber on the border (Figure 2) of region (#5), (smaller sugar crystal of the second cell) and region (#6), (intercrystalline sucrose solution of the second smaller cell) with the relative time of boiling sugar massecuite  $\tau/\tau_c = 0.15$ ;**  
 [value  $j_{s6}(\tau) > 0$  if sucrose is transferred from region (#5) (smaller sugar crystal of the second cell) to region (#6) (intercrystalline sucrose solution of the second smaller cell), (Figure 2, bottom footnote)].

**\* Designations:**

1 – all thermophysical characteristics (coefficients): for the crystal, for the intercrystalline sucrose solution and for the massecuite there are constant values (option I);

2 – thermophysical characteristics (coefficients):

all for the crystal, diffusion coefficient for the intercrystalline sucrose solution and all for the massecuite are constant values;

thermal conductivity coefficient, heat capacity coefficient and density for the intercrystalline sucrose solution, are variable values (option II, a);

3 – thermophysical characteristics (coefficients):

all for intercrystalline sucrose solution and all for massecuite are constant values;

thermal conductivity coefficient, heat capacity coefficient and density for the crystal are variable quantities (option II, b);

4 – thermophysical characteristics (coefficients):

all for the crystal, all for the intercrystalline solution are constant values;

thermal conductivity coefficient, heat capacity coefficient and density for massecuite, are variable quantities (option II, c);

5 – all thermophysical characteristics (coefficients):

for the crystal, for the intercrystalline solution, and for the massecuite are variable values (option III).

The obtained results of calculations and studies of the distribution of non-stationary diffusion mass flows of sucrose  $j_{mn}(\tau)$ , ( $m=1-5$ ,  $n=m+1$ ), at the boundaries of intercrystalline sucrose solutions regions (#1), (#3), (#4) and (#6), (Figure 2) depending on the contact time  $\tau$  of the «two cells–massecuite» system with the inner surface of the heating tube of the vacuum apparatus heating chamber at eight values of the relative boiling time  $\tau/\tau_c = (0.2 - 0.9)$ , – it is not possible to submit due to the limited scope of this article.

We will present only the results of boiling at a relative time of  $\tau/\tau_c = 1.0$ .

Distribution of unsteady diffusion mass flows of sucrose  $j_{mn}(\tau)$ , ( $m=1-5$ ,  $n=m+1$ ), at the boundaries of intercrystalline sucrose solutions regions (#1), (#3), (#4) and (#6), (Figure 2) depending on the contact time  $\tau$  of the «two cells–massecuite» system with the inner surface of the heating tube of the vacuum apparatus heating chamber at the relative time of boiling sugar massecuite  $\tau/\tau_c = 1.0$  is presented in the following graphs below:

- unsteady diffusion mass flow of sucrose  $j_{12}(\tau)$  on the right border of the area (#1), where the positive direction is taken (as in Figure 3), the movement of matter from the area (#2) of the larger crystal of the first cell to the area (#1) intercrystalline solution of sucrose, (Figure 8);
- unsteady diffusion mass flow of sucrose  $j_{23}(\tau)$  on the left border of the region (#3), where the positive direction is taken (as in Figure 4) to be the movement of matter from the region (#2) of the larger crystal of the first cell to the region (#3) intercrystalline solution of sucrose, (Figure 9);
- unsteady diffusion mass flow of sucrose  $j_{34}(\tau)$  between the right border of the region (#3) and the left border of the region (#4), where the positive direction is taken (as in Figure 5) to be the movement of matter from the region (#3) the intercrystalline sucrose solution of the larger crystal of the first cell into the region (#4) of the intercrystalline sucrose solution of the smaller crystal of the second cell (Figure 10);
- unsteady diffusion mass flow of sucrose  $j_{45}(\tau)$  on the right border of the area (#4), where the positive direction is taken (as in Figure 6) to be the movement of matter from the area (#5) of the smaller crystal of the second cell to the area (#4) intercrystalline sucrose solution, (Figure 11);
- unsteady diffusion mass flow of sucrose  $j_{56}(\tau)$  on the left border of the region (#6), where the positive direction is taken (as in Figure 7) to be the movement of matter from the region (#5) of the smaller crystal of the second cell to the region (#6) intercrystalline sucrose solution, (Figure 12).

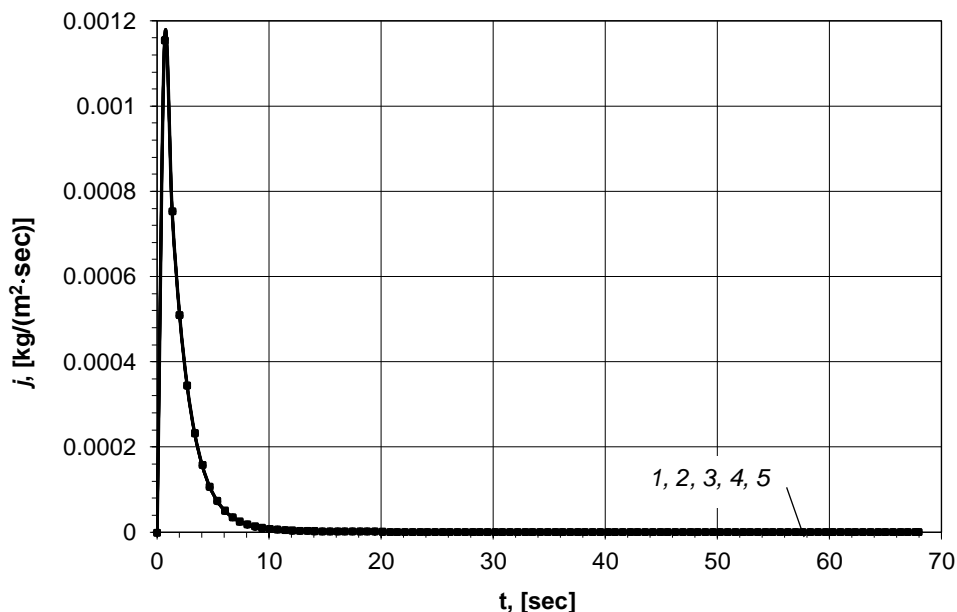


**Figure 8. Dependence of the sucrose diffusion mass flow  $j_{12}(\tau)$  on the contact time  $\tau$  of the «two cells–massecuite» system with the inner surface of the heating tube of the vacuum apparatus heating chamber on the border (Figure 2) of area (#1), (intercrystalline sucrose solution of the first larger cell) and area (#2), (larger sugar crystal of the first cell) with the relative time of boiling sugar massecuite  $\tau/\tau_c = 1.0$ ; [value  $j_{12}(\tau) > 0$  if sucrose is transferred from region (#2) (larger sugar crystal of the first cell) to region (#1) (intercrystalline sucrose solution of the first larger cell), (Figure 2, bottom footnote)].**

**\* Designations:**

- 1 – all thermophysical characteristics (coefficients): for the crystal, for the intercrystalline sucrose solution and for the massecuite there are constant values (option I);
- 2 – thermophysical characteristics (coefficients): all for the crystal, diffusion coefficient for the intercrystalline sucrose solution and all for the massecuite are constant values; thermal conductivity coefficient, heat capacity coefficient and density for the intercrystalline sucrose solution, are variable values (option II, a);
- 3 – thermophysical characteristics (coefficients): all for intercrystalline sucrose solution and all for massecuite are constant values; thermal conductivity coefficient, heat capacity coefficient and density for the crystal are variable quantities (option II, b);
- 4 – thermophysical characteristics (coefficients): all for the crystal, all for the intercrystalline solution are constant values; thermal conductivity coefficient, heat capacity coefficient and density for massecuite, are variable quantities (option II, c);
- 5 – all thermophysical characteristics (coefficients): for the crystal, for the intercrystalline solution, and for the massecuite are variable values (option III).

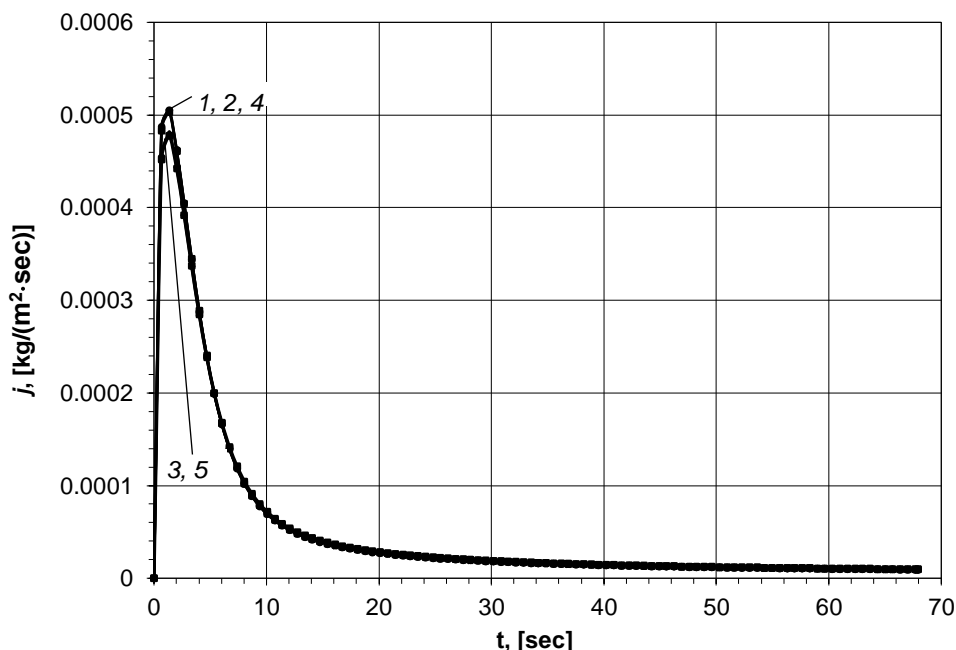


**Figure 9. Dependence of the sucrose diffusion mass flow  $j_{23}(\tau)$  on the contact time  $\tau$  of the «two cells–massecuite» system with the inner surface of the heating tube of the vacuum apparatus heating chamber on the border (Figure 2) of region (#2), (larger sugar crystal of the first cell) and region (#3), (intercrystalline sucrose solution of the first larger cell) with the relative time of boiling sugar massecuite  $\tau/\tau_c = 1.0$ ;**  
**[value  $j_{23}(\tau) > 0$  if sucrose is transferred from region (#2) (larger sugar crystal of the first cell) to region (#3) (intercrystalline sucrose solution of the first larger cell), (Figure 2, bottom footnote)].**

**\* Designations:**

1 – all thermophysical characteristics (coefficients): for the crystal, for the intercrystalline sucrose solution and for the massecuite there are constant values (option I);

2 – thermophysical characteristics (coefficients):

all for the crystal, diffusion coefficient for the intercrystalline sucrose solution and all for the massecuite are constant values;

thermal conductivity coefficient, heat capacity coefficient and density for the intercrystalline sucrose solution, are variable values (option II, a);

3 – thermophysical characteristics (coefficients):

all for intercrystalline sucrose solution and all for massecuite are constant values;

thermal conductivity coefficient, heat capacity coefficient and density for the crystal are variable quantities (option II, b);

4 – thermophysical characteristics (coefficients):

all for the crystal, all for the intercrystalline solution are constant values;

thermal conductivity coefficient, heat capacity coefficient and density for massecuite, are variable quantities (option II, c);

5 – all thermophysical characteristics (coefficients):

for the crystal, for the intercrystalline solution, and for the massecuite are variable values (option III).

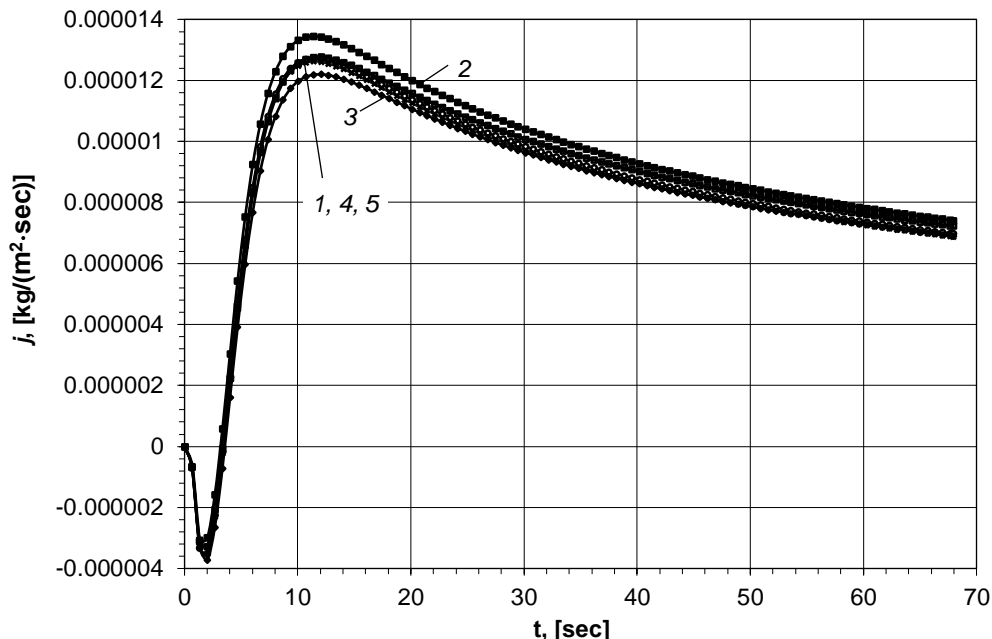


**Figure 10. Dependence of the sucrose diffusion mass flow  $j_{34}(\tau)$  on the contact time  $\tau$  of the «two cells–massecuite» system with the inner surface of the heating tube of the vacuum apparatus heating chamber on the border (Figure 2) of region (#3), (intercrystalline sucrose solution of the first larger cell) and region (#4), (intercrystalline sucrose solution of the second smaller cell) with the relative time of boiling sugar massecuite  $\tau/\tau_c = 1.0$ ;**

[value  $j_{34}(\tau) > 0$  if sucrose is transferred from region (#3) (intercrystalline sucrose solution of the first larger cell) to region (#4) (intercrystalline sucrose solution of the second smaller cell), (Figure 2, footnote)].

**\* Designations:**

1 – all thermophysical characteristics (coefficients): for the crystal, for the intercrystalline sucrose solution and for the massecuite there are constant values (option I);

2 – thermophysical characteristics (coefficients):

all for the crystal, diffusion coefficient for the intercrystalline sucrose solution and all for the massecuite are constant values;

thermal conductivity coefficient, heat capacity coefficient and density for the intercrystalline sucrose solution, are variable values (option II, a);

3 – thermophysical characteristics (coefficients):

all for intercrystalline sucrose solution and all for massecuite are constant values;

thermal conductivity coefficient, heat capacity coefficient and density for the crystal are variable quantities (option II, b);

4 – thermophysical characteristics (coefficients):

all for the crystal, all for the intercrystalline solution are constant values;

thermal conductivity coefficient, heat capacity coefficient and density for massecuite, are variable quantities (option II, c);

5 – all thermophysical characteristics (coefficients):

for the crystal, for the intercrystalline solution, and for the massecuite are variable values (option III).

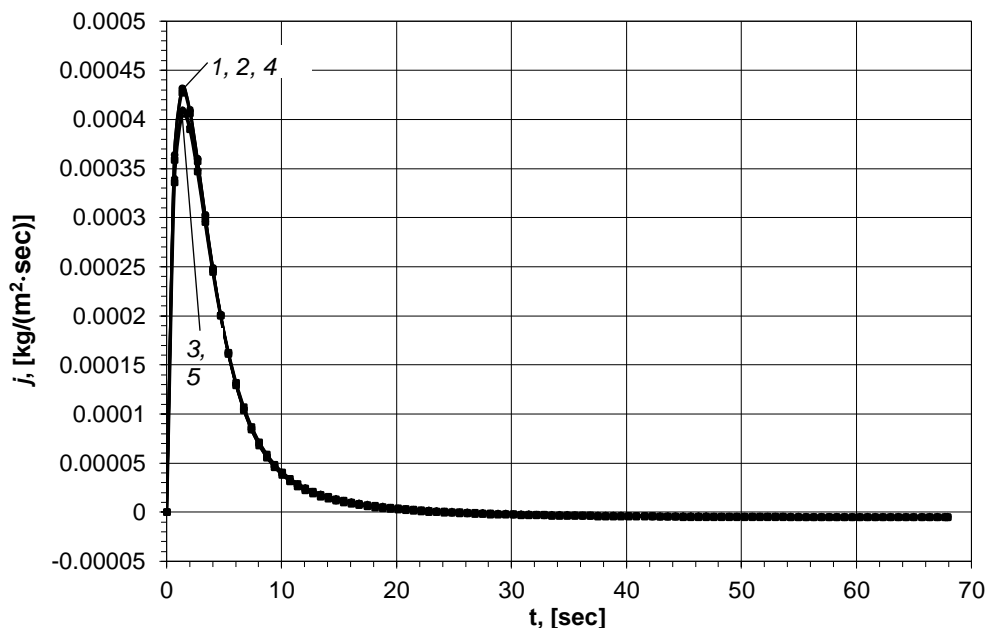


**Figure 11. Dependence of the sucrose diffusion mass flow  $j_{45}(\tau)$  on the contact time  $\tau$  of the «two cells–massecuite» system with the inner surface of the heating tube of the vacuum apparatus heating chamber on the border (Figure 2) of area (#4), (intercrystalline sucrose solution of the second smaller cell) and area (#5), (smaller sugar crystal of the second cell) with the relative time of boiling sugar massecuite  $\tau/\tau_c = 1.0$ ;  
[value  $j_{45}(\tau) > 0$  if sucrose is transferred from region (#5) (smaller sugar crystal of the second cell) to region (#4) (intercrystalline sucrose solution of the second smaller cell), (Figure 2, bottom footnote)].**

**\* Designations:**

- 1 – all thermophysical characteristics (coefficients): for the crystal, for the intercrystalline sucrose solution and for the massecuite there are constant values (option I);
- 2 – thermophysical characteristics (coefficients): all for the crystal, diffusion coefficient for the intercrystalline sucrose solution and all for the massecuite are constant values; thermal conductivity coefficient, heat capacity coefficient and density for the intercrystalline sucrose solution, are variable values (option II, a);
- 3 – thermophysical characteristics (coefficients): all for intercrystalline sucrose solution and all for massecuite are constant values; thermal conductivity coefficient, heat capacity coefficient and density for the crystal are variable quantities (option II, b);
- 4 – thermophysical characteristics (coefficients): all for the crystal, all for the intercrystalline solution are constant values; thermal conductivity coefficient, heat capacity coefficient and density for massecuite, are variable quantities (option II, c);
- 5 – all thermophysical characteristics (coefficients): for the crystal, for the intercrystalline solution, and for the massecuite are variable values (option III).

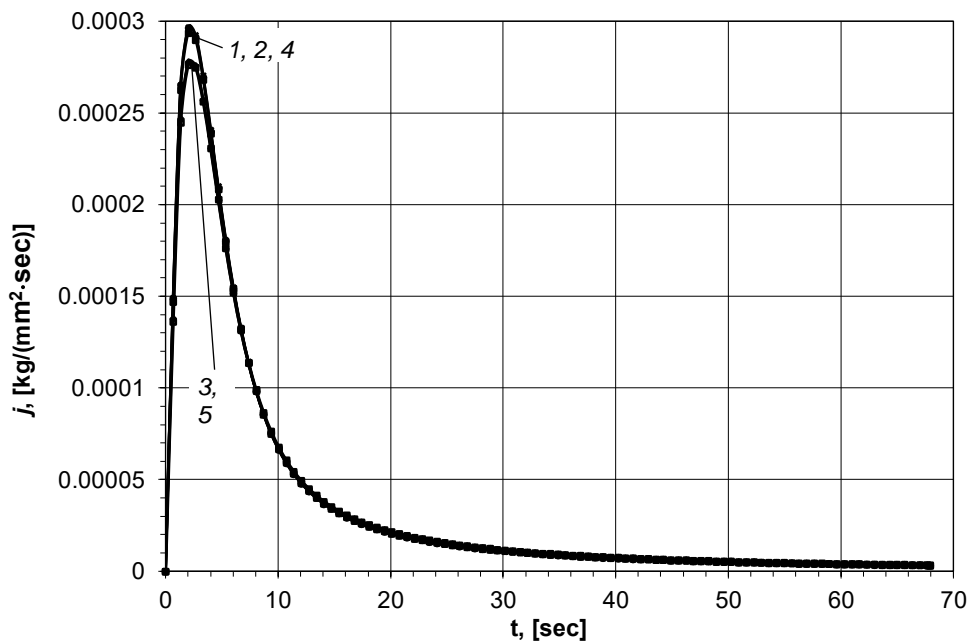


**Figure 12. Dependence of the sucrose diffusion mass flow  $j_{s6}(\tau)$  on the contact time  $\tau$  of the «two cells–massecuite» system with the inner surface of the heating tube of the the vacuum apparatus heating chamber on the border (Figure 2) of region (#5), (smaller sugar crystal of the second cell) and region (#6), (intercrystalline sucrose solution of the second smaller cell) with the relative time of boiling sugar massecuite  $\tau/\tau_c = 1.0$ ;**  
 [value  $j_{s6}(\tau) > 0$  if sucrose is transferred from region (#5) (smaller sugar crystal of the second cell) to region (#6) (intercrystalline sucrose solution of the second smaller cell), (Figure 2, bottom footnote)].

**\* Designations:**

1 – all thermophysical characteristics (coefficients): for the crystal, for the intercrystalline sucrose solution and for the massecuite there are constant values (option I);

2 – thermophysical characteristics (coefficients):

all for the crystal, diffusion coefficient for the intercrystalline sucrose solution and all for the massecuite are constant values;

thermal conductivity coefficient, heat capacity coefficient and density for the intercrystalline sucrose solution, are variable values (option II, a);

3 – thermophysical characteristics (coefficients):

all for intercrystalline sucrose solution and all for massecuite are constant values;

thermal conductivity coefficient, heat capacity coefficient and density for the crystal are variable quantities (option II, b);

4 – thermophysical characteristics (coefficients):

all for the crystal, all for the intercrystalline solution are constant values;

thermal conductivity coefficient, heat capacity coefficient and density for massecuite, are variable quantities (option II, c);

5 – all thermophysical characteristics (coefficients):

for the crystal, for the intercrystalline solution, and for the massecuite are variable values (option III).

The graphs (Figures 3, 4, 8, 9) show that the larger crystal of the first cell is dissolving. As can be seen from the obtained graphs (Figs. 3, 4), the nature of the change in diffusion mass flows from one side of the larger crystal of the first cell (Figs. 1, 2), which is closer to the heating wall of the vacuum apparatus heating chamber (Figure 3), is not quite coincides with the nature of the change in diffusion mass flows from the other side (Figure 4) at the relative time of boiling sugar massecuite  $\tau/\tau_c = 0.15$ . But we get a completely different situation when  $\tau/\tau_c = 1.0$ , where the nature of the change in the form of diffusion mass flows is almost the same (Figs. 8, 9). It is clear that the closer the cell is to the heating wall of the vacuum apparatus heating chamber, the faster the process of heating the components of this cell of the «two cells–massecuite» system occurs, and therefore the diffusion mass flow reaches its maximum in time earlier than from the other side of the crystal.

As for the second, smaller cell of the «two cells–massecuite» system, which is located further from the heating wall (Figs. 1, 2), the nature of the change in diffusion mass flows from one and the other side of the smaller crystal of the second cell (Figure 6, 7), practically coincide with each other at the relative time of boiling sugar massecuite  $\tau/\tau_c = 0.15$ , and at  $\tau/\tau_c = 1.0$ . Although, again, the graphs show that the intercrystalline solution on the side of the heating wall heats up faster, and as a result, the diffusive mass flows reach their maximum faster. The decline of diffusive mass flows after reaching their maximum can be explained by the fact that a saturated state is reached in each region of the intercrystalline sucrose solution.

The uneven movement nature of diffusion mass flows between cells (Figs. 5, 10), that is, between regions of intercrystalline sucrose solutions, can also be explained by the fact that the first cell warms up faster than the second. As a result, at the first stage, the intercrystalline sucrose solution of the first cell moves from the saturated state to the unsaturated state faster than the second cell. This leads to the dissolution of the first crystal faster than the second. But the rate of the crystal dissolution does not cover the need to reach a saturated state of the intercrystalline sucrose solution in the first cell, as a result of which sucrose is transferred from the second cell to the first (Figure 5, 10).

At the second stage, the saturated state of the first cell is equalized and at the same time the second cell has time to warm up sufficiently. At the same time, the saturation coefficient also decreases in its intercrystalline sucrose solution. Then the flow of sucrose already begins to occur from the intercrystalline sucrose solution of the first cell to the intercrystalline sucrose solution of the second cell.

All this plays an indicative role in the recrystallization process. It is clear that predicting the nature of the sucrose movement within one cell, and even more so between the cells itself, was quite a difficult task before conducting research. But now we have obtained the main indicators of diffusional flow of sucrose between cells and inside cells, albeit on the basis of an idealized mathematical model.

In order to compare the effect of taking into account variable thermophysical coefficients on the diffusion mass transfer process in an intercrystalline solution with constant thermophysical coefficients, a study was conducted and the maximum and minimum values of the relative deviations of the diffusion mass flows values  $j_{mn}(\tau)$ , ( $m = 1-5$ ,  $n = m + 1$ ), were found, (Figure 2).

Let us denote the diffusive mass flows, which were calculated at constant thermophysical coefficients by  $j_{mn, \text{const}}(\tau)$ , ( $m = 1-5$ ,  $n = m + 1$ ). Similarly, let's denote diffusion mass flows, which were calculated with variable thermophysical coefficients through  $j_{mn, \text{var}}(\tau)$ , ( $m = 1-5$ ,  $n = m + 1$ ).

The relative change of diffusion mass flows will be carried out in two cases:

- during the entire stay of the «two cells–massecuite» system (Figures 1, 2) in the heating tube of the vacuum apparatus heating chamber;
- at the time of exit of the «two cells–massecuite» system from the heating tube.

For comparison, we will find the largest deviation of diffusion mass flows  $j_{mn,var}(\tau)$ , ( $m = 1-5, n = m + 1; 0 \leq \tau \leq \tau_{c,end}$ ), from  $j_{mn,const}(\tau)$ , ( $m = 1-5, n = m + 1; 0 \leq \tau \leq \tau_{c,end}$ ). And then already on the basis of these data we will be able to draw a conclusion: which method should be used for further mathematical modeling. For this, it is necessary to find the maximum and minimum deviation of the values of diffusion mass flows  $j_{mn,var}(\tau)$ , ( $m = 1-5, n = m + 1; 0 \leq \tau \leq \tau_{c,end}$ ), from  $j_{mn,const}(\tau)$ , ( $m = 1-5, n = m + 1; 0 \leq \tau \leq \tau_{c,end}$ ).

Relative changes in diffusion mass flows  $j_{mn}(\tau)$ , ( $m = 1-5, n = m + 1; 0 \leq \tau \leq \tau_{c,end}$ ), at the boundaries of the corresponding regions of intercrystalline sucrose solutions (#1), (#3), (#4) and (#6), (Figure 2), calculated during the entire contact time  $\tau$  of the «two cells–massecuite» system with the inner surface of the heating tube of the vacuum apparatus heating chamber at the relative time of boiling sugar massecuite  $\tau/\tau_c = 0.15$  given in Table 1.

**Table 1**  
**Relative changes in diffusion mass flows  $j_{mn}(\tau)$ , ( $m = 1-5, n = m + 1; 0 \leq \tau \leq \tau_{c,end}$ ), calculated during the entire contact time  $\tau$  at the relative time of boiling sugar massecuite  $\tau/\tau_c = 0.15$**

$\tau_c = (0.0-3.95) c$ ( $\tau/\tau_c = 0,15$ ) (Min–Max)	II, a(lq.var) / I(all.const), %	II, b(cr.var) / I(all.const), %	II, c(ms.var) / I(all.const), %	III(all.var) / I(all.const), %
$(j_{12,var}(\tau) / j_{12,const}(\tau) - 1) _{min} \cdot 100\%$	- 2.5 ( $\tau = 0.03$ s)	0.0 $\tau = 0.39-3.95$ s)	0.0 $\tau = 0.00-3.95$ s)	- 2.1 ( $\tau = 0.03$ s)
$(j_{12,var}(\tau) / j_{12,const}(\tau) - 1) _{max} \cdot 100\%$	0.0 $\tau = 0.69-3.95$ s)	+ 0.5 $\tau = 0.03-0.06$ s)	0.0 $\tau = 0.00-3.95$ s)	0.0 $\tau = 0.51-3.95$ s)
$(j_{23,var}(\tau) / j_{23,const}(\tau) - 1) _{min} \cdot 100\%$	- 0.8 $\tau = 0.36-0.48$ s)	- 6.2 ( $\tau = 0.6-0.72$ s)	0.0 ( $\tau = 0.0-2.91$ s)	- 6.8 $\tau = 0.57-0.69$ s)
$(j_{23,var}(\tau) / j_{23,const}(\tau) - 1) _{max} \cdot 100\%$	0.1 $\tau = 3.18-3.95$ s)	0.0 ( $\tau = 0.0-0.06$ s)	0.1 $\tau = 3.03-3.95$ s)	0.0 $\tau = 0.0-0.03$ s)
$(j_{34,var}(\tau) / j_{34,const}(\tau) - 1) _{min} \cdot 100\%$	0.0 ( $\tau = 0.0-0.48$ s)	- 10.3 $\tau = 3.93-3.95$ s)	- 0.5 $\tau = 3.84-3.95$ s)	- 3.3 $\tau = 2.93-2.95$ s)
$(j_{34,var}(\tau) / j_{34,const}(\tau) - 1) _{max} \cdot 100\%$	8.1 $\tau = 3.87-3.95$ s)	0.5 $\tau = 0.69-0.84$ s)	0.0 ( $\tau = 0.0-1.8$ s)	1.3 $\tau = 0.99-1.26$ s)
$(j_{45,var}(\tau) / j_{45,const}(\tau) - 1) _{min} \cdot 100\%$	- 1.0 ( $\tau = 0.6-0.96$ s)	- 5.7 $\tau = 0.75-0.96$ s)	0.0 ( $\tau = 0.0-2.25$ s)	- 6.6 $\tau = 0.68-0.9$ s)
$(j_{45,var}(\tau) / j_{45,const}(\tau) - 1) _{max} \cdot 100\%$	0.0 ( $\tau = 0.0-0.09$ s)	0.0 ( $\tau = 0.0-0.06$ s)	0.1 $\tau = 2.28-3.95$ s)	0.0 $\tau = 0.0-0.06$ s)
$(j_{56,var}(\tau) / j_{56,const}(\tau) - 1) _{min} \cdot 100\%$	- 0.8 $\tau = 0.87-1.86$ s)	- 6.4 $\tau = 1.44-1.74$ s)	0.0 ( $\tau = 0.0-1.41$ s)	- 7.1 $\tau = 1.53-1.56$ s)
$(j_{56,var}(\tau) / j_{56,const}(\tau) - 1) _{max} \cdot 100\%$	0.0 ( $\tau = 0.0-0.21$ s)	0.0 ( $\tau = 0.0-0.15$ s)	0.2 $\tau = 2.61-3.95$ s)	0.0 $\tau = 0.0-0.15$ s)

Relative changes in diffusion mass fluxes  $j_{mn}(\tau_{c,end})$ , ( $m=1-5, n=m+1$ ), at the boundaries of the corresponding regions of intercrystalline sucrose solutions (#1), (#3), (#4) and (#6), (Figure 2), calculated at the moment of time  $\tau_{c,end}$  of the exit of the entire system «two cells–massecuite» from the heating tube of the vacuum apparatus heating chamber at the relative time of boiling sugar massecuite  $\tau/\tau_c = 0.15$  given in Table 2.

Relative changes in diffusion mass flows  $j_{mn}(\tau)$ , ( $m = 1-5$ ,  $n = m + 1$ ;  $0 \leq \tau \leq \tau_{c,end}$ ), at the boundaries of the corresponding regions of intercrystalline sucrose solutions (#1), (#3), (#4) and (#6), (Figure 2), calculated during the entire contact time  $\tau$  of the «two cells–massecuite» system with the inner surface of the heating tube of the vacuum apparatus heating chamber at the relative time of boiling sugar massecuite  $\tau/\tau_c = 1.0$  given in Table 3.

Relative changes in diffusion mass fluxes  $j_{mn}(\tau_{c,end})$ , ( $m=1-5$ ,  $n=m+1$ ), at the boundaries of the corresponding regions of intercrystalline sucrose solutions (#1), (#3), (#4) and (#6), (Figure 2), calculated at the moment of time  $\tau_{c,end}$  of the exit of the entire system «two cells–massecuite» from the heating tube of the vacuum apparatus heating chamber at the relative time of boiling sugar massecuite  $\tau/\tau_c = 1.0$  given in Table 4.

In Tables 1–4, the notation of various variants of the performed calculations is used:

- option I<sub>(all.const)</sub>, – constant thermophysical coefficients;
- option (II, a)<sub>(liq.var)</sub>, – variable thermophysical coefficients only for regions of intercrystalline sucrose solutions (#1), (#3), (#4) and (#6), (Figure 2);
- (II, b)<sub>(cr.var)</sub>, – variable thermophysical coefficients only for regions of sugar crystals (#2) and (#5), (Figure 2);
- (II, c)<sub>(ms.var)</sub>, – variable thermophysical coefficients only for the massecuite region (#7), (Figure 2);
- (III)<sub>(all.var)</sub>, – variable thermophysical coefficients for all regions (#1)–(#7), (Figure 2), simultaneously.

From Tables 1 and 2, it can be concluded that taking into account the influence of variable thermophysical coefficients on the non-stationary process of diffusion mass transfer is clearly non-linear and non-uniform in nature.

For an example in Table 1, the relative change in diffusion mass flow  $j_{34}(\tau)$  in the case of variable thermophysical coefficients only for sugar crystals for the case  $\tau/\tau_{II} = 0.15$ , with contact time  $\tau = 0.69-0.84$  s, is 0.5%, and already at the contact time  $\tau = 3.93-3.95$  s, it is – 10.3%. Similarly, according to Table 3, the relative change in the diffusion mass flow  $j_{23}(\tau)$  in the case of all simultaneously changing thermophysical coefficients for the case of  $\tau/\tau_c = 1.0$ , with a contact time of  $\tau = 0.67$  s, is – 6.2%, and already at the contact time  $\tau = 7.37-11.39$  s, it is 0.3%.

That is, the deviation of diffusive mass flows with variable thermophysical coefficients from constant ones during the entire contact time of the "two cell-heater" system with the heating tube is positive at one point in time, and negative at another point in time (that is, it has a clearly expressed variable character). It is clear that in such cases it is possible to find moments of time  $\tau$  where diffusive mass flows with variable thermophysical coefficients will completely coincide with diffusive mass flows with constant thermophysical coefficients.

Let's examine in more detail the weight of the impact of taking into account variable thermophysical coefficients on the process of diffusion mass transfer in comparison with constant coefficients. For this purpose, we will find the maximum relative deviations of diffusive mass flows with variables, where the case with constant coefficients was taken as the basic values.

Diffusion mass flows with variable coefficients only in the region of the intercrystalline sucrose solution (option II-a) differ the most from diffusion mass flows with constant coefficients (I) by 8.1% at the relative time of boiling sugar massecuite  $\tau/\tau_c = 0.15$ , and by 4.7% at the relative time of boiling sugar massecuite  $\tau/\tau_c = 1.0$  (in both cases for  $j_{34}(\tau)$ ).

**Table 2**

**Relative changes in diffusion mass fluxes  $j_{mn}(\tau_{c, \text{end}})$ , ( $m=1-5, n=m+1$ ), calculated at the moment of time  $\tau_{c, \text{end}}$  at the relative time of boiling sugar massecuite  $\tau/\tau_c = 0.15$**

$\tau_c = \tau_{c, \text{end}} = 3.95 \text{ c}$ ( $\tau/\tau_c = 0.15$ )	II a (lq.var) / I (all.const), %	II b (cr.var) / I (all.const), %	II c (ms.var) / I (all.const), %	III (all.var) / I (all.const), %
$(j_{12, \text{var}}(\tau) / j_{12, \text{const}}(\tau) - 1) _{\text{end}} \cdot 100\%$	0.028	- 0.010	0.001	0.018
$(j_{23, \text{var}}(\tau) / j_{23, \text{const}}(\tau) - 1) _{\text{end}} \cdot 100\%$	0.131	- 0.683	0.065	- 0.517
$(j_{34, \text{var}}(\tau) / j_{34, \text{const}}(\tau) - 1) _{\text{end}} \cdot 100\%$	8.065	- 10.299	- 0.473	- 3.298
$(j_{45, \text{var}}(\tau) / j_{45, \text{const}}(\tau) - 1) _{\text{end}} \cdot 100\%$	- 0.173	- 0.413	0.092	- 0.509
$(j_{56, \text{var}}(\tau) / j_{56, \text{const}}(\tau) - 1) _{\text{end}} \cdot 100\%$	- 0.254	- 2.870	0.191	- 2.949

**Table 3**

**Relative changes in diffusion mass flows  $j_{mn}(\tau)$ , ( $m = 1-5, n = m + 1; 0 \leq \tau \leq \tau_{c, \text{end}}$ ), calculated during the entire contact time  $\tau$  at the relative time of boiling sugar massecuite  $\tau/\tau_c = 1.0$**

$\tau_c = (0.0-67.93) \text{ c}$ ( $\tau/\tau_c = 1.0$ ) (Min-Max)	II a (lq.var) / I (all.const), %	II b (cr.var) / I (all.const), %	II c (ms.var) / I (all.const), %	III (all.var) / I (all.const), %
$(j_{12, \text{var}}(\tau) / j_{12, \text{const}}(\tau) - 1) _{\text{min}} \cdot 100\%$	- 0.3 ( $\tau = 0.67 \text{ s}$ )	0.0 ( $\tau = 1.34-67.93 \text{ s}$ )	0.0 ( $\tau = 0.0-67.93 \text{ s}$ )	- 0.2 ( $\tau = 0.67 \text{ s}$ )
$(j_{12, \text{var}}(\tau) / j_{12, \text{const}}(\tau) - 1) _{\text{max}} \cdot 100\%$	0.1 ( $\tau = 2.01-7.37 \text{ s}$ )	0.1 ( $\tau = 0.67 \text{ s}$ )	0.0 ( $\tau = 0.0-67.93 \text{ s}$ )	0.1 ( $\tau = 2.01-6.03 \text{ s}$ )
$(j_{23, \text{var}}(\tau) / j_{23, \text{const}}(\tau) - 1) _{\text{min}} \cdot 100\%$	- 0.8 ( $\tau = 0.67 \text{ s}$ )	- 6.2 ( $\tau = 0.67 \text{ s}$ )	0.0 ( $\tau = 0.0-2.01 \text{ s}$ ) ( $\tau = 9.38-67.93 \text{ s}$ )	- 6.9 ( $\tau = 0.67 \text{ s}$ )
$(j_{23, \text{var}}(\tau) / j_{23, \text{const}}(\tau) - 1) _{\text{max}} \cdot 100\%$	0.2 ( $\tau = 4.69-17.42 \text{ s}$ )	0.3 ( $\tau = 7.37-11.39 \text{ s}$ )	0.1 ( $\tau = 2.68-8.71 \text{ s}$ )	0.6 ( $\tau = 7.37-8.71 \text{ s}$ )
$(j_{34, \text{var}}(\tau) / j_{34, \text{const}}(\tau) - 1) _{\text{min}} \cdot 100\%$	0.1 ( $\tau = 0.67 \text{ s}$ )	- 5.0 ( $\tau = 6.03 \text{ s}$ )	- 0.7 ( $\tau = 8.04-47.55 \text{ s}$ )	- 1.2 ( $\tau = 6.03-6.7 \text{ s}$ )
$(j_{34, \text{var}}(\tau) / j_{34, \text{const}}(\tau) - 1) _{\text{max}} \cdot 100\%$	4.7 ( $\tau = 4.02-6.03 \text{ s}$ )	0.2 ( $\tau = 0.67 \text{ s}$ )	0.0 ( $\tau = 0.0-1.34 \text{ s}$ )	1.6 ( $\tau = 32.16-57.62 \text{ s}$ )
$(j_{45, \text{var}}(\tau) / j_{45, \text{const}}(\tau) - 1) _{\text{min}} \cdot 100\%$	- 1.1 ( $\tau = 0.67 \text{ s}$ )	- 5.4 ( $\tau = 0.67 \text{ s}$ )	0.0 ( $\tau = 0.0-1.34 \text{ s}$ ) ( $\tau = 14.74-67.93 \text{ s}$ )	- 6.4 ( $\tau = 0.67 \text{ s}$ )
$(j_{45, \text{var}}(\tau) / j_{45, \text{const}}(\tau) - 1) _{\text{max}} \cdot 100\%$	0.0 ( $\tau = 0.0 \text{ s}$ )	0.6 ( $\tau = 7.37-8.04 \text{ s}$ )	0.2 ( $\tau = 4.02-6.03 \text{ s}$ )	0.6 ( $\tau = 7.37-8.71 \text{ s}$ )
$(j_{56, \text{var}}(\tau) / j_{56, \text{const}}(\tau) - 1) _{\text{min}} \cdot 100\%$	- 1.0 ( $\tau = 1.34 \text{ s}$ )	- 6.2 ( $\tau = 1.34-2.01 \text{ s}$ )	0.0 ( $\tau = 0.0-0.67 \text{ s}$ ) ( $\tau = 14.07-67.93 \text{ s}$ )	- 7.0 ( $\tau = 1.34 \text{ s}$ )
$(j_{56, \text{var}}(\tau) / j_{56, \text{const}}(\tau) - 1) _{\text{max}} \cdot 100\%$	0.1 ( $\tau = 8.71-14.07 \text{ s}$ )	0.4 ( $\tau = 11.39-14.07 \text{ s}$ )	0.3 ( $\tau = 2.68-6.03 \text{ s}$ )	0.5 ( $\tau = 10.05-14.07 \text{ s}$ )

**Table 4**

**Relative changes in diffusion mass fluxes  $j_{mn}(\tau_{c,end})$ , ( $m=1-5, n=m+1$ ), calculated at the moment of time  $\tau_{c,end}$  at the relative time of boiling sugar massecuite  $\tau/\tau_c = 1.0$**

$\tau_c = \tau_{c,end} = 67.93 \text{ c}$ ( $\tau/\tau_c = 1.0$ )	II a (lq.var) / I (all.const), %	II b (cr.var) / I (all.const), %	II c (ms.var) / I (all.const), %	III (all.var) / I (all.const), %
$(j_{12,var}(\tau) / j_{12,const}(\tau) - 1) \cdot 100\%$	0.001	0.000	0.000	0.001
$(j_{23,var}(\tau) / j_{23,const}(\tau) - 1) \cdot 100\%$	0.089	0.021	-0.024	0.085
$(j_{34,var}(\tau) / j_{34,const}(\tau) - 1) \cdot 100\%$	2.665	-0.487	-0.606	1.512
$(j_{45,var}(\tau) / j_{45,const}(\tau) - 1) \cdot 100\%$	-0.094	0.055	0.018	-0.019
$(j_{56,var}(\tau) / j_{56,const}(\tau) - 1) \cdot 100\%$	0.009	0.074	-0.010	0.073

Diffusion mass flows with variable coefficients only in the region of the crystal (II-b) differ the most from diffusion mass flows with constant coefficients (I) by  $-10.3\%$  at the relative time of boiling sugar massecuite  $\tau/\tau_c = 0.15$  (the case for  $j_{34}(\tau)$ ), and by  $-6.2\%$  at the relative time of boiling sugar massecuite  $\tau/\tau_c = 1.0$  (cases for  $j_{23}(\tau)$  and  $j_{56}(\tau)$ ).

Diffusion mass flows with variable coefficients only in the region of massecuite (II-c) differ the most from diffusion mass flows with constant coefficients (I) by  $-0.5\%$  at the relative time of boiling sugar massecuite  $\tau/\tau_c = 0.15$ , and by  $-0.7\%$  at the relative time of boiling sugar massecuite  $\tau/\tau_c = 1.0$  (in both cases for  $j_{34}(\tau)$ ).

Diffusion mass flows with simultaneously all variable coefficients (III) differ the most from diffusion mass flows with constant coefficients (I) by  $-7.1\%$  at the relative time of boiling sugar massecuite  $\tau/\tau_c = 0.15$ , and by  $-7.0\%$  at the relative time of boiling sugar massecuite  $\tau/\tau_c = 1.0$  (in both cases for  $j_{56}(\tau)$ ).

As can be seen from Table 1, the closest to the obtained results of sucrose diffusion mass flows in intercrystalline solutions with constant thermophysical coefficients (option I) is the result with variable thermophysical coefficients only for the massecuite region (option II-c), where the maximum relative deviation is  $-0.7\%$ .

In second place in terms of the relative deviation from the obtained results of sucrose diffusion mass flows in intercrystalline solutions with constant thermophysical coefficients (option I) is the variant of diffusion mass flows with all simultaneously variable thermophysical coefficients (option III), where the maximum relative deviation is  $-7.1\%$ .

In third place in terms of the relative deviation from the obtained results of sucrose diffusion mass flows in intercrystalline solutions with constant thermophysical coefficients (option I) is the variant of diffusion mass flows with variable coefficients only for intercrystalline sucrose solutions (option II-a), where the maximum relative deviation is  $8.1\%$ .

Finally, in the last fourth place in terms of relative deviation from the obtained results of sucrose diffusion mass flows in intercrystalline solutions with constant thermophysical coefficients (option I) there is a variant of diffusion mass flows with variable coefficients only for crystals (option II-b), where the maximum relative deviation is  $-10.3\%$ .

That is, in the last, fourth case, we get the maximum relative deviations of diffusive mass transfers from the case obtained with constant thermophysical coefficients.

It is worth noting that the thermophysical coefficients of the massecuite are a certain combination of the corresponding thermophysical coefficients for the crystal and the intercrystalline solution. As we can see from the conducted studies, the option only for

intercrystalline solutions of sucrose (option II-a) has the maximum impact with a «+» sign (8.1%). While the variant for sugar crystals only (variant II-b) has the maximum impact with a «-» sign (-10.3%). Their simultaneous influence was expected to be obtained as the sum of such two influences. However, in reality, we got a slightly different result (-0.5%), which does not match the numerical value with the expected  $8.1\% - 10.3\% = -2.2\%$  by almost 4.4 times. The only explanation the author can offer is that the process of sugar crystallization is quite complex to understand. Note that in such a complex process as sugar crystallization, the values of certain thermophysical characteristics for massecuite (for example, density, thermal conductivity coefficient) are not calculated based on simple ratios of the thermophysical characteristics of massecuite components (i.e., crystal, intercrystalline sucrose solution).

Before starting the study of the dependence of non-stationary diffusion mass flows on the method used to calculate the process (with constant or variable thermophysical coefficients; alternately or all at once), it was expected to obtain a result that would confirm that the simultaneous consideration of all variable thermophysical characteristics makes the biggest impact.

In fact, we found that taking into account all variable thermophysical coefficients is not the first place, but only the second place. The largest relative deviations were obtained when variable coefficients for crystals were taken into account separately, as well as when variable coefficients were taken into account for intercrystalline sucrose solutions.

Again, this can be explained only by the fact that the sucrose mass crystallization process is very complex and has a pronounced nonlinear character. Moreover, the crystallization process investigated in this work is non-stationary.

Summing up, it can be concluded that the influence of variable thermophysical coefficients on the relative changes in the values of diffusive mass flows in comparison with constant thermophysical coefficients during the entire time of contact of the «two cells–massecuite» system with the inner wall of the heating tube of the vacuum apparatus heating chamber is within the range of -10.3% to +8.1%.

With regard to the final results at the final moment of time  $\tau = \tau_{c,end}$  of the «two cells–massecuite» system contact at the exit from the heating tube the deviations are as follows:

- at  $\tau/\tau_c = 0.15$ , the largest relative deviations were obtained when taking into account variable thermophysical coefficients only for sugar crystals (-10.3%), then variable thermophysical coefficients only for intercrystalline sucrose solutions (+8.1%); then with all variable coefficients at the same time (-3.3%); and finally, taking into account variable coefficients only for massecuite (-0.5%);
- at  $\tau/\tau_c = 1.0$ , the largest relative deviations were obtained when taking into account variable thermophysical coefficients only for intercrystalline solutions of sucrose (+2.7%); then with all variable coefficients at the same time (+1.5%); further, taking into account variable coefficients only for massecuite (-0.6%); and finally, taking into account variable coefficients only for sugar crystals (-0.5%).

Summing up, it can be concluded that the influence of variable thermophysical coefficients on the relative changes in the values of diffusive mass flows in comparison with constant thermophysical coefficients at the output of the «two cells–massecuite» system from the heating tube of the vacuum apparatus heating chamber is within the range of -10.3% up to +8.1%.

Also, it was established that at the value of the relative time of boiling sugar massecuite  $\tau/\tau_c = 0.15$ , when the entire system of cells moves along the heating tube, the substance is first transferred from the region of the intercrystalline sucrose solution of a smaller crystal to the region

of the intercrystalline sucrose solution of a larger crystal during  $\tau_{c,2} = 2.41\text{--}2.7$  s depending on constant or variable thermophysical characteristics (Figure 5). Starting from the moment of time  $\tau_{c,2}$  to the moment of time  $\tau_{c,\text{end}} = 3.95$  s (at  $\tau/\tau_c = 0.15$ ) when the system of cells leaves the heating tube, the situation changes to the opposite (Figure 5). So, in this case, only one extreme of the diffusion mass flow was clearly expressed (the minimum on the graph, which is reached at the moment of time  $\tau_{c,1} = 1.29\text{--}1.45$  s, determines the maximum mass transfer of sucrose from a smaller crystal to a larger crystal). There is no clear maximum in this case.

At the relative time of boiling sugar syrup  $\tau/\tau_c = 1.0$ , two extremes were clearly expressed (Figure 10):

- minimum at  $\tau_{c,2} = 1.34\text{--}2.01$  s and
- maximum at  $\tau_{c,2} = 11.39\text{--}12.06$  s, depending on constant or variable thermophysical characteristics.

## Conclusions

The effect of taking into account variable thermophysical coefficients on the results of calculations of unsteady diffusion mass flows of sucrose for the system «two cells–massecuite» (Figure 1, 2) was investigated, as for the case of their alternate change (only separately for the intercrystalline solution of sucrose, only separately for sugar crystals and only separately for utfel), as well as for the case of simultaneous change of all thermophysical coefficients.

The distribution of non-stationary diffusive mass flows was obtained on the basis of the simultaneous solution of a large system of partial differential equations consisting of a non-stationary heat conduction problems system and simultaneously three different systems for non-stationary diffusive mass transfers problems. Solving such a complex system of problems was carried out using numerical methods.

For a deeper understanding, cases were considered for a certain series of relative time of boiling sugar massecuite  $\tau/\tau_c = 0.15; -1.0$ .

This paper presents the distribution of non-stationary diffusion mass flows of sucrose only for the case of relative boiling time:  $\tau/\tau_c = 0.15$  and  $\tau/\tau_c = 1.0$ .

To determine the influence of variable thermophysical coefficients on the calculations, the obtained unsteady diffusion mass flows of sucrose at variable thermophysical coefficients were compared with the unsteady diffusion mass flows of sucrose obtained at constant thermophysical coefficients (subject to the same other conditions).

The comparison was made for two cases:

- a) during the entire time of contact of the «two cells–massecuite» system with the inner surface of the heating tube of the vacuum apparatus heating chamber ( $0 \leq \tau \leq \tau_{c,\text{end}}$ );
- b) at the moment of time when the «two cells–massecuite» system leaves this heating tube ( $\tau = \tau_{c,\text{end}}$ ).

For option (a), the following studies were conducted:

- to determine the weight of the impact of taking into account variable thermophysical coefficients on the obtained result of diffusion mass flows of sucrose; they give reasons to accept the calculations made with constant coefficients close to the calculations made with variable coefficients only for massecuite; the maximum relative deviation in this case is:  $-0.5\%$  at  $\tau/\tau_c = 0.15$ , and  $-0.7\%$  at  $\tau/\tau_c = 1.0$ ;

- unsteady diffusive mass flows with variable thermophysical coefficients only in the region of the crystal differ from the calculation option with constant coefficients by – 10.3% at the relative time of boiling sugar massecuite  $\tau/\tau_c = 0.15$ , and by – 6.2% at to the relative time of boiling sugar syrup  $\tau/\tau_c = 1.0$ ;
- non-stationary diffusive mass flows with variable thermophysical coefficients only in the region of the intercrystalline sucrose solution differ from the calculation option with constant coefficients by 8.1% at the relative time of boiling sugar massecuite  $\tau/\tau_c = 0.15$ , and by 4.7% at to the relative time of boiling sugar massecuite  $\tau/\tau_c = 1.0$ ;
- finally, the conducted studies of non-stationary diffusion mass flows with all simultaneously variable thermophysical coefficients differ from the calculation option with constant coefficients by – 7.1% at the relative time of boiling sugar massecuite  $\tau/\tau_c = 0.15$ , and – 7.0% with the relative time of boiling sugar massecuite  $\tau/\tau_c = 1.0$ .

Summarizing the research carried out for option (b), it can be concluded that the influence of variable thermophysical coefficients on the relative changes in the values of diffusion mass flows in comparison with constant thermophysical coefficients at the output of the «two cells–massecuite» system from the heating tube of the vacuum apparatus heating chamber is ranges from – 10.3% to + 8.1%.

A general conclusion can be made as follows. Taking into account variable thermophysical coefficients affects the non-stationary process of diffusion mass transfer for intercrystalline solutions of sucrose in the components of the «two cells–massecuite» system. The limits of this influence are from – 10.3% to + 8.1% of relative units.

If the researcher is satisfied with deviations of this order, he can further use thermophysical coefficients for calculations of steel (note that the calculation time of the entire system of problems in this case is significantly reduced by many times). Otherwise, it is worth using a more accurate model in which variable thermophysical coefficients will be taken into account, and all components of the «two cells–massecuite» system at the same time (maximum relative deviations in this case will be 7.1%).

## References

- Alewijn W.F., Honig P. (2013), Chapter 9. Technology of sugar crystallization, *Crystallization*, Elsevier, pp. 318–370.
- Bruno J. C. de Castro, Melécio Marciniuk Junior, Marco Giulietti, André Bernardo (2019), Sucrose crystallization: modeling and evaluation of production responses to typical process fluctuations, *Brazilian Journal of Chemical Engineering*, 36(3), pp. 1237–1253, dx.doi.org/10.1590/0104-6632.20190363s20180240.
- Crestani C. E., Bernardo A., Costa C.B.B., Giulietti M. (2021), An artificial neural network model applied to convert sucrose chord length distributions into particle size distributions, *Powder Technology*, 384, pp. 186–194, <https://doi.org/10.1016/j.powtec.2021.01.075>
- Duroudier J.P. (2016), *Crystallization and Crystallizers*, Industrial Equipment for Chemical Engineering Set, London.
- Eymard R. Gallouët, T. R. Herbin R. (2000), *The finite volume method. Handbook of Numerical Analysis*, VII, pp. 713–1020.

- Gakhovych N., Savhenko I. (2022), Strategic priorities of Ukraine's economy recovery based on the sustainable development principles, *Selected papers of IV International Conference on European Dimensions of Sustainable Development, October 20–21, 2022, Kyiv, NUFT, Kyiv*.
- Georgieva P., Feye de Azevedo S., Goncalves M.J., Ho P. (2003). Modeling of sugar crystallization through knowledge integration, *Engineering in Life Sciences*, 3, pp. 146–153, <http://doi.org/10.1002/elsc.200390019>
- Hartel R.W., Shastry A.V. (1991), Sugar crystallization in food products, *Critical Reviews in Food Science and Nutrition*, 30(1), pp. 49–112. <https://doi.org/10.1080/10408399109527541>
- Kulinchenko V., Mironchuk V. (2012), *Industrial Crystallization of Sugary Substances*, NUFT, Kyiv.
- LeVeque R. (2002), *Finite Volume Methods for Hyperbolic Problems*, Cambridge University Press.
- Nagy Z.K., Fevotte G., Kramer H., Simon L.L. (2013), Recent advances in the monitoring, modelling and control of crystallization systems, *Chemical Engineering Research and Design*, 91(10), pp. 1903–1922.
- Osmanbegovic N., Alopaeus V., Han B., Vuorinen V., Louhi-Kultanen M. (2022), Experimental and CFD study on influence of viscosity on layer melt crystallization, *Separation and Purification Technology*, 284, pp. 1–8, <https://doi.org/10.1016/j.seppur.2021.120170>
- Pogoriliy T. (2015a), The distribution of temperatures in the sucrose solution–sugar crystal–sucrose solution–massecuite cells depending on the boiling sugar massecuite time, *Ukrainian Journal of Food Science*, 3(1), pp. 139–148.
- Pogoriliy T. (2015b), Temperatures distribution in the «larger sugar crystal–larger crystal sucrose solution–less crystal sugar sucrose solution–smaller sugar crystal–massecuite» cells system depending on the boiling sugar massecuite time, *Ukrainian Food Journal*, 4(4), pp. 648–661.
- Pogoriliy T. (2015c) Simultaneous unsteady calculation of temperature distribution in the «larger sugar crystal–larger sugar crystal sucrose solution–less sugar crystal sucrose solution–smaller sugar crystal–massecuite» system cells and sucrose solutions cells concentrations in the same system depending on the boiling sugar massecuite time, *Ukrainian Journal of Food Science*, 3(2), pp. 322–341.
- Pogoriliy T. (2016a), Non-stationary sucrose diffusion mass flow calculation for sucrose solution cells from the «larger sugar crystal–larger sugar crystal sucrose solution–less sugar crystal sucrose solution–smaller sugar crystal–massecuite» system cells depending on the boiling sugar massecuite time, *Ukrainian Food Journal*, 5(2), pp. 350–367.
- Romero-Bustamante J.A., Velazquez-Camilo O., Garcia-Hernandez A., Rivera V.M., Hernandez-Martinez E., (2022), Monitoring of cane sugar crystallization process by multiscale time-series analysis, *Chaos, Solitons & Fractals*, 156, p. 111848, <https://doi.org/10.1016/j.chaos.2022.111848>.
- Rózsa L., Rózsa J., Kilpinen S. (2016), Crystal growth and crystallization control tactics in industrial sugar crystallizers Part 1. Crystal growth, *International Sugar Journal*, 118, pp. 746–755.
- Sánchez-Sánchez K.B., Bolaños-Reynoso E.; Urrea-García, G.R. (2017), Analysis of operating conditions for cane sugar batch crystallization based on MSZW coupled with mechanistic kinetic models, *Revista Mexicana de Ingeniería Química*, 16(3), pp. 1029–1052, Available at: <https://www.redalyc.org/pdf/620/62053304028.pdf>

- Shamim F., Hernández R., Paulen R., Engell S.A. (2016), A hierarchical coordination approach to the optimal operation of a sugar crystallization process, *Computer Aided Chemical Engineering*, 38, pp. 703–708, DOI; 10.1016/B978-0-444-63428-3.50122-3.
- Suarez L.A.P., Georgieva P., de Azevedo S.F. (2011), Model Predictive Control Strategies for Batch Sugar Crystallization Process, In (Ed.), *Advanced Model Predictive Control, IntechOpen*, Available at: <https://www.intechopen.com/chapters/16065>
- Tkachenko S.V., Sheiko T.V, Petrenko V.V., Anisimova O.M., Kuznietsova I.V., Khomichak L.M., Obodovych O.M. (2020), Influence of crystallizing agent on sugar quality, *Acta Scientiarum Polonorum-Technologia Alimentaria*, 19(4), pp. 457–465. <http://doi.org/10.17306/J.AFS.2020.0867>
- Vetter F.L., Strube J. (2022), Enabling total process digital twin in sugar refining through the integration of secondary crystallization influences, *Processes*, 10(373), <https://doi.org/10.3390/pr10020373>.
- Zhong X., Huang C., Chen L., Yang Q., Huang Y. (2022), Effect of ultrasound on the kinetics of anti-solvent crystallization of sucrose, *Ultrasonics Sonochemistry*, 82(105886), pp. 1–10, <https://doi.org/10.1016/j.ultsonch.2021.105886>

## Determining the parameters of demarcation of heat exchange modes in the film during vaporization

Valentyn Petrenko, Oleksiy Pylypenko,  
Oleksandr Ryabchuk, Maksym Nalyvaiko

National University of Food Technologies, Kyiv, Ukraine

---

### Abstract

---

#### Keywords:

Heat exchange  
Film  
Liquid  
Temperature  
Turbulence  
Velocity

**Introduction.** The purpose of the research is to analytically determine the parameters of the separation of two characteristic modes of heat transfer to the boiling film under the condition of its cyclic mixing by large waves, which takes place in the long pipes of film evaporators of the sugar industry.

**Materials and methods.** Analytical methods of analysis of heat transfer processes in flowing laminar and turbulent films of liquids during vaporization are applied in the study.

**Results and discussion.** Mathematical modeling of the temperature field in a liquid flowing down the vertical surface of a boiling film with a developed wave structure in the presence of an accompanying vapor flow at the time of the appearance of a temperature gradient at the film-vapor interfacial surface was carried out. The perturber of cyclic temperature fluctuations in the film in long channels are large low-frequency waves that roll along the interfacial surface. The limiting curve for separating heat transfer modes in the film is obtained on the basis of the approximate solution of the differential equation of heat conduction with a convective term for both laminar and turbulent modes of film motion using the algebraic form of dependence for turbulent viscosity in the film provided under the condition of zero temperature gradient on the surface of the film. As a result of solving the problem, an analytical expression was obtained, which is the initial condition of the boundary value problem of heat transfer in a boiling film, which arises at the moment of stirring the film by a large wave. It was found that with a change in the volume density of irrigation from 0.0001 to 0.0005 m<sup>2</sup>/s, the length of the film run, during which the heat exchange mode changes, is 50–140 mm for laminar films and 10–35 mm for turbulent films, respectively.

**Conclusions.** From the equations of convective heat conduction for laminar and turbulent films under the condition of zero temperature gradient on the surface of the film, expressions are obtained that are the initial conditions of the boundary value problem of heat exchange in a boiling film, which occurs at the time of mixing of the film by a large wave.

---

#### Article history:

Received  
30.11.2022  
Received in  
revised form  
3.03.2023  
Accepted  
31.03.2023

---

#### Corresponding author:

Valentyn  
Petrenko  
E-mail:  
ufi\_nuft@meta.ua

---

#### DOI:

10.24263/2304-  
974X-2023-12-1-  
9

## Introduction

Transfer processes in flowing films of liquids with interaction with a gas (vapor) flow are characterized by high intensity due to the powerful interaction of the gas flow with the surface of the film covered by a complex system of surface waves. In addition, film processes are fast-moving, which is especially important in the processes taking place in heat and mass exchange devices of the food industry, where the determining factor in improving the quality of products during their heat treatment in evaporation devices is a short stay in the zone of elevated temperature.

Considering the variety and complexity of the structural forms of surface waves, which have a decisive influence on the intensity of transfer processes in films, a large number of works are devoted to the study of wave characteristics of films and modeling of thermal-hydrodynamic processes in films. But the majority of them are devoted to the analysis of thermohydrodynamic processes in films on short sections of pipes, where the wave structure is formed by a system of high-frequency capillary waves on the surface of laminar films of water (Dietze et al., 2014; Lel et al., 2015) and viscous liquids (Gourdon et al., 2015). Turbulence in films has also been studied on short sections and has a specific structure associated with the damping of turbulent pulsations by the interfacial surface (Mascarenhas et al., 2013). There is a limited number of experimental and theoretical works on the study of heat transfer and hydrodynamics of film flows in long pipes, where the structure of large low-frequency waves is formed (Kostoglou et al., 2010; Malamataris et al., 2008). However, the large waves that are formed at a distance of 1.5–3 m from the entrance play a decisive role in the processes of heat exchange in long steam-generating channels. Since the speed of the large waves exceeds the speed of the interphase surface of the film (by 2.5–1.5 times depending on the Re number), and their amplitude is 2–3 times greater than the average thickness of the film, deformed large waves act on the film like a bulldozer, rolling over the interfacial surface. It was established that a large wave during its movement has a central vortex (Demekhin et al., 2005), due to which the film is mixed during its movement of the wave. Taking into account the above, the following mechanism of heat exchange in the presence of large waves appears: at the moment of the passage of a large wave, the mass of liquid superheated relative to the saturation temperature moves from the wall layer to the interphase surface, where, as a result of self-evaporation, it cools to the saturation temperature. In the time interval between the passage of two large waves, two successive processes take place: the first begins immediately after mixing the film and continues until the state when the temperature wave reaches the interphase surface; the second begins from the moment of the appearance of a positive temperature gradient on the interphase surface and, accordingly, is manifested by the beginning of evaporation. The intensity of evaporation increases with the growth of the temperature gradient on the interfacial surface and this process continues until the next big wave passes. The limit state of the heating of the film in the second period is a temperature curve that corresponds to the steady mode of heat exchange, but this state, due to the significant frequency of passing waves (7–10 Hz), is not reached.

Thus, taking into account the development of the temperature field along the surface of the heat exchange, the temperature profile in the period between the passage of large waves can be obtained from the equation of convective heat conduction, in which, under the laminar regime of motion of the film, the convective term is written in the form of a parabolic velocity profile

$$\left[ \left( \frac{\tau_i}{\rho\nu} + \frac{g\delta}{\nu} \right) y - \frac{g}{2\nu} y^2 \right] \frac{\partial t(x, y)}{\partial x} = a_i \frac{\partial^2 t(x, y)}{\partial y^2}, \quad (1)$$

and for turbulent – in the form of a power equation:

$$u_i \left( \frac{y}{\delta} \right)^{1/n} \frac{\partial t(x, y)}{\partial x} = \frac{\partial}{\partial y} (a_i + a_t) \frac{\partial t(x, y)}{\partial y}, \quad (2)$$

where  $x$  and  $y$  are the longitudinal and transverse coordinates, respectively;  $\tau_i$  is a shear stress on the interfacial surface of the film;  $t$  is a temperature;  $\delta$  is an average film thickness;  $\nu, \rho$  – kinematic viscosity, liquid density, respectively;  $g$  – acceleration of free fall;  $u_i$  – velocity of the liquid in the film on the interfacial surface;  $a_i, a_t$  – molecular and turbulent thermal conductivity, respectively.

The exponent  $n$  varies from 1/5 to 1/7 depending on the Reynolds number (irrigation density). Turbulent thermal conductivity  $a_t$ , which is included in equation (2), is determined through turbulent viscosity  $V_t$ , since these parameters are related by the equation

$$\frac{a_t}{a_i} = \frac{\nu_t}{\nu} \frac{\text{Pr}}{\text{Pr}_t},$$

where  $\text{Pr}, \text{Pr}_t$  are the molecular and turbulent Prandtl numbers, respectively.

A list of the main dependencies for the algebraic form of relations for turbulent viscosity in flowing films of liquids is given in (Mascarenhas et al., 2013). Among the latest relations proposed in the literature for the algebraic form of turbulent viscosity for film flows with accompanying vapor flow in vertical evaporation channels is the relation (Petrenko et al., 2020)

$$\frac{\nu_t}{\nu} = 5 \cdot 10^{-5} \text{Re}^{1.4} \left\{ 1 + 3,6 \left[ 1 - \exp \left( 1 - \frac{d}{d_o} \right) \right] \right\} f_u \eta^2 (1 - \eta^2), \quad (3)$$

where  $f_u = C_u \left[ 1 - 0,1 \exp(-1,1086 \sqrt{We}) \right]$ ,

$$C_u = 1,119 - 0,122 \sqrt{We} + \left( 0,07424 + \frac{\text{Re}}{9,153 \cdot 10^6} \right) (\sqrt{We})^2 - 0,01808 (\sqrt{We})^3 + 1,775 \cdot 10^{-3} (\sqrt{We})^4 - 7,8 \cdot 10^{-5} (\sqrt{We})^5 + 1,28 \cdot 10^{-6} (\sqrt{We})^6,$$

$We = \frac{\rho_2 u_2^2 d_o}{\sigma}$  – the Weber number;  $u_2$  – steam core velocity;  $\rho_2$  – density of steam;  $\sigma$  –

surface tension;  $d_o = 0,02 \text{ m}$ .

Ratio (3) is correct in the range  $We \leq 250$  for pipes with diameters from 20 to 32 mm (investigated range).

Graphical interpretation (3) for different phase costs is shown in Fig.1

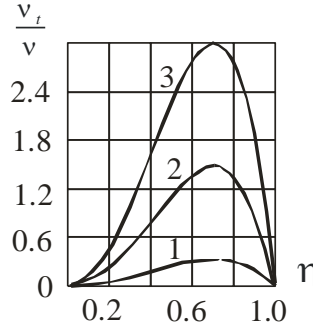


**Figure 1. Dependence  $\frac{v_t}{v} = f(\eta)$  on the ratio (3) for water**

**at  $t = 100\text{ }^\circ\text{C}$ ,  $d = 0,02\text{ m}$  and  $u_2 = 10\text{ m/s}$ ;**

**1 –  $Re = 1356$ ; 2 –  $4068$ ; 3 –  $6780$ .**

Boundary conditions (on the heat exchange wall ( $y = 0$ ) and the interphase surface ( $y = \delta$ ) for the first period:  $y = 0, t = t_w$ ;  $y = \delta, \frac{\partial t}{\partial y} = 0$  and initial conditions  $x = x_m, t = t(x_m, y)$ . For the second period, the boundary conditions are:  $y = 0, t = t_w$ ;  $y = \delta, t = t_{sat}$ , and initial conditions  $x = x_m, t = t(x_m, y)$ . The index "w" refers to the wall, "sat" – the state of saturation; "m" corresponds to the transition conditions from period 1 to period 2. The function  $t(x_m, y)$  is a solution of equations (1, 2) (depending on the mode of motion of the film) at the moment when  $\frac{\partial t}{\partial y}|_{y=\delta} = 0$ . Equations (1, 2, 3) with the given boundary conditions make it possible to obtain the temperature distribution for both the first and second periods of the development of the temperature field in the film.

This work is devoted to the determination of the longitudinal coordinate  $x_m$  under which the condition is met  $\frac{\partial t}{\partial y}|_{y=\delta} = 0$  and the obtaining of the boundary temperature curve under these boundary conditions for laminar and turbulent films  $t = t(x_m, y)$ , which is the curve separating the two regimes of heat exchange in boiling films.

## Materials and methods

The paper examines the parameters of distinguishing two modes of heat exchange in the model of heat exchange in boiling liquid films with a developed structure of large waves.

Research methods – analytical research based on the equations of convective heat conduction, using empirical coefficients in the ratio for turbulent viscosity, obtained based on the analysis of experimental data from the study of heat exchange processes in turbulent films (Petrenko et al., 2020).

The range of changes in regime parameters in which the obtained research results are correct is determined by the range of changes in parameters for which the empirical coefficients in the relation for turbulent viscosity were obtained (Petrenko et al., 2020) and is: the volumetric liquid flux varied in the range of  $0,05\text{--}0,55 \times 10^{-3} \text{ m}^3/\text{s}$ . Steam speed  $0\text{--}35 \text{ m/s}$ , pipe diameter  $20\text{--}34 \text{ mm}$ ; the length of the pipes is  $1,5\text{--}9 \text{ m}$ .

## Results and discussion

Schematically, the temperature and velocity profiles in the film before and after the passage of a large wave are shown in Figure 2.

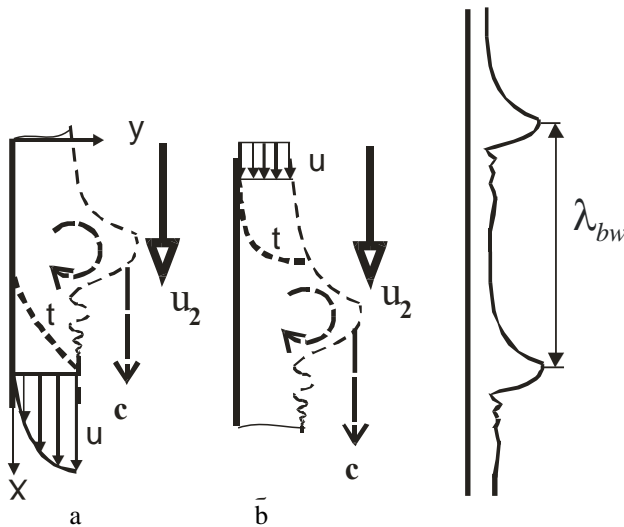


**Figure 2. Scheme of the movement of a large wave on the surface of a turbulent film:**

a – velocity and temperature profile before the passage of a large wave; b – after.

c – phase speed of large waves;  $\lambda_{bw}$  – length of large waves, accordingly.

### Laminar mode of motion of the liquid film

We assume that in the laminar mode of motion at the time of appearance of the temperature gradient  $\frac{\partial \theta}{\partial \eta_{\eta=1}}$  at the interphase boundary, the film travels the distance at which the velocity profile becomes parabolic or close to it. Then the convective heat transfer equation (1) in the presence of shear stress on the interphase surface  $\tau_i$  in dimensionless form will be written as

$$\left[ \left( \frac{\tau_i}{\rho \delta} + \frac{g}{v} \right) \eta - \frac{g}{2v} \eta^2 \right] \frac{\delta^3}{a_i} \frac{\partial \theta(\eta, \xi)}{\partial \xi} = \frac{\partial^2 \theta(\eta, \xi)}{\partial \eta^2}, \quad (4)$$

where  $\theta(\eta, \xi) = \frac{t(\eta, \xi) - t_{sat}}{t_w - t_{sat}}$  – the dimensionless temperature;  $\eta = \frac{y}{\delta}$ ,  $\xi = \frac{x}{\delta}$  – dimensionless transverse and longitudinal coordinates.

The task of finding the coordinate where the two modes of heat exchange in the film are separated during vaporization is formulated as follows. A liquid film flows down a vertical surface and is uniformly heated to the saturation (boiling) temperature  $t_{sat}$ . The temperature of the heat exchange surface, along which the film flows, instantly increases to  $t_w$ . Let's find the longitudinal coordinate  $\xi_m$ , or the distance covered by the film, at which the temperature profile will develop to the state at which a temperature gradient will appear on the interfacial surface of the film  $\frac{\partial \theta}{\partial \eta} \Big|_{\eta=1} \geq 0$ .

It can be solved (4) using an approximate method. To do this, replace the left part of (4) with the average value

$$\int_0^1 \left[ \left( \frac{\tau_i}{\rho \delta} + \frac{g}{v} \right) \eta - \frac{g}{2v} \eta^2 \right] \frac{\delta^3}{a_i} \frac{\partial \theta(\eta, \xi)}{\partial \xi} d\eta = \left( \frac{\tau_i \delta^2}{2\rho v} + \frac{g \delta^3}{3v} \right) \frac{1}{a_i} \frac{\partial \theta_{av}(\xi)}{\partial \xi}.$$

Given that the average speed is defined as

$$\bar{u} = \frac{1}{\delta} \int_0^\delta \left[ \left( \frac{\tau_i}{\rho v} + \frac{g \delta}{v} \right) y - \frac{g}{2v} y^2 \right] dy = \frac{\tau_i \delta}{2\rho v} + \frac{g \delta^2}{3v},$$

and the film thickness and the average velocity are related by a cubic equation

$$G_v = \bar{u} \delta = \frac{\tau_i \delta^2}{2\rho v} + \frac{g \delta^3}{3v}, \quad (5)$$

equation (4) takes the form

$$\frac{Pe}{4} \frac{\partial \theta(\eta, \xi)}{\partial \xi} = \frac{\partial^2 \theta(\eta, \xi)}{\partial \eta^2}, \quad (6)$$

where  $Pe = \frac{4G_v}{a_i} = \frac{4\bar{u}\delta}{a_i}$  – the Peclet number;  $G_v$  – volumetric liquid flux.

Double integration (6) under boundary conditions

$$\eta = 0, \theta = 1; \quad \eta = 1, \frac{\partial \theta}{\partial \eta} = 0, \quad (7)$$

gives

$$\theta(\eta, \xi) = \frac{Pe}{4} \frac{\partial \theta_{av}(\xi)}{\partial \xi} \left( \frac{\eta^2}{2} - \eta \right) + 1. \quad (8)$$

It was found the derivative  $\frac{\partial \theta_{av}(\xi)}{\partial \xi}$  from the expression for the average temperature  $\theta_{av}$ , which we give as mass average

$$\theta_{av} = \int_0^1 \theta(\eta, \xi) \frac{u(\eta)}{\bar{u}} d\eta = \int_0^1 \theta(\eta, \xi) \frac{\left[ \left( \frac{\tau_i}{\rho v} + \frac{g\delta}{v} \right) \eta - \frac{g\delta}{2v} \eta^2 \right]}{\left( \frac{\tau_i}{2\rho v} + \frac{g\delta}{3v} \right)} d\eta. \quad (9)$$

Integration (9) gives

$$\theta_{av} = 1 - \frac{\partial \theta_{av}(\xi)}{\partial \xi} \frac{Pe}{80} \frac{25\tau_i + 16\rho g\delta}{3\tau_i + 2\rho g\delta} = 1 - \frac{\partial \theta_{av}(\xi)}{\partial \xi} D, \quad (10)$$

where  $D = \frac{Pe}{80} \frac{25\tau_i + 16\rho g\delta}{3\tau_i + 2\rho g\delta}$ .

Integrating the differential equation (10) under the initial condition:  $\xi = 0$ ,  $\theta_{av} = 0$ , we obtain an expression for the average temperature

$$\theta_{av} = 1 - \exp\left(-\frac{\xi}{D}\right). \quad (11)$$

Differentiating (11) and substituting the derivative of (11)  $\frac{d\theta_{av}(\xi)}{d\xi}$  into (8), we obtain the temperature distribution in the film at  $\xi = \xi_m$ , which is the boundary curve between the first and second characteristic regimes of heat exchange in the film

$$\theta(\eta, \xi_m) = \left( \frac{Pe}{4} \right) \frac{1}{D} \exp\left(-\frac{\xi_m}{D}\right) \left( \frac{\eta^2}{2} - \eta \right) + 1. \quad (12)$$

The graphic interpretation of (12) is shown in Figure 3.

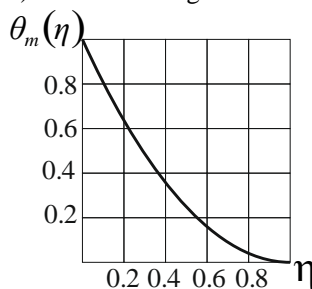


**Figure 3. Graphic representation of the limiting temperature curve (12) at:**

$$Gv = 0,5 \cdot 10^{-3} \text{ m}^2/\text{s}; u_2 = 20 \text{ m/s}; \tau_i = 2,7 \text{ N/m}; \delta = 0,256 \cdot 10^{-3} \text{ m}.$$

The coordinate  $\xi_m$  is determined from (12) under the condition that when  $\xi = \xi_m$  the dimensionless temperature is zero, ( $\theta(1, \xi_m) = 0$ )

$$\xi_m = D \ln \left( \frac{Pe}{8D} \right). \quad (13)$$

With free flow ( $\tau_i = 0$ )  $D = \frac{Pe}{80} \frac{25\tau_i + 16\rho g\delta}{3\tau_i + 2\rho g\delta} = \frac{Pe}{10}$ , and the expression (13) for  $\xi_m$  takes the form

$$\xi_m = D \ln \left( \frac{Pe}{8D} \right) = \frac{Pe}{10} \ln \left( \frac{5}{4} \right) = 0,0223 Pe. \quad (14)$$

Actual (physical) distance when defined as

$$x_m = \xi_m \delta.$$

The thickness of the laminar film during free flow on a vertical surface is defined as

$$\delta = \sqrt[3]{\frac{3G_v v}{g}},$$

and in the presence of accompanying steam (gas) flow – as a result of solving the cubic equation (5). The results of dimensionless distance  $\xi_m$  and physical length  $x_m$  calculations for different vapor core velocities are shown in Figure 4.

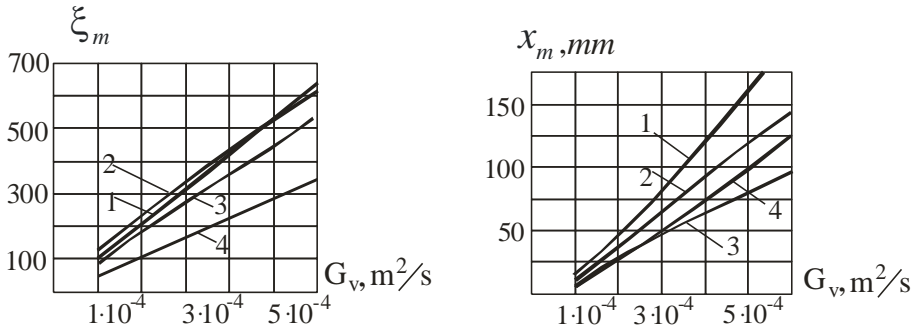


**Figure 4. Dependence of the dimensionless  $\xi_m$  (a) and physical  $x_m$  (b) length overcome by a laminar film, at which the heat transfer regimes to the film change from the volumetric liquid flux  $G_v$ .**

u, m/s: 1 – 15; 2 – 25; 3 – 35;  
4 – free flow.

### Turbulent mode of motion of a liquid film

For the turbulent motion of the film, we give the convective heat conduction equation (2) in dimensionless form

$$\frac{6\delta}{5} \bar{u}(\eta)^{1/5} \frac{\partial \theta(\xi, \eta)}{\partial \xi} = \frac{\partial}{\partial \eta} (a_i + a_t) \frac{\partial \theta(\xi, \eta)}{\partial \eta} \quad (15)$$

In relation (15), the power profile of the speed  $u = u_i \eta^{1/n}$  is given by the average speed

$$u = u_i \left( \frac{y}{\delta} \right)^{1/5} = \frac{6}{5} \bar{u} \left( \frac{y}{\delta} \right)^{1/5} = \frac{6}{5} \bar{u} \eta^{1/5}, \quad (\text{at } n = 1/5).$$

By replacing the left side of equation (15) with the average value

$$\int_0^1 \frac{6\delta}{5} \bar{u}(\eta)^{1/5} \frac{\partial \theta(\xi, \eta)}{\partial \xi} \partial \eta = \delta \bar{u} \frac{\partial \theta_{av}(\xi)}{\partial \xi},$$

we will get

$$\frac{Pe}{4} \frac{\partial \theta_{av}(\xi)}{\partial \xi} = \frac{\partial}{\partial \eta} \left( 1 + \frac{a_t}{a_i} \right) \frac{\partial \theta(\xi, \eta)}{\partial \eta}. \quad (16)$$

Since  $\frac{a_t}{a_i} = \frac{\nu_t}{\nu} \frac{Pr}{Pr_t}$ , expression (16) will be rewritten in the form

$$\frac{Pe}{4} \frac{\partial \theta_{av}(\xi)}{\partial \xi} = \frac{\partial}{\partial \eta} \left( 1 + \frac{\nu_t Pr}{\nu Pr_t} \right) \frac{\partial \theta(\xi, \eta)}{\partial \eta}. \quad (17)$$

The boundary and initial conditions under which the boundary temperature curve in the film is located are similar to the laminar flow regime of the film (7)

$$\eta = 0, \theta = 1; \quad \eta = 1, \frac{\partial \theta}{\partial \eta} = 0; \quad \xi = 0, \theta = 0.$$

Integrating (17) under the condition  $\eta = 1, \frac{\partial \theta}{\partial \eta} = 0$ , gives

$$\theta(\eta, \xi) = \frac{Pe}{4} \frac{\partial \theta_{av}(\xi)}{\partial \xi} \left[ \int \frac{\eta d\eta}{\left( 1 + \frac{\nu_t Pr}{\nu Pr_t} \right)} - \int \frac{d\eta}{\left( 1 + \frac{\nu_t Pr}{\nu Pr_t} \right)} \right]. \quad (18)$$

We give the turbulence function in the film in the form (3)

$$\frac{\nu_t}{\nu} = \varepsilon_m \eta^2 (1 - \eta^2), \quad (19)$$

where  $\varepsilon_m = 5 \cdot 10^{-5} \text{Re}^{1.4} \left\{ 1 + 3,6 \left[ 1 - \exp \left( 1 - \frac{d}{d_o} \right) \right] \right\} \left[ 1 - 0,1 \exp(-1,1086\sqrt{We}) \right] C_u$ .

Provided that  $\text{Pr}_r = 1$ , expression (18) taking into account (19) will be rewritten as

$$\theta(\eta, \xi) = \frac{Pe}{4} \frac{\partial \theta_{av}(\xi)}{\partial \xi} \left[ \int \frac{\eta d\eta}{(1 + \varepsilon_m (\eta^2 - \eta^4)) \text{Pr}} - \int \frac{d\eta}{(1 + \varepsilon_m (\eta^2 - \eta^4)) \text{Pr}} \right],$$

and its integration under boundary conditions  $\eta = 0, \theta = 1$  gives

$$\theta(\eta, \xi) = 1 + \frac{Pe}{4} \frac{\partial \theta_{av}(\xi)}{\partial \xi} \left[ \frac{1}{H} \text{Arth} \left( \frac{P(2\eta^2 - 1)}{H} \right) + \frac{\sqrt{2}H}{(4+P)A} \text{Arth} \left( \frac{\sqrt{2}P}{A} \eta \right) - \frac{\sqrt{2}H}{(4+P)B} \text{Arth} \left( \frac{\sqrt{2}P}{B} \eta \right) + \frac{1}{H} \text{Arth} \left( \frac{P}{H} \right) \right], \quad (20)$$

where  $H = \sqrt{4P + P^2}$ ;  $A = [P - [P(4+P)]^{1/2} P]^{1/2}$ ;  $B = [P + [P(4+P)]^{1/2} P]^{1/2}$ ;  $P = \varepsilon_m \text{Pr}$ .

The derivative  $\frac{\partial \theta_{av}(\xi)}{\partial \xi}$  is unknown. The average temperature, which is included in equation (20) and which is subject to determination, is defined as average mass

$$\theta_{av} = \int_0^1 \theta(\eta, \xi) \frac{u(\eta)}{\bar{u}} d\eta = \int_0^1 \frac{6}{5} \eta^{\frac{1}{5}} \theta(\eta, \xi) d\eta. \quad (21)$$

There is no analytical expression for the integral (21), but assuming the fullness of the velocity profile, with a certain approximation with respect to the average temperature  $\theta_{av}(\xi)$ , we apply the simplification

$$\theta_{av}(\xi) = \int_0^1 \theta(\eta, \xi) \frac{u(\eta)}{\bar{u}} d\eta \approx \int_0^1 \theta(\eta, \xi) d\eta. \quad (22)$$

Then as a result of integration (22) we get:

$$\theta_{av}(\xi) = 1 + \frac{Pe}{4} \frac{\partial \theta_{cp}}{\partial \xi} \left[ \begin{aligned} & \frac{H}{2P(P+4)} \ln \left( \frac{A^2 - 2P^2}{B^2 - 2P^2} \right) + \frac{2}{H} \operatorname{Arth} \left( \frac{P}{H} \right) + \\ & + \frac{\sqrt{2}(P-H)}{2aH} \operatorname{Arth} \left( \frac{\sqrt{2}P}{a} \right) - \frac{\sqrt{2}(P+H)}{2bH} \operatorname{Arth} \left( \frac{\sqrt{2}P}{b} \right) + \\ & + \frac{\sqrt{2}H}{(P+4)} \left( \frac{1}{A} \operatorname{Arth} \left( \frac{\sqrt{2}P}{A} \right) - \frac{1}{B} \operatorname{Arth} \left( \frac{\sqrt{2}P}{B} \right) \right) + \frac{H}{P(4+P)} \ln \left( \frac{B}{A} \right) \end{aligned} \right],$$

where  $a = \sqrt{P^2 - PH}$ ;  $b = \sqrt{P^2 + PH}$ .

Denoting the expression in square brackets as

$$S = \frac{Pe}{4} \left[ \begin{aligned} & \frac{H}{2P(P+4)} \ln \left( \frac{A^2 - 2P^2}{B^2 - 2P^2} \right) + \frac{2}{H} \operatorname{Arth} \left( \frac{P}{H} \right) + \\ & + \frac{\sqrt{2}(P-H)}{2aH} \operatorname{Arth} \left( \frac{\sqrt{2}P}{a} \right) - \frac{\sqrt{2}(P+H)}{2bH} \operatorname{Arth} \left( \frac{\sqrt{2}P}{b} \right) + \\ & + \frac{\sqrt{2}H}{(P+4)} \left( \frac{1}{A} \operatorname{Arth} \left( \frac{\sqrt{2}P}{A} \right) - \frac{1}{B} \operatorname{Arth} \left( \frac{\sqrt{2}P}{B} \right) \right) + \frac{H}{P(4+P)} \ln \left( \frac{B}{A} \right) \end{aligned} \right],$$

we come to the differential equation

$$\theta_{av} = 1 + S \frac{d\theta_{av}}{d\xi},$$

solution of which, under the initial condition  $\xi = 0$ ;  $\theta = 0$ , gives an expression for the average temperature

$$\theta_{av} = \left[ 1 - \exp \left( \frac{\xi}{S} \right) \right].$$

Derivative from  $\theta_{av}$  to  $\xi$

$$\frac{d\theta_{av}}{d\xi} = -\frac{1}{S} \exp \left( \frac{\xi}{S} \right).$$

By substituting the obtained derivative into the original equation, we obtain the limiting curve  $\theta_m(\eta, \xi_m)$  at the distance  $\xi_m$ , at which the condition  $\frac{\partial \theta}{\partial \eta} = 0$

$$\theta_m(\eta, \xi_m) = 1 - \frac{Pe}{4S} \exp\left(\frac{\xi_m}{S}\right) \left[ \begin{aligned} & \frac{1}{H} \operatorname{Arth}\left(\frac{P(2\eta^2 - 1)}{H}\right) + \frac{\sqrt{2}H}{(4+P)A} \operatorname{Arth}\left(\frac{\sqrt{2}P}{A}\eta\right) - \\ & - \frac{\sqrt{2}H}{(4+P)B} \operatorname{Arth}\left(\frac{\sqrt{2}P}{B}\eta\right) + \frac{1}{H} \operatorname{Arth}\left(\frac{P}{H}\right) \end{aligned} \right] \quad (23)$$

A graphic representation of the obtained function  $\theta_m(\eta, \xi_m)$  is shown in Figure 5.

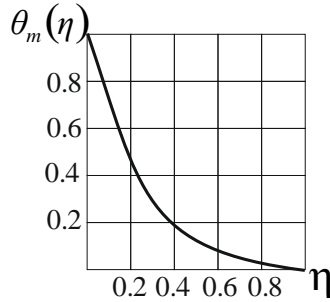


**Figure 5. Graphic representation of the limiting temperature curve (23) from the dimensionless transverse coordinate  $\theta_m = f(\eta)$  with the parameters:  $P = 10$ ,  $Pe = 12000$ .**

The coordinate  $\xi_m$  for which  $\frac{\partial \theta}{\partial \eta} = 0$  is found from the condition  $\eta = 1$ ,  $\theta(1, \xi_m) = 0$

$$0 = 1 - \frac{Pe}{4S} \exp\left(\frac{\xi_m}{S}\right) \left[ \begin{aligned} & \frac{1}{H} \operatorname{Arth}\left(\frac{P}{H}\right) + \frac{\sqrt{2}H}{(4+P)A} \operatorname{Arth}\left(\frac{\sqrt{2}P}{A}\right) - \\ & - \frac{\sqrt{2}H}{(4+P)B} \operatorname{Arth}\left(\frac{\sqrt{2}P}{B}\right) + \frac{1}{H} \operatorname{Arth}\left(\frac{P}{H}\right) \end{aligned} \right].$$

Denoting the expression in square brackets as  $K$

$$K = \left[ \begin{aligned} & \frac{1}{H} \operatorname{Arth}\left(\frac{P}{H}\right) + \frac{\sqrt{2}H}{(4+P)A} \operatorname{Arth}\left(\frac{\sqrt{2}P}{A}\right) - \\ & - \frac{\sqrt{2}H}{(4+P)B} \operatorname{Arth}\left(\frac{\sqrt{2}P}{B}\right) + \frac{1}{H} \operatorname{Arth}\left(\frac{P}{H}\right) \end{aligned} \right],$$

we will get the ratio for calculation  $\xi_m$  in the turbulent mode of motion of the film

$$\xi_m = S \ln\left(\frac{4S}{PeK}\right). \quad (24)$$

The graphical interpretation of (24) is shown in Figure 6.

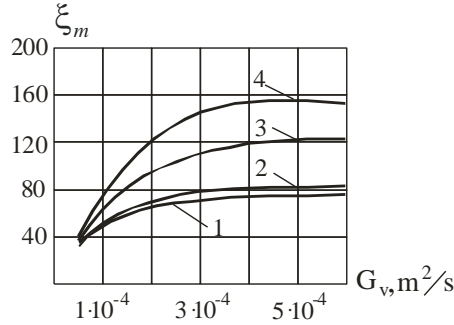


**Figure 6. Dependence of the dimensionless  $\xi_m$  length overcome by a turbulent film, at which the heat transfer regimes to the film change from the volumetric liquid flux  $G_v$  :**

1 – free flow;  
u, m/s: 2 – 15 m/s; 3 – 25; 4 – 35.

To obtain the physical length of the boundary of the zones  $x_m$  under the turbulent regime, it is necessary to determine the thickness of the film from the equation of motion using the dependence for turbulent viscosity (3)

$$\frac{\tau_i \delta}{\rho \nu} + \frac{g \delta^2}{\nu} (1 - \eta) = \left[ 1 + \varepsilon_m (\eta^2 - \eta^4) \right] \frac{du}{d\eta}. \quad (25)$$

From (25) under boundary conditions  $\eta = 0, u = 0$ , we obtain the velocity profile

$$u = \left( \frac{\tau_i \delta}{\rho \nu} + \frac{g \delta^2}{\nu} \right) \frac{\sqrt{2} h}{(4 + \varepsilon_m)} \left[ \frac{1}{r} \text{Arth} \left( \frac{\sqrt{2} \varepsilon_m \eta}{r} \right) - \frac{1}{j} \text{Arth} \left( \frac{\sqrt{2} \varepsilon_m \eta}{j} \right) \right] - \frac{g \delta^2}{\nu h} \left[ \text{Arth} \left( \frac{\varepsilon_m (2\eta^2 - 1)}{h} \right) + \text{Arth} \left( \frac{\varepsilon_m}{h} \right) \right], \quad (26)$$

Where  $h = \sqrt{4\varepsilon_m + \varepsilon_m^2}$ ;  $j = \sqrt{\varepsilon_m^2 - \varepsilon_m h}$ ;  $r = \sqrt{\varepsilon_m^2 + \varepsilon_m h}$ ;

$$n = \left[ \frac{1}{r} \text{Arth} \left( \frac{\sqrt{2} \varepsilon_m}{r} \right) - \frac{1}{j} \text{Arth} \left( \frac{\sqrt{2} \varepsilon_m}{j} \right) \right].$$

The average speed  $\bar{u} = \int_0^1 u d\eta$  is obtained from (26):

$$\bar{u} = \left( \frac{\tau_i \delta}{\rho \nu} + \frac{g \delta^2}{\nu} \right) \frac{\sqrt{2} h}{(4 + \varepsilon_m)} \left[ n - \frac{\sqrt{2}}{4\varepsilon_m} \ln \left( \frac{j^2 - 2\varepsilon^2}{r^2 - 2\varepsilon^2} \right) - \frac{\sqrt{2}}{2\varepsilon_m} \ln \left( \frac{r}{j} \right) \right] - \frac{g \delta^2}{\nu h} \left[ 2 \text{Arth} \left( \frac{\varepsilon_m}{h} \right) - \frac{\sqrt{2} h}{2} \left( \frac{1}{r} \text{Arth} \left( \frac{\sqrt{2} \varepsilon_m}{r} \right) + \frac{1}{j} \text{Arth} \left( \frac{\sqrt{2} \varepsilon_m}{j} \right) \right) - \frac{\sqrt{2} \varepsilon_m n}{2} \right]. \quad (27)$$

The thickness of the film  $\delta$  and the average speed  $\bar{u}$  are related to the volumetric liquid flux  $G_v$  by dependence  $\delta = \frac{G_v}{\bar{u}}$ . Whence the expression for the average thickness of the film takes the form of a cubic equation

$$G_v = \left( \frac{\tau_i \delta^2}{\rho \nu} \right) D + \frac{g \delta^3}{\nu h} (Dh - B), \quad (28)$$

where

$$B = \left[ 2 \operatorname{Arth} \left( \frac{\varepsilon_m}{h} \right) - \frac{\sqrt{2}h}{2} \left( \frac{1}{r} \operatorname{Arth} \left( \frac{\sqrt{2}\varepsilon_m}{r} \right) + \frac{1}{j} \operatorname{Arth} \left( \frac{\sqrt{2}\varepsilon_m}{j} \right) \right) - \frac{\sqrt{2}\varepsilon_m n}{2} \right],$$

$$D = \frac{\sqrt{2}h}{(4 + \varepsilon_m)} \left[ n - \frac{\sqrt{2}}{4\varepsilon_m} \ln \left( \frac{j^2 - 2\varepsilon_m^2}{r^2 - 2\varepsilon_m^2} \right) - \frac{\sqrt{2}}{2\varepsilon_m} \ln \left( \frac{r}{j} \right) \right].$$

In the case of free flow ( $\tau_i = 0$ ), the film thickness is directly from (28)

$$\delta = \sqrt[3]{\frac{G_v \nu h}{g(Dh - B)}}. \quad (29)$$

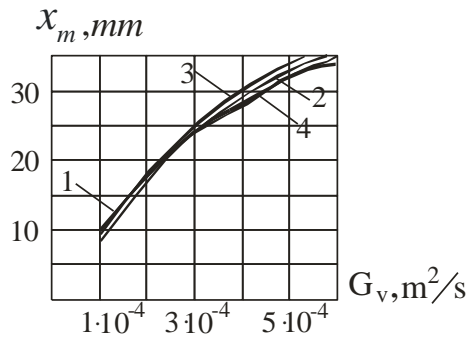


**Figure 7. Dependence of the physical  $x_m$  length overcome by a turbulent film, at which the heat transfer regimes to the film change from the volumetric liquid flux  $G_v$ :**  
 1 – free flow;  $u_2, m/s$ : 2 – 15; 3 – 25; 4 – 35.

Regarding the distance covered by the film during the period between the passage of two large waves. The phase speed of the large wave  $c$  exceeds the average speed of the film  $\bar{u}$ , so a selected section of the film moving at speed  $\bar{u}$  will be crossed by the next wave in time  $\tau$  at a distance of  $x$ .

$$\tau = \frac{\lambda_{bw}}{c - \bar{u}},$$

where  $c, \lambda_{bw}$  – face velocity and length of large waves, respectively.

The distance  $x$  covered by the film in time  $\tau$ , moving at speed  $\bar{u}$ , between the crests of large waves is equal to

$$x = \bar{u}\tau = \frac{\bar{u}\lambda_{bw}}{c - \bar{u}} = \frac{\bar{u}c}{f_{bw}(c - \bar{u})} = \frac{c}{f_{bw}\left(\frac{c}{\bar{u}} - 1\right)}, \quad (30)$$

where  $f_{bw}$  – is the frequency of large waves. The quantities  $c, \lambda_{bw}, f_{bw}$  are functions of irrigation density, interfacial tangential stress, and channel geometry. According to data known from the literature, the phase speed exceeds the average speed of the film by 2.5– 1.5 times, and the length of large waves  $\lambda_{bw}$  in long pipes is 100–140 mm, depending on the density of irrigation. If we take the average value of the phase speed  $c = 2\bar{u}$ , we get the distance covered by the film during the passage of two large waves, which, according to (30), is equal to the wavelength of  $x \cong \lambda_{bw}$ . Thus, since  $x_m \leq \lambda_{bw}$  two modes of heat exchange are realized during a wave cycle on the entire gap of the film surface between two large waves. The initial condition for finding the temperature profile in the second period is equation (12) for laminar and (23) for turbulent film motion modes.

## Conclusions

1. The obtained relations (13) for the laminar flow and (24) for the turbulent flow allow us to calculate the length of the film movement between two large waves up to the limit ( $\xi = \xi_m$ ), at which the character of the heat transfer to the boiling film changes – from the heating mode to the saturation state on the interfacial surface to the evaporation mode with of the interfacial surface with an increase in the heat flux in the process of movement to the steady state.
2. As a result of solving the convective heat conduction equation with the boundary conditions  $\eta = 0, \theta = 1; \eta = 1, \frac{\partial \theta}{\partial \eta} = 0$  and the initial condition:  $\xi = 0, \theta_{av} = 0$ , obtained solutions for laminar (12) and turbulent (23) flows, which are the initial conditions for the equation of convective heat conduction in the second period of development of the temperature field in the film at  $\xi = \xi_m$ .
3. The parameter  $x_m$  for the turbulent flow is not very sensitive to changes in the velocity of the vapor core, since as the film thickness decreases due to the dynamic action of the flow core on the film, the intensity of turbulence in the film also decreases.

## References

- Demekhin E.A., Kalaidin E.N., Rastarukhin A.A. (2005), Influence of wave regimes on mass transfer in falling liquid films, *Thermophysics and Aeromechanics*, 12(2), pp. 259–269.
- Dietze G.F. (2016), On the Kapitza instability and the generation of capillary waves, *Journal of Fluid Mechanics*, 789, pp. 368–401, <https://doi.org/10.1017/jfm.2015.736>

- Dietze G.F., Rohlfis W., Kneer R. (2014), Three-dimensional flow structures in laminar liquid films, *Journal of Fluid Mechanics*, 743, pp. 75–123, <https://doi.org/10.1017/S0022112009008155>
- Gourdon M., Karlsson E., Innings A., Vamling L. (2015), Heat transfer for falling film evaporation of industrially relevant fluids up to very high Prandtl numbers, *Heat and Mass Transfer*, 52(2), pp. 379–391.
- Kostoglou M., Samaras K., Karapantsios T.D. (2010), Large wave characteristics and their downstream evolution at high Reynolds number falling films, *AIChE Journal*, 56(1), pp. 11–23.
- Lel V.V., Al-Sibai F., Kneer R. (2009), Thermal Entry Length and Heat Transfer Phenomena in Laminar Wavy Falling Films, *Microgravity Science and Technology*, 21(S1), pp. 215 – 220
- Malamataris N.A., Balakotaiah V. (2008), Flow structure underneath the large amplitude waves of a vertically falling film, *AIChE Journal*, 54(7), pp. 1725–1740.
- Mascarenhas N., Mudawar I. (2013), Investigation of eddy diffusivity and heat transfer coefficient for free-falling turbulent liquid films subjected to sensible heating, *International Journal of Heat and Mass Transfer*, 64, pp. 647–660, <https://doi.org/10.1016/j.ijheatmasstransfer.2013.04.061>
- Mascarenhas N., Mudawar I. (2013), Study of the influential waves on heat transfer in turbulent falling films, *International Journal of Heat and Mass Transfer*, 67, pp. 1106–1121, <https://doi.org/10.1016/j.ijheatmasstransfer.2013.08.100>
- Petrenko V., Pryadko M., Ryabchuk O. (2020), Modeling heat transfer in down flowing annular weakly turbulent vapor-liquid flows during evaporation, *Ukrainian Food Journal*, 9(4), pp. 901–916, <https://doi.org/10.24263/2304-974X-2020-9-4-14>

# Phosphate recovery and fertilizer production from wastewater using iron-reducing bacteria

Viktor Stabnikov<sup>1</sup>, Dmytro Stabnikov<sup>1,2</sup>, Zubair Ahmed<sup>3</sup>

1 – National University of Food Technologies, Kyiv, Ukraine

2 – University of Wrocław, Wrocław, Poland

3 – Mehran University of Engineering and Technology, Jamshoro, Pakistan

---

## Abstract

---

### Keywords:

Phosphate  
Biotechnology  
Iron ore  
Wastewater  
Fertilizer  
Plant growth

**Introduction.** Food production is based on the use of fertilizers, in particular those containing phosphorus. Recovery of phosphorus from wastewater can prevent eutrophication of water bodies, meanwhile the removed phosphate can be used as a fertilizer.

**Materials and methods.** Wastewater containing phosphorous, iron ore, iron reducing bacteria are the main components of the proposed technology for phosphorous recovery. Microscopic observations were done using laser scanning confocal microscopy. Obtained fertilizer was tested for plant growth.

**Results and discussion.** An effective biological method for removal and recovery of phosphate from phosphate containing liquid wastes using precipitation of phosphate by microbially-produced ferrous ions was proposed. Performance of this biotechnology on the example of reject water (liquid fraction of anaerobic sludge) from municipal wastewater treatment plant was shown. This biotechnology is based on the application of iron ore treated by iron-reducing bacteria *Stenotrophomonas maltophilia* strain BK. Dissolved ferrous are produced from solid iron ore using iron-reducing bacteria and precipitate phosphate present in wastewater.

Phosphate-iron precipitate was assessed as a phosphorus fertilizer by addition of it to sandy soil poor with nutrients using for cultivation of three plants, namely *Lycopersicum esculantum* L. (tomato), *Casicum annuum* L. (pepper) and *Ipomoea aquatica* (water spinach). Addition of phosphorous precipitate to soil increased dry weight of stems and leaves of test plants by up to 5 times in comparison with control.

**Conclusion.** The biotechnology of anaerobic removal and recovery of phosphate from reject water of municipal wastewater treatment plants using iron-reducing bacteria *Stenotrophomonas maltophilia* strain BK and iron ore as a source of ferric has been developed. Produced phosphate – iron precipitate could be used as a phosphorus fertilizer.

---

### Article history:

Received  
29.09.2022  
Received in  
revised form  
12.02.2023  
Accepted  
31.03.2023

---

### Corresponding author:

Viktor Stabnikov  
E-mail:  
vstabnikov1@  
gmail.com

---

### DOI:

10.24263/2304-  
974X-2023-12-1-  
10

---

## **Introduction**

This is due to the fact that a large part of soil phosphorus is adsorbed onto mineral particles or is present in form of slightly soluble salts and also is removed from soil because of water erosion (Alewell et al., 2020; Günther et al., 2018). Thus, not much soil phosphorus can be used by the plants for their growth. Phosphorus for agriculture is obtained from phosphate rock, which is a non-renewable resource and, according to preliminary calculations, its world reserves can be depleted in 50–100 years (Cordell et al., 2009). Phosphorus has even been called a "disappearing nutrient" (Gilbert, 2009). Therefore, recovery of phosphorus from various wastes in order to use it later as a fertilizer is a significant contribution to the problem of phosphorus shortage for agriculture.

From the other side, concentration of total phosphorus above 0.5 mg/l in freshwater systems causes their eutrophication. Growth and decay of phototrophic biomass lead to decrease of dissolved oxygen concentration in natural water that kills aquatic life and decreases quality of drinking water. According to European legislation, the concentration of phosphorus in purified municipal wastewater (discharged effluent from Municipal Wastewater Treatment Plant, MWWTP) should be below 0.5–1.0 mg/l (Sunner, 2017). According to the standards of United States Environmental Protection Agency (US EPA) the content of total phosphorus in streams that discharge directly into water systems should be less than 0.05 mg/l (US EPA, 1986). Meanwhile, concentration of phosphorus in municipal wastewater varied from 5 to 20 mg/l and only 30% of this concentration is removed by secondary treatment (Cieślik and Konieczka, 2017).

Concentration of total phosphorus in reject water (liquid fraction of anaerobic sludge) in MWWTP is in the range from 50 to 130 mg/l (Pitman, 1999). So, phosphorus, which is present in reject water, is from 10 to 50% of total phosphorus load to the aeration tank (Van Loosdrecht and Salem, 2006). Removal of phosphate from reject water can significantly decrease the phosphorus load on the aeration tanks of MWWTP, and helps to prevent eutrophication of natural water bodies. Besides that, removed phosphate probably can be used as a fertilizer in agriculture.

Ferrous chloride and ferrous sulphate are conventionally used for chemical removal of phosphate from wastewater (Günther et al., 2018). The main disadvantage of this chemical precipitation of phosphate is the high cost of iron salts. Application of iron-reducing bacteria (IRB) for reduction of Fe(III), which is supplying to reject water as a cheap iron ore mining waste, produces dissolved Fe(II), which will precipitate phosphate. This technology can be a new method for phosphate removal and recovery (Ivanov et al., 2005; 2006; Korniienko et al., 2023; Stabnikov et al., 2004; Stabnikova et al., 2023; Tay et al., 2008). Altogether, obtained precipitate contains phosphorus, which is a non-renewable nutrient needed for plant growth.

The aim of the present study was to propose technological scheme for anaerobic removal and recovery of phosphate from reject water of MWWTP based on application of iron-reducing bacteria at the presence of iron ore and check the possibility to use of phosphate-iron precipitate as a fertilizer.

## **Materials and methods**

### **Microscopic observations**

The interaction of iron-reducing bacteria cells with Fe(OH)<sub>3</sub> particles was observed using a confocal laser scanning microscope Fluoview300 (Olympus, Japan). The

combination of SYTO 9™ nucleic acid stain and propidium iodide was used according to the manufacturer's instructions for the LIVE/DEAD BacLight™ dye kit (Molecular Probes, Eugene, OR, USA). This kit is used to detect live and dead bacterial cells due to the ability of propidium iodide to selectively penetrate dead cells (Boulos et al., 1999). The green fluorescence of SYTO 9™ dye and the red fluorescence of propidium iodide were induced by a 10 mW argon laser at 488 nm, separated into two channels at 570 nm with a filter, and determined in channel 1 with a filter that transmitted light 1 with a filter that transmitted light from a wavelength of 580 nm to 640 nm.

### **Microbiological analysis**

A 24-h direct plating method for fecal coliform enumeration at  $37 \pm 1$  °C for  $21 \pm 3$  h using Coliforms Chromogenic Agar was performed to assess the possibility of phosphate-iron precipitate application as a fertilizer.

### **Plant cultivation**

Tomatoes (*Lycopersicon esculantum* L.), chili peppers (*Capsicum annuum* L.), and water spinach (*Ipomoea aquatica*) were selected to study the effect of phosphate-iron precipitate (PIP) obtained from wastewater on the growth of plants in ceramic pots (23 cm diameter, 18 cm high), each of which contained 4 kg of nutrient-poor soil with a moisture content of 14%. As controls, only soil without impurities (C1), soil with the addition of nitrogen fertilizer (C2), and soil with the addition of phosphate fertilizer (C3) were used. Ammonium sulfate was used as a nitrogen fertilizer in the amount of 0.46 g per kg of soil (0.098 g of nitrogen), which corresponded to the recommended rate of its use for nitrogen-poor soils (Roman et al., 1990). As a phosphate fertilizer,  $\text{KH}_2\text{PO}_4$  was used, which was set in an amount corresponding to the amount of phosphorus in the experiment using obtained phosphate-iron precipitate. In the experiment, iron phosphate precipitate was added in an amount that corresponded to 0.0475 g P per 1 kg of soil and ammonium sulfate in the same amount as in C2. All chemicals were applied to the soil, thoroughly mixed and left for a week before making 10 seeds in each pot. After three weeks, 5 strong seedlings were left, which were grown for 8 weeks. At the end of cultivation, all plants were carefully removed from the soil and the roots were washed with distilled water. The length of the ground part of the plants and the root system was measured. The dry weight of the aerial part of the plant and roots was determined after drying at 60 °C for 48 hours.

### **Statistics**

Experiments were carried out in triplicates. Statistical processing of the experimental results was carried out using special computer programs for personal computers.

Data on the effect of iron phosphate on plant growth were analysed by ANOVA and Tukey statistical procedures using the Statistical Package for the Social Sciences (SPSS) version 12.0 program (SPSS Inc, Chicago, Illinois).

## Results and discussion

### Production of phosphate fertilizer

The main processes for removing phosphate from any phosphorus-containing liquid waste using iron-reducing bacteria are: (a) anoxic bacterial reduction of  $\text{Fe}^{3+}$  from a cheap natural mineral such as iron ore and converting it into a soluble form  $\text{Fe}^{2+}$ ; (b) precipitation of phosphate due the formation of an insoluble phosphate-iron precipitate:



Ferrous phosphate could be further chemically or biologically oxidized by oxygen:



The process of phosphorus recovery from phosphorus-containing wastewater, including reject water from municipal water treatment plants, using the reduction of iron from cheap iron ore sources by iron-reducing bacteria, has been studied and described in works (Ivanov et al., 2005; 2007; 2014; Stabnikov and Ivanov, 2004), as well as in a US patent (Tay J. H., Tay S. T. L., Ivanov V., Stabnikova O., Wang J.Y. US Patent 7 393452, Compositions and methods for the treatment of wastewater and other waste). The principal scheme of phosphate recovery and fertilizer production from reject water of the wastewater treatment plant using iron-reducing bacteria is shown in Fig. 1.

After mechanical treatment, wastewater enters the aeration tank A1. Wastewater after aerobic treatment in A1 is supplied by the pump P2 in the settling tank S3. A portion of activated sludge is returning to the aeration tank A1, but the excessive activated sludge is supplied by the pump P4 to the anaerobic reactor AR5. Treated wastewater after the aeration tank is discharged into aquatic systems. Biogas, which is produced during anaerobic digestion of activated sludge in the reactor AR5, can be used for heating and/or electricity generation. Anaerobic sludge after sedimentation in the settling tank S7 and dewatering is disposed of, for example as concrete from the mixture of cement and sewage sludge. Reject water with phosphate concentration from 100 to 200 mg/L is supplied to the reactor R8 for its precipitation by Fe(II). Part of the reject water is supplied for production of ferrous solution in the reactor R16. Settling of phosphate-iron precipitate (PIP) is going in the settling tank S9. Purified liquid from the settling tank S9 is returned to the aeration tank A1 for further treatment, but the precipitate in the form of suspension with the moisture content 90% is dewatered on the centrifuge C10 to the final moisture content 25%. PIP is drying on the belt dryer BD11 to the moisture content from 5 to 10%. Hot air with a temperature 170°C is used as a heating agent. Final product enters the loading pocket LD12 and through screw conveyor SC13 is going for the packing to packing machine PM14.

Anaerobic cultivation of iron-reducing bacteria is going at temperature  $28 \pm 2^\circ\text{C}$  in the sealed reactor R15, which is filled by 90% medium (NM) with the following composition, g/l:  $\text{NaHCO}_3$ , 2.5;  $\text{NH}_4\text{Cl}$ , 1.5;  $\text{NaH}_2\text{PO}_4$ , 0.6;  $\text{KCl}$ , 0.1; yeasts extract 0.5; ferric citrate,  $\text{C}_6\text{H}_8\text{O}_7\text{Fe}$ , 5.0; ethanol, 1.0; tap water to 1 l; pH 7.0. Nitrogen gas is supplied into the reactor R14 to ensure anaerobic conditions. Inoculum (I) is preparing in the laboratory by anaerobic cultivation of IRB *Stenotrophomonas maltophilia* strain BK (Ivanov et al., 2005) on the solid medium (solidified reject water) and then by the submerged cultivation in the liquid medium with the composition described above.



*S. maltophilia* strain BK is Gram-negative, rod-shaped, non-spore forming bacteria, facultative aerobe. *S. maltophilia* strain BK is able to reduce Fe(III) using m-cresol, 2,4-dichlorophenol, p-phenylphenol and diphenylamine, a third by importance compound in the European Union list of priority pollutants, as a sole source of carbon under anaerobic conditions. This property of strain BK can be used in the anaerobic (anoxic) treatment of wastewater or reject water polluted with xenobiotics. Image of iron-reducing bacteria on iron hydroxide particles obtained using a confocal laser scanning microscope is shown in Fig. 2.

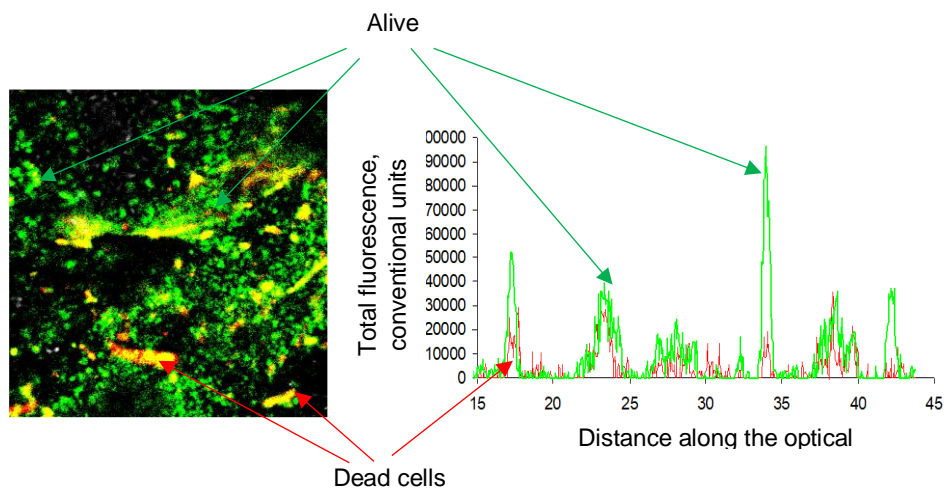


**Figure 2. Image of iron-reducing bacteria on iron hydroxide particles (image obtained using a confocal laser scanning microscope):**

- a – cells were stained with nucleic acid dye SYTO 9™ (green fluorescence) and propidium iodide (PI), penetrating only into cells with a broken membrane.  
Dead cells are yellow due to a combination of green and red fluorescence;
- b – fluorescence indices of SYTO 9 (upper curve) and PI (lower curve) in the optical section of the image.

Suspension of IRB biomass is supplied to the reactor R15 for initiation of ferric reduction from iron ore particles with size less than 4.75 mm and the content of Fe(III) higher than 65%, which is periodically loaded in the reactor R15. Further reduction of Fe(III) is performed by IRB present in the reactor R16. Reject water is continuously supplied to the reactor R17 from the settling tank S7.

Reduction of iron from iron ore leads to production of Fe(II) solution, which is used for phosphate precipitation in the form of phosphate iron precipitate, PIP. PIP after dewatering and drying can be used as a phosphorus fertilizer in agriculture.

#### **Assessment of biological safety of use in the cultivation of agricultural plants**

An important aspect of the use of wastewater treatment products in agriculture is to check its safety, in particular, the presence of pathogenic microorganisms. The United States Standard for the use of anaerobically treated activated sludge (biological solid waste) includes allowable limits for faecal coliforms (US EPA, 1999). An important aspect of the

use of wastewater treatment products in agriculture is to check its safety, in particular, the presence of pathogenic microorganisms. The United States Standard for the Use of Anaerobically Treated Activated Sludge (Biological Solid Waste) includes allowable limits for faecal coliforms. According to the content of faecal coliforms, biological solid waste is divided into two classes: class B with a faecal coliforms content of less than  $2 \times 10^6$  cells per gram of dry matter and class A with a faecal coliforms content of less than  $1 \times 10^3$  cells per gram of dry matter. Unlike class B biological solid waste, class A waste has virtually no restrictions regarding the place of application and the regarding the place of use and the nature of crops.

The concentration of faecal coliforms was  $(4.0 \pm 0.6) \times 10^6$  cells/ml in suspensions of anaerobic sludge (activated sludge after anaerobic treatment) with a solids concentration of 5.5%;  $(3.1 \pm 0.8) \times 10^1$  cells/ml in the liquid fraction of anaerobic sludge;  $(1.8 \pm 0.2) \times 10^2$  cells per 1 g of dry matter in phosphorus-iron sediment with moisture content of 75%. The growth of colonies of faecal coliforms was not observed in the analysis of the dried phosphorus-iron sediment, which makes it possible to consider the possibility of its use as a fertilizer.

### Application of phosphate iron precipitate as fertilizer for plant cultivation

The chemico-physical characteristics of the sandy soil used in the experiment are given in Table 1.

Table 1

Chemico-physical characteristics of soil

Parameters	Soil	Parameters	Soil
pH	6.4±0.1	N, % from dry matter	0.29±0.02
Organic substances, % from dry matter	4.8±0.2	P, % from dry matter	0.00±0.00
Density, g/cm <sup>3</sup>	1.26±0.11	K, % from dry matter	0.16±0.01

Sandy loam soil poor by nutrients was used as control (C). Plants were grown in soil with addition only a nitrogen fertilizer (C1), in soil with addition only a phosphorus fertilizer (C2) and in soil with addition of ammonium sulphate as a nitrogen fertilizer and phosphate iron precipitate as a phosphorus fertilizer in ratio N: P = 2:1 (E). Quality of phosphate iron precipitate as the phosphorus fertilizer was tested using cultivation of three plants: *Lycopersicum esculantum L.* (tomato), *Casicum annum L.* (pepper) and *Ipomoea aquatica* (water spinach). Results are shown in Table 2.

Data were analysed using one-way ANOVA and Tukey's HSD tests by the SPSS statistical package. The length and dry weight of stems in the experiment was increased significantly: for pepper by 3.1 and 19; for tomato by 4.4 and 40; for water spinach by 2.1 and 5 times in comparison with controls, respectively (Figures 3 and 4).

The length and dry weight of the ground part of the plant (stem) increased when phosphate iron precipitate was added as a phosphorus fertilizer (E) to the soil containing nitrogen fertilizer (C1): pepper by 3.1 and 19; tomatoes by 4.4 and 40; water spinach by 2.1 and 5 times, respectively.

Table 2

Influence of phosphate iron precipitate addition to soil on the plant growth

Parameters of plants	C	C1 (with N)	C2 (with P)	E
<b>Pepper</b>				
Length of stem, cm	6.0±0.4 <sup>a</sup>	6.1±0.3 <sup>a</sup>	5.9±0.4 <sup>a</sup>	19.0±1.4 <sup>b</sup>
Length of root, cm	4.7±0.8 <sup>a</sup>	4.7±0.7 <sup>a</sup>	4.6±0.8 <sup>a</sup>	12.6±1.5 <sup>b</sup>
Dry weight of stem, g	0.02±0.00 <sup>a</sup>	0.02±0.00 <sup>a</sup>	0.02±0.00 <sup>a</sup>	0.38±0.14 <sup>b</sup>
Dry weight of root, g	0.01±0.00 <sup>a</sup>	0.01±0.00 <sup>a</sup>	0.01±0.00 <sup>a</sup>	0.08±0.03 <sup>b</sup>
<b>Tomato</b>				
Length of stem, cm	7.6±0.7 <sup>a</sup>	7.2±0.4 <sup>a</sup>	7.0±0.4 <sup>a</sup>	31.8±2.2 <sup>b</sup>
Length of root, cm	6.0±1.1 <sup>a</sup>	5.8±0.6 <sup>a</sup>	5.9±0.4 <sup>a</sup>	10.4±2.3 <sup>b</sup>
Dry weight of stem, g	0.04±0.0 <sup>a</sup>	0.04±0.0 <sup>a</sup>	0.04±0.0 <sup>a</sup>	1.59±0.37 <sup>b</sup>
Dry weight of root, g	0.05±0.0 <sup>a</sup>	0.04±0.0 <sup>a</sup>	0.05±0.0 <sup>a</sup>	0.32±0.11 <sup>b</sup>
<b>Water spinach</b>				
Length of stem, cm	19.2±0.5 <sup>a</sup>	16.2±0.8 <sup>b</sup>	11.6±1.3 <sup>b</sup>	33.6±3.7 <sup>b</sup>
Length of root, cm	15.1±2.0 <sup>b</sup>	10.4±1.3 <sup>a</sup>	7.8±1.1 <sup>a</sup>	15.3±1.6 <sup>b</sup>
Dry weight of stem, g	0.32±0.03 <sup>a</sup>	0.23±0.01 <sup>a</sup>	0.16±0.02 <sup>a</sup>	1.17±0.27 <sup>b</sup>
Dry weight of root, g	0.15±0.03 <sup>ab</sup>	0.12±0.02 <sup>ab</sup>	0.10±0.02 <sup>a</sup>	0.18±0.03 <sup>b</sup>

Note: Values in the same line followed by the same letter are not statistically different at P<0.05 according to the least significant difference test (calculated using statistical procedures ANOVA and Tukey).

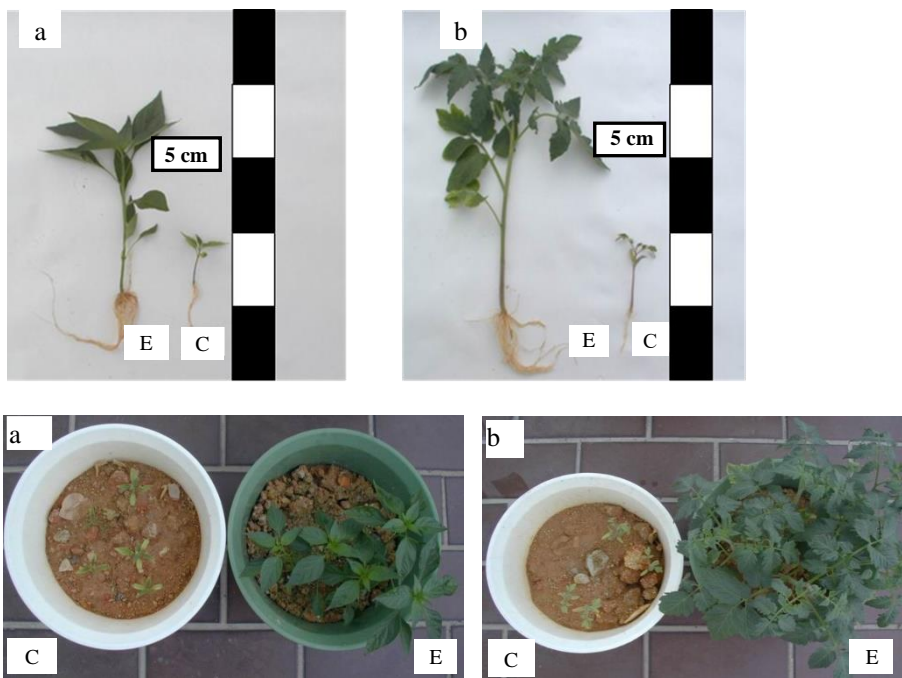
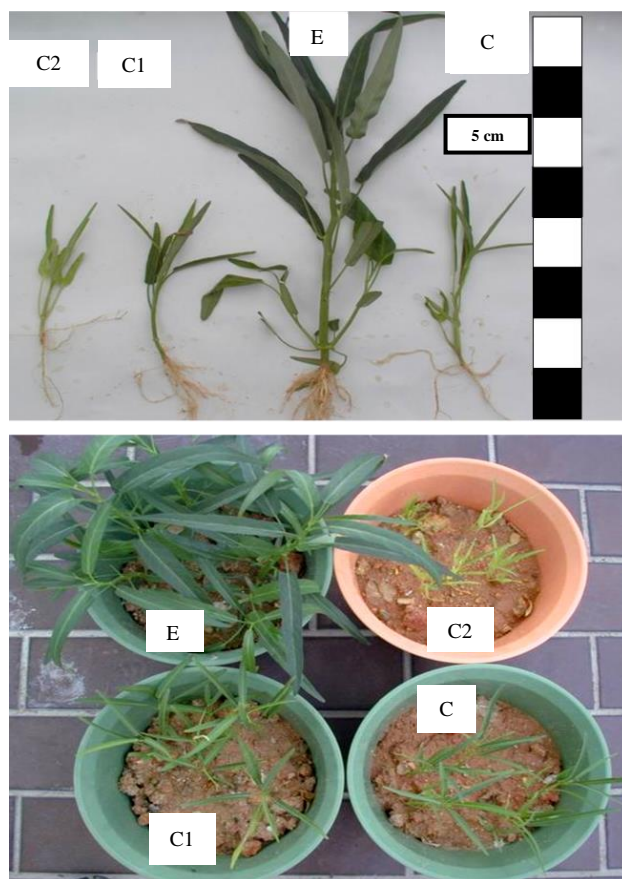


Figure 3. Growth of pepper (a) and tomatoes (b) in control (C) and in the experiment with phosphate-iron precipitate (E).



**Figure 4. Growth of water spinach in control (C), in control added with nitrogen fertilizer (C1), in control added with phosphorus fertilizer (C2) and in the experiment with phosphate iron precipitate (E).**

## Conclusions

The biotechnology of anaerobic removal and recovery of phosphate from reject water of municipal wastewater treatment plant using iron-reducing bacteria *Stenotrophomonas maltophilia* strain BK and iron ore mining waste as a source of ferric has been developed. Produced phosphate – iron precipitate could be used as a phosphorus fertilizer. Addition of phosphate iron precipitate in poor by nutrients soil increased the dry weight of stems and leaves of test plants by 4–5 times in comparison with control.

## References

- Alewell C., Ringeval B., Ballabio C., Robinson D. A., Panagos P., Borrelli P. (2020), Global phosphorus shortage will be aggravated by soil erosion, *Nature Communication*, 11(1), p. 4546, <https://doi.org/10.1038/s41467-020-18326-7>
- Boulos L., Prevost M., Barbeau B., Coallier J., Desjardins R. (1999), LIVE/DEAD BacLight: application of a new rapid staining method for direct enumeration of viable and total bacteria in drinking water, *Journal of Microbiological Methods*, 37(1), pp. 77–86, [https://doi.org/10.1016/s0167-7012\(99\)00048-2](https://doi.org/10.1016/s0167-7012(99)00048-2)
- Cieślak B., Konieczka P. (2017), A review of phosphorus recovery methods at various steps of wastewater treatment and sewage sludge management, The concept of “no solid waste generation” and analytical methods, *Journal of Cleaner Production*, 142(4), pp. 1728–1740, <https://doi.org/10.1016/j.jclepro.2016.11.116>
- Cordell D., Drangert, J. O., White S. (2009), The story of phosphorus: global food security and food for thought, *Global Environmental Change*, 19(2), pp. 292–305, <https://doi.org/10.1016/j.gloenvcha.2008.10.009>
- Gilbert N. (2009), Environment: The disappearing nutrient, *Nature*, 461(7265), pp. 716–718, <https://doi.org/10.1038/461716a>
- Günther S., Grunert M., Müller S. (2018), Overview of recent advances in phosphorus recovery for fertilizer production, *Engineering in Life Science*, 8(7), pp. 434–439, <https://doi.org/10.1002/elsc.201700171>
- Ivanov V., Stabnikov V., Zhuang W.Q., Tay J.H., Tay S.T.L. (2005), Phosphate removal from return liquor of municipal wastewater treatment plant using iron-reducing bacteria, *Journal of Applied Microbiology*, 98(5), pp.1152–1161, <https://doi.org/10.1111/j.1365-2672.2005.02567.x>
- Ivanov V., Kuang S. L., Stabnikov V., Guo C. H. (2009), The removal of phosphorus from reject water of municipal wastewater treatment plant using iron ore, *Journal of Chemical Technology and Biotechnology*, 84(1), pp. 78–82, <https://doi.org/10.1002/jctb.2009>
- Ivanov V., Stabnikov V., Guo C. H., Stabnikova O., Ahmed Z., Kim I. S., Shuy E. B. (2014), Wastewater engineering applications of BioIronTech process based on the biogeochemical cycle of iron bioreduction and (bio)oxidation, *AIMS Environmental Journal*, 1(2), pp. 53–66, <https://doi.org/10.3934/environsci.2014.2.53>
- Korniienko I., Kuznietsova O., Kuskova V., Gulyaev V., Anatskyi A., Korniienko Yu. (2023), Biotransformation of vegetable waste using modern em-technologies: European experience and Ukrainian realities, *Selected papers of IV International Conference on European Dimensions of Sustainable Development, October 20–21, 2022, Kyiv, NUFT, Kyiv*.
- Pitman A.R. (1999), Management of biological nutrient removal plant sludges – Change the Paradigms? *Water Research*, 33(5), pp. 1141–1146, [https://doi.org/10.1016/S0043-1354\(98\)00316-9](https://doi.org/10.1016/S0043-1354(98)00316-9)
- Roman I.S. (1990), Handbook of fertilizer and plant protection in collective gardens and household plots, Kyiv, Harvest.
- Sokolska T., Lobachova S., Osypenko B. (2023), Ukraine agricultural policy adaptation to the natural environment challenges, *Selected papers of IV International Conference on European Dimensions of Sustainable Development, October 20–21, 2022, Kyiv, NUFT, Kyiv*.
- Stabnikov V.P., Tay S.T.L., Tay J.H., Ivanov V.N. (2004), Effect of iron hydroxide on phosphate removal during anaerobic digestion of activated sludge, *Applied*

- Biochemistry and Microbiology*, 40(4), pp. 376–380,  
<https://doi.org/10.1023/B:ABIM.0000033914.52026.e5>
- Stabnikova O., Stabnikov V., Krasinko V., Ahmed Z. (2023). Microbial reduction and oxidation of iron for wastewater treatment. In O. Stabnikova, O. Shevchenko, V. Stabnikov, O. Paredes-López (Eds.) *Bioconversion of Waste to Value-Added Products*, (pp. 169-189), CRC Press, Boca Raton, <https://doi.org/10.1201/9781003329671-6>
- Sunner N. (2017), Meeting the new low phosphorus standards, *Water and sewerage*, May 31, 2017, <http://www.waterjournal.co.uk/features/processes/meeting-the-new-low-phosphorus-standards>
- Tay J.H., Tay S.T.L., Ivanov V., Stabnikova O., Wang J.Y. (2008), US Patent 7 393452, Compositions and methods for the treatment of wastewater and other waste, Publication date: 07.01.2008, Filing date: 04.11.2003, International Classes: C02F3/30; C02F3/34.
- US EPA. (1986), Quality criteria for water, Washington, DC, US Environmental Protection Agency, Report 440/5-86-001.
- US EPA. (1999), United States Environmental Protection Agency, 1999, Part 503, Standards for the use or disposal of sewage sludge as amended, <https://www.govinfo.gov/content/pkg/CFR-2011-title40-vol30/pdf/CFR-2011-title40-vol30-part503.pdf>
- Van Loosdrecht M.C.M., Salem S. (2006), Biological treatment of sludge digester liquids, *Water Science and Technology*, 53(12), pp. 11–20, <https://doi.org/10.2166/wst.2006.401>

## Employment status of Hungarian food delivery workers in the post pandemic era

Ali Ilhan, Frank Füredi

*Szechenyi Istvan University, Budapest, Hungary*

---

### Abstract

#### Keywords:

Employment  
status  
Food  
Delivery  
Worker  
Flexibility  
Hungary  
Sharing  
economy

**Introduction.** The Covid pandemic had a great impact on the sharing economy. As a result, food delivery platforms continue to flourish. Today, several challenges recently appeared, and this research explores the ambiguous employment status of food delivery workers in Hungary. They are uncertain as to whether they are employees or independent contractors.

**Materials and methods.** This research provided use of techniques including "word frequency inquiry" and "exploration diagrams," which are supported by the NVivo qualitative research software. Through interviews and participant observation this paper attempts to illuminate how food delivery workers perceive their employment status and the information is gathered directly from them.

**Results and discussion.** This study attempted to determine how Hungarian food delivery workers felt about their status as independent contractors or employees. The data revealed that the majority of food delivery employees work full-time, but a large proportion of them do not view it as a long-term source of income due to concerns about their health and working conditions. Also, despite being referred to as "independent contractors," many of them claimed to be "employees," indicating that they were skeptical and confused about their employment status. Food delivery employees struggle in the sharing economy because they do not receive assistance from organizations such as labor unions. Based on these results, it appears that there is a need for more clarity and norms regarding the classification of individuals in the sharing economy. When it is unclear whether an individual is an independent contractor or an employee, they can be exploited, particularly if they have no other employment options. Also, the incapacity of organizations such as labor unions demonstrates the importance of finding alternative means to defend and support food delivery workers. This study helps us understand the issues that food delivery workers in the sharing economy face, particularly with regard to their employment and the absence of institutional support. The results demonstrate that policymakers must address these issues by implementing the appropriate rules and support systems to safeguard and assist workers in the sharing economy.

**Conclusions.** Our research indicates that the attitudes of the food delivery workers are influenced by the trade-off between the flexibility of working conditions and the lack of employee benefits.

---

#### Article history:

Received  
12.12.2022  
Received in  
revised form  
15.03.2023  
Accepted  
31.03.2023

---

#### Corresponding author:

Ali Ilhan  
E-mail:  
alihilhan00@  
gmail.com

---

#### DOI:

10.24263/2304-  
974X-2023-12-1-  
11

## **Introduction**

The sharing economy is gradually growing, and we cannot neglect the increasing number of food delivery workers, especially during the pandemic. However, there are critical challenges for these workers (Vinod and Sharma, 2021). The current situation has brought to light the challenges delivery workers face, such as employment contracts and employment benefits, especially before and after the COVID-19 pandemic.

As Barton (2001) highlights that gig workers in the sharing economy face identity problems of whether they are independent contractors or employees. There might be several reasons behind this uncertainty, where flexibility and benefits are the main drivers.

The flexibility arises when workers indicate the advantage of being able to choose where and when to work. By doing so, they are able to control and modify their earnings based on their working hours. Food delivery workers have the opportunity of deciding working hours by enabling their phones to show an online or offline status. This situation indicates flexibility.

Lin et al. (2020) highlights the importance of the flexibility that the just-in-time workforce has become, much more valuable than before in the sharing economy. The platforms provide flexibility for many people who choose the starting time and duration of work. It is an essential component for food delivery workers and their working conditions. Rosso et al. (2010) also highlights the relation between the work and its value to workers, and this dimension is necessary, especially for workers in the sharing economy.

The food delivery workers' employment status varies from country to country depending on its regulations. Some nations identify them as independent contractors, whereas other countries accept them as employees.

During the pandemic, food delivery workers face many difficulties. Moreover, essential needs, such as holiday pay and sick leave, became more important among the workers. Governments also aim to leverage these difficulties among workers, and the employment status of workers play a crucial role in receiving governmental assistance during this pandemic. Moreover, Schwab and Malleret (2020) also expresses that many workers in the sharing economy face difficulties in obtaining government assistance during the pandemic. Their employment contract status plays a crucial role. Food delivery workers are part of the sharing economy that faces the same difficulties in receiving financial help during the pandemic.

This research aims to explore the employment status of food delivery workers in Hungary from the perspective of these workers. This study focuses on the uncertainty of employment contracts and employment benefits that arises, especially during the pandemic.

People use social media platforms to gather and categorize a diverse array of user perspectives and opinions. The primary objective is to highlight the different viewpoints and perspectives of food delivery workers, as well as answer specific queries.

For the purpose of gaining a deeper and more detailed comprehension, in-depth interviews are used to obtain complete responses to a wide range of queries.

## **Materials and methods**

### **Materials**

Through the implementation of a rigorous research methodology that integrates comprehensive in-depth interviews, open-ended inquiries on various social media platforms, and specialized software, we are able to collect an extensive and precise array of

interpretations from individuals who engage in food delivery workers. In order to effectively manage and evaluate the large quantity of data obtained from open-ended inquiries on social media platforms, it is necessary to initially classify the majority of short responses into distinct categories. Subsequently, qualitative research methods are employed to carry out comprehensive interviews, which facilitates deeper understanding of the experiences and perspectives of these workers. Eventually, specialized software tools, such as "Nvivo," are employed to facilitate word frequency inquiries and exploration diagrams. These tools allow for the identification and analysis of patterns that arise from the data. By adopting a comprehensive approach, we have been able to generate detailed and elaborate insights into the experiences of gig workers among the food delivery workers. This has enabled us to contribute to a greater understanding of this rapidly expanding sector within the gig economy.

## **Methodology**

This paper reviews the available sources regarding the food delivery workers in Hungary as part of the sharing economy. The main aim is to reinterpret a certain number of articles from various sources. For this reason, employment contract status and employment benefits are widely discussed to analyze the perspective of the food delivery workers in the sharing economy.

The research is based on a qualitative method, and it is not limited to only particular sources, such as published articles, specialized authors, professors, or companies. Instead, the scope of the paper includes participants' responses and public interpretations to achieve the entire content beyond the disciplines. An eclectic approach is taken by combining different disciplines and research methods.

NVivo software, which specializes in exploring qualitative data in research-based investigations, is also used in this research. The two methods are "word frequency inquiry" and "explore diagrams," respectively. These methods assist in efficiently merging the interview materials and analyzing them in specificity (QSR International Pty Ltd. 2020). Graphs were created using the qualitative data-specific software Nvivo, and its data reflects a "word frequency query and exploration diagrams." The most highlighted terms are the most prevalent coping expressions from interviews.

The research includes in-depth interviews with local food delivery people in Hungary. The in-depth interviews were taken by people who work in the food delivery sector of the sharing economy in Hungary. There are both full-time and part-time food delivery workers among participants. The age range of the participants is between 25-40, and the length of work experience is from one month to over two years. Males predominate, and almost half of the workers are not Hungarian citizens. Moreover, specific questions are asked on social media platforms to gather information from the food delivery worker community, specifically from the Facebook group Futárok – Wolt – Netpincér. This group includes most of the delivery sector workers in Budapest comprised of 10.2K members (Banyai et al., 2014). The closed-ended questions are posted with specific time cycles to collect most of the answers. The first question aims to understand whether participants provide food delivery services as part-time or full-time. Almost 150 pieces of feedback were collected. After having the results, the following question is asked to understand participants' expectations for their long-term activities. The question is aimed to observe whether participants undertook their current activity as long-term or not related to the previous question. Almost 250 pieces of feedback were collected. Additionally, 13 personal comments that respond to the questions are included as part of the survey discussion. The first and second questions referred to the

current and desired length of working cycles based on participant preferences. The third and last questions refer to whether the participant is aware of their working status and the implications of said status, such as employment conditions and benefits. Therefore, the third question asks to understand whether participants count themselves as independent contractor or employees. The third question aimed to observe whether food delivery workers recognize themselves as independent contractor or employee. The answers are collected from over 100 pieces of feedback.

In the following part, personal comments in response to the questions are shared. These comments are not directly relevant to the questions, and therefore, they are partly shared in this section.

The participant observation is also part of the research, and results are shared based on participant observation experience. The main concern of participant observation is understanding how other workers perceive their employment status in this field. As part of the participant observation, this study includes personal experiences working in the delivery sector for a limited time and observing working conditions. Observations were made through discussions with other food delivery workers as much as possible while working with them. The food delivery workers' feelings and interpretations in the working field played important roles, especially in terms of their employment status according to their perspectives.

The database includes mainly Google Scholar, Scopus, and Science-Direct platforms. Gale and Ebsco sources are included for further literature review, and literature sources only began to emerge in the last 2–5 years.

## **Results and discussion**

### **Employment contract status**

This study exposes how food delivery workers in the sharing economy are unaware of their employment rights and benefits, especially during the pandemic. In other words, there is a lack of clarity regarding their employment status. The people who were interviewed appear to be uncertain about their work status. They are confused about where they stand in relation to the labour market and their position of uncertainty. In this chapter, readers will obtain information about the employment contract statuses and different approaches of food delivery workers.

#### ***Distinguish between two categories***

In order to better explain employment contract status, it is crucial to interpret the main difference between independent contractor and employee. There are both similarities and differences between these two categories. The employee is assigned to work under an employer/manager for any business environment, and the independent contractor may also work under an employer/manager. However, the employment benefits are not the same for both categories. For instance, an employee is supported with the primary benefits governed by employment laws, such as holiday pay and sick leave. On the other hand, the independent contractor is not afforded the same benefits due to their employment contract status. Independent contractors do, however, possess greater flexibility in their jobs, such as the ability to choose their working hours (Thelen, 2018).

It is crucial to remember that independent contractors should be valued the same as any administrators or business owners in the sharing economy. Ravenelle (2017) highlights "*the ethos of being your own boss and setting your own hours*" for the players in the sharing economy. In other words, even though food delivery workers are identified as independent contractors, they do not receive the same flexibility compared to any "manager/boss" in the traditional economy. Moreover, food delivery workers receive less employment benefits due to their contract status. In other words, food delivery workers are classified as independent contractors and therefore are not given the same employment benefits as employees.

Additionally, sharing economy is an emerging concept, and therefore, the relationship between independent contractors or employees with ongoing business fields is newly created. The adaptation of new concepts into existing platforms, such as the food delivery business, creates uncertainty.

### **Approaches towards the uncertainty**

In order to leverage this uncertainty between the independent contractor and employee, Rogers (2016) highlights the need for a minimum wage for most workers in the sharing economy. It should be feasible for companies to provide these essential employment conditions, such as minimum wage and specific employee benefits. In order to set a minimum wage, the government must be involved. Exposing the issues for workers of the sharing economy will thus help to improve the political economy accordingly. In the long run, innovative policies will be essential and sufficient for the growth of the sharing economy.

Furthermore, food delivery workers in the sharing economy are identified as independent contractors. Their status allows them to decide where and when to work due to the sharing economy concept. Therefore, this opportunity provides them with essential flexibility. On the other hand, workers may not decide the price mechanism and do not have bargaining power during contract procedures. Food delivery workers are only obligated to confirm the employment contract online without any discussion opportunities. In this case, the question appears whether or not food delivery workers have value as independent contractors. The food delivery workers are excluded from particular benefits, such as sick leave and holiday pay.

Despite these uncertainties, Inman (2021) highlights the essential development by referencing Uber Technologies, Inc. (Uber). Uber Eats, a subsidiary of Uber, guaranteed that 70,000 food delivery workers are classified as employees by having a minimum hourly wage and holiday pay aligned with the superior court. This is a sign that the current issue is already deeply discussed in the UK.

Another article highlights the consensus view that existing laws are insufficient to support workers' rights in the sharing economy. Therefore, the classification of independent contractors has to be improved significantly for these participants. Indeed, workers' flexibility should be considered in employment status, as employment protection is essential to the digital economy's growth (Means and Seiner, 2015).

Adversely, the emerging economies and new concepts lead many businesses to benefit from existing laws. Many companies recognize the diminished employee responsibilities. In the sharing economy, employee classification as independent contractors allow business owners to take less responsibility. Moreover, this situation leads companies to shortcut their costs. For example, companies do not pay immense taxes or social benefits for sharing economy workers because these platforms classify them as independent contractors. However, as pandemics increase, social benefits become essential. Therefore, gig workers recognize their lack of rights to obtain these benefits.

On the other hand, Cunningham-Parmeter (2016) highlights that several American companies hire people by not employing them in the traditional sense. The growth of new economies critically underestimates labour standards. Sharing economy and traditional economy will differ, especially in terms of contract status, as long as platform economies hire workers as independent contractors. Moreover, this dilemma requires an urgent call for governments to review existing labour laws.

### **Concept of food delivery in Hungary**

In this chapter, the reader will obtain more profound information about food delivery workers in Hungary. The central part of the study is to overview the case of Hungary during the pandemic. In this part of the study, the focus is on how the food delivery sector plays a role in Hungary as part of the sharing economy.

Recently, the food delivery sector is increasingly in high demand. Lin et al. (2020) also indicate that the sharing economy is an emerging pattern that grows in various sectors. Primarily, the food delivery sector in the sharing economy plays an essential role during the pandemic.

The food delivery sector plays an essential role in Hungary. There are three leading brands: Wolt, Netpincer and Bolt. These three brands belong to the sharing economy, especially in the food delivery sector.

Technically, online platform applications are user interfaces where workers can communicate with restaurants. After registering on the application, users are required to sign an online contract that indicates a partnership with the company. In other words, the contract is prepared between food delivery workers and companies as a partnership agreement, which is partly different from the employment contract of an employee in the traditional economy. Additionally, users have to register to the tax system as a service provider owner.

### **In-depth Interview**

In this section, participant interpretations will be about the uncertainty between being/feeling like an independent contractor or employee depending on circumstances.

The term flexibility becomes a critical factor in identifying the employee status, especially after the pandemic and the growing food delivery sector in the sharing economy. Flexibility is an excellent option and one of the most attractive features for food delivery workers. Most of the participants highlight that they can decide where and when to work, and the duration of working hours based on their availability. Most of the interview participants emphasize flexibility. Interviewee #2 states that the given contract by food delivery companies provides flexibility to workers. According to Interviewee #3, flexibility is the most significant reason why he is eager to work full-time as a food delivery worker, as he feels more free in this line of work. Also, the literature reviewed shows that companies in the sharing economy offer workers freedom and flexibility to work wherever and whenever they prefer to work (Cano et al., 2021).

Moreover, participants often mention the independence of a personal income based on their efficiency. They indicate that they can estimate and arrange their pay, as they determine their own working hours. These are the main reasons why food delivery workers feel like independent contractors.

On the other hand, there are some circumstances where food delivery workers feel like employees than independent contractors. Interviewee #7 indicates that he has worked as a



The most common words are “*boss*” and “*employee*”, which they follow concerning working durations and their payments. The most notable connection between this chart and our foundational findings is the dilemma faced by Hungarian workers, who feel either as employers (bosses) or employees. In the following, Hungarian workers link this difficulty to their income and hours worked. In other words, food delivery workers compare their working hours and compensation to their employment status.

### Exploring Diagrams

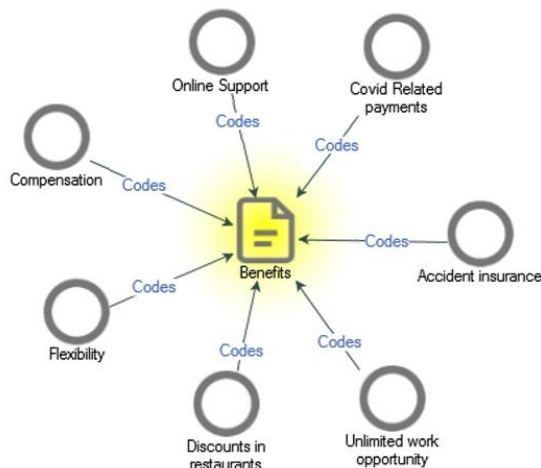


**Figure 2. The benefits of being delivery workers**  
 Source: NVivo (released in December 2022)

The graph mainly illustrates responses about the advantages the food delivery sector offers. “*flexibility*” and “*unlimited work opportunity*” is related to the primary of the study, which demonstrates why food delivery workers feel conflicted between the roles of employee and employer. In addition, the “*accident insurance*” and “*compensation options*” (i.e. Covid-related payments) were significant advantages.

This graph depicts the Hungarian delivery workers’ anticipation of obtaining the future. The highlighted areas focus mostly on aspects of representation, where employees perceive a lack of support for being represented by unions or even countries. In addition, some of the responses indicate that in the future, delivery positions may be considered as a temporary occupation in order to “*save money for difficult situation*”, such as economic or career-related ones. Some of the replies also highlight the unclarity between employee and employer because a couple of the results demonstrate represented responses “*paid holiday*” and “*voucher*”, which are mainly applied to employees.

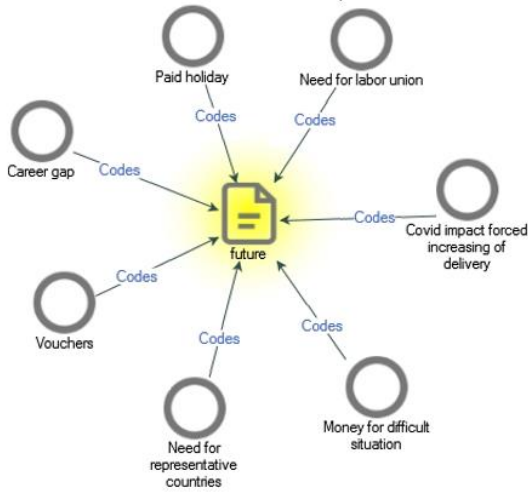


**Figure 3: The future expectation of being delivery workers**  
Source: NVivo (released in December 2022)

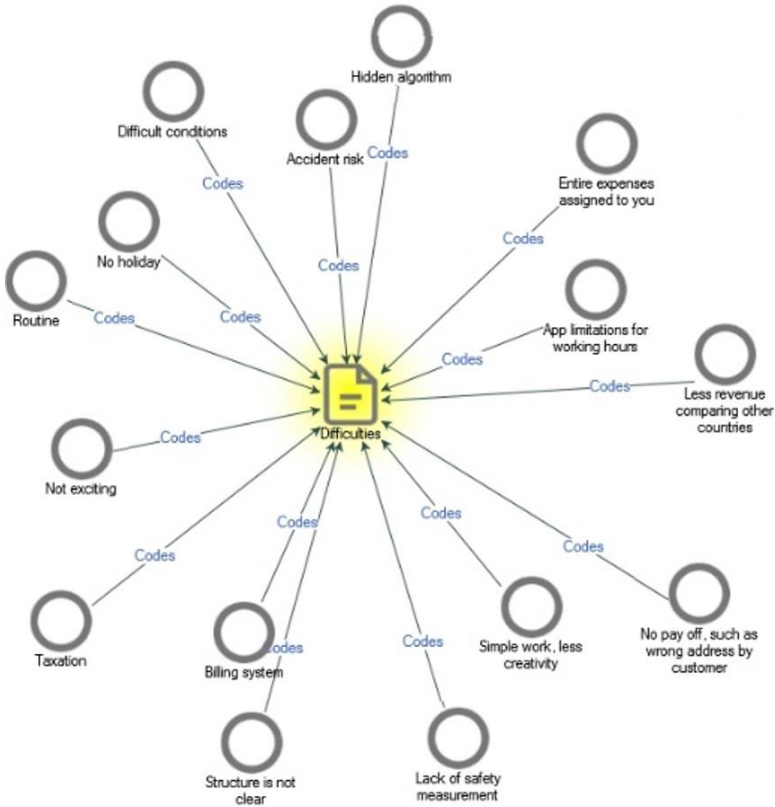


**Figure 4. The difficulties delivery workers**  
Source: NVivo (released in December 2022)

In this graph, many issues are presented, with an emphasis on accounting-related topics such as “*billing system*” and “*taxation.*” In addition, app-related difficulties are highlighted due to the complexity and uncertainty of the algorithm and limited usage entries, such as “*app limitation for working hours*”. The complexity arrives due to some responses on whether employees are supposed to work based on given responses, such as without “*app limitations for working hours*” or “*entire expenses assigned to you*”.

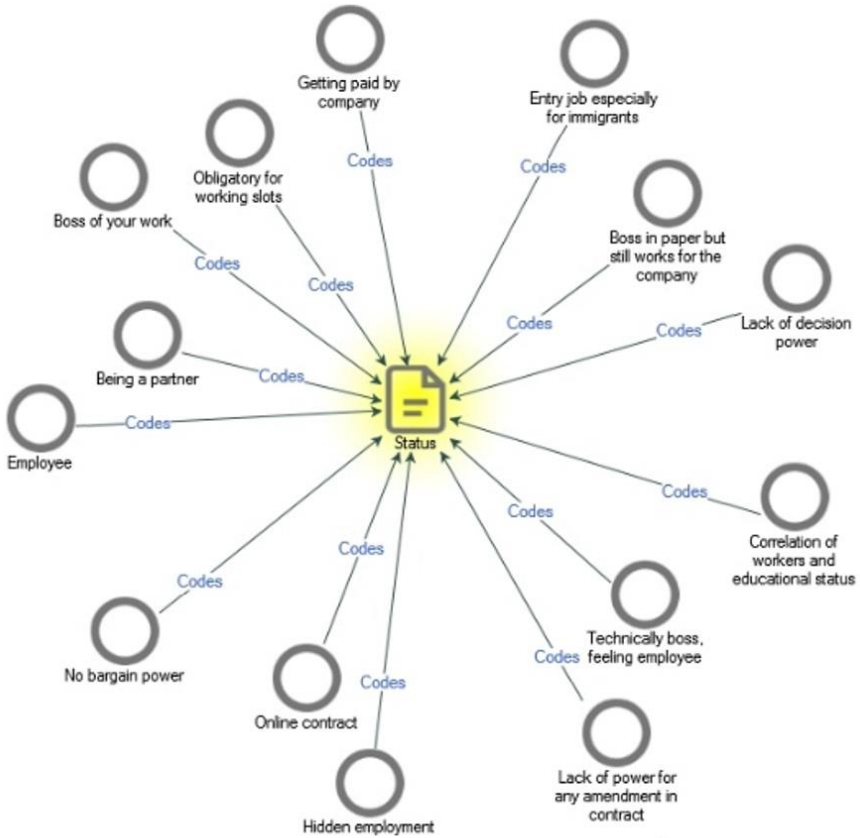


**Figure 5. The status delivery workers**

Source: NVivo (released in December 2022)

This graph depicts the current status of delivery employees, with being a boss, employer, or feeling like an employee as the most attractive result. Being an employer is supported by responses such as “*being a partner*” and “*being the boss of your job,*” but being an employee is indicated by responses such as “*being paid by a firm*” and “*being the boss on paper but still working for the company.*” In addition, there is uncertainty that can be

explained by responses such as "hidden employment," "no bargaining power," and "lack of power."

### Food delivery workers' perspective on the social media

This section will include the interpretation of answers given by participants through social media. Four questions were asked to food delivery workers located in Hungary.

The questions were posted in a specific Facebook group that includes most food delivery workers from the sharing economy located in Hungary. Participants were able to answer closed-ended questions as well as share their own comments below the questions.

#### Question 1

According to the results:

Q1: Are you doing this job part-time or full-time?

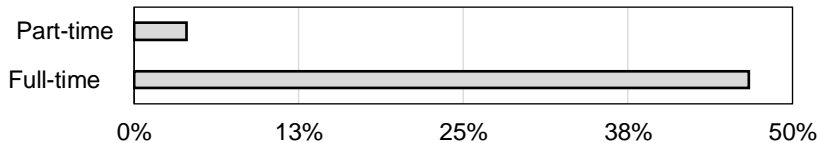


Figure 6. Comparison data by poll results

Source: own data

- 47% of the participants claim full-time activity;
- 4% of the participants claim part-time activity.

The result shows that many participants take on food delivery services as a full-time opportunity. According to the result, we can assume that most of the people do not have other jobs and do not work as food delivery workers as an additional job but rather choose to be full-time delivery workers.

#### Question 2

According to the results:

Q2: Do you see this job as long-term gainful activity?

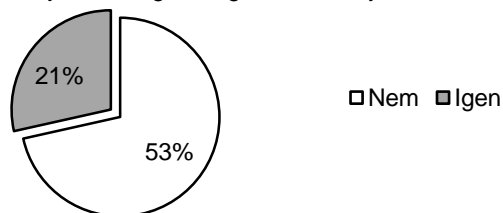


Figure 7. Comparison data by poll results

Source: own data

- 53% of the participants claim that they do not see this job as a long-term gainful activity;
- 21% of the participants claim that they see this job as a long term gainful activity

The result shows that a high portion of the answers belongs to negative intention. According to the results, we may assume that food delivery workers do not anticipate working for a more extended period in the future in the delivery sector. Therefore, a dilemma appears where participants primarily work full-time; however, they are also not willing to prolong it in the future.

Additionally, there are personal comments under the questions where users share their opinions about not seeing this job as a long-term gainful activity. Participants highlight that working conditions and health issues are the vital causes behind this negative intention.

### Question 3

According to the results:

Q3: Do you regard yourself as an independent contractor or employee?

employee  individual entrepreneur



**Figure 8. Comparison data by poll results**

Source: *own data*

- 44% of the total result indicates that people identify themselves as an employee
- 32% of the total result indicates that people identify as an independent contractor

The result shows that most of the independent contractor food delivery workers recognize themselves as employees despite being independent contractors.

### Personal Comments of Questions

Personal comments to the second question provide assumptions that food delivery cannot be a long-term activity. Participants highlight that working conditions and health issues are the vital causes behind this negative intention.

The poll results provide the two central answers as yes and no to the last question. However, participants created their comments, and two of the comments are highlighted among other comments.

According to the personal comments:

- 61% indicate that they are employees
- 28% indicate that they are immigrants with no specific information about their employment rights

It is possible that food delivery workers may misunderstand the questions. Though the question asks about their employee benefits and rights, most of the commenters respond, “We are an employee.” The comment shows that 61% of participants perceive that any

benefits or rights are not within their scope unless they are employees. Moreover, the rest of the comments belong to foreigners, as they indicated in the comments that they are immigrants. They claim that foreigners, referred as immigrants, are not aware of their benefits due to their residential status.

Additionally, the word immigrant used in the comments might refer to expatriate or foreigner as well. Therefore, this study includes this comment under foreigner.

Results show that food delivery workers in Hungary prefer to work in the sharing economy as full-time workers instead of being idle. However, they are also unwilling to invest in this field for a more extended period. Moreover, food delivery workers assume that employment benefits or rights are only available when working as an employee. Employment benefits and rights are crucial factors in determining whether food delivery workers identify themselves as independent contractors or employees.

What is more, food delivery workers in the sharing economy recognize themselves more as employees than as independent contractors as demonstrated by the collected answers. Food delivery companies in the sharing economy implemented the idea of being the owner of your business. In other words, they are supposed to be called independent contractors in the sharing economy. As proof, a food delivery worker must sign a partnership employment contract with companies under the title of service provider. This is not the same contract where a single worker signs a bilateral employment contract with a company in the traditional economy. Consequently, the dilemma arises whether food delivery workers are employees or individual entrepreneurs as part of the sharing economy.

### **Participant observation**

The aggregate feedback from the participant observation exposes that having incremental earnings and facing difficulties during a pandemic may be the main reasons for being a full-time independent contractor of food delivery in the sharing economy. Most of the workers find this field as an opportunity for incremental earnings, and they highlight that the more they work, the higher their earnings become. Most of the participants also indicate that the pandemic is a strong factor why many people turn to the food delivery sector after facing many difficulties in other business fields.

Besides, food delivery sectors in the sharing economy provide flexibility for where and when to work. The employment contract, which is called a partnership agreement as a service provider, also supports their identity as an independent contractor. However, food delivery workers highlight that they also feel like employees based on current working conditions, such as bargaining power, application restrictions, and revenue cycles, widely discussed in the in-depth interviews section.

### **Limitation of the study**

There were a couple of essential difficulties that impacted our study. This study aimed to review the sharing economy in Hungary. Therefore, a language barrier existed, especially with comments made in different languages in response to the questions.

Also, the posting pool questions are deleted more than twice on the social platform. The social platform for given poll questions was managed by an administrator and four moderators. Since communication issues exist between moderators and managers of the group's page, the given questions were suddenly removed even though they had prior approval from the administrator, which impacted our study negatively.

This study aimed to collect an aggregate number of participants during interviews and questions. However, social platform owners were unwilling to assist in this study. There was

hesitation among moderators about whether these activities on their platforms played an essential role or not while this study aimed to get in touch with Hungarian food delivery workers directly through these social platforms.

### **Questions for future**

The study exposes that most participants are dissatisfied with health conditions during work, and they also highlight avoiding working in the same sector for longer periods. Another research may delve into exposing the underlying reasons.

In the poll question answers, some of the participants indicated that they are foreigners and do not have any idea about their employment rights. Further research can be helpful in understanding how foreigners identify themselves in terms of their employment benefits and rights.

This study is limited in scope, as the research only addresses the local citizens and foreigners working in Hungary. Alongside this research, however, there were some discussions with a couple of delivery sector workers in Sweden and Gotland, Iceland, and these workers indicate that Swedish food delivery workers are the minority of total food delivery workers based on a short analysis. Therefore, this point may need further investigation in the future.

### **Conclusion**

This paper exposes how the pandemic situation creates remarkable changes in the sharing economy. This study mainly focused on food delivery workers in the sharing economy and significant changes in employment contract status and benefits during the COVID-19 pandemic.

This study discloses that ambiguity is a significant factor, where uncertainty exists between being an independent contractor or an employee. As explained before, it is an interesting phenomenon, as there seems to be no concern regarding employment status until the pandemic occurs. However, this uncertainty is not the primary concern for food delivery workers in the sharing economy in the case of Hungary. The participants do not seem particularly concerned about this ambiguity but are more focused on the working conditions and standards. As an illustration, Barton (2001) emphasizes the issue of identity, whereas Thelen (2018) explains that the right to choose working hours is an indicator of identity. To support the idea, Ravenelle. (2017) highlights "the ethos of being your own boss and setting your own hours" Rogers (2016), however, emphasizes the minimum wage's crucial function in this regard.

Finally, the study shows that food delivery workers started to be concerned about their employee benefits and rights after the pandemic. Rosso et al. (2010) describes the relationship between the value of work, whereas Lin et al. (2020) emphasizes flexibility. It shows that employment contract status is not the main challenge for workers unless critical times arise, such as a pandemic. For instance, food delivery workers face difficulty regarding their social benefits since their employment status involves barriers compared to traditional workers. The lack of support from institutions or agencies, such as labor unions, for food delivery workers in the sharing economy, as mentioned by Interviewee #6, highlights the need for further advocacy and regulation in this sector. Impact of the pandemic made these people much more aware or interested in their labour market status.

## References

- Angrist J.D., Caldwell S., Hall J. V. (2017), *Uber vs taxi: A driver's eye view* (No. w23891), National Bureau of Economic Research.
- Banyai, D., Emese H., Miklos T. (2014), Futárok – Wolt – Foodpanda, Available at: <https://www.facebook.com/groups/213840165488998>
- Barton L.H. (2001), Reconciling the independent contractor versus employee dilemma: a discussion of current developments as they relate to employee benefit plans, *Capital University Law Review*, 29, 1079.
- Cano M.R., Espelt R., Morell M.F. (2021), Flexibility and freedom for whom? Precarity, freedom and flexibility in on-demand food delivery, *Work Organisation, Labour & Globalisation*, 15(1), pp. 46-68, <https://doi.org/10.13169/workorgalaboglob.15.1.0046>
- Cunningham-Parmeter K. (2016), From Amazon to Uber: Defining employment in the modern economy, *BUL Rev.*, 96, 1673.
- Davidov, G. (2016), The status of Uber workers: A purposive approach, *Forthcoming Hebrew University of Jerusalem Legal Research*, 17-7.
- Federal Register (2021), Temporary Rules to Include Certain "Platform Workers" in Compensatory Offerings Under Rule 701 and Form S-8., *Securities and Exchange Commission*, Available at: <https://www.federalregister.gov/documents/2020/12/11/2020-26374/temporary-rules-to-include-certain-platform-workers-in-compensatory-offerings-under-rule-701-and>
- Inman P. (2021), After Uber's U-turn, ministers must stop giving gig economy bosses an easy ride., *The Guardian*, Available at: <https://www.theguardian.com/business/2021/mar/21/after-uber-u-turn-ministers-must-stop-giving-gig-economy-bosses-an-easy-ride>
- Kenney M., Zysman J. (2016), The rise of the platform economy, *Issues in Science and Technology*, 32(3), 61.
- Larkin P. (2020), Relationship between Employment Status and Scope of Social Security Protection: The United Kingdom Example, In: *Social Law 4.0*, pp. 117–146), Nomos Verlagsgesellschaft mbH & Co. KG.
- Lin P.M.C., Au W.C., Leung V.T.Y., Peng K.-L. (2020), *Exploring the meaning of work within the sharing economy: A case of food-delivery workers*. *International Journal of Hospitality Management*, 91, 102686, <https://doi.org/10.1016/j.ijhm.2020.102686>
- Meaker M. (2021), The Gig Economy's Days in Europe Are Numbered., *Wired UK*. Available at: [https://www.wired.co.uk/article/gig-economy-european-commission-law?utm\\_source=newsletter&utm\\_medium=email&utm\\_campaign=08%2F12%2F2021](https://www.wired.co.uk/article/gig-economy-european-commission-law?utm_source=newsletter&utm_medium=email&utm_campaign=08%2F12%2F2021)
- Means B., Seiner J. A. (2015), Navigating the Uber economy, *University of California, Davis, Law Review*, 49, 1511.
- QSR International Pty Ltd. (2020), *NVivo* (released in March 2020), Available at: <https://www.qsrinternational.com/nvivo-qualitative-data-analysis-software/home>
- Ravenelle A. J. (2017), Sharing economy workers: selling, not sharing, *Cambridge Journal of Regions, Economy and Society*, 10(2), pp. 281–295, DOI:10.1093/cjres/rsw043
- Rogers B. (2016), Employment rights in the platform economy: Getting back to basics, *Harvard Law & Policy Review*, 10, 479.
- Rosso B.D., Dekas, K.H., Wrzesniewski A. (2010), On the meaning of work: a theoretical integration and review, *Research in Organizational Behavior.*, 30, pp. 91–127.
- Sahinyilmaz T. (2021), Gig Workers I: Gig Economy Employment Issues – Employment and HR, Available at: <https://www.mondaq.com/unitedstates/employee-rights-labour-relations/1047712/gig-workers-1-gig-economy-employment-issues>
- Schwab K., Malleret T. (2020), The Great Reset, *World Economic Forum*, Geneva.

- Thelen K.A. (2018), Regulating Uber: The politics of the platform economy in Europe and the United States, *Perspectives on Politics*, 16(4), pp. 938–953.
- Tooze, A. (2021), Talk of a global economic reset must not ignore grim realities., *Financial Times*, Available at: <https://www.ft.com/content/5834df03-d8d4-456a-b08f-fa2ee0203141>
- Vinod P.P., Sharma D. (2021), COVID-19 impact on the sharing economy post-pandemic, *Australasian Accounting, Business and Finance Journal*, 15(1), pp. 37-50, <https://doi.org/10.14453/AABFJ.V15I1.4>

# Historical and contemporary perspectives of the sugar industry in sub-Saharan Africa

Joshua Mabeta, Luboš Smutka

University of South Bohemia in České Budějovice, Czech Republic

---

## Abstract

### Keywords:

Sugar  
Sugarcane  
Sub-Saharan  
Africa,  
Yield  
Production

**Introduction.** This paper analyses the trends in sugar and sugarcane production in sub-Saharan Africa, including the core drivers of production by reviewing the current institutional and production arrangements.

**Materials and methods.** The analysis is based on 35 African countries categorized into 4 regions based on the United Nations M49 classification. A detailed literature review was conducted to explain the observed trends and to provide context for the various institutional and production arrangements. The literature reviewed key sugar-related documents at national level, websites of the core companies producing sugar in each country including their annual reports and previous empirical studies undertaken in the major sugarcane producing countries.

**Results and discussion.** The sugarcane industry in South Africa has grown significantly over the last 6 decades, with raw sugar production and sugarcane production increasing by 200 and 215%, respectively. In terms of regional production, the average growth rate for raw sugar production over the period 1961 to 2020 was 2, 3, 3, and 13% for Eastern, Middle, Southern and Western Africa regions, respectively. The Eastern and Southern Africa regions produce a major share of both sugar and sugarcane production accounting for 90 and 86% of total production. Yields have consistently remained low and only Eswatini, Malawi, Tanzania, South Africa, Uganda and Zambia have remained competitive and low cost producers in the region. Some countries like Kenya, Uganda, and Tanzania are not self-sufficient and have consistently been net importers of sugar. The countries in question have in the past imposed import restrictions particularly on import tariffs as a way of boosting domestic production.

Threats to steady supply of sugar and sugarcane, especially for countries that depend on rain fed agriculture, have continued to emanate from periodic droughts, particularly the major producing Eastern and Southern regions in the early 1990s. The institutional review revealed that the proportion of sugarcane production supplied by smallholder farmers under outgrower schemes compared to the nucleus estate dictates the stability of sugar production in Africa. Outgrowers dominate the production of sugarcane, as is the case in South Africa (92%) and Kenya (90%), which poses a high risk to the steady supply of sugarcane to the milling company involved in sugar production. This may arise because outgrowers may fail to honor their contracts and engage in opportunistic behavior to side-sell their sugarcane to other offtakers.

**Conclusion.** Key to resolving the low yields and threats to sustainable sugarcane production in sub-Saharan Africa will be addressing the institutional and production arrangements of sugarcane production, particularly addressing the issues surrounding outgrower schemes that are the major production models.

---

### Article history:

Received  
21.12.2022  
Received in  
revised form  
20.03.2023  
Accepted  
31.03.2023

---

### Corresponding author:

Luboš Smutka  
E-mail:  
smutka@pef.czu.cz

---

### DOI:

10.24263/2304-  
974X-2023-12-1-  
12

## **Introduction**

The sugar industry in sub-Saharan Africa is characterized by complexity and diversity with a vast spectrum of participants and stakeholders involved in its production, processing, and distribution. The sugar industry has key aspects that are distinct from those of other agricultural commodities in relation to production traits, trade structures, and related political economy issues (McDonald et al., 2004). The sugar industry is important to most sub-Saharan Africa countries not only in terms of its contribution to Gross Domestic Product but also in terms of its potential to create employment opportunities along the value chain and contributing to rural development (Hassan, 2008). A crucial product in the region, demand and production of sugar is driven by domestic consumption, export markets and international prices. Some of the best-run sugar enterprises have recently suffered greatly from persistently low sugar prices, particularly following the reforms in the European Union sugar industry (Chudasama, 2021). According to the International Sugar Organization (ISO, 2018), sub-Saharan Africa is the fourth-largest producer of sugar in the world, making up around 10% of total world and 5% of global sugarcane production (Macháček et al., 2017; Thibane et al., 2023).

The sub-Saharan Africa region holds a unique position. With below-average per capita consumption and above-average population growth, it has the biggest potential for sugar consumption increase of any region in the world (ISO, 2019). The continent boasts the lowest average per capita consumption of 17.42 kg, which is about 6 kg less than the global average, and a deficit of over 10 million tons (ISO, 2019). The production and consumption dynamics are likely to change given the rate of growth of population of sub-Saharan Africa (Smutka et al., 2011). On the production side, the sub-Saharan Africa region also has potential to increase its market share of sugar on the world market given its favorable climatic conditions, economies of scale, favorable government policies and availability of water and arable land (Hess et al., 2016; Macháček et al., 2017), and recent increase in investment flows in the sugar industry (Chudasama, 2021; Macháček et al., 2017).

The main feedstocks for sugar production are sugarcane and sugar beet with sugarcane alone accounting for about 80% of the total world production of sugar (Macháček et al., 2017; Rumánková Smutka, 2013; Smutka et al., 2011). In sub-Saharan Africa, sugarcane accounts for about 83% of total sugar production (Hinke et al., 2018).

Recent studies in sub-Saharan Africa have focused on production and its determinants (Jones and Singels, 2015; Macháček et al., 2017; Owiti, 2019; Smutka et al., 2011; Tena et al., 2016; Thibane et al., 2023), trade liberalization and export performance (Macháček et al., 2017; McDonald et al., 2004), market structure and competitiveness (Chisanga et al., 2014; Hinke et al., 2018) impact of European Union trade reforms on the African sugar industry (Goodison, 2007; Gotor and Tsigas, 2011; Paha et al., 2021; Richardson, 2009). Maltitz et al. (2019) analyzed institutional arrangements but the study was only focused on 4 southern African countries. While a number of studies have revealed salient features about sugar production in Africa, there is scanty evidence on the core drivers of production, especially the institutional and production arrangements for sugarcane production. Institutional and ramifications not only on the supply of throughput used to ultimately produce sugar but also on the output and price stability of national and international sugar markets. This paper contributes to the ongoing work on the growth of the sugar industry by providing an elaborate and holistic analysis of the sub-Saharan Africa sugar industry from a historical and contemporary perspective. The aim of this research is to review the key features of the sugar market in sub-Saharan Africa not only in terms of production but also in relation to other indicators such as area harvested, yields and institutional arrangements at regional and country level over a long time horizon.

## **Materials and methods**

### **Materials**

The analysis is based on 35 African countries in sub-Saharan Africa categorised into 4 regions based on the United Nations M49 classification widely used by the Food and Agricultural Organization. Data on production, area harvested, yield and raw sugar production by region and country were obtained from FAOSTAT website of the Food and Agricultural Organization. The sub-Saharan Africa geographic sub-region comprises Eastern Africa (22 countries), Middle Africa (9 countries), Southern Africa (5 countries) and Western Africa (17 countries) (UN, 2023). The sub-Saharan Africa countries that form part of this study on average account for 74% of total raw sugar production and 77% of total sugarcane production in Africa. Although Ethiopia, Reunion Island and South Sudan are sugarcane producers, the three countries are excluded in the analysis due to non-availability of data for the period 2015 to 2020.

### **Methods**

This study is descriptive in nature and provides a historical and current perspective of the development of the sugar industry for selected indicators over the past 6 decades (1961 to 2020), where data is available. The analysis is conducted at both country and regional level to highlight regional discrepancies and changes that have occurred in both raw sugar and sugarcane production over the entire analysis period. Some basic descriptive statistics such as means and percentages were used to describe the trends. A detailed literature review was conducted to explain the intuition behind the observed trends and to provide context for the various institutional and production arrangements. The literature reviewed key sugar-related documents at national level, websites of the core companies producing sugar in each country including their annual reports, previous studies undertaken in the major sugarcane producing countries.

## **Results and Discussion**

### **Trends in sugarcane and sugar production in sub-Saharan Africa**

Sugarcane and raw sugar production in sub-Saharan Africa follows similar patterns and trajectories (Figure 1A and 1B).

Between 1961 and 2020, raw sugar and sugarcane production increased by 200% and 215% respectively. Between the periods 1961 and 1970, 1971 and 1980, 1981 and 1990, 1991 and 2000, 2001 and 2010 and 2011 and 2020, raw sugar production increased by 53%, 10%, 4%, 14%, 6% and 8%, respectively. On the other hand, except for the period 1980 to 1990, when sugarcane production reduced by 0.4%, sugarcane production increased by 54%, 13%, 11%, 2%, and 12% for the same periods under review, respectively.

The underlying drivers for this growth are mainly increased local and international demand due to population growth and expansion of sugarcane production brought about by large inflows of foreign direct investment (Ngcobo and Jewitt, 2017). Advancement in technology, use of better production methods and improved cane crop varieties have also contributed to the general positive trend in sugarcane production during this period. It is also worth noting that the area harvested may have contributed to the increase in total sugarcane and raw sugar production. Between 1988 and 2020, the increase in the area harvested coincided with the increase in sugarcane production. Figure 2 shows the correlation between the area harvested and sugarcane production.

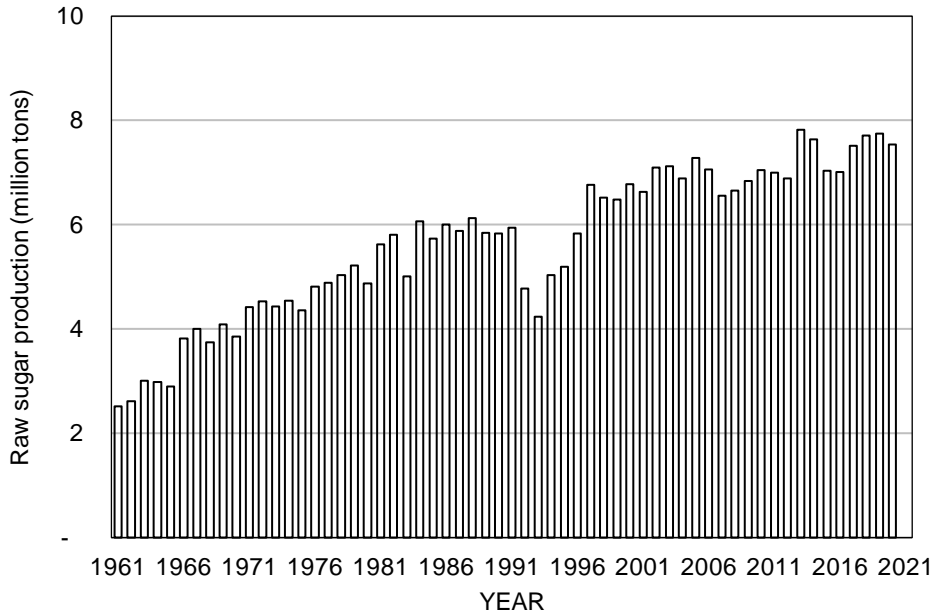


**Figure 1A. Raw sugar production in sub-Saharan Africa**

Source: FAOSTAT, 2023

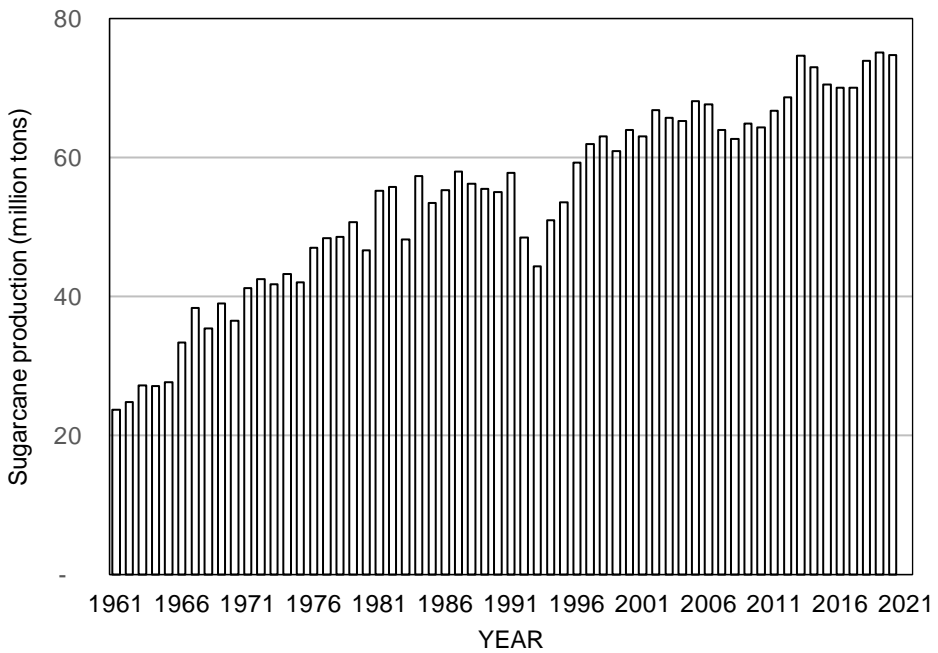


**Figure 1B. Sugarcane production in sub-Saharan Africa**

Source: FAOSTAT, 2023

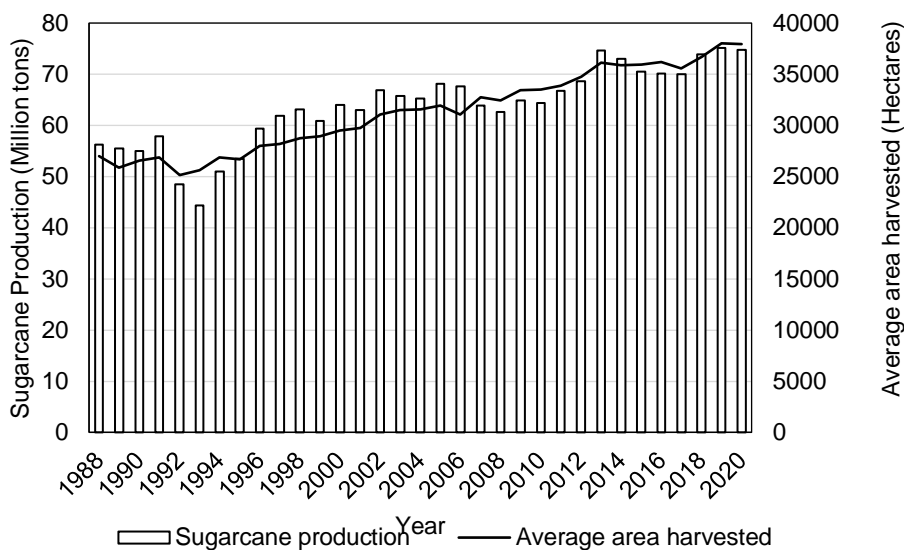


**Figure 1. Relationship between sugarcane production and area harvested**

Source: FAOSTAT, 2023

Despite the positive trajectory between 1961 and 2020, sugarcane production dipped in some years mainly due to droughts (Hess et al., 2016), especially for countries that depend on rain fed agriculture. Sub-Saharan Africa had in the past numerous severe and protracted droughts in northwest Africa (1999-2002), the Sahel (1970 and 1980), the Horn of Africa (2010–2011) and the southern and southeast Africa (2001–2003) (Masih et al., 2014).

### Sugar and sugarcane production by region

Raw sugar and sugarcane production among the regions in sub-Saharan Africa has alternated between periods of growth and decline. The fluctuations in raw sugar and sugarcane production are evident in the Eastern and Southern Africa regions, particularly during the 1991/1992 season due to prolonged drought spells (Sandrey and Vink, 2007). Overall, there has been an upward trend in the production of both commodities (Figure 3A and 3B). The average growth rate for raw sugar production over the period 1961 to 2020 was 2%, 3%, 3%, and 13% for Eastern, Middle, Southern and Western Africa regions, respectively. Sugarcane production, on the other hand, grew by 2%, 3%, 3% and 6% on average during the same period for the respective regions. The Eastern and Southern Africa regions dominate both sugarcane and raw sugar production. The former has recorded significant growth and overtaken the Southern Africa region in sugar raw sugar and sugarcane production, particularly between 2001 and 2020. The Eastern and Southern African regions contribute 90% and 86% to raw sugar and sugarcane production in sub-Saharan Africa.

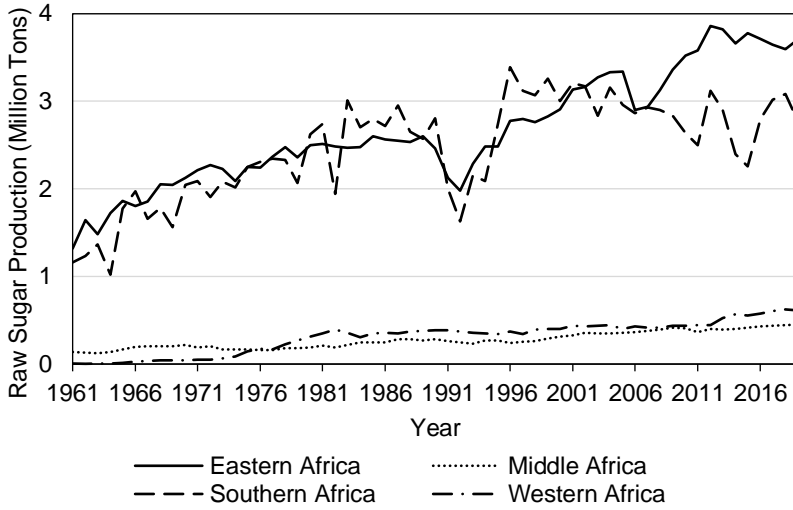


**Figure 2A. Trends in raw sugar production by region**  
Source: FAOSTAT, 2023

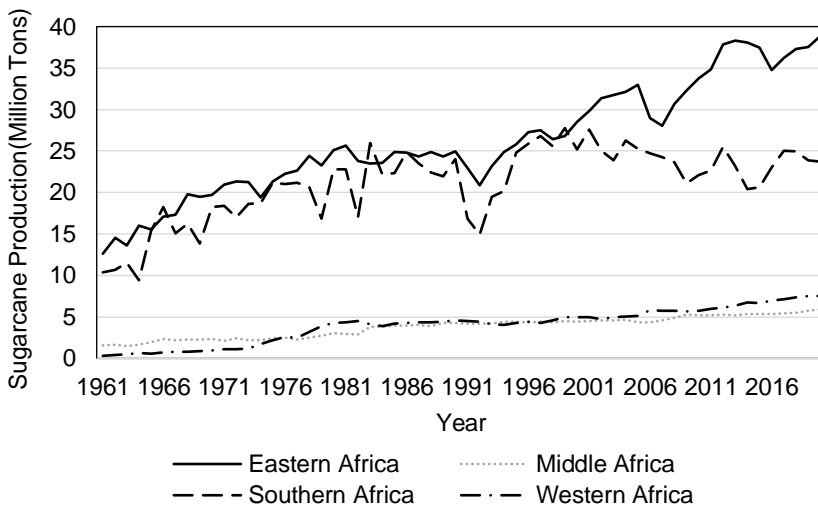


**Figure 3B. Trends in sugarcane production by region**  
Source: FAOSTAT, 2023

The average raw sugar production for Eastern, Middle, Southern and Western Africa regions was 2.64, 0.27, 2.44 and 0.31 million metric tons (MT), respectively. On the other hand, sugarcane production averaged 25.94 million MT, 3.73 million MT, 20.91 million MT and 3.94 million MT for the respective regions. Each ton of sugarcane harvested and processed is expected to produce 120 kg of sugar (FAO, 1984), translating into a conversion rate of 12%. A review of the production trends from a historical and contemporary perspective shows that all the four sub-Saharan Africa regions are not far off this target, with the Southern African region having the highest conversion rate close to 12% (Figure 4).

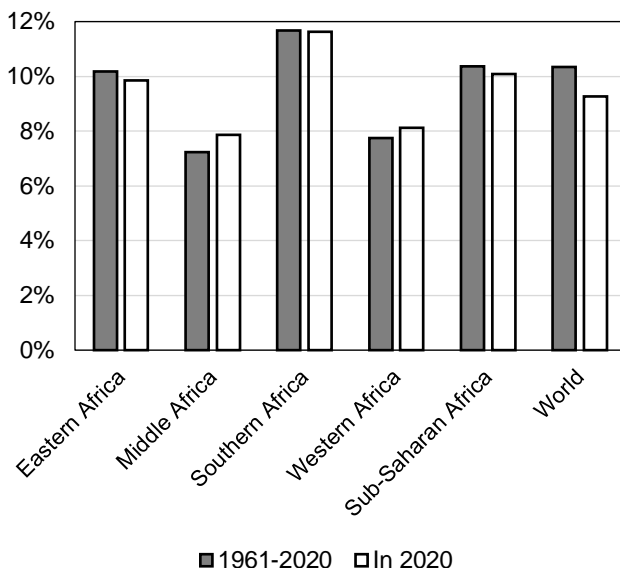


**Figure 4. Ratio of sugarcane harvested raw produced**

Source: FAOSTAT, 2023

However, this must be interpreted with caution as a low conversion rate below the target might not necessarily imply low levels of efficiency but could be due to the use of sugarcane to produce other competing products such as ethanol, biofertilizers or bagasse for electricity generation.

### Countries with high cane yields in Sub-Saharan Africa

The amount of cane harvested per hectare varies depending on several factors including the duration of the growing season, the type of crop, watering system used (FAO, 2023), climatic conditions, types of soil and human factors (Hassan, 2008). Under rainfed conditions, cane yields can vary substantially with good yields ranging from 70 to 100 tons per hectare of cane in the wet tropics while the dry tropics and subtropics can produce crops yields of 110 to 150 tons per hectare with irrigation (FAO, 2023). With this benchmark, it is clear that average yields for most sub-Saharan Africa countries are low. In all of these countries, average yields have either remained essentially stable or declined. Therefore, it is imperative to investigate the causes of such low yields if the sub-Saharan Africa region is to increase its sugar output share on the world market as expanding the area cultivated may prove to be unsustainable. From Table 1, only 12 sub-Saharan Africa countries have had good cane yields on average between 1988 and 2020, albeit some fluctuations, particularly for Zimbabwe, Tanzania and Mauritius. The average cane yields for the 12 countries have been in the recommended range of 70 to 100 tons per hectare.

**Table 1**

**Top 12 sub-Saharan Africa countries with high cane yields**

Country	Average Yield (hg/ha) (1988-2020)	Average Yield (hg/ha) in 2020	Variance
Senegal	1,130,827	1,147,597	16,770
Malawi	1,058,137	1,078,256	20,119
Zambia	1,036,815	1,035,811	1,004
Burkina Faso	998,233	1,020,816	22,583
Eswatini	980,008	969,331	10,677
Chad	963,092	1,043,764	80,672
Zimbabwe	883,324	753,994	129,330
Kenya	839,416	758,452	80,964
Tanzania	813,591	700,052	113,539
Mauritius	722,882	599,591	123,291
Mali	709,718	725,057	15,339
Burundi	706,977	690,109	16,868

Source: FAOSTAT, 2023

### **Main Sugar and Sugarcane Producers in sub-Saharan Africa in 2020**

In 2020, sub-Saharan Africa's share of total world sugarcane and raw sugar production was both 4%. The top 10 producers account for about 78 percent of total sugarcane and 81% of raw sugar production in sub-Saharan Africa. South Africa is the largest producer and has dominated the sugar industry over the years producing 2.1 million MT of sugar and 18 million MT of sugarcane in 2020 (Figure 5A and 5B). Apart from South Africa, none of the top 10 countries produce above 1 million MT of raw sugar and above 5 million MT of sugarcane (except for Eswatini, Kenya and Uganda that produce slightly above these thresholds). It is worth noting that despite being major producers, countries like Kenya, Uganda, and Tanzania are not self-sufficient and have consistently been net importers of sugar (Chisanga et al., 2014; Sandrey and Moobi, 2015). The countries in question have in the past imposed import restrictions particularly on tariffs as a way of boosting domestic production (Andae, 2018; Kalagho, 2014; Olingo, 2018). Among the major producers, only Eswatini, Malawi, Tanzania, South Africa, Uganda and Zambia are competitive due to their low cost of production (Gro Intelligence, 2015; Sandrey and Vink, 2007; SASA, 2023b), although somewhat this conclusion may be contentious due to various distortions that characterize the sugar industry. The European Union sugar reforms are likely to reduce demand for African sugar (Paha et al., 2021; Viljoen, 2014) although some African countries could still benefit from the European Union market under the African, Caribbean and Pacific Group of States (Viljoen, 2014) and other various Economic Partnership Agreements.

In this section, we review the various institutional and production arrangements that drive the observed trends in yields and production of raw sugar and sugarcane discussed in previous sections. To analyze the various institutional and production arrangements in sub-Saharan Africa, we collated recently published literature on sugarcane dynamics across some of the major sugar producing countries.

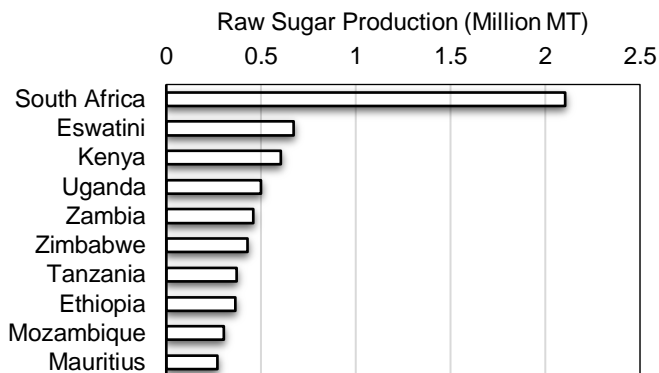


**Figure 5A. Main sugar producers in sub-Saharan Africa in 2020**  
Source: FAOSTAT, 2023

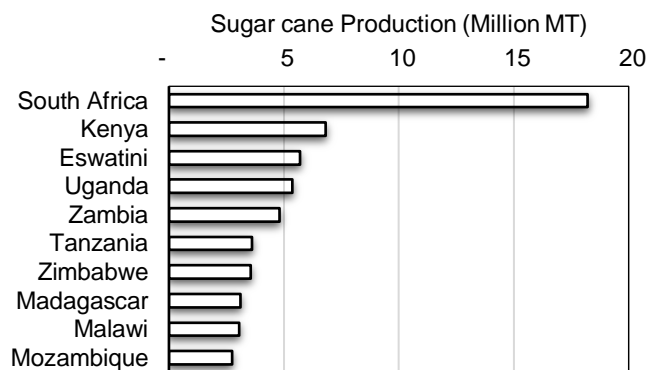


**Figure 6B. Main sugar cane producers in sub-Saharan Africa in 2020**  
Source: FAOSTAT, 2023

### **Institutional and production arrangements of major sugarcane producing countries**

The sub-Saharan African sugar market's reliance on smallholder farmers for production is one of its distinguishing features. Although there are some large-scale plantations, especially in South Africa, Kenya, and Zambia, most of the region's sugar is produced by small-scale farmers who grow sugarcane on small plots of land. These farmers frequently lack access to cutting-edge equipment and inputs, which can reduce their yields and competitiveness. For most African countries, sugarcane is produced under outgrower schemes. Typically, for Africa's top sugarcane producers, the nucleus estate plantation, in which the milling companies farm their own land, incorporates the surrounding producers as outgrowers.

Outgrower schemes can be defined as “a contractual arrangement for a fixed term between a farmer and a firm, agreed verbally or in writing before production begins, which

provides resources to the farmer and/or specifies one or more conditions of production, in addition to one or more marketing conditions, for agricultural production on land owned or controlled by the farmer, which is non-transferable and gives the firm, not the farmer, exclusive rights and legal title to the crop” (Prowse, 2012).

These outgrowers may be single farmers or farming communities organized into trusts, cooperatives, or businesses and enter into a contract to cultivate sugarcane especially for a processing plant or milling company (von Maltitz et al., 2019). Such schemes allow the farmer to have guaranteed access to markets, technology, skills and inputs (Prowse, 2012). The key aspects to stability of the sugar industry and constant supply of sugar and sugarcane production for such outgrower schemes relate to land ownership and land management. Table 2 highlights some of these aspects.

**Table 2**  
**Production arrangements for major sugarcane producing African countries**

Country	Number of Core Companies	Sugarcane crushed (million tons/annum)	Sugar produced ('000 tons/annum)	Ownership	Outgrower production (% of total cane production)
Malawi	2	2.4 (2021) (↑9%)	279 (↑17%)	State-run trust, Individual outgrowers	22% (Illovo Sugar)
Eswatini	3	1.9 (2022) (↓8%)	270 (↓6%)	Outgrowers through shareholdings	41% (RES), 63% (Illovo)
Zambia	3	3.2 (2021) (↓4%)	468 (↓15%)	Outgrower-owned trust, Company 14 year lease	44% (Zambia Sugar PLC)
South Africa	6	4.84 (2021) (↓6%)	535 (↓11%)	Joint Venture with millers, Cooperative,	92% overall. 88% (Tongaat Hulett), 60% (Illovo Sugar)
Kenya	16	0.4 (2019) (↓23%)	24 (↓30%)	State-owned, Outgrower-owned	90% overall

↓ and ↑ Denotes percentage decrease and increase from previous year respectively/interannual change

Source: Various sources (Bomett et al., 2020; Chisanga et al., 2014; Illovo, 2023c, 2023b, 2023a; Malawi Investment Forum (MIF), 2020; Royal Eswatini Sugar Corporation (RES), 2023; Samboko and Dlamini, 2017; SASA, 2023a; Tongaat and Hulett, 2023; von Maltitz et al., 2019)

The proportion of sugarcane production supplied by outgrowers compared to the nucleus estate is likely to dictate the stability of sugar production given. This may be particular the case for sugarcane production in Africa which is dominated by smallholder outgrowers (von Maltitz et al., 2019). When outgrowers dominate the production of

sugarcane, as is the case in South Africa (92%) and Kenya (90%), this poses as a high risk to the steady supply of sugarcane to the milling company involved in sugar production. This may arise because outgrowers may fail to honor their contracts and engage in opportunistic behavior to side-sell their sugarcane to other offtakers (Chisanga et al., 2014). This may be widespread for markets that are not monopsonistic in a given location or indeed if the market is less concentrated, such as the Kenyan sugar milling industry. There is overwhelming evidence on side-selling with regards to such contractual arrangements for various crops (Alemu et al., 2021; Blackmore et al., 2018; Ewusi Koomson et al., 2022; Mugwagwa et al., 2020). This risk may be lower in case of Malawi, Eswatini and Zambia, in which outgrowers supply 16, 41 and 44%, respectively. However, even for such countries with relatively low proportions of outgrower sugarcane supply, other risks may emanate from decisions about investing in other enterprises and not adhering to laid down production methods. This is typically common in cases where agricultural plots for sugarcane production are individually owned (Samboko and Dlamini, 2017).

These risks however may be averted through use of block plantations, mostly used in all the 5 countries highlighted as shown in Table 3.

**Table 3**

**Institutional Arrangements for Sugarcane Production in Africa**

<b>Type of outgrower scheme</b>	<b>Type of fields</b>	<b>Institutional structure (establishment and support)</b>
Irrigated, rainfed	Block plantations, individual fields	Government in charge of land, loans and sales. Farmer Associations purchase cane and controls marketing links to millers. Industry associations exist without supporting legislation.
Irrigated	Block plantations	Government scheme initiation and support; strong industry associations supported by legislation.
Irrigated	Block plantations, individual fields	Government provides funding and land in some cases. Milling and outgrower Companies: oversees all farming activities. Industry associations exist without supporting legislation.
Irrigated, rainfed, hybrid	Block plantations, individual fields	Community and Industry: Support; strong industry associations supported by legislation.
Irrigated, rainfed	Block plantations, individual fields	Government currently owns 5 out of the 12 operational milling companies. Milling Companies oversees all farming activities. Industry associations exist without supporting legislation.

Source: F.O.Licht, International Sugar and Sweetener Report, 2022

Most of the outgrower projects reviewed had land tenure rights alterations from individually owned land to block plantations, while in some cases governments or traditional leaders allocated land to farmers in blocks prior to the establishment of the outgrower project. Heavy government support and ownership is prevalent in countries like Eswatini and Kenya. Out of the 12 operating milling companies in Kenya, 5 are owned by the government although there are ongoing plans to privatize some of them owing to inherent inefficiencies of the state owned enterprises that have hampered production and contributed to the current sugar deficits (Bomett et al., 2020). For other countries, government involvement is mainly in the nascent

stages by initiating some projects, while for some projects that were initiated by the milling companies, government did provide some funding and technical support. Farmer associations and outgrower companies are mainly involved in the marketing aspects and overseeing farming activities carried out by the farmers. Strong institutional and industrial support is key in ensuring a win-win situation between the outgrower companies and the farmers. This is the case in South Africa and Eswatini in which some sugar associations, backed by legislation involved in enhancing the welfare of the farmers play a critical role in relation to the pricing of sugarcane.

## Conclusions

1. Sugar and sugarcane production has increased by 200% and 215%, respectively over the last 6 decades. The Eastern and Southern Africa regions produce a lion's share of both sugar and sugarcane production accounting for 90% and 86% respectively of total production in SSA.
2. Despite the positive trajectory, SSA only accounts for a meagre 4% of the world's sugar and sugarcane production. SSA has immense potential to increase sugarcane and sugar production at global level given the availability of arable land and its rich endowment of natural resources.
3. The upward trajectory in sugar and sugarcane production between 1961 and 2020 coincided with the expansion in area cultivated and not necessarily the increase in yields. Yields in SSA are quite low, averaging 56 metric tons against a benchmark of 70 to 100 tons per hectare with only 12 countries producing above this threshold.
4. The institutional and production arrangements in Africa highlight the importance of outgrower schemes and smallholder farmers in the sugarcane value chain. Their dominance in the supply of sugarcane to milling companies, particularly in South Africa (92%) and Kenya (90%) poses as a high risk to the steady supply of sugarcane given the reported opportunistic behavior to sell their sugarcane to other offtakers, hence abrogating their contracts.
5. Key to resolving the low yields and boosting Africa's share on the global market will be addressing the institutional and production arrangements of sugar and sugarcane production, particularly addressing the issues surrounding outgrower schemes that are the major production models. This will entail improving extension services and incentives to outgrowers, organization of farmers into associations, enhanced adoption of modern technology and inputs (improved sugarcane varieties) and improving irrigation facilities especially in the light of increasing adverse weather conditions associated with climate change.

## References

Alemu D., Guinan A., Hermanson J. (2021), Contract farming, cooperatives and challenges of side selling: Malt barley value-chain development in Ethiopia, *Development in Practice*, 31(4), pp. 496–510, <https://doi.org/10.1080/09614524.2020.1860194>

- Andae G. (2018), *Kenya seeks fresh Comesa sugar import safeguard*, Available at: <https://www.tralac.org/news/article/13264-kenya-seeks-fresh-comesa-sugar-import-safeguard.html>
- Blackmore E., Kabwe S., Mujeyi K., Muzenda J., Vorley B. (2018), *Informal trade in cotton: Understanding drivers and working towards solutions in Zambia and Zimbabwe*, Available at: <https://www.jstor.org/stable/resrep16753>
- Bomett M., Wambua J., Odhiambo V. (2020), *Sugar Sub-Sector Profile*, Available at: [https://kam.co.ke/bfd\\_download/kam-sugar-sub-sector-profile/](https://kam.co.ke/bfd_download/kam-sugar-sub-sector-profile/)
- Chisanga B., Gathiaka J., Nguruse G., Onyancha S. (2014), Competition in the regional sugar sector: The case of Kenya, South Africa, Tanzania and Zambia, *Proceedings of the Fifth Meeting of the UNCTAD Research Partnership Platform, July 11, 2014*, Geneva, pp. 48–60
- Chudasama A. (2021), *International Sugar Journal-World Sugar Yearbook 2021*, Available at: <https://internationalsugarjournal.com/>
- Ewusi Koomson J., Donkor E., Owusu V. (2022), Contract farming scheme for rubber production in Western region of Ghana: Why do farmers side sell?, *Forests Trees and Livelihoods*, 31(3), pp. 139–152, <https://doi.org/10.1080/14728028.2022.2079007>
- FAO (1984), Animal Production and Health, *Proceedings of The Fao Expert Consultation on The Substitution of Imported Concentrate Feeds in Animal Production Systems in Developing Countries, September 9-13, 1985*, Bangkok, Available at: <https://www.fao.org/3/x6930e/X6930E00.htm>
- FAO (2023), *Land Water: Sugar cane*, Available at: <https://www.fao.org/land-water/databases-and-software/crop-information/sugarcane/en/>
- Goodison P. (2007), *EU Trade Policy the Future of Africa's Trade Relationship with the EU*, 34(112), pp. 247–266, <https://doi.org/10.1080/03056240701449646>
- Gotor E., Tsigas M.E. (2011), The impact of the EU sugar trade reform on poor households in developing countries: A general equilibrium analysis, *Journal of Policy Modeling*, 33(4), pp. 568–582, <https://doi.org/10.1016/j.jpolmod.2010.10.001>
- Gro Intelligence (2015), *Global Sugar Markets*, Available at: <https://gro-intelligence.com/insights/global-sugar-markets>
- Hassan S. F. (2008), Development of sugar industry in Africa, *Sugar Tech*, 10(3), pp. 197–203, <https://doi.org/10.1007/s12355-008-0037-6>
- Hess T. M., Sumberg J., Biggs T., Georgescu M., Haro-Monteagudo D., Jewitt G., Ozdogan M., Marshall M., Thenkabail P., Daccache A., Marin F., Knox J. W. (2016), A sweet deal? Sugarcane, water and agricultural transformation in sub-Saharan Africa, *Global Environmental Change*, 39, pp. 181–194, <https://doi.org/10.1016/j.gloenvcha.2016.05.003>
- Hinke J., Smutka L., Pulkrábek J. (2018), Selected aspects of the sugar market in the African region, *Listy Cukrovarnické a Řepářské*, 134(9), pp. 332–337
- Illovo (2023a), *Illovo Sugar Africa – About Us*, Available at: <https://www.illovosugarafrika.com/about-us>
- Illovo (2023b), *Illovo Sugar Africa—Eswatini—Ubombo Sugar Limited—About Us*, Available at: <https://www.illovosugarafrika.com/about-us/eswatini>
- Illovo (2023c), *Illovo Sugar Africa—Malawi—Illovo Sugar Malawi—About Us*, Available at: <https://www.illovosugarafrika.com/about-us/malawi>
- ISO (2018), International Sugar Organization, *World Sugar Market and Trade*, Available at: <https://www.isosugar.org/world-sugar-market-and-trade/>

- ISO (2019), International Sugar Organization, *Profiling the African Sugar Market Future Trade Landscape*, Available at: [https://www.isosugar.org/publication/118/profiling-the-african-sugar-market-&-future-trade-landscape---mecas\(18\)08-](https://www.isosugar.org/publication/118/profiling-the-african-sugar-market-&-future-trade-landscape---mecas(18)08-)
- Jones M.R., Singels A. (2015), Analysing yield trends in the South African sugar industry, *Agricultural Systems*, 141, pp. 24–35, <https://doi.org/10.1016/j.agry.2015.09.004>
- Kalagho K. (2014), *Tanzania restricts sugar imports – Tralac trade law centre*, Available at: <https://www.tralac.org/news/article/5815-tanzania-restricts-sugar-imports.html>
- Macháček J., Syrovátka M., Harmáček J. (2017), Sugar production and trade in sub-Saharan Africa, *Listy Cukrovarnické a Řepářské*, 133(7), pp. 258–261
- Malawi Investment Forum (MIF) (2020), *The Salima Medium Scale Farmers 1000ha Project*, Available at: <https://mif.mw/index.php/projects/agriculture/sugar-project>
- Masih I., Maskey S., Mussá F. E. F., Trambauer P. (2014), A review of droughts on the African continent: A geospatial and long-term perspective, *Hydrology and Earth System Sciences*, 18(9), pp. 3635–3649, <https://doi.org/10.5194/hess-18-3635-2014>
- McDonald S., Punt C., Leaver R. (2004), Trade Liberalisation, Efficiency and South Africa's Sugar Industry, [Working Paper No. 2004012], Available at: <https://eprints.whiterose.ac.uk/9898/1/SERP2004012.pdf>
- Mugwagwa I., Bijman J., Trienekens J. (2020), Typology of contract farming arrangements: A transaction cost perspective, *Agrekon*, 59(2), pp. 169–187, <https://doi.org/doi.org/10.1080/03031853.2020.1731561>
- Ngcobo S., Jewitt G. (2017), Multiscale drivers of sugarcane expansion and impacts on water resources in Southern Africa, *Environmental Development*, 24, pp. 63–76, <https://doi.org/10.1016/j.envdev.2017.07.004>
- Olingo A. (2018), *Kenya bags Comesa sugar safeguards for another two years, but with conditions*, Available at: <https://www.tralac.org/news/article/13290-kenya-bags-comesa-sugar-safeguards-for-another-two-years-but-with-conditions.html>
- Owiti O. (2019), *Socio-Economic Determinants of Sugarcane Production among Small Scale Farmers in Nyando Sugarbelt, Kenya* [Maseno University], Available at: <https://repository.maseno.ac.ke/handle/123456789/3613>
- Paha J., Sautter T., Schumacher R. (2021), Some Effects of EU Sugar Reforms on Development in Africa, *Intereconomics*, 56(5), pp. 288–294, <https://doi.org/10.1007/s10272-021-1001-x>
- Prowse M. (2012), *Contract Farming in Developing Countries: A Review*, Agence Française de Développement, Imprimerie de Montligeon. Savoir, Paris. Available at: <https://lup.lub.lu.se/search/ws/files/5824557/5218915.pdf>
- Richardson, B. (2009), Restructuring the EU–ACP sugar regime: Out of the strong there came forth sweetness, *Review of International Political Economy*, 16(4), pp. 673–697, <https://doi.org/10.1080/09692290802529751>
- Royal Eswatini Sugar Corporation (RES). (2023), *RES integratd report 2022*, [Annual Report], Available at: <https://www.res.co.sz/admin/documents/RES%20integratd%20report%202022.pdf>
- Rumánková L., Smutka L. (2013), Global sugar market – the analysis of factors influencing supply and demand, *Acta Universitatis Agriculturae et Silviculturae Mendelianae Brunensis*, 61(2), pp. 463–471, <https://doi.org/10.11118/actaun201361020463>
- Samboko P.C., Dlamini C. (2017), *Institutional arrangements for biofuel feedstock production in Zambia*, [Working Paper Working Paper, No. 2017/54], Available at: <https://doi.org/10.35188/UNU-WIDER/2017/278-6>

- Sandrey R., Moobi M. (2015), *Sugar: Production, trade and policy profiles for South Africa and other selected African countries*, [Working Paper Working Paper No. S15WP25/2015], Available: <http://rgdoi.net/10.13140/RG.2.1.1179.4005>
- Sandrey R., Vink N. (2007), *Future prospects for African sugar: Sweet or sour?*, [Working Paper Working Paper No. 11/2007], Available: <https://www.tralac.org/publications/article/4235-future-prospects-for-african-sugar.html>
- SASA (2023a), *Cane growing in South Africa*, Available at: <https://www.sasugarindustrydirectory.co.za/growers/overview/>
- SASA (2023b), *The Sugar Industry: The South African Sugar Association*, Available at: <https://sasa.org.za/the-sugar-industry/>
- Smutka L., Pokorna I., Pulkrábek J. (2011), World production of sugar crops, 127(3), *Listy Cukrovarnické a Řepářské*, pp. 78–82
- Tena E., Mekbib F., Shimelis H., Mwadzingeni L. (2016), Sugarcane production under smallholder farming systems: Farmers preferred traits, constraints and genetic resources, *Cogent Food Agriculture*, 2(1), pp. 1–15, <https://doi.org/10.1080/23311932.2016.1191323>
- Thibane Z., Soni S., Phali L., Mdoda L. (2023), Factors impacting sugarcane production by small-scale farmers in KwaZulu-Natal Province-South Africa, *Heliyon*, 9(1), pp. e13061, <https://doi.org/10.1016/j.heliyon.2023.e13061>
- Tongaat Hulett (2023), *Overview of the South Africa Sugar Industry*, Available at: <https://www.tongaat.com/our-business/sugar/south-africa/>
- UN (2023), *UNSD Methodology-Standard country or area codes for statistical use (M49)*, Available at: <https://unstats.un.org/unsd/methodology/m49/>
- Viljoen W. (2014), *The end of the EU sugar quota and the implication for African producers*, Available at: <https://www.tralac.org/discussions/article/5684-the-end-of-the-eu-sugar-quota-and-the-implication-for-african-producers.html>
- von Maltitz G. P., Henley G., Ogg, M., Samboko P.C., Gasparatos A., Read M., Engelbrecht F., Ahmed A. (2019), Institutional arrangements of outgrower sugarcane production in Southern Africa, *Development Southern Africa*, 36(2), pp. 175–197, <https://doi.org/10.1080/0376835X.2018.1527215>

## Анотації

### Харчові технології

#### Оцінка якості бісквітних тістечок з додаванням насіння розторопші

Євгенія Ковальов, Татьяна Капканарь, Владислав Решітка, Ауріка Кірсанова  
*Технічний університет Молдови, Кишинів, Республіка Молдова*

**Вступ.** У дослідженні наведено характеристики бісквітних тістечок із частковою заміною пшеничного борошна порошком з насіння розторопші.

**Матеріали і методи.** Порошок насіння розторопші (*Silybum marianum* L.) використовувався для часткової заміни пшеничного борошна під час приготування бісквіту. У бісквіті з порошком насіння розторопші загальновідомими методами визначали втрати при випіканні, вміст вологи, активність води, об'єм, пористість, текстуру, колір скоринки та м'якушки, сенсорні показники, антиоксидантну активність і загальний вміст фенолу.

**Результати і обговорення.** Із заміною пшеничного борошна порошком розторопші від 0 до 20% об'єм і пористість бісквітів зменшуються. Додавання порошку розторопші вплинуло на текстуру і колір м'якушки випечених бісквітів. Твердість і жувальна здатність випечених бісквітів мали тенденцію до зростання зі збільшенням кількості порошку розторопші, а зв'язність і пружність демонстрували зворотну тенденцію. Для кольору скоринки та м'якушки значення  $L^*$  і  $b^*$  зменшилися, тоді як значення  $a^*$  збільшилося. Отримані зразки були темніші, червоніше та менш жовті. Додавання розторопші позитивно вплинуло на загальний вміст фенолів – з 63,93 (контрольний зразок) до 121,94 (GAE)/100 g. Водночас найвищу антиоксидантну активність (44,70%) зафіксовано у зразка з 20% порошку насіння розторопші. Органолептичний аналіз показав, що найбільш прийнятним є бісквіт із заміною пшеничного борошна 5 і 10% порошку з насіння розторопші.

**Висновки.** Включення порошку насіння розторопші в рецептури бісквіту збагатило його біологічну цінність з точки зору загального вмісту фенолу та антиоксидантної активності. Проте деякі технологічні показники якості знизилися. Для отримання якісних бісквітів заміна пшеничного борошна на порошок насіння розторопші не повинна перевищувати 10%.

**Ключові слова:** бісквіт, розторопша, колір, текстура.

## Вплив попередньої ферментативної обробки на структуру клітин і вилучення олії з гарбузового насіння

Ганна Вовк<sup>1</sup>, Кванкао Карнпакді<sup>2</sup>, Ольга Голубець<sup>3</sup>,  
Ірина Левчук<sup>3</sup>, Роланд Людвиг<sup>2</sup>, Тамара Носенко<sup>1</sup>

1 – Національний університет харчових технологій, Київ, Україна

2 – Університет природних ресурсів і природничих наук (БОКУ), Відень, Австрія

3 – Державне підприємство «Укрметртестстандарт», Київ, Україна

**Вступ.** Досліджено вплив попередньої обробки гарбузового насіння протеолітичними, целюлолітичними та пектолітичними ферментними препаратами на клітинну структуру, вихід пресової олії та її якість.

**Матеріали і методи.** Використовували папаїн, пектиназу, целюлазу та Viscozyme L виробництва Sigma-Aldrich (USA), пепсин – Sigma-Aldrich (США) і Carl Roth (Німеччина). Кількість зруйнованих клітин визначали методом миттєвої екстракції. Для дослідження мікроструктури клітин ультрамікроміт зрізи гарбузового насіння обробляли або індивідуальними ферментними препаратами, або їх сумішами. Антиоксидантну активність пресової гарбузової олії визначали за реакцією гасіння радикалів DPPH.

**Результати і обговорення.** Визначення цілісності клітин гарбузового насіння методом миттєвого струшування показало, що зразки, оброблені різними ферментними препаратами, мали вищий вихід олії в діапазоні від 33,2 до 34,1%, ніж контрольний зразок (32,1%), і вищу кількість зруйнованих клітин, ніж контроль (64,4%), – від 67,6 до 69,5%. Найвища кількість зруйнованих клітин (71,0 та 71,1%) була у зразках насіння, обробленого ферментними сумішами пепсин+Viscozyme L+пектиназа та пепсин+целюлаза+пектиназа відповідно. Також найвища кількість зруйнованих клітин була в зразках, оброблених Viscozyme L та сумішшю пепсин+Viscozyme L+пектиназа. Вихід пресової олії з насіння, обробленого сумішшю пепсин+Viscozyme L+пектиназа, був на 7% вищим, ніж у контрольному зразку. Ферментативна обробка не впливає суттєво на вміст вільних жирних кислот, пероксидне число, склад жирних кислот і фітостеролів. Антиоксидантна активність, виражена за здатністю гасіння радикалів DPPH, була на 2,7% вищою в зразках олії з насіння, обробленого сумішшю ферментів, ніж у контролі.

**Висновки.** Попередня обробка гарбузового насіння целюлолітичними і протеолітичними ферментами є перспективним методом збільшення виходу пресової олії та одночасного підвищення її біологічної цінності.

**Ключові слова:** ферментативна обробка, пресова олія, гарбузове насіння, протеаза, целюлаза, пектиназа.

## Вплив гарбузової клітковини на конформаційні перетворення в тісті та хлібі з пшеничного борошна

Анастасія Шевченко, Світлана Літвинчук,  
Віра Дробот, Олександр Шевченко

*Національний університет харчових технологій, Київ, Україна*

**Вступ.** Метою дослідження є визначення впливу гарбузової клітковини на конформаційні перетворення в структурі тіста та хліба з пшеничного борошна.

**Матеріали і методи.** Досліджували гранулометричний склад, функціонально-технологічні властивості, амінокислотний склад гарбузової клітковини в порівнянні з пшеничним борошном вищого сорту. Вплив гарбузової клітковини в поєднанні з фосфоліпідами на конформаційні перетворення в структурі тіста та хліба були досліджені методом інфрачервоної спектроскопії у ближній інфрачервоній області.

**Результати і обговорення.** Встановлено, що 96% частинок пшеничного борошна вищого сорту пройшло через сито з отворами 132 мкм, решта 4% – через сито з отворами 260 мкм. Гарбузова клітковина має більші розміри частинок, адже всі 100% залишаються на ситі з розміром отворів 670 мкм. Здатність гарбузової клітковини зв'язувати й утримувати вологу була значно вищою, ніж пшеничного борошна, через вищий вміст харчових волокон. Вологозв'язувальна здатність гарбузової клітковини була вищою у 3,6 раза, а вологоутримувальна – у 2,8 раза. Амінокислотний скор лімітуючої амінокислоти – лізину, в пшеничному борошні становив 0,44. Амінокислотний скор лімітуючої амінокислоти – метіоніну, гарбузової клітковини становив 3,16, а лізину – 3,49, що значно вище, ніж у пшеничному борошні. Додавання в хліб гарбузової клітковини (5 – 15%) підвищувало цей показник для лізину на 6,5–15,2%. Встановлено, що інфрачервоні спектри зразків тіста після замішування (контрольного зразка та зразка із заміною) практично накладаються у всьому діапазоні довжин хвиль. У процесі бродіння інтенсивно відбувалися конформаційні зміни функціональних груп тіста, змінювалися його структурно-механічні властивості. Кулька тіста контрольного зразка розріджувалася швидше. Формоутримувальна здатність покращувалася при збільшенні частки заміни пшеничного борошна на гарбузову клітковину.

**Висновки.** Внесення гарбузової клітковини в рецептуру пшеничного хліба підвищило його біологічну цінність завдяки більш високому вмісту харчових волокон, білка та повноцінного амінокислотного профілю. Додаток також впливає на структурно-механічні властивості та структурні елементи тіста й хліба.

**Ключові слова:** *гарбуз, борошно, клітковина, хліб, тісто, спектроскопія.*

## Порівняльне дослідження властивостей рису басматі та інших сортів

Рошанлал Ядав, Сакші Хурана, Суніл Кумар

1 – Коледж Лакимібай, Університет Делі, Індія

2 – Коледж прикладних наук Бхаскарачар'я Делійського університету, Індія

3 – Університет Махараджа Ганга Сінгха, Індія

**Вступ.** Метою дослідження був аналіз фізико-хімічних, кулінарних, текстурних та подрібнювальних властивостей рису басматі та рису інших сортів.

**Матеріали та методи.** Очищення від лушпиння і подрібнення рису проводили за допомогою лабораторного млина, а вихід рису з головки визначали за методами Адейра. Шліфований рис аналізували на вміст вологи, золи, білка та амілози. Текsturні характеристики вареного зерна аналізували за допомогою профілю текстури.

**Результати і обговорення.** Досліджено хімічні властивості різних сортів рису, які впливають на якість і ринкову вартість рису. Так, вихід шліфованого рису залежить від сорту, причому Pusa Basmati (PB)-6 демонструє найвищий вихід, а PB-1121 має найвищий відсоток лушпиння. Вихід головного рису був найвищим у P-44 і найнижчим у PB-6, тоді як вміст вологи в подрібненому рисовому зерні коливався від 10,75 до 11,84%. PB-1121 мав найвищу зольність, а P-2819 – найменшу зольність і вміст білка. Сорти басматі мали значно нижчий вміст крохмалю і більший вміст амілози, ніж інші сорти. Вимірювання насипної густини показали, що PB-6 мав найнижчу насипну густину, тоді як P-44 – найвищу. P-2819 мав найвищу дійсну густину. Сорти басматі, як правило, мають довші зерна порівняно з іншими. PB-1121 вирізнявся найвищим співвідношенням довжини до ширини через відносно тонку та подовжену форму зерна. Кулінарні властивості сортів рису виявили цікаві варіації. P-2819 продемонстрував найкоротший час приготування, тоді як PB-1121 – найдовший. Коефіцієнт подовження виявився вищим у сортах басматі порівняно з іншими. Якщо розглядати поглинання води, PB-1121 продемонстрував найвищий коефіцієнт. Це означає, що він поглинав більше води під час приготування. Крім того, тверді втрати були найвищими в P-2819 і найменшими в PB-1121. Що стосується текстурних властивостей, P-2819 показав найвищу твердість, тоді як PB-1121 – найнижчу. Адгезивність сортів басматі була нижчою порівняно з іншими, що вказує на більш липку текстуру інших сортів. PB-1121 мав найнижчу клейкість, що вказувало на меншу тенденцію зерна ставати клейкими. Дослідження кореляції виявило значні зв'язки між властивостями рису. Час приготування позитивно корелює зі справжною густиною, співвідношенням довжини та ширини, твердістю, клейкістю і жувальністю. Коефіцієнт подовження позитивно корелював із вмістом амілози, пористістю, довжиною, співвідношенням довжини до ширини та вагою 1000 зерен. Коефіцієнт поглинання води показав численні позитивні кореляції.

**Висновок.** Використовуючи цю інформацію, зацікавлені сторони можуть підвищити якість, ринкову вартість і загальне задоволення від споживання рисових продуктів.

**Ключові слова:** рис, басматі, амілоза, шліфування, текстура.

## Ряжанка з гарбузовим пюре та насінням льону

Олег Кузьмін<sup>1</sup>, Вікторія Кійко<sup>1,2</sup>, Олена Хареба<sup>3</sup>,  
Олена Гавриленко<sup>2</sup>, Марія Янчик<sup>1</sup>, Наталія Мельник<sup>1</sup>

1 – Національний університет харчових технологій, Київ, Україна

2 – Український державний науково-дослідний інститут «Ресурс», Київ, Україна

3 – Національна академія аграрних наук України, Київ, Україна

**Вступ.** Метою цього дослідження було покращення нутрієнтного складу та сенсорних властивостей ряжанки шляхом включення гарбузового пюре та насіння льону, а також стабілізація її фізико-хімічні параметрів.

**Матеріали і методи.** Зразки ряжанки готували з додаванням гарбузового пюре та насіння льону. Титровану кислотність ряжанки визначали за методом Тернера, активну кислотність – рН-метрією. Вміст жиру аналізували за допомогою кислотного методу Гербера, сенсорну оцінку проводили експертною групою.

**Результати і обговорення.** Досліджено вплив гарбузового пюре та насіння льону на активну й титровану кислотність ряжанки. Встановлено, що додавання 4–8% насіння льону до ряжанки з 10% гарбузового пюре знижує титровану кислотність до 64–70 °Т і підвищує активну кислотність до 4,60–4,69 рН. Додавання 4–8% насіння льону з 15% гарбузового пюре знижувало титровану кислотність до 61–68 °Т і підвищувало активну кислотність до 4,62–4,74 рН. При одночасному додаванні 20% гарбузового пюре і 4–8% насіння льону титрована кислотність знижувалася до 60–65 °Т, а активна кислотність підвищувалася до 4,62–4,75 рН. Оптимальні умови гарбузового пюре та вмісту насіння льону в ряжанці – 10% гарбузового пюре та 4% насіння льону. Оптимальними умовами досягнення фізико-хімічної стабільності ряжанки є використання 10% гарбузового пюре та 4% насіння льону.

Додавання до ряжанки гарбузового пюре (10%) і насіння льону (4%) призвело до підвищення вмісту водорозчинних вітамінів: С – на 0,570 мг (184%), В<sub>1</sub> – на 0,062 мг (295%), вітаміну В<sub>2</sub> – 0,003 мг (2%). Також підвищився вміст жиророзчинних вітамінів, включаючи 0,010 мг вітаміну Е і 0,051 мг β-каротину. Окрім того, додавання насіння льону підвищило вміст поліненасичених жирних кислот, причому вміст омега-3 жирних кислот збільшився з 0 до 0,80 г, а омега-6 жирних кислот – з 0 до 0,20 г.

При порівнянні з контрольним зразком встановлено, що додавання гарбузового пюре та насіння льону до ряжанки вплинуло на термін її зберігання за температури від 0 °С до 6 °С, подовжуючи його не більше ніж на 7 діб.

**Висновки.** Запропонована рецептура ряжанки з гарбузовим пюре та насінням льону покращує її поживний склад, стабілізує фізико-хімічні показники, покращує сенсорні властивості та розширює спектр можливостей для задоволення смаків любителів кисломолочного напою.

**Ключові слова:** ряжанка, гарбузове пюре, насіння льону.

## Процеси і обладнання

### Моделювання тепломасообміну нестационарних процесів за комірчастою моделлю масової кристалізації сахарози

Тарас Погорілий

*Національний університет харчових технологій, Київ, Україна*

**Вступ.** Метою дослідження є визначення впливу змінних теплофізичних характеристик на нестационарні дифузійні масові потоки сахарози під час масової кристалізації цукру.

**Матеріали і методи.** Для отримання кількісних величин нестационарних дифузійних масових потоків для міжкристалних розчинів сахарози, що оточують кристали цукру, було проведено чисельний розрахунок одночасно для двох систем задач тепло- та масообміну: 1) система із семи нестационарних задач теплопровідності; 2) система, що складалась з трьох нестационарних задач дифузійного масообміну.

**Результати і обговорення.** Для ряду значень відносного часу уварювання цукрового утфелю 0,15–1,0 на основі одночасного чисельного розв'язку двох систем (10 підсистем) нестационарних диференціальних рівнянь у частинних похідних параболічного типу (перша система складалась із 7 підсистем – для нестационарних задач теплопровідності по кожній із 7 областей; друга система включає три підсистеми – для нестационарних задач дифузійного масообміну для 4 областей) знайдено відповідно: нестационарні розподіли температур в кожній із 7 областей (4 області з міжкристалними розчинами, 2 кристалами цукру та утфель); нестационарні розподіли дифузійних масових потоків сахарози в кожній із 4 областей міжкристалних розчинів сахарози всієї розглянутої системи двох комірок та утфелю. При значенні відносного часу уварювання цукрового утфелю 0,15 при русі всієї системи комірок вздовж нагрівальної трубки спочатку відбувається перенесення речовини з області міжкристалного розчину сахарози меншого кристала в область міжкристалного розчину сахарози більшого кристала протягом  $\tau_{к,2}=2,41-2,7$  с (залежно від сталих чи змінних теплофізичних характеристик). Починаючи з цього часу, до 3,95 с (при відносному часі уварювання цукрового утфелю 0,15) виходу системи комірок з нагрівальної трубки ситуація змінюється на протилежну. Отримано чітко виражений лише один екстремум дифузійного масового потоку (мінімум на графіку, який досягається в момент часу 1,29–1,45 с, що визначає максимальне масове перенесення сахарози від меншого кристала до більшого кристала). Явного максимуму не встановлено. При відносному часі уварювання цукрового утфелю 1,0 отримали два чітко виражених екстремуми (мінімум і максимум) як для сталих, так і для змінних теплофізичних характеристик.

**Висновки.** Показано особливості впливу змінних теплофізичних характеристик на нестационарні дифузійні масові потоки.

**Ключові слова:** температура, концентрація, розчин, кристал, утфель.

**Визначення параметрів розмежування режимів теплообміну  
в плівці під час пароутворення**

Валентин Петренко, Олексій Пилипенко,  
Олександр Рябчук, Максим Наливайко

*Національний університет харчових технологій, Київ, Україна*

**Вступ.** Мета дослідження – аналітичне визначення параметрів розмежування двох характерних режимів тепловіддачі до киплячої плівки за умови її циклічного перемішування великими хвилями, що має місце в довгих трубах плівкових випарних апаратів цукрової промисловості.

**Матеріали і методи.** Застосовані аналітичні методи аналізу процесів теплоперенесення в стікаючих ламінарних і турбулентних плівках рідин під час пароутворення.

**Результати і обговорення.** Здійснено математичне моделювання температурного поля в стікаючій по вертикальній поверхні киплячої плівки рідини з розвинутою хвильовою структурою за наявності супутнього парового потоку в момент появи температурного градієнта на міжфазній поверхні плівка-пара. Збудовачем циклічних температурних коливань в плівці в довгих каналах виступають великі низькочастотні хвилі, які прокочуються по міжфазній поверхні. Гранична крива розмежування режимів теплообміну в плівці отримана на основі наближеного розв'язку диференціального рівняння теплопровідності з конвективним членом як для ламінарного, так і турбулентного режимів руху плівки з використанням алгебраїчної форми залежності для турбулентної в'язкості в плівці за умови нульового температурного градієнта на поверхні плівки. В результаті розв'язання задачі отримано аналітичний вираз, який є початковою умовою крайової задачі теплообміну в киплячій плівці, що виникає в момент перемішування плівки великою хвилею. Встановлено, що зі зміною об'ємної щільності зрошення від 0,0001 до 0,0005 м<sup>2</sup>/с довжина пробігу плівки, за якої відбувається зміна режиму теплообміну, становить, відповідно, 50–140 мм для ламінарних плівок та 10–35 мм – для турбулентних.

**Висновки** З рівнянь конвективної теплопровідності для ламінарних і турбулентних плівок за умови нульового температурного градієнта на поверхні плівки отримані вирази, які є початковими умовами крайової задачі теплообміну в киплячій плівці, що виникає в момент перемішування плівки великою хвилею.

**Ключові слова:** *рідина, плівка, температура, теплообмін, турбулентність, швидкість.*

## Біотехнологія, мікробіологія

### Отримання фосфатвмісного добрива зі стічних вод при використанні залізівідновлювальних бактерій

Віктор Стабніков<sup>1</sup>, Дмитро Стабніков<sup>1,2</sup>, Зубер Ахмет<sup>3</sup>

1 – Національний університет харчових технологій, Київ, Україна

2 – Вроцлавський університет, Польща

3 – Механський інженерно-технологічний університет, Джамшиоро, Пакистан

**Вступ.** Виробництво продуктів харчування засноване на використанні добрив, зокрема фосфоровмісних. Вилучення фосфору зі стічних вод може запобігти евтрофікації водойм, а віддалений фосфат можна використовувати як добриво.

**Матеріали і методи.** Стічні води, що містять фосфоровмісні сполуки, залізну руду, залізівідновлювальні бактерії є основними компонентами запропонованої технології вилучення фосфору. Мікроскопічні спостереження проводилися з використанням лазерної конфокальної скануючої мікроскопії. Отримане добриво випробували для вирощування рослин.

**Результати і обговорення.** Запропоновано ефективний біологічний метод видалення і вилучення фосфатів з рідких відходів з використанням осадження фосфатів мікробно-продукованими іонами заліза. Показано ефективність цієї біотехнології на прикладі скидної води (рідка фракція анаеробного мулу) міських очисних споруд.

Ця біотехнологія заснована на застосуванні залізної руди, обробленої залізівідновлювальними бактеріями *Stenotrophomonas maltophilia*, штам ВК. Розчинене залізо, одержане з твердої залізної руди внаслідок активності залізівідновлювальних бактерій, осаджує фосфат, присутній у стічних водах.

Фосфат-залізний осад оцінювали як фосфорне добриво шляхом внесення його в бідний поживними речовинами піщаний ґрунт, що використовувався для вирощування трьох рослин: *Lycopersicon esculantum* L. (томат), *Capsicum annuum* L. (перець) і *Ipomea aquatica* (водяний шпинат). Внесення в ґрунт фосфорного осаду збільшувало суху масу стебел та листя дослідних рослин до 5 разів, якщо порівняти з контролем.

**Висновок.** Розроблено біотехнологію анаеробного видалення фосфатів зі зворотної води міських очисних споруд з використанням залізо-відновлювальних бактерій і залізної руди як джерело заліза. Отриманий фосфат-залізний осад можна використовувати як фосфорне добриво.

**Ключові слова:** фосфат, біотехнологія, залізна руда, стічні води, добриво.

## Економіка і управління

### Історичні та сучасні перспективи цукрової промисловості в Африці на південь від Сахари

Джошуа Мабета, Любош Смутка

*Університет Південної Богемії в Ческе-Будейовіце, Чеська Республіка*

**Вступ.** Проаналізовано тенденції у виробництві цукру і цукрової тростини в Африці на південь від Сахари разом з основними факторами виробництва шляхом перегляду поточних інституційних і виробничих механізмів.

**Матеріали і методи.** Аналіз базується на 35 африканських країнах, розділених на чотири регіони на основі класифікації ООН М49. Було проведено детальний огляд літератури для пояснення наявних тенденцій і забезпечення контексту для різних інституційних та виробничих механізмів. Розглядаються ключові документи, пов'язані з цукром на національному рівні, вебсайти основних виробників цукру в кожній країні, їхні річні звіти та попередні емпіричні дослідження, проведені в основних країнах-виробниках цукрової тростини.

**Результати і обговорення.** За останні шість десятиліть виробництво цукру-сирцю і цукрової тростини в Південній Африці зросло на 200 і 215% відповідно. З точки зору регіонального виробництва, середній темп зростання виробництва цукру-сирцю за період з 1961 р. по 2020 р. становив 2, 3, 3 і 13% для регіонів Східної, Середньої, Південної та Західної Африки відповідно. Регіони Східної та Південної Африки виробляють основну частку як цукру, так і цукрової тростини, на які припадає 90 і 86% загального виробництва. Урожайність постійно залишалася низькою, і тільки Есватіні, Малаві, Танзанія, Південна Африка, Уганда і Замбія залишалися конкурентоспроможними та дешевими виробниками в регіоні. Деякі країни, такі як Кенія, Уганда і Танзанія, не є самодостатніми і вважаються нетто-імпортерами цукру. Ці країни в минулому вводили обмеження на імпорт, зокрема на імпортні тарифи, намагаючись таким чином стимулювати внутрішнє виробництво.

Загрози стабільному постачанню цукру і цукрової тростини, особливо для країн, які залежать від богарного сільського господарства, продовжували виникати через періодичні посухи, особливо в східних і південних регіонах на початку 1990-х років. Частка виробництва цукрової тростини, яку постачають дрібні фермери за схемами вирощування, порівняно з основними виробниками, визначає стабільність виробництва цукру в Африці. Найбільша частка таких виробників у Південній Африці (92%) і Кенії (90%), що створює високий ризик для сталого постачання цукрової тростини для компаній, які займаються виробництвом цукру, адже дрібні фермери можуть не виконувати свої контракти та вдаватися до опортуністичної поведінки, щоб продавати свою цукрову тростину іншим покупцям.

**Висновок.** Для сталого виробництва цукрової тростини в Африці на південь від Сахари важливо задіяти інституційні та виробничі механізми виробництва цукрової тростини, які б сприяли розв'язанню проблем, пов'язаних із основними моделями виробництва.

**Ключові слова:** *цукор, цукрова тростина, Африка, Сахара, врожайність, виробництво.*

# Instructions for authors



**Dear colleagues!**

The Editorial Board of scientific periodical  
“**Ukrainian Food Journal**”  
invites you for publication of your research results.

A manuscript should describe the research work that has not been published before and is not under consideration for publication anywhere else. Submission of the manuscript implies that its publication has been approved by all co-authors as well as by the responsible authorities at the institute where the work has been carried out.

It is mandatory to include a covering letter to the editor which includes short information about the subject of the research, its novelty and significance; state that all the authors agree to submit this paper to Ukrainian Food Journal; that it is the original work of the authors.

## **Manuscript requirements**

Authors must prepare the manuscript according to the guide for authors. Editors reserve the right to adjust the style to certain standards of uniformity.

Language – English

Manuscripts should be submitted in Word.

Use 1.0 spacing and 2 cm margins.

Use a normal font 14-point Times New Roman for text, tables, and signs on figures, 1.0 line intervals.

Present tables and figures in the text of manuscript.

Consult a recent issue of the journal for a style check.

Number all pages consecutively.

Abbreviations should be defined on first appearance in text and used consistently thereafter. No abbreviation should be used in title and section headings.

Please submit math equations as editable text and not as images (It is recommend software application MathType or Microsoft Equation Editor)

Minimal size of the article (without the Abstract and References) is 10 pages. For review article is 25 pages (without the Abstract and References).

## **Manuscript should include:**

**Title** (should be concise and informative). Avoid abbreviations in it.

**Authors' information:** the name(s) of the author(s); the affiliation(s) of the author(s), city, country. One author has been designated as the corresponding author with e-mail address. If available, the 16-digit ORCID of the author(s).

**Declaration of interest**

**Author contributions**

**Abstract.** The **abstract** should contain the following mandatory parts:

**Introduction** provides a rationale for the study (2–3 lines).

**Materials and methods** briefly describe the materials and methods used in the study (3–5 lines).

**Results and discussion** describe the main findings (20–26 lines).

**Conclusion** provides the main conclusions (2–3 lines).

The abstract should not contain any undefined abbreviations or references to the articles.

**Keywords.** Immediately after the abstract provide 4 to 6 keywords.

**Text of manuscript**

**References**

## **Manuscripts should be divided into the following sections:**

- **Introduction**
- **Materials and methods**
- **Results and discussion**
- **Conclusions**
- **References**

**Introduction.** Provide a background avoiding a detailed review of literature and declare the aim of the present research. Identify unexplored questions, prove the relevance of the topic. This should be not more than 1.5 pages.

**Materials and methods.** Describe sufficient details to allow an independent researcher to repeat the work. Indicate the reference for methods that are already published and just summarize them. Only new techniques need be described. Give description to modifications of existing methods.

**Results and discussion.** Results should be presented clearly and concisely with tables and/or figures, and the significance of the findings should be discussed with comparison with existing in literature data.

**Conclusions.** The main conclusions should be drawn from results and be presented in a short Conclusions section.

**Acknowledgments**(if necessary). Acknowledgments of people, grants, or funds should be placed in a separate section. List here those persons who provided help during the research. The names of funding organizations should be written in full.

Divide your article into sections and into subsections if necessary. Any subsection should have a brief heading.

**References**

Please, check references carefully.

The list of references should include works that are cited in the text and that have been published or accepted for publication.

All references mentioned in the reference list are cited in the text, and vice versa.

Cite references in the text by name and year in parentheses. Some examples:

(Drobot, 2008); (Qi and Zhou, 2012); (Bolarinwa et al., 2019; Rabie et al., 2020; Sengev et al., 2013).

Reference list should be alphabetized by the last name of the first author of each work. If available, please always include DOI links in the reference list.

## Reference style

### Journal article

Please follow this style and order: author's surname, initial(s), year of publication (in brackets), paper title, *journal title (in italic)*, volume number (issue), first and last page numbers, DOI. e.g.:

Popovici C., Gitin L., Alexe P. (2013), Characterization of walnut (*Juglans regia* L.) green husk extract obtained by supercritical carbon dioxide fluid extraction, *Journal of Food and Packaging Science, Technique and Technologies*, 2(2), pp. 104-108, <https://doi.org/11.1016/22-33-85>

Journal names should not be abbreviated.

### Book

Deegan C. (2000), *Financial Accounting Theory*, McGraw-Hill Book Company, Sydney.

### Book chapter in an edited book

Coffin J.M. (1999), Molecular biology of HIV, In: Crandell K.A. ed., *The Evolution of HIV*, Johns Hopkins Press, Baltimore, pp. 3–40.

Fordyce F.M. (2013), Selenium deficiency and toxicity in the environment. In: Selinus O. (ed.), *Essentials of Medical Geology*, pp. 375–416, Springer, [https://doi.org/10.14453/10.1007/978-94-007-4375-5\\_16](https://doi.org/10.14453/10.1007/978-94-007-4375-5_16)

### Online document

Mendeley J.A., Thomson, M., Coyne R.P. (2017), *How and When to Reference*, Available at: <https://www.howandwhentoreference.com>

### Conference paper

Arych M. (2018), Insurance's impact on food safety and food security, *Resource and Energy Saving Technologies of Production and Packing of Food Products as the Main Fundamentals of Their Competitiveness: Proceedings of the 7th International Specialized Scientific and Practical Conference, September 13, 2018*, NUFT, Kyiv, pp. 52–57, <https://doi.org/11.1016/22-33-85>

### Figures

All figures should be made in graphic editor using a font Arial.

The font size on the figures and the text of the article should be the same.

Black and white graphic with no shading should be used.

The figure elements (lines, grid, and text) should be presented in black (not gray) colour.

Figure parts should be denoted by lowercase letters (a, b, etc.).

All figures are to be numbered using Arabic numerals.

Figures should be cited in text in consecutive numerical order.

Place figure after its first mentioned in the text.

Figure captions begin with the term **Figure** in bold type, followed by the figure number, also in bold type.

Each figure should have a caption describing what the figure depicts in bold type.

Supply all figures and EXCEL format files with graphs additionally as separate files.

Photos are not advisable to be used.

If you include figures that have already been published elsewhere, you must obtain permission from the copyright owner(s).

### **Tables**

Number tables consecutively in accordance with their appearance in the text.

Place footnotes to tables below the table body and indicate them with superscript lowercase letters.

Place table after its first mentioned in the text.

Ensure that the data presented in tables do not duplicate results described elsewhere in the article.

### **Suggesting / excluding reviewers**

Authors are welcome to suggest reviewers and/or request the exclusion of certain individuals when they submit their manuscripts.

When suggesting reviewers, authors should make sure they are totally independent and not connected to the work in any way. When suggesting reviewers, the Corresponding Author must provide an institutional email address for each suggested reviewer. Please note that the Journal may not use the suggestions, but suggestions are appreciated and may help facilitate the peer review process.

### **Submission**

Email for all submissions and other inquiries:

**[ufj\\_nuft@meta.ua](mailto:ufj_nuft@meta.ua)**

## Шановні колеги!

Редакційна колегія наукового періодичного видання «**Ukrainian Food Journal**» запрошує Вас до публікації результатів наукових досліджень.

### Вимоги до оформлення статей

- Мова статей – англійська.  
Мінімальний обсяг статті – **10 сторінок** формату А4 (без врахування анотацій і списку літератури).  
Для всіх елементів статті шрифт – **Times New Roman**, кегль – **14**, інтервал – 1.  
Всі поля сторінки – по 2 см.

### Структура статті:

1. УДК.
2. **Назва статті.**
3. Автори статті (ім'я та прізвище повністю, приклад: Денис Озеряно).
4. *Установа, в якій виконана робота.*
5. Анотація. **Обов'язкова** структура анотації:
  - Вступ (2–3 рядки).
  - Матеріали та методи (до 5 рядків)
  - Результати та обговорення (пів сторінки).
  - Висновки (2–3 рядки).
6. Ключові слова (3–5 слів, але не словосполучень).

### Пункти 2–6 виконати англійською і українською мовами.

7. Основний текст статті. Має включати такі обов'язкові розділи:
  - Вступ
  - Матеріали та методи
  - Результати та обговорення
  - Висновки
  - Література.

За необхідності можна додавати інші розділи та розбивати їх на підрозділи.

8. Авторська довідка (Прізвище, ім'я та по батькові, вчений ступінь та звання, місце роботи, електронна адреса або телефон).
9. Контактні дані автора, до якого за необхідності буде звертатись редакція журналу.

Рисунки виконуються якісно. Скановані рисунки не приймаються. Розмір тексту на рисунках повинен бути **співрозмірним (!)** тексту статті. **Фотографії можна використовувати лише за їх значної наукової цінності.**

Фон графіків, діаграм – лише білий. Колір елементів рисунку (лінії, сітка, текст) – чорний (не сірий).

Рисунки та графіки EXCEL з графіками додатково подаються в окремих файлах.

Скорочені назви фізичних величин в тексті та на графіках позначаються латинськими літерами відповідно до системи СІ.

У списку літератури повинні переважати англомовні статті та монографії, які опубліковані після 2010 року.

## Оформлення цитат у тексті статті:

Кількість авторів статті	Приклад цитування у тексті
1 автор	(Arych, 2019)
2 автора	(Kuievda and Bront, 2020)
3 і більше авторів	(Bazopol et al., 2022)

**Приклад тексту із цитуванням:** It is known (Arych, 2019; Bazopol et al., 2022), the product yield depends on temperature, but, there are some exceptions (Kuievda and Bront, 2020).

У цитуваннях необхідно вказувати одне джерело, звідки взято інформацію.

Список літератури сортується за алфавітом, літературні джерела не нумеруються.

## Правила оформлення списку літератури

В Ukrainian Food Journal взято за основу загальноприйняте в світі спрощене оформлення списку літератури згідно стандарту Garvard. Всі елементи посилання розділяються **лише комами**.

### 1. Посилання на статтю:

**Автори А.А. (рік видання), Назва статті, Назва журналу (курсивом), Том (номер), сторінки, DOI.**

Ініціали пишуться після прізвища.

Всі елементи посилання розділяються комами.

Приклад:

Popovici C., Gitin L., Alexe P. (2013), Characterization of walnut (*Juglans regia* L.) green husk extract obtained by supercritical carbon dioxide fluid extraction, *Journal of Food and Packaging Science, Technique and Technologies*, 2(2), pp. 104–108, <https://doi.org/5533.935-3>.

### 2. Посилання на книгу:

**Автори (рік), Назва книги (курсивом), Видавництво, Місто.**

Ініціали пишуться після прізвища.

Всі елементи посилання розділяються комами.

Приклад:

Deegan C. (2000), *Financial Accounting Theory*, McGraw-Hill Book Company, Sydney.

### 3. Посилання на розділ у редактованій книзі:

**Автори (рік), Назва глави, In: Редактори, Назва книги (курсивом), Видавництво, Місто, сторінки.**

Приклад:

Coffin J.M. (1999), Molecular biology of HIV, In: Crandell K.A. ed., *The Evolution of HIV*, Johns Hopkins Press, Baltimore, pp. 3–40.

Fordyce F.M. (2013), Selenium deficiency and toxicity in the environment. In: Selinus O. (ed.), *Essentials of Medical Geology*, pp. 375–416, Springer, DOI: 10.1007/978-94-007-4375-5\_16

#### 4. Тези доповідей конференції:

Arych M. (2018), Insurance's impact on food safety and food security, *Resource and Energy Saving Technologies of Production and Packing of Food Products as the Main Fundamentals of Their Competitiveness: Proceedings of the 7th International Specialized Scientific and Practical Conference, September 13, 2018*, NUFT, Kyiv, pp. 52–57, <https://doi.org/5533.935-3>.

#### 5. Посилання на електронний ресурс:

Виконується аналогічно посиланню на книгу або статтю. Після оформлення даних про публікацію пишуться слова **Available at:** та вказується електронна адреса.

Приклад:

Cheung T. (2011), *World's 50 most delicious drinks*, Available at: <http://travel.cnn.com/explorations/drink/worlds-50-most-delicious-drinks-883542>

Список літератури оформлюється лише латиницею. Елементи списку українською та російською мовою потрібно транслітерувати. Для транслітерації з українською мови використовується паспортний стандарт.

Зручний сайт для транслітерації з української мови: <http://translit.kh.ua/#lat/passport>

Стаття надсилається за електронною адресою:

[ufj\\_nuft@meta.ua](mailto:ufj_nuft@meta.ua)

**Ukrainian Food Journal** публікує оригінальні наукові статті, короткі повідомлення, оглядові статті, новини та огляди літератури.

#### Тематика публікацій в **Ukrainian Food Journal**:

Харчова інженерія	Процеси та обладнання
Харчова хімія	Нанотехнології
Мікробіологія	Економіка та управління
Фізичні властивості харчових продуктів	Автоматизація процесів
Якість та безпека харчових продуктів	Упаковка для харчових продуктів

#### Періодичність виходу журналу 4 номери на рік.

Результати досліджень, представлені в журналі, повинні бути новими, мати чіткий зв'язок з харчовою наукою і представляти інтерес для міжнародного наукового співтовариства.

**Ukrainian Food Journal** індексується наукометричними базами:

- Index Copernicus (2012)
- EBSCO (2013)
- Google Scholar (2013)
- UlrichsWeb (2013)
- CABI full text (2014)
- Online Library of University of Southern Denmark (2014)
- Directory of Open Access scholarly Resources (ROAD) (2014)
- European Reference Index for the Humanities and the Social Sciences (ERIH PLUS) (2014)
- Directory of Open Access Journals (DOAJ) (2015)
- InfoBase Index (2015)
- Chemical Abstracts Service Source Index (CASSI) (2016)
- FSTA (Food Science and Technology Abstracts) (2018)
- Web of Science (Emerging Sources Citation Index) (2018)
- Scopus (2022)

**Рецензія рукопису статті.** Матеріали, представлені для публікування в «Ukrainian Food Journal», проходять «Подвійне сліпе рецензування» двома вченими, призначеними редакційною колегією: один є членом редколегії і один незалежний учений.

**Авторське право.** Автори статей гарантують, що робота не є порушенням будь-яких авторських прав, та відшкодовують видавцю порушення даної гарантії. Опубліковані матеріали є правовою власністю видавця «Ukrainian Food Journal», якщо не узгоджено інше.

Детальна інформація про Журнал, інструкції авторам, приклади оформлення статті та анотацій розміщені на сайті:

<http://ufj.nuft.edu.ua>

## Редакційна колегія

### Головний редактор:

**Олена Стабнікова**, д-р., *Національний університет харчових технологій, Україна*

### Члени міжнародної редакційної колегії:

**Агота Гедре Райшене**, д-р., *Литовський інститут аграрної економіки, Литва*  
*В. І. Вернадського НАН України*

**Бао Тхи Вуронг**, д-р., *Університет Меконгу, В'єтнам*

**Віктор Стабніков**, д.т.н., проф., *Національний університет харчових технологій, Україна*

**Годвін Д. Ндоссі**, професор, *Меморіальний університет Хуберта Кайрукі, Дар-ес-Салам, Танзанія*

**Дора Марінова**, професор, *Університет Кертіна, Австралія*

**Егон Шніцлер**, д-р, професор, *Державний університет Понта Гросси, Бразилія*

**Ейрін Марі Скійондал Бар**, д-р., професор, *Норвезький університет науки і техніки, Тронхейм, Норвегія*

**Йорданка Стефанова**, д-р, *Пловдивський університет "Паїсій Хілендарскі", Болгарія*

**Кірстен Брандт**, професор, *Університет Ньюкасла, Великобританія*

**Крістіна Луїза Міранда Сілва**, д-р., професор, *Португальський католицький університет – Біотехнологічний коледж, Португалія*

**Крістіна Попович**, д-р., доцент, *Технічний університет Молдови*

**Лелівельд Хуб**, асоціація «Міжнародна гармонізаційна ініціатива», *Нідерланди*

**Марія С. Тапіа**, професор, *Центральний університет Венесуели, Каракас, Венесуела*

**Мойзес Бурачик**, д-р., *Інститут сільськогосподарської біотехнології Покапіо (INDEAR), Покапіо, Аргентина*

**Марк Шамцян**, д-р., доцент, *Чорноморська асоціація з харчової науки та технологій, Румунія*

**Нур Зафіра Нур Хаснан**, доктор філософії, *Університет Путра Малайзії, Селангор, Малайзія*

**Октавіо Паредес Лопес**, д-р., проф., *Центр перспективних досліджень Національного політехнічного інституту, Мексика*

**Олександр Шевченко**, д.т.н., проф., *Національний університет харчових технологій, Україна*

**Рана Мустафа**, д-р., *Глобальний інститут продовольчої безпеки, Університет Саскачевана, Канада*

**Семіх Отлес**, д-р., проф., *Університет Еге, Туреччина*

**Соня Амарей**, д-р., проф., *Університет «Штефан чел Маре», Сучава, Румунія*

**Станка Дам'янова**, д.т.н., проф., *Русенський університет «Ангел Канчев», філія Разград, Болгарія*

**Стефан Стефанов**, д.т.н., проф., *Університет харчових технологій, Болгарія*

**Тетяна Пирог**, д.т.н., проф., *Національний університет харчових технологій, Україна*

**Умезуруйке Лінус Опара**, професор, *Стелленбошський університет, Кейптаун, Південна Африка*

**Шейла Кілонзі**, *Університет Каратіна, Кенія*  
**Юлія Дзязько**, д-р. хім. наук, с.н.с., *Інститут загальної та неорганічної хімії імені Юн-Хва Пеггі Хсі*, д-р, професор, *Університет Флориди, США*  
**Юрій Білан**, д-р., проф., *Університет Томаша Баті в Зліні, Чехія*  
**Ясмiна Лукiнак**, д.т.н., професор, *Університет Осієка, Хорватія*  
**Ясмiна Лукiнак**, д-р, проф., *Осієкський університет, Хорватія.*

#### **Члени редакційної колегії:**

**Агота Гедре Райшене**, д-р., *Литовський інститут аграрної економіки, Литва*  
**Бао Тхи Вуронг**, д-р., *Університет Меконгу, В'єтнам*  
**Валерій Мирончук**, д-р. техн. наук, проф., *Національний університет харчових технологій, Україна*  
**Віктор Стабніков**, д.т.н., проф., *Національний університет харчових технологій, Україна*  
**Володимир Ковбаса**, д-р. техн. наук, проф., *Національний університет харчових технологій, Україна*  
**Галина Сімахіна**, д-р. техн. наук, проф., *Національний університет харчових технологій, Україна*  
**Годвін Д. Ндоссі**, професор, *Меморіальний університет Хуберта Кайрукі, Дар-ес-Салам, Танзанія*  
**Дора Марінова**, професор, *Університет Кертіна, Австралія*  
**Егон Шніцлер**, д-р, професор, *Державний університет Понта Гросси, Бразилія*  
**Ейрін Марі Скійондал Бар**, д-р., професор, *Норвезький університет науки і техніки, Тронхейм, Норвегія*  
**Йорданка Стефанова**, д-р, *Пловдивський університет "Паїсій Хілендарскі", Болгарія*  
**Кірстен Брандт**, професор, *Університет Ньюкасла, Великобританія*  
**Крістіна Луїза Міранда Сілва**, д-р., професор, *Португальський католицький університет – Біотехнологічний коледж, Португалія*  
**Крістіна Попович**, д-р., доцент, *Технічний університет Молдови*  
**Лада Шерінян**, д-р. екон. наук, професор., *Національний університет харчових технологій, Україна*  
**Лелівельд Хуб**, асоціація «Міжнародна гармонізаційна ініціатива», *Нідерланди*  
**Марія С. Тапіа**, професор, *Центральний університет Венесуели, Каракас, Венесуела*  
**Мойзес Бурачик**, д-р., *Інститут сільськогосподарської біотехнології Покапіо (INDEAR), Покапіо, Аргентина*  
**Марк Шамцяня**, д-р., доцент, *Чорноморська асоціація з харчової науки та технології, Румунія*  
**Нур Зафіра Нур Хаснан**, доктор філософії, *Університет Путра Малайзії, Селангор, Малайзія*  
**Октавіо Паредес Лопес**, д-р., проф, *Центр перспективних досліджень Національного політехнічного інституту, Мексика.*  
**Олександр Шевченко**, д.т.н., проф., *Національний університет харчових технологій, Україна*  
**Ольга Рибак**, канд. техн. наук, доц., *Тернопільський національний технічний університет імені Івана Пулюя, Україна*  
**Рана Мустафа**, д-р., *Глобальний інститут продовольчої безпеки, Університет Саскачевана, Канада*  
**Семіх Отлес**, д-р., проф, *Університет Еге, Туреччина*

**Соня Амарей**, д-р., проф., *Університет «Штефан чел Маре», Сучава, Румунія*  
**Станка Дам'янова**, д.т.н., проф., *Русенський університет «Ангел Канчев», філія Разград, Болгарія*  
**Стефан Стефанов**, д.т.н., проф., *Університет харчових технологій, Болгарія*  
**Тетяна Пирог**, д.т.н., проф., *Національний університет харчових технологій, Україна*  
**Тетяна Пирог**, д-р. біол. наук, проф., *Національний університет харчових технологій, Україна*  
**Умезуруйке Лінус Опара**, професор, *Стелленбошський університет, Кейптаун, Південна Африка*  
**Шейла Кілонзі**, *Університет Каратіна, Кенія*  
**Юлія Дзязько**, д-р. хім. наук, с.н.с., *Інститут загальної та неорганічної хімії імені В. І. Вернадського НАН України*  
**Юн-Хва Пеггі Хсі**, д-р, професор, *Університет Флориди, США*  
**Ясмїна Лукїнак**, д-р, проф., *Осієкський університет, Хорватія.*

**Олексій Губеня** (відповідальний секретар), канд. техн. наук, доц., *Національний університет харчових технологій, Україна.*

Наукове видання

## **Ukrainian Food Journal**

**Volume 12, Issue 1  
2023**

**Том 12, № 1  
2023**

Підп. до друку 25.05.2023 р. Формат 70x100/16.

Обл.-вид. арк. 12.71. Ум. друк. арк. 12.73.

Гарнітура Times New Roman. Друк офсетний.

Наклад 100 прим. Вид. № 12н/23.

НУХТ. 01601 Київ–33, вул. Володимирська, 68

Свідоцтво про державну реєстрацію  
друкованого засобу масової інформації

КВ 18964–7754Р

видане 26 березня 2012 року.